UNIVERSITY OF NEUCHATEL
SCIENCES FACULTY

GEOLOGICAL INSTITUTE
HYDROGEOLOGICAL CENTER

Spatial variability in porous aquifer properties.

Synthetical approach by geophysics, tracer techniques and groundwater flow parameters.

THESIS

Presented to the Science Faculty of the University of Neuchâtel
For the grade of
Docteur ès Sciences

by
Amélia Carvalho Dill
Geologist graduated in the Classical University of Lisbon (Portugal)

Defence at November the 5 th, 1993 for the jury composed of:

Professor F. Zwahlen, University of Neuchâtel.	Co-Director of Thesis
Professor Ch. Leibundgut, University of Freiburg (Germany).	Co-Director of Thesis
Professor I. Müller, University of Neuchâtel.	Examiner
Professor L. Ribeiro, Technical University of Lisbon (Portugal).	Examiner
Dr. habil. W. Käss, University of Freiburg (Germeny).	Examiner
Dr. M. Bouzelboudjen, University of Neuchâtel.	Examiner

IMPRIMATUR POUR LA THÈSE

Spatial variability in porous aquifer properties. Synthetical approach by geophysics, tracer techniques and groundwater flow parameters.

de Madame Amélia de Carvalho Dill

UNIVERSITÉ DE NEUCHÂTEL

FACULTÉ DES SCIENCES

La Faculté des sciences de l'Université de Neuchâtel
sur le rapport des membres du jury,

MM. F. Zwahlen, Ch. Leibundgut et H. Käss (Freiburg i.Br.), I. Muller, L. Ribeiro (Liabonne) et M. Bouzelboudjen

autorise l'impression de la présente thèse.

Neuchâtel, le 22 novembre 1993

Le doyen:

H.-E. Nägeli

Dedication:

To the memories of my father and brother,
to my husband and my daughters Barbara and Leonor,
to my mother and to all my brothers and sisters,
who are my guiding light,...the beautiful sight of life...

Acknowledgements

This work is successful thanks to the financial support of several institutions and persons:

- The University of the Algarve (Portugal) gave me the opportunity to come abroad and invested in my professional training as a hydrogeologist.

- The Junta Nacional de Investigaçao Cientifica e Tecnológica (Portugal) helped me with a four year scholarship.

- The Erziehungsdirektion des Kantons Berns (Switzerland) subsidize one year of my training.

- My husband Eduard Dill.

Many people helped me along the way and I would like to express my gratitude to all of them. Among them:

Prof. F. Zwahlen opened the doors of the Centre d'Hydrogeology to me and gave me the possibility to continue my research project. Without his interest and support I would never have finished this work.

Prof. Leibundgut (University of Freiburg, Germany) introduced me to the theme of my work and agreed for me to carry it on despite his departure.

Prof. I. Müller (Centre d'Hydrogeology de Neuchâtel) helped and encouraged me right from the start . It was a privilege to work with him and discover the fascinating world of the electromagnetic methods. He will always remain for me the example of the field scientist, selflessly dedicated to investigation. And, above all, a friend.

U. Schotterer (Physikalisches Institut der Universität Bern) assisted and advised me in the most critical period of this undertaking. He and H.Burki contributed an important part of this work : the isotopes analysis.

Prof. W. Käss (University of Freiburg, Germany) performed most of the tracer analyses. He offered me the opportunity to work on his site, giving me all the information and data I needed for my project. I was very fortunate to meet such a person, both a true scientific mind and profoundly humane. My sincere admiration goes to him and his wife.

Dr. Mahmoud Bouzelboudjen (Centre d'Hydrogeology de Neuchâtel) with whom I worked during the last year advised me tirelessly, encouraged me and criticised my writings. I can but admire his work methodology and his promptitude to help.

Prof. L. Kiraly (Centre d'Hydrogeology de Neuchâtel) gave me lots of incentive. His advice and critical remarks were very stimulating and always invited deeper reflection.

My Portuguese colleague Dr. Luis Ribeiro was always helpful and interested.

Dr. Carlos Beck (*LASUR* Chemical Laboratory) and all his team, especially Olga Sierra helped me a lot with the chemical analyses. To them: *Um enorme Obrigado! Bem hajam!*

All the chemical and clay mineral identifications were always promptly carried out by the Chemistry and Geology Departments of the Universidade de Trás-os-Montes e Alto Douro. For this, I must thank my brother Dr. Luis Carvalho, Prof. Dr. J. Féria Seita, Dr. Vilela de Matos and the staff of the UTAD.

I do not forget all the colleagues I met in Neuchâtel:

Pierre Rossi (Laboratoire de Microbiology) shared the work of the last tracer experiment.

Pascal Turberg (Centre d'Hydrogeology de Neuchâtel) patiently listened and answered all my doubts and questions, notwithstanding his own work.

Catherine Fischer (Laboratoire de Microbiology) corrected the English of this text with remarkable promptitude and efficiency.

I would also like to thank Nathalie Doerflinger, Laurent Eisenlohr, Yvan Rossier, Abdallah Mdaghri, A.Dodo, P-Y. Jeannin, Laurent Tacher, R.Kozel and my Bernese colleagues Bernhard Schudel and Thomas Wagner.
I am also grateful to Mr. Manuel Silva (Uni. Neuchâtel), who encouraged me frequently .

... And of course I thank most particularly my husband and my daughters, Barbara and Leonor, who not only showed a lot of understanding despite my many absences, but also encouraged me constantly and participated in the field work.

Some of the data used in this work was kindly provided by the WEA (Wasser- und Energiewirtschaftsamt des Kantons Bern), the Büro Werner (Burgdorf), the Landeshydrologie (Bern), and the SMA (Schweizerischen Meteorologischen Anstalt).

Spatial variability in porous aquifer properties.

Synthetical approach by geophysics, tracer techniques and groundwater flow parameters.

Keywords:

Porous aquifers, electromagnetics, heterogeneities, piezometry, dyes, isotopes, water chemistry, Swiss Plateau (Wilerwald), Upper Rhine Valley (Merdingen,Germany).

Abstract:

Natural porous formations are quite heterogeneous and of a complex nature, with highly variable geometrical and hydraulic properties. They are often important water reservoirs, very vulnerable to contaminatioo by agriculture or other pollution sources. Therefore, tracer tests under field conditions, simulating contamination problems, have become of increasing importance.

This work was developed on a test site - Wilerwald [canton Bern, Swiss Plateau] - equipped to perform tracer experiments on post glacial Holoceoe sandy gravels. Artificial tracer tests had already been made, but gave results very inconsistent with what had beeo expected :

- In wells lying just 7 meters apart, differences of several orders of magnitudes in arrival times as well as in concentrations were observed!
- Simultaneously, we repeatedly observed a deflection of the tracer, diverging from what was considered the main direction of water flow.

In order to interpret solute transport in such formations, it is necessary to have sufficient information about the aquifer, that is, about the mechanisms of flow and about its structure and permeability distribution. Electromagnetical surveys* - Radio Magnetotelluric - Resistivity (RMT-R 12-240 kHz) and Very Low Frequency - Electromagnetic (VLF-EM) were fundamental for collecting such detailed data, otherwise impossible to obtain, by classical geoelectrics or drilling.

We discovered a paleochannel, responsible for the above-mentioned deflection, as well as significant differences in resistivities (and consequently in permeabilities) around each piezometer, thus plausibly explaining the erratic behaviour of the tracers.

In November 1992, the last tracer campaign using classical dyes (Naphtionate, Uranin and Amidorhodamine) and bacteriophages, once again confirmed the electromagnetic conclusions. Almost daily observations of the piezometric level, performed simultaneously, exposed the spatial and temporal variations of the groundwater level, induciog each time new directions and velocities of flow .

To interpret RMT-R raw data a new approach was used, based oo the indirect relationship between resistivities and graio size distribution. This is a rapid method for determining both the horizontal and vertical distribution of heterogeneities. It differentiates the vertical distribution of layers and resistivities, and also defines the influence of the upper conductive layer on the resistivity data.

According to the prevailing heterogeneities a regional flow system can thus be differentiated into local systems, each with a different flow-line pattern, a different residence time of the water, and consequently different chemical properties. The same applies to the test-site scale. Some chemical analyses (conductivity , nitrate, sulphate, chloride determinations and hardness) were carried out : they showed only small differences but quite significant ones.

The concentration of two water isotopes was measured

- oxygeo 18, to evaluate the respective contributions of rain water and the river Emme to the renewal of the water reserves.
- Tritium, to determine the residence-time of the water in the aquifer.

This work points out:

1) the real degree of heterogeneity of Wilerwald's quaternary formation,
2) the importance of this factor in the evaluation of hydraulic parameters,
3) its implications for transport processes,
4) and the importance of electromagnetical methods for hydrogeological studies.

Résumé:

Les aquifères poreux en milieu alluvial sont caractérisés par des dépôts très hétérogènes. Leurs propriétés hydrauliques et géométriques sont souvent extrêmement variables.
Par ailleurs, ils constituent des aquifères très importants mais aussi très vulnérables à la contamination liées aux activités agricoles et industrielles. Pour cette raison, l'intérêt de la réalisation d'essais de traçage, simulant les problèmes de contamination, a considérablement augmenté .

Ce travail a été réalisé dans un champ expérimental - Wilerwald - [Canton de Berne, Plateau suisse] conçu pour effectuer des essais de traçage. L'aquifère y étant constitué par des graviers sableux du Holocène.
Les résultats des essais déjà réalisés semblaient contradictoires :

- Des différences en temps d'arrivée et aussi en concentration, parfois de plusieurs ordres de grandeur ont été détectés dans des piézomètres distants de 7 mètres!
- Simultanément il parait exister une déviation du nuage du traceur, s'éloignant de la direction d'écoulement principal supposée.

Pour pouvoir interpréter les essais de traçage dans ces formations hétérogènes, il faut connaître d'abord les processus des écoulements souterrains, identifier l'aquifère, sa structure et ses paramètres physiques.
Nous avons réalisés des sondages électromagnétiques (Radio Magnetotelluric-Resitivité -RMT-R 12 a 240 kHz ,et Very Low Frequency - Electromagnétique - VLF-EM-) fondamentales pour l'acquisition des données détaillés sur la lithologie et la structure des dépôts. Il est clair que cette partie constitue une phase importante du travail.

Les principaux résultats ont permis de déceler :

- Un paléochenal, responsable de la déviation du nuage du traceur ;
- des différences significatives de résistivité constatées entre les piézomètres, et qui semblaient donner une explication plausible à la migration "aléatoire" du traceur.

Nous avons injecté différents traceurs colorants traditionnelles (Uranin, Naphtionat et Amidorhodamin) ainsi que des bactériophages. Les résultats de ces essais (dernière campagne de novembre 1992) ainsi que des mesures piézométriques presque journalières effectuées simultanément, nous ont permis de confirmer une fois de plus les conclusions des méthodes électromagnétiques.

Par ailleurs les mesures piézométriques ont révélé l'extrême variabilité de situations possibles créant à chaque fois variations spatiaux ou temporelles locales de direction et vitesse de flux.

Pour mieux interpréter les données RMT-R, nous avons utilisé une nouvelle approximation, basée sur la relation indirecte entre la résistivité et la granulométrie. Cette méthode nous a permis de montrer la distribution spatiale et verticale de l'hétérogénéité, de relier rapidement les valeurs de résistivité et de la phase aux modèles de remplissage plausibles et également d'évaluer l'influence de la couche de couverture (existante ou non) sur les valeurs mesurées.

Dans un système d'écoulement régional il est possible d'individualiser des systèmes locaux avec des temps de séjour d'eau différents et conséquemment des propriétés chimiques distinctes, liées aux hétérogénéités existantes. À l'échelle du site et du fait de l'hétérogéneité des phénomènes similaires peuvent exister. Ainsi, les résultats des analyses chimiques de l'eau (conductivité, nitrates, sulfates, chlorures et dureté) ont révélé des petites différences significatives.

Conjointement nous avons utilisé les techniques isotopiques, pour évaluer la contribution des eaux de la rivière et des eaux météoriques dans le renouvellement des réserves (l' oxygène- 18) et pour estimer le temps de séjour des eaux dans l'aquifère (le tritium).

Ce travail nous a permis de mettre en évidence:

1) le degré de l'hétérogénéité réelle de la formation quaternaire du site de Wilerwald,
2) l'importance de ce facteur dans l'évaluation des paramètres hydrauliques,
3) les implications dans les processus de transport,
4) l'importance de la géophysique électromagnétique dans les études des dépôts alluvionnaires complexes.

Kurzfassung

Die porösen Medien sind sehr heterogeo und komplex und ihre hydraulischen Eigenschaften sind stark wechselhaft. Gleichzeitig sind sie wichtige Wasser-Reserven, sehr empflindlich gegen landwirtschaftlische oder industrielle Pollution. Tracer Tests können Kontaminationsprobleme simulieren, deswegen ist das Interesse in den letzten Jahren dafür stark gewachsen.

Diese Arbeit ist im Testfeld Wilerwald (Kanton Bern, Bernermittelland) durchgeführt worden. Der Aquifer besteht aus holozaco sandigem Kies (jüngere Schottern). Künstliche Tracer wurden schon früher eingespeist, doch die Resultate scheinten wiedersprüchlich zu sein:

- Piezometer, welche nur 7 Meter vno einander entfernt waren, wiesen extrem grosse Unterschiede in den Durchgangskurven auf.
- Gleichzeitig scheinten die Tracer immer wieder deflektiert zu sein und zwar in Richtung West, weit von der gedachte Hauptfliessrichtung abweichend.

Um die Stofftransport in solchen Formationen interpretieren zu können, ist es notwendiggenügend Informationeo über den Grundwasserleiter, seine Struktur und Durchlässigkeitsverteilung und über die Fliessmechanismen zu haben. Elektromagnetische Methoden - Radiomagnetotellurische-Resistivität (RMT-R, 12-240 kHz) und Very Low Frequency- Electromagnetik (VLF-EM) sind deswegen durchgeführt wordeo. Sie erlaubten auch eine detaillierte Aufnahme, die mit anderen Methoden sonst unmöglich zu bekommeo ist.
Es wurde auch,

- Eine Paleorinne, die verantwortlich ist für die Tracer-Deflektion, entdeckt;
- Gleichzeitig sind bedeutende Unterschiede der Widerstandswerte (indirekte Durchlässigkeitswerte) bei jedem Piezometer festgestellt worden.

Bei dem letzen Tracerversuch im November 1992 sind gleichzeitig die klassischen Tracer (Naphtionate, Amidorhodamine G und Uranin) zusammen mit Bakteriophagen eingespeist worden, diese bestätigten wieder die RMT-R Resultate.
Gleichzeitig sind tägliche Messungen des Grundwasserspiegels bei jedem Piezometer durchgeführt worden. Sie haben wieder die starke räumliche und vertikale Veränderlichkeit dieser quartäreo Formation, welche ständige Veränderungen der Fliessrichtungen und Fliessgeschwindigkeiten induzieren können, bewiesen.

Eine neue approximative Methode, welche auf der Beziehung zwischen elektrischen Widerstand und der Korngrössenverteilung beruht, wurde eingesetzt, um die RMT-R Daten anders interpretieren zu könneo. Die vertikale und horizontale Heterngeneitätsverteilung wurdeo damit schnell determiniert. Gleichzeitig konnte die unregelmässige Verteillung einer obersten, undurchlässigen Schicht bestimmt werden.

Ein regionales Fliesssystem kann in mehrere lokale und intermediäre Fliesssysteme differenziiert werden, jedes mit bestimmteo Fliesslinienmuster, verschiedenen Verweilzeiten und entsprecheden chemischen Eigenschaften, in Bezug auf die herrschende Heterogeneität. Dasselbe kann sich im kleinen Massstab des Versuchsfeldes wiederholen. Um das beweisen zu können, sind chemische Analysen durchgeführt worden : (Leitfähigkeit, Nitrat, Sulfat, Chloride, und Härte) : sie zeigten kleine aber bedeutende Unterschiede zwischen den Piezometern.

Zwei Wasserisotopen sind auch gemessen worden : Sauerstoff-18 und Tritium. Das erste wurde gebraucht, um eine relative Komponententrennung - mit welcher der Prozent-Anteil von lokalem Regenwasser und Emme-Wasser berechnet werden konnte, zu bestimmen. Tritium erlaubte eine relative Datierung des Grundwassers.

Diese Arbeit ermöglichte:

1) den reelen Veränderlichkeitsgrad des Wilerwalds Grundwasserleiters zu beweisen,
2) die Wichtigkeit dieses Faktors für die Ermittlung hydraulischer Parameter,
3) die Konzequenzen für die Stofftransportvorgänge,
4) und die Wichtigkeit der elektromagnetischen Methoden für die Hydrogeologie.

Resumo:

Os meios porosos de natureza aluvial são caracterisados pela sua grande heterogeneidade e pelas suas propriedades hidráulicas e geométricas apresentarem frequentemente grande variabilidade. Em geral comportam-se como bons aquíferos, vulneráveis à contaminação associada às actividades agrícolas e industriais. Por esse motivo, a simulação de problemas de transporte utilizando ensaios com traçadores é uma técnica de crescente importância.

Este trabalho desenrolou-se no campo experimental - Wilerwald - situado no cantão de Berna, no planalto suiço. Trata-se de um campo concebido para efectuar ensaios de traçadores. O aquífero é constituido por cascalheiras e calhaus arenosos e siltosos , de origem fluvio-glaciar holocénica.

Nesse campo já tinham sido efectuados no passado ensaios deste tipo. Os resultados então obtidos mostraram-se contradictórios, em relação ao esperado, dado que:

- Em alguns piezometros distanciados apenas de sete metros, quer as diferenças de tempo de chegada quer as de concentrações obtidas eram por vezes de várias ordens de magnitude!
- Ao mesmo tempo parecia existir sistemáticamente um desvio da ouvem de traçadores, afastando-se do que se considerava ser a direcção de escoamento principal.

De modo a interpretar os ensaios de traçadores em formações heterogéneas é necessário conhecer de antemão os processos que regem o escoamento subterrâneo, identificar a estrutura e os parâmetros físicos do aquífero.

Para isso foram realizadas sondagens electromagnéticas (Radio-Magnetotelúricas- de resistividade RMT-R, entre 12 a 240 kHz e sondagens electromagnéticas de muito baixa frequência VLF-EM) que são fundamentais no processo de aquisição de dados mais pormenorizados sobre a litologia e estrutura dos depósitos.

Como resultado dessas aplicações foram individualisados :

- Um paleocanal, responsável pelo desvio repetitivo das núvens de traçadores ;
- diferenças significativas nas resistividade na vizinhanças dos piezómetros que permitem explicar as migrações "erráticas" dos traçadores.

Na última campanha de novembro de 1992 foram injectados traçadores corantes tradicionais (Uranin, Naphtionat et Amidorhodamin) e bacteriófagos. Tanto os resultados obtidos nesses ensaios como as medições observadas nos níveis piezométricos, efectuadas simultaneamente, confirmaram uma vez mais os conclusões dos métodos electromagnéticos.

Quase todas as medidas piezométricas observadas diáriamente revelaram a extrema diversidade de situações, contribuindo para as variações espaciais e temporais da direcção e da velocidade de fluxo.

Para melhor interpretar os dados de RMT-R , ensaiou-se novo método aproximativo, baseado na relação indirecta existente entre a resistividade e a granulometria. Os resultados evidenciam uma vez mais o grau de heterogeneidade do meio. Obteve-se de igual modo uma imagem da variabilidade espacial e vertical dos terrenos, ao mesmo tempo que se conseguiu associar rápidamente aos valores de resistividade e de desfasagem modelos sedimentógicos plausiveis. Foi possível igualmente delinear áreas contendo terrenos mais desenvolvidos de cobertura siltosa, cuja natureza intrínseca se reflecte nos valores de resistividade e de fases medidos.

Num sistema de escoamento regional é possível individualisar sistemas locais e intermediários, cada qual possuindo tempos de residência diferentes, e consequentemente distintas propriedades químicas ligadas às heterogeneidades regionais existentes. O mesmo pode ocorrer à escala do campo experimental. Para o constatar foram realizadas análises químicas das águas . Os resultados das análises (conductividade, nitratos, sulfatos, cloretos, e de dureza) revelaram diferenças significativas embora pequenas.

As técnicas isotópicas permitiram *grosso modo* avaliar o tempo de permanência (tritium) e a contribuição relativa das águas da chuva e do rio Emme (oxigénio-18) , para a renovação das reservas de água subterrânea.

Com este trabalho foi possível evidenciar:

1) o grau de heterogeneidade do Quaternário em Wilerwald,
2) a importância deste factor na determinação de parâmetros hidráulicos,
3) as implicações no processo de transporte,
4) e finalmente a importância dos métodos geofísicos electromagnéticos no estudo de depósitos aluviais complexos.

Contents:

Aknowledgments

Abstract

Contents

List of figures

List of tables

CONTENTS :

Part I: Introduction to the theme of the work

1. General framework
   1.1 Introduction
   1.2 Work orientation

2. Presentation of the test site
   2.1 Geographic locatioo and site description
   2.2 Regional geology and hydrogeology - previous studies
   2.3 Local characterisation and previous works
   2.3.1 General aspects
   2.3.2 Tracer tests
   2.3.3 Interpretation of tracer tests : modelling attempts - Sansoni et al (1988) and Schneider(1992)

Part II: Regional Framework

3. Regional Studies
   3.1 Identification and geometry of the aquifer
   3.1.1 Literature Overview
   3.1.2 Very Low Frequency - Electromagnetic Surveys
   3.1.2 Audio-Magneto-Tellury
   3.2 Hydrodynamic aspects: piezometric observations
   3.3 Hydrochemistry
   3.4 Synthesis and conclusions

Part III: Local Studies, Field Experiments and analyses

4. Identification and geometry of the aquifer

4.1 Geophysical Methods:

4.1.1 Electromagnetical methods

A RMT-R

A.1 RMT-R Results

A.2 Methods of interpretation

A.2.1.-Application of Kriging

A.2.2.-Interpretation based on raw data

A.3 Interpretation based on MT. inversion

B multidirectional RMT-R

C VLF-EM

D audiomagneto-tellurics

4.1.2 Electrical method: Schlumberger configuration

4.1.3 Seismic surveys

4.2 Local Geological Aspects

4.3 Synthesis and conclusions

5. Hydrodynamic aspects:

5.1 Experimental work

5.2 Conclusions about local hydrodynamic aspects

6. Chemical analyses:

6.1 Analyses performed:

1- Conductivity (K)

2- Hardness

3- Nitrates

4- Chlorides

5- Sulphates

6- Temperature

6.2 Synthesis

7. Isotope hydrology in Wilerwald

7.1 Tritium (^{3}H)

7.2 Oxygen-18 (^{18}O)

8. Artificial tracers: Experiments performed in 1988 and 1992 : differences and analogies
8.1 Tracer test of 1988
8.2 Tracer test performed at 1992
8.3 Conclusions about the tracer results of 1992

Part IV: Merdingen test site (Germany)

9. Merdingen
9.1 Description of the site
9.2 Geology and Hydrology
9.3 Electromagnetic surveys
9.3.1 RMT-R
9.3.1.1 Performance and Results
9.3.1.2 Interpretation based on raw data
9.3.1.3 Kriging at Merdingen
9.3.2 VLF-EM
9.4 Synthesis and conclusions

Part V: Final Conclusions

10. Brief Overview

Bibliography

Appendix :

Appendix 1

A : Geophysical methods used:
Electromagnetic methods: RMT-R, VLF-EM; seismic and electric methods
B Applied geostatistic :
Theory of the regionalized variables
Variogram
Kriging

Appendix 2 Regional :

figures and tables

Appendix 3 Local :

figures and tables

Curriculum Vitae

List of Figures :

Part I: Introduction to the theme of the work

Fig. 1 Relationship between real system, abstracted scheme and model (after Kiraly, 1992)

Fig. 2 Flow and transport organigram (after Gerlinger, K. in Carvalho Dill (1992).

Fig. 3 Location of the Wilerwald testsite - Swiss map (a); limits of the aquifer and limits of the catchmeot basin (b) and the Wilerwald testsite showing the disposition of the piezometers in three half-circulated ranges, C, D and F. EP_I = injection well (1986); C_d = borehole (1988); R1, R2...R6 and RP = piezometers just for ground water level measurements (1992) .

Fig. 4 Vertical section showing a piezometer settled on the soil, and its division system, for the sampling at three levels -5,8,11 m after **Sansoni et al,1987.**

Fig. 5 Simplified hydrogeological map with springs and wells inventoryin in the "Unteres Emmental".

Fig. 6 Schematic profile representing the quaternary sedimeots found in the Emme Valley, after WEA (1981).

Fig. 7 1979 groundwater isohypsen map, (after **WEA,1981**)

Fig. 8 1986 piezometric map : indicating the main direction of flow towards NW and the existence of small irregularities on the isohypsen, a indicator of heterogeneity.

Part II : Regional Framework

Fig. 9 Two geological profiles (after WEA) enveloping the site, showing the geological units referred above and the extreme different development of these formations (Window : location of the geological profiles).

Fig. 10 Regional map with the localisation of the drill cores of the stations used for piezometric head level measurements (**WEA,1981**) and drill cores logs (**WEA,1981**).

Fig. 11 Map with Aqufer thickness isolines (**WEA,1981**).

Fig. 12 Localisation of the VLF-EM profiles. The Wilerwald test site is represented by a shadow area. The map used as a basis is the geological map 1:25000 (**Ledermann, H.,1977**).

Fig. 13 Representing the graphic profiles, a qualitative division of classes , and the topographic contour lines. The site is represented by a dotted line. Only the paleochannel (chapter 4) is delineated at the site area (pointed area).

Fig. 14 Aquifer thickness isolines (after Wea, 1981), and the VLF-EM profiles, illustrating the danger of interpolation using punctual and scattered informatinn in a heterogeneous formation.

Fig. 15 Annual Precipitatioo for the the period 1.Jan 1992 till 31 Jan 1993, measured at the Oeschberg Station.

Fig. 16 Map representing the **Fig. 10** and the amplitude of the ground water level during Nov./Dec. 1992 : w/ altitude, date of maximal level, amplitude (cm) and depth of water level: lowest amplitudes in stations near discharge areas (sources), relative high amplitude (1 - 1.4 meters in the central part : important contribution of the Emme, main ground water drainage); higher amplitude : WAB 57, confined aquifer (q4vsB - gravels and sand with low permeability, covered by moraine sediments q4mB).

Fig. 17 Delta head fluctuations during the rain period Nov./Dec. 1992.

Fig. 18 Groundwater level evolution during about 6 months (22 Mai 1992 - 31 Dec. 1992) for the observatioo well WAB 57 - exemplifying the cumulative aspect referred above.

Part III : Local studies, field experiments and analyses

Fig. 19 a) & b). Map with location of the geophysical observatioo net: geoelectrics,VLF-EM, RMT-R, seismic.

Fig. 20 Location of the RMT-R profiles mentioned above

Fig. 21 Apparent resistivity contour map obtained with 183 kHz, clearly indicating the existence of a higher resistant channel (Rho >300 Ohm.m) and its disposition relative to the net of observation wells.

Fig. 22 a) & b) RMT-R results: apparent resistivity map (183 kHz) and standard error maps.

Fig. 23 a) & b) RMT-R results: phase maps and standard error maps (existence of a structure oriented northwards and bisecting the channel .

Fig. 24 Profiles passing through the C, D and F galleries, representing the Rho apparent values at Y1 (left axis) and the phase values at Y2 (right axis).

Fig. 25 Histograms of the Rho ap values (transformed into logarithms) - A bimodal distribution at 183 kHz.

Fig. 26 Hypothetical cumulative distribution curves of apparent resistivities values, representing:
1) an extremely homogeneous sediment where all the values are the same,
2) a situation of symmetrical distribution with a modal class, the case of a relatively homogeneous deposit,
3) a very heterogeneous deposit, where practically all classes are represented.

Fig. 27 Cumulative percent distribution curves. For the separating domains, please see the text.

Fig. 28 100 Ohm.m separating borderline, separating the more conductive NNE region, detectable at all frequencies.

Fig. 29 Possible models corresponding to the 5 classes illustrating that within each class, different situations can occur.

Fig. 30 Map of Classes : a trial to get a qualitative integrated information with the rho ap. values at three depths, simultaneously reflecting the influence of the structure and nature of the materials (see text).

Fig. 31 Cumulative distribution curves of all Wilerwald values and of the 5 classes.

Fig. 32 Map with the results of RMT-R multidirectional.

Fig. 33 Map showing the VLF-EM profiles inside the site, in correspondence with RMT-R results.

Fig. 34 Map of electrical soundings. The following features can be observed:

1) the situation of D1, R1, RP, F2 and F4 (confined);
2) the increased thickness of the silty clay layer in the east part of the site;
3) the aquifer thickness, greater in the channel (C7, D6), and also the increase of resistivity values (increase of the gravel dimensions) there.

Fig. 35 Seismic results confirming the paleochannel.

Fig. 36 Grain size cumulative distribution curves of the samples taken from the borehole CD. The depth of the sample is indicated and is in meters. One can observe that aquifer curves reflect the heterogeneity of the sediments (very inclined, almost horizontal curves). Some lenses have very distinguish curves reflecting the more percent on the sand fraction. The passage to the aquitard (?) can be clearly seen at 14.5 m depth. At 15 m depth the curve is dislocated toward the silt domain.

Fig. 37 Lithological log from the borehole CD.

Fig. 38 Schlumberger resistivity log of the borehole CD.

Fig. 39 Graphics representing the depth distribution of the resistance to penetration of the piezometers installed in May 1992 for ground water level measurements. For the localisation of the piezometers please regard Fig. 3.

Fig. 40 Representing some observation wells , during the tracer test performance (graphic below). The rain fall events and their magnitudes are plotted on the graphic above.- to be compared with **Fig. 3B-2.**

Fig. 41 Differences on head max. and minimal values, for the periods June-Sept. and Nov.-Dec. 92)

Fig. 42 Representing the Schlumberger information of the depth of the aquifer, of the humic layer and the maximal and minimal water level (Nov.-Dec. 92). The piezometers D1, R1, F4, F2 and Rp are in a captive situation.

Fig. 43 Represents the depth of the ground water level relative to the observation wells.

Fig. 44 Piezometric maps representing the three situations of the isohypsen during the tracer experiment Nov./Dec 1992. 10 Nov. day of the injection; 16. Dec. last day of the experiment; 27 Nov. an intermediate situation.

Fig. 45 Longitudinal profile along the line considered to be the main direction of water flow .

Fig. 46 Conductivity values for the C (a) and D gallery (b) with simultaneous representation of the rainfall events during 1992.

Fig. 47a) & b) Conductivity values for the C (a) and D gallery (b) with simultaneous representation of the rainfall events during during the tracer experiment at Nov. 1992.

Fig. 48 Conductivity and temperature profiles for the observation well B4 measured in Sept 1992 (a) and Nov 1992 (b) The profile b2 is the same as b3, with only a different scale.

Fig. 49 Total hardness values (Dto) measured during June and September 1992.

Fig. 50 Nitrates values for the C (a) and D gallery (b) with simultaneous representation of the rainfall events.

Fig. 51 Chlorides values for the C (a) and D gallery (b) with simultaneous representation of the rainfall events.

Fig. 52 Sulphates values for the C and D galleries with simultaneous representation of the rainfall events.

Fig. 53a) & b) Temperature values for the C (a) and D gallery (b) with simultaneous representation of the rainfall events during July till Nov. 1992.

Fig. 54a) & b) Temperature values for the C (a) and D gallery (b) with simultaneous representation of the rainfall events during during the tracer experiment at Nov. 1992.

Fig. 57(a) & (b) Tritium in precipitation (a) Tritium in the investigation area and exponential model output (b)

Fig. 58(a),(b) & (c) Oxygen-18 in Kleine Scheidegg and Grimsel (a) (Schotterer et al, 1993), in spring water (b) and in precipitation Burgdorf (six months gliding means, 1984-1992,, Emme and Zielebach (c).

Fig. 59(a)&(b) Oxygen-18 in surface water and in the investigation area (a), and comparison of Oxygen-18 in ground and surface water in Wilerwald (b).

Fig. 58. Uranine, Lithium and Sulforhodamine B breakthrough curves at four chosen observation wells, D1 and D7 set 50 meters apart (D gallery) and C7 and C8 (separated by only 7 meters (C gallery). The contrasts between C8 and C7 are outstanding.

Fig. 59 Hand drawed apparent resistivity map and the Uranine breakthrough curves at four observation wells.

Fig. 60 Uranine breakthrough curves at 1988 (a) and 1993 (b). Both injection occurred at the 10th of November.

Fig. 61 Peak concentrations at different observations well.

Fig. 62a) & b) Naphtionate breakthrough curves at the C gallery (a) and D gallery (b).

Fig. 63a) & b Amidorhodamine breakthrough curves at the C gallery (a) and D gallery (b).

Fig. 64a) & b Uranine breakthrough curves at the C gallery (a) and D gallery (b).

Part IV: Merdingen test site (Germany)

Fig. 65 Location of the Merdingen test site.

Fig. 66 Merdingen test area showing the two sub-sites A and B.

Fig. 67 Map representing the RMT-R profiles and the measuring points

Fig. 68 Some profiles, showing the Rho apparent values at y1 (left axis) and the Phase values at y2 (right axis).

Fig. 69 Appareot resistivity contour map at 1&3 kHz, drawn by hand. The figure also shows:
1) the actual tracer path (arrows);
2) the piezometers which received the greatest amount of tracer.

Fig. 70 Histograms of the resistivities and phases values

Fig. 71 Cumulative frequency curves at the Merdingen test site

Fig. 72a) & b RMT-R results: apparent resistivity map (183 kHz) and standard error maps.

Fig. 73a) & b RMT-R results: phase map (183 kHz) and standard error maps.

Part V: Final conclusions

Fig. 74 3-D picture of the true resistivity distribution at the Wilerwald site ("piece of pie"). The small blocks diagrams showing qualitative models for chosen punctual RMT-R soundings (sticks=penetration depths),illustrate the variability of possible situations within the test area .

List of tables :

Part I: Introduction to the theme of the work

Table 1 Main units found in the Unteres Emmental (WEA): .

Table 2 Hydrological caracterisation of the geological unities.

Table 3 Hydraulic parameters determined by Sansoni et al, 1987.

Table 4 Chemical analyses performed at the test site Wilerwald

Part III : Local studies, field experiments and analyses

Table 5 main characteristics of the kriging interpolation function.

Table 6 Selection degree in a grain size analysis after **Folk and Ward (1957).**

Table 7 Assimetry degree in a grain size analysis after **Folk and Ward (1957).**

Table 8 Folk and Ward parameters **Folk and Ward (1957).**

Table 9 Statistical parameters of the Rho apparent values (logarithms) calculed after **Folk and Ward (1957).**

Table 10 multidirectional RMT-R data. The position of the stations can be seen on the Map of **Fig. 32.**

Table 11 Nitrate content at the Wilerwald test site (summer 1992).

Table 12 Chlorides concentrations

Table 13 Sulphate concentrations

Table 14 Comparison of the transport parameters calculed by different methods using the conservative tracer Uranine .

Table 15 Tracer test, 1988 : main differences on peak concentrations and peak times.

Table 16 Tracer test, 1992 : main differences on peak concentrations and peak times.

Part IV: Merdingen test site (Germany)

Table 17 Hydrochemical data for the groundwater in the testfield Merdingen (extracted from **Käss** *in* **Carvalho Dill et al, 1992).**

Table 18 : main characteristics of the kriging interpolation function.

List of tables :

Part I: Introduction to the theme of the work

Table 1 Main units found in the Unteres Emmental (WEA):

Table 2 Hydrological caracterisation of the geological unities.

Table 3 Hydraulic parameters determined by Sansoni et al, 1987.

Table 4 Chemical analyses performed at the test site Wilerwald

Part III : Local studies, field experiments and analyses

Table 5 main characteristics of the kriging interpolation function.

Table 6 Selectioo degree in a grain size analysis after **Folk and Ward (1957).**

Table 7 Assimetry degree in a grain size analysis after **Folk and Ward (1957).**

Table 8 Folk and Ward parameters **Folk and Ward (1957).**

Table 9 Statistical parameters of the Rho apparent values (logarithms) calculed after **Folk and Ward (1957).**

Table 10 multidirectional RMT-R data. The position of the stations can be seen on the Map of **Fig. 32**.

Table 11 Nitrate content at the Wilerwald test site (summer 1992).

Table 12 Chlorides concentrations

Table 13 Sulphate concentrations

Table 14 Comparison of the transport parameters calculed by different methods using the conservative tracer Uranine .

Table 15 Tracer test, 1988 : main differences on peak concentrations and peak times.

Table 16 Tracer test, 1992 : main differences on peak concentrations and peak times.

Part IV: Merdingen test site (Germany)

Table 17 Hydrochemical data for the groundwater in the testfield Merdingeo (extracted from **Käss** *in* **Carvalho Dill et al, 1992).**

Table 18 : main characteristics of the kriging interpolatioo function.

Part I: Introduction to the theme of the work

1. General framework

1.1 Introduction

1.2 Work orientation

2. Presentation of the test site

2.1 Geographic location and site description

2.2 Regional geology and hydrogeology - previous studies

2.3 Local characterization and previous works

2.3.1 General aspects

2.3.2 Tracer tests

2.3.3 Interpretation of tracer tests : modelling attempts - Sansoni et al (1988) and Schneider (1991).

Spatial variability in porous aquifer properties.

Synthetical approach by geophysics, tracer techniques and groundwater flow parameters.

I Part : Introduction

1. Generalities

1.1 Introduction

Tracer tests under field conditions in porous media, are a subject of great interest and actuality. They are used to study the water flow, to determine aquifer parameters, mean residence times of water and to simulate contamination problems. However, the interpretation of tracer tests, is not always an easy task, due to the intrinsic heterogeneity of the porous media.

Wilerwald testsite was set up for tracer experiments in the aquifer, in the lower (unteres) Emme valley aquifer composed of post-glacial Holocene sandy gravels.

This formation is an important water reserve, lying under land intensively cultivated and pastured. The ground water reserve is renewed, directly by the river Emme, or by infiltration. Therefore the system is vulnerable to contaminations from agriculture or other pollution sources. In consequence, it is necessary to study the groundwater transport processes and to preserve water quality. For this reason, the Wasser- und Energiewirtschaftsamt des Kantons Bern has been carrying out hydrogeological studies in this region for more than 20 years.

The regional heterogeneity of the aquifer was already known. Nevertheless, at the time of the installation of the site, it was thought that because of its small dimensions the aquifer in Wilerwald could be considered ideal for analytical modelling. This meant that it was supposed:
- homogeneous,
- of almost constant depth,
- with an uniform hydraulic gradient oriented towards North,
- steady-state flow conditions,
- a laminar and uniform flow,
- and with practically no human disturbance.

In short it was thought to possess the ideal characteristics for calibration of flow models and the acquisition of transport parameters.
Soon after the first experiments (**Sansoni,1987**), it became obvious that the heterogeneity was a dominant feature : not only the tracer transport did not correspood to the theoretical predictions, but the results varied a lot from experiment to experiment, making them more difficult to interpret. It was important to discover the reasons of this behaviour and try to improve the modelling techniques. This was initially to be my task.

A model is a simplified version of a real situation ,which is known through a limited number of punctual data. The validity of a model is measured by its capacity to simulate the aquifer's behaviour, and to answer specific events (**Fig. 1**, after **Kiraly, L.,1992**). Despite the progress in modelling techniques, many problems still remain. For example, how should one quantify the different parameters, define of boundary conditions, or the relation between local and regional scales?

Keywords :Porous aquifers, electromagnetics, heterogeneities, anisotropy, piezometry, dyes, isotopes, water chemistry, Swiss Plateau (Wilerwald), Upper Rhine valley (Merdingen,Germany).

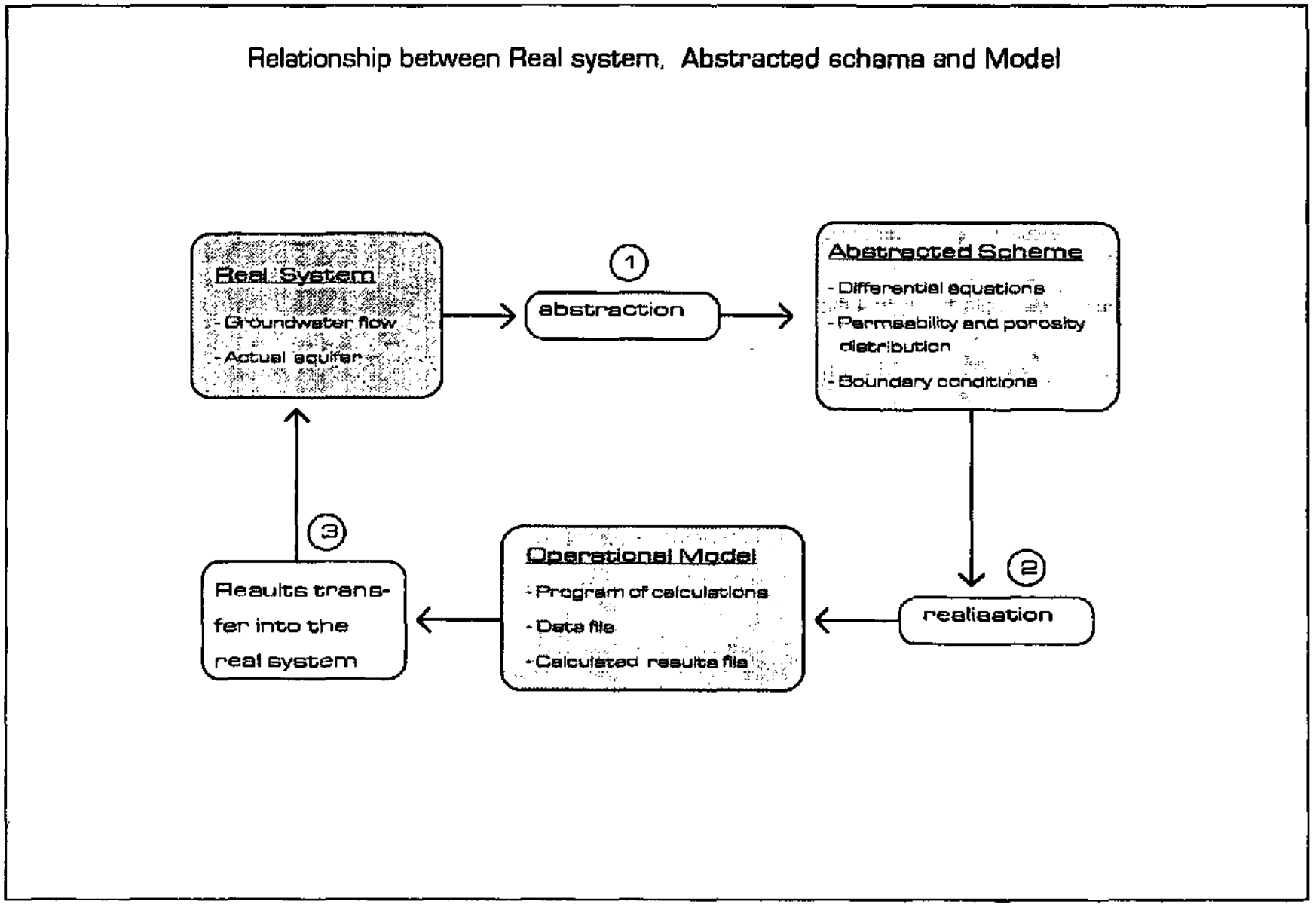

Fig 1.- Relationship between the real world of groundwater systems, abstracted scheme and model.- adapted from L. Kiraly,1992.

To model solute transport a number of steps must be followed (Fig 2):

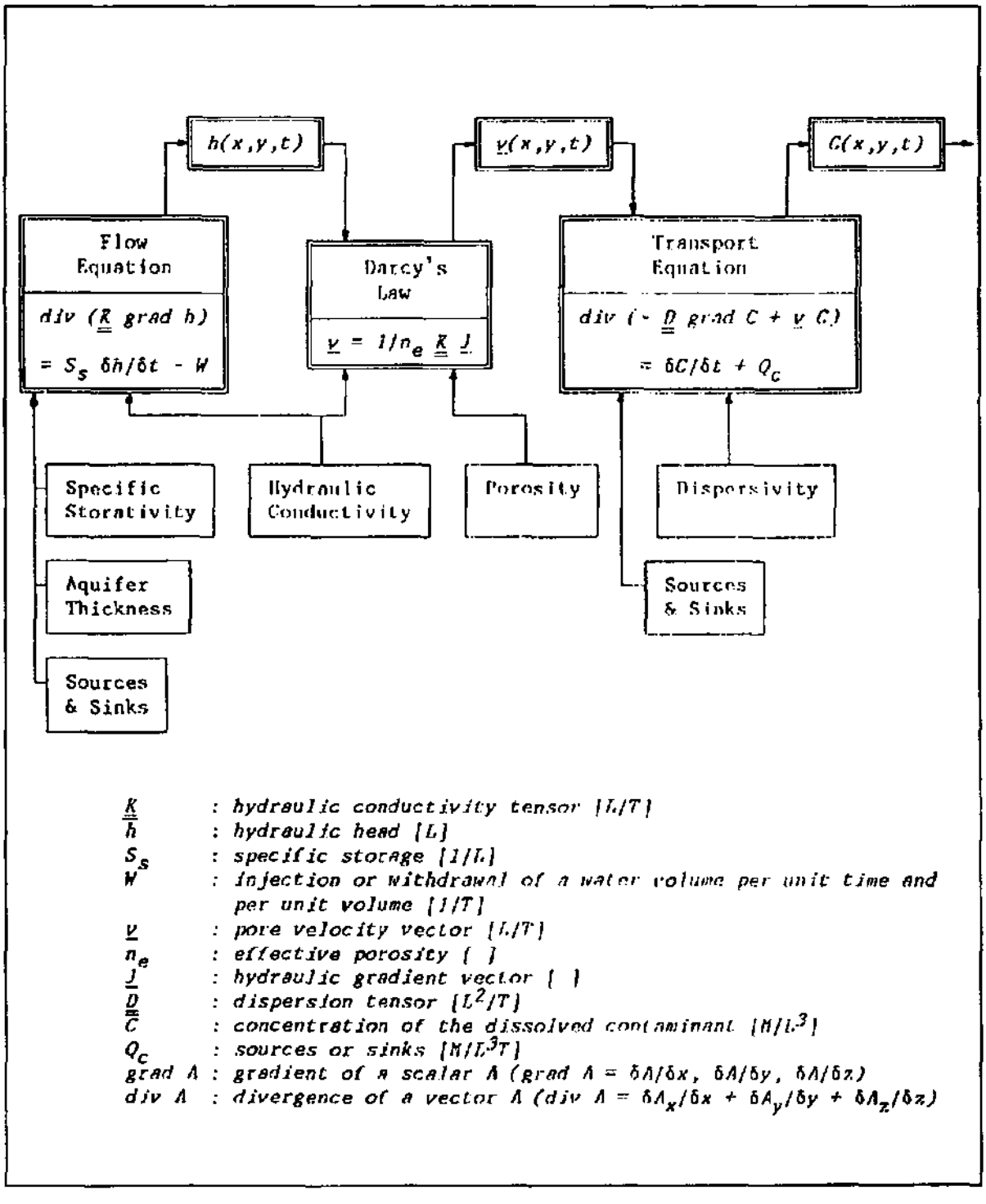

Fig 2.- Organigram showing the main steps to be followed in a transport model (after **Gerlinger, K.** *in* **Carvalho Dill,A. 1992**).

It is clear, that the identificatioo of the aquifer, the degree of its heterogeneity, its structure and individualisation of the main flow directions, constitute the fundamental basis of modelling.

Therefore the aim of this work changed. We now wanted:

1) to determine the actual degree of heterogeneity of this quaternary formation,
2) prove the importance of this factor in the evaluation of hydraulic parameters,
3) its consequences for transport processes,
4) and finally, show the importance of electromagnetical methods for hydrogeology.

1.2 Orientation of this work

Conceptually, local scales require 3-D models which in turn demand a detailed knowledge of the aquifer. This isn't easy to obtain, due to the limitations of field procedures.

Large scale multiwell pumping tests performed in the entire regioo will give vertical and horizootal average values of permeabilities. Single well pumping tests or hydraulic cooductivity tests carried out at the bottom of cased boreholes can give punctual information. These punctual values can be interpolated and used in models to outline regions of equal permeability. This type of ioformatioo did exist beforehand for the area, but wasn't very useful for interpreting tracer experiments where each piezometer showed a totally different breakthrough curve, even those lying only 5 meters apart! (Fig. 58, Chapter 8).

Single well pumping tests were also performed at the Wilerwald testsite (Sansoni et al,1987), so information about the permeability around each piezometer was available, assuming it was correct to suppose that the installation procedure "by penetration" did not compact the particles, thus diminishing the porosity around the piezometers walls.
The results were oot clear enough to explain tracer behaviour, but already pointed out that the local degree of heterogeneity had to be investigated further.

Since the site was designed to reproduce the natural situation of the flow field, the piezometers had small diameters so as to avoid extra convection fluxes within them. This made it impossible to use other hydraulic techniques (such as flow meters), which could have supplied useful information about the vertical distributioo of permeabilities.

Boreholes give direct access to the aquifer, allowing the construction of logs, but their high cost reduces their possibilities of use. Furthermore they give no informatioo about the lateral expansion of a lithological unity. Once again, one is in possession of punctual information, which cannot be easily interpolate.

So, we made use of all the information available about the geology, geomorphology, local and regional experiments. We also used indirect methods like geophysics or obtained punctual information, like ground-resistance to penetration during the installatioo of the observation wells, to try to study the local transport situatioo framed regionally.

The planning and conception of any site should always start with geophysical surveys, which will rapidly give information about the geometry and distributioo of properties of the aquifer. This would then serve as a guide to the best location for the observation network and for the drillings which have to be done.
In Wilerwald the geophysical methods were done after. But they were vital for the significance of this work.

Among all the geophysical methods used, I would like to point out the electromagnetic RMT (radio magnetotellurics) methods, using the prototypes developed at the Centre d'Hydrogeologie de Neuchâtel, (**I. Müller**), and the VLF-EM.
The dense punctual information of the RMT-R, or the permanent recording of the VLF-EM will give a very good picture of the geometry and composition of the aquifer. Contour maps can be drawn, giving a good surface image of the distribution of apparent resistivity. Different profiles were also outlined and average values of true resistivities were calculated and plotted. All this enable us to formulate plausible explanation of the tracer's erratic behaviour in Wilerwald. The RMT-R and VLF-EM methods were also successfully applied at the Merdingen testsite in Germany (Chap 9).

Classical Schlumberger soundings were performed, to evaluate the thickness of the upper bed. Situations of confined waters and of free water table were detected, revealing not only one of the features affecting the water level measurements and their interpretation, but also places where rainfall waters can directly recharge the groundwater.

Geology, geomorphology, distribution of discharge and recharge areas, topography, all these factors condition the flow system, and they are all interrelated.
As a consequence, regional flow systems can be devised into intermediate and local systems, with different flow-line patterns. Different residence times of water and consequently different chemical properties, can coexist within the same aquifer and also at the test site scale. So it was also important to perform chemical and isotopes analysis (Physikalisches Institut, Uni Bern).

This work is divided in 5 Parts. The first part is merely descriptive. It includes the introduction (Chapter 1) and the presentation of the test site within its regional frame (Chapter 2). The second part refers more specifically to the works performed regionally (Ch. 3). The third deals with the works carried out at the test-site scale (Ch.4, 5 , 6, 7 & 8). In the next part the results of the electromagnetic surveys made at the German test site Merdingen are discussed separately (Ch.9). As this site is also a porous aquifer, they are interesting for comparison. The fifth part contains the final conclusions. A resume of the principles of the electromagnetical methods used and the kriging can be found in the Appendix, at the end of this volume. A very detailed description of tracers and measuring techniques can be found in Geohydrologische Markierungstechnik (Käss,1992). For the flow and solute transport equations in porous media, the following authors are indicated: **Freeze & Cherry,1979; de Marsily,1981; Wang & Anderson,1982; Kiraly,1985&1992; Dagan,1989; Klotz et al,1988; Maloszewski P.,1981; Cameron, D. R., Klute, A. ,1977; Bear,1979; Kinzelbach,W.,1986.**

2. Presentation of the test site Wilerwald

2.1 Wilerwald: geographic location and site description

The Wilerwald test site is located 6 Km south of Solothurn, on the edge of the forest surrounding Wiler b. Utzenstorf (Canton Bern) (**Fig. 3**).

The place was judiciously selected (**Sansoni, Schudel & Wagner, 1987**), so as to dispose of an optimal test field representing the Swiss Central Plateau aquifers while at the same time meeting the border conditions required by analytical models, among others:

- a non confined groundwater,
- a relation of width to length of over 1:3,
- a depth of the aquifer of less than 15 m,
- stable flow conditions.

Good accessibility, a depth of the groundwater table of less than 5m (pumping problems may occur if it is deeper than 5m), a hydraulic conductivity between 10^{-2} and 10^{-3} m/s, isotropy and homogeneity and no human disturbance completed the criteria, and Wilerwald was thought to fulfill them best.

After a pilot tracer test, twenty-one observation wells and an injection well were installed in three half-circles (C, D and F) oriented towards the main water flow (**Fig. 3**).

The wells, 1 1/2 inch in diameter and covering the whole aquifer thickness, were conceived in order to enable water sampling at 3 different levels: 5, 8 and 11 m, with the help of an automatic sampling device (**Sansoni et all,1987**). Its conception can be seen in **Fig. 4**.

One borehole for the sedimentological characterization of the substrate was drilled in 1988, increasing the number of observation wells. Finally, six piezometers (**Fig. 3**) were installed in May 1992, exclusively for measurements of the groundwater level, in anticipation of their possible use in a numeric model.

2.2 Regional geology and hydrogeology - previous works

The Wilerwald test site lies in the large Emme valley.The aquifer (**Fig. 5**) is situated south of Gerlafingen between Oberburg and the Bern/Solothurn cantonal border, in the region called "Unteres Emmental" (**WEA, 1981**). It is extremely heterogeneous and anisotropic.

This aquifer consists of gravels, sometimes clean, sometimes sandy but only rarely silty and containing a variable proportion of pebbles, cobbles and even boulders. They can be differentiated into 3 units :

- Holocene sandy gravels (post-glacial Emmeschotter q_s);
- Würm sandy gravels ("Vorstossschotter" **q4vsB** and **q4vsW**);
- Pre-Würm sandy gravels ("Ältere Emmeschotter", **q3s-4s**).

In general it is a very permeable formation, with a widely variable thickness (from a few meters up to 50 m). Its composition, structure and properties vary laterally and vertically very quickly, thus reflecting its geographical situation (the floodplain of the actual river Emme, a sedimentary basin of the Alpine foreland in the Swiss Central Plateau) and its quaternary genesis, with continuous alternation of erosion/sedimentation cycles.

According to Wanner (1981), (in Grundlagen für die siedlungswasserwirtschaftliche Planung des Kantons Bern, Teil III, Wasser- und Energie Wirtschaftsamt des Kantons Bern, (WEA)), the aquifer is composed of 40 to 60% quartzite, 30 to 50% Flysch and calcareous sandstones and 5 to 15% crystalline rocks.

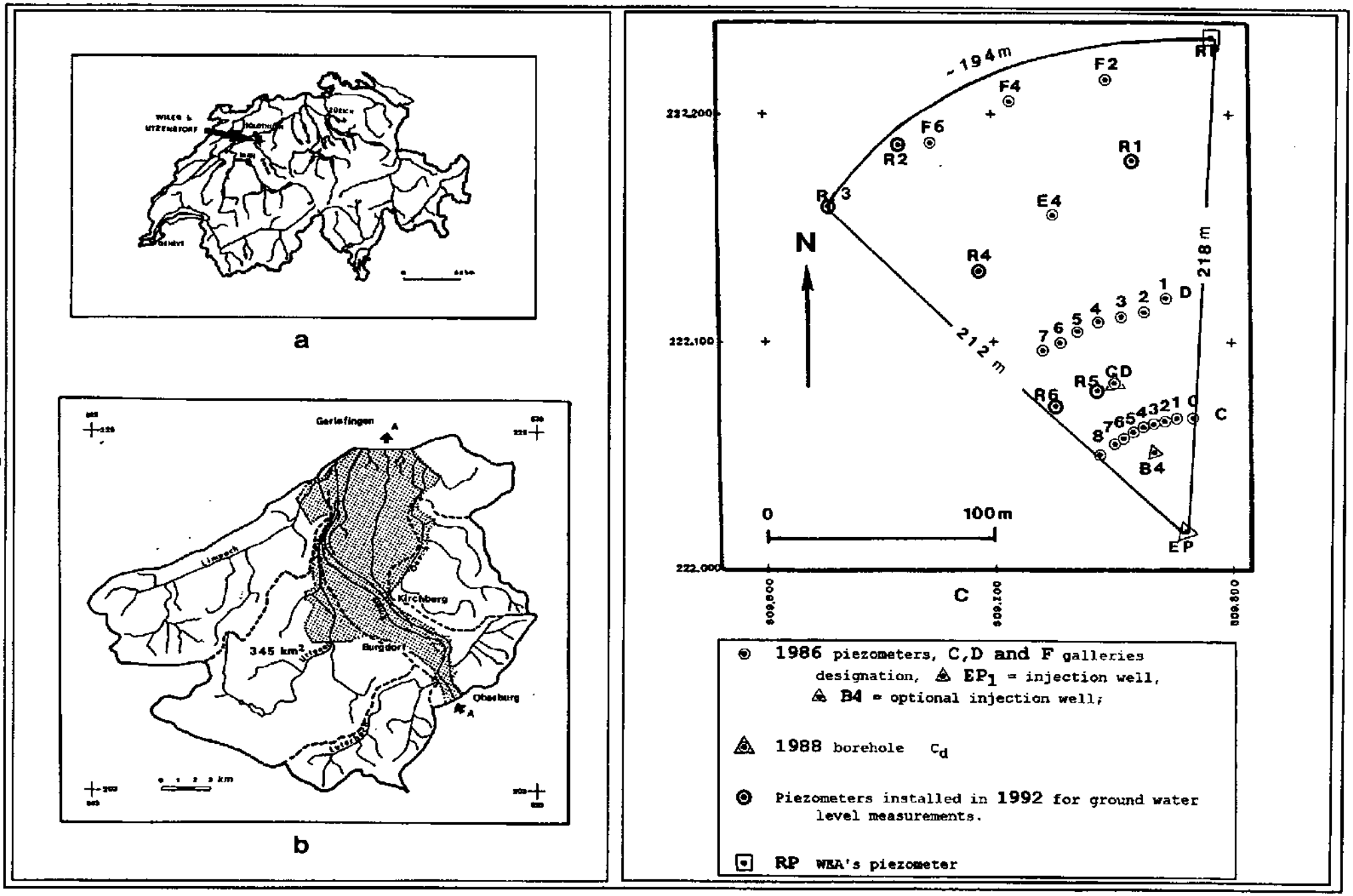

Fig. 3 Location of the Wilerwald testsite - Swiss map (a); limits of the aquifer and limits of the catchment basin (b) and the Wilerwald testsite showing the disposition of the piezometers in three half- circulated ranges (c).

The aquifer is covered by alluvial sediments, made up of sand, silt, gravel and clay in varying proportions, and sometimes by moraine relics. It overlays a very irregular Miocene surface of impervious mollassic marls m_1 (Aquitanian), intensely eroded at some points (Fig. 5). This stratum functions as an aquitard.

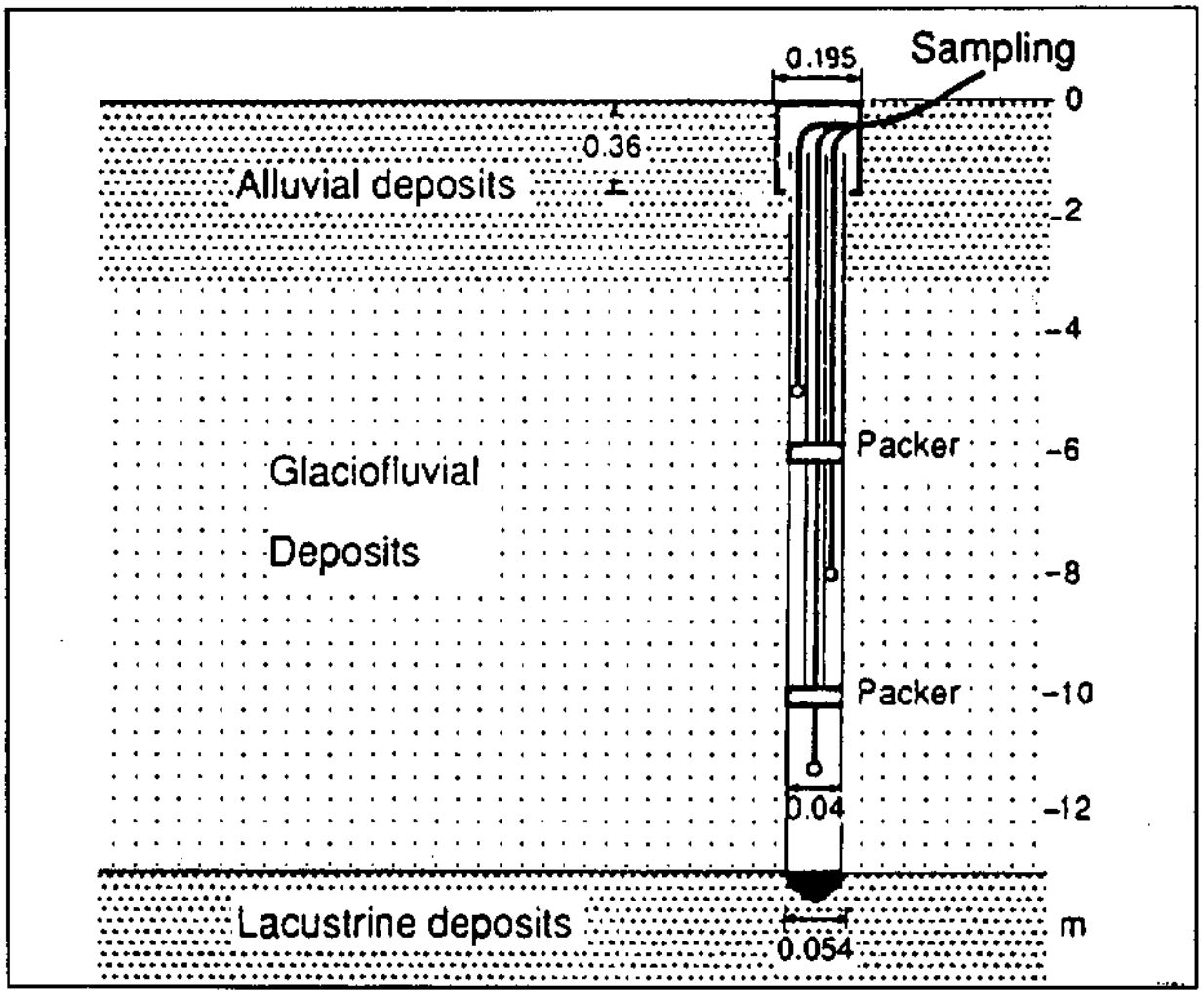

Fig. 4: Vertical section showing a piezometer driven into the soil, and its division system, for the sampling at three levels (5, 8 and 11 m) after Sansoni, Schudel & Wagner, (figure extracted from **Leibnndgut Ch., 1992**).

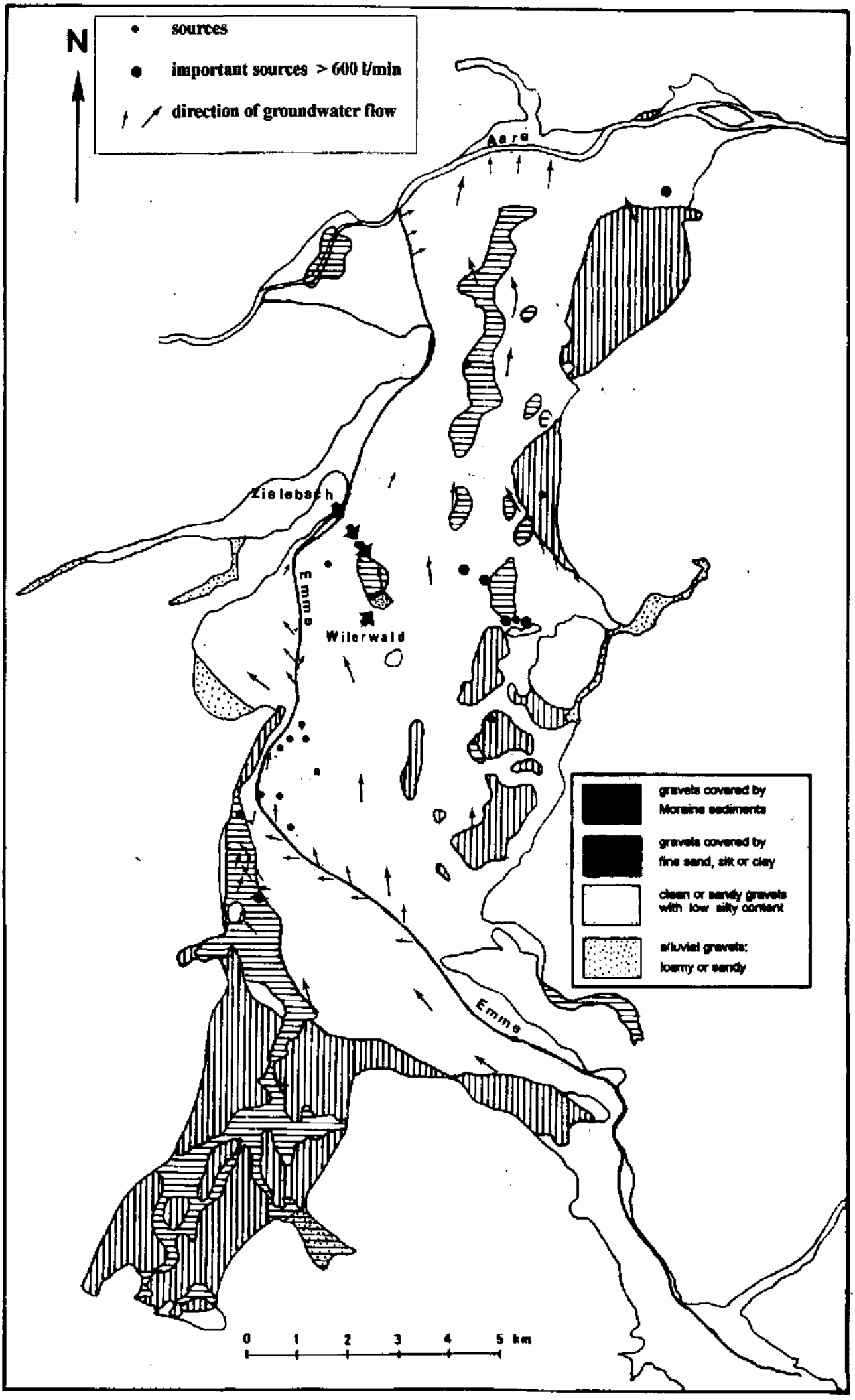

Fig. 5.- Simplified hydrogeological map, with a representation of the aquifer and its overlying deposits and with the inventory of springs and wells of the "Unteres Emmental" region.

Some moraine relics may exist, interspersed between the Aquitanian and Holocene gravels, (q4mW, q4mB), and the lacustrioe sediments (q4r). The thickness of the lacustrine sediments may even reach circa 75 meters. These formations act as aquitards too.

The lateral limits of the aquifer are well established in the regions where it adjoins the molasse. Difficulties in delimiting areas occur at the junctioos with the tributaries (Oesch, Limpach, Urtenen and Luterbach) and when moraine deposits border the aquifer (as in the case of South Burgdorf).

The **Fig. 3** shows also the limits catchment basin of about 347 km^2 (after **WEA**), and those of the aquifer in the area called Unteres Emmental, covering a surface of about 74 km^2.

The following figure (**Fig. 6**) and **Table 1**, taken from **WEA (1981)**, resume the maio characteristics of the units found in the "Uoteres Emmental":

Designation	Age	Geological Unity	Lithology	Hydraulic Function
a		alluvial deposits	Silt,Sand, gravel and clay	covering deposits
gs		suspension debris	Silt,Sand, gravel and pebbles	Origin of local sources
qs	Würm	Emme's gravels	gravels and sand	aquifer
q4mB q4mW		Würm's moraine	pebbles,gravels, sand and silt	covering deposits on hills, aquitard in the depressions
q4vsB q4vsW		Vorstossschotter	gravels and sand	aquifer
q4r		lacustrine sediments	sand, silt, clay	aquitard
q4l		Stauletten	sand, silt, clay	local aquitard
q4st		Stauschotter	gravels and sand	local aquifer
q3s-4s	Pre-Würm	Emme's older gravels	gravels and sand	aquifer
m2	Miocene	Burdigalian	sand, silt, marls	aquitard
m1		Aquitanian		

Table 1 Main units found in the Unteres Emmental (WEA):

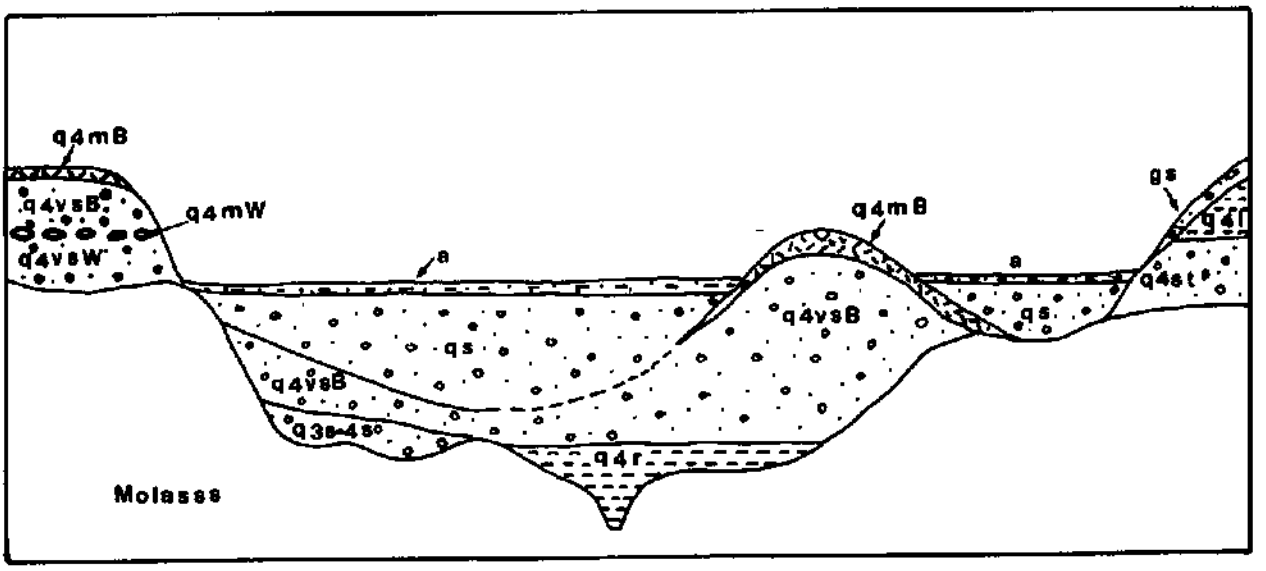

Fig. 6 Schematic profile representing the quaternary sediments found in the Emme Valley, after WEA (1981).

The following aquifer parameters were also calculated (after WEA):

Geological unity	Designation	Permeability (10^{-3} m/s)	Storativity %
Post glacial Emme gravel	qs	6 - 20	7 - 14
Vorstossschotter	q4v	1 - 4	5 - 10
Moraine	q4m	ca.0,8	5 - 9
suspensions debris	gs		1 - 6
alluvial deposits	a		1 - 6

Table 2 Hydrological caracterisation of the geological unities

A permeability map (WEA) with the location of Wilerwald can be seen in **Appendix 2. B (Fig 2B-1).**

The groundwater is renewed by precipitation waters, as well as by the infiltrated waters of the Emme and lateral rivers. Studies carried out in the area and published by WEA, show the important contribution of the Emme to the renewal of the groundwater stock. The Emme water predominantly infiltrates the central part of the aquifer (Burgdorf-Schalunen). It has a beneficial dilution effect, counterbalancing the increase in pollution due to the infiltration of rainwater in regions where soils are intensely cultivated.

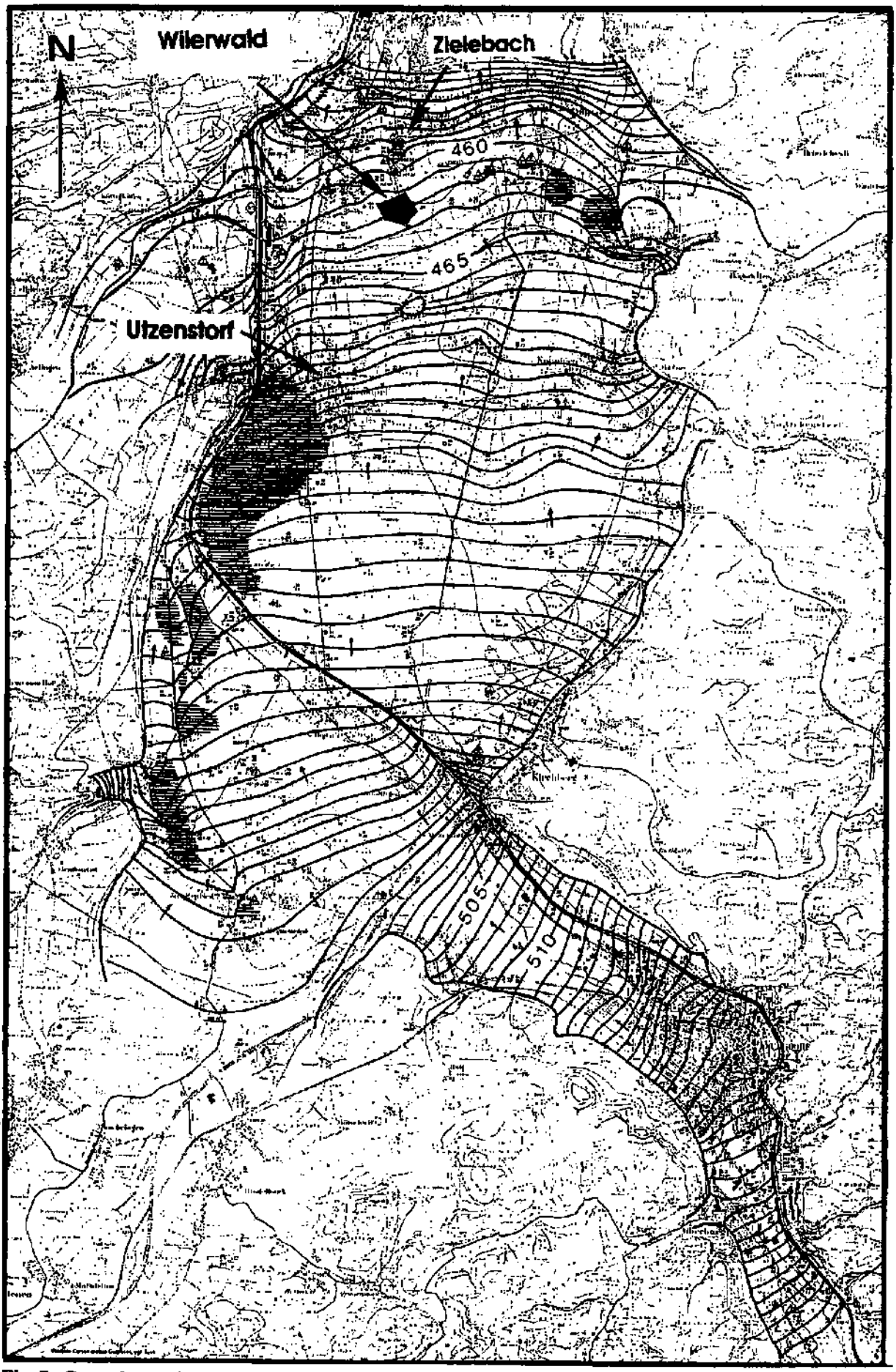

Fig. 7 Ground water isohypsen map, 1981 (WEA)

Small rivers and channels can also infiltrate the aquifer, but their contribution is rather small as they predominantly exfiltrate.
The figure above (Fig. 7) shows the exfiltration areas by means of straight parallel lines, also corresponding to regions where the isolines are closer. One of these areas, 500 m north of the Wilerwald test site, is at the origin of the Zielebach, a small tributary of the Emme.
The groundwater isohypsen map also shows irregularities in the spacing of the contour isolines. Besides the reasons referred to just above, it is known from the literature that many other situations can be at the origin of the smaller spacing of the isolines. If we are in the presence of a *free nappe*, this can be due to:

- the elevation of the aquifer substratum,
- the proximity of a river or stream, or
- to the passage to a less permeable medium.

If instead, one is in presence of a *confined aquifer* the following reasons can than play a role:

- a decrease of the aquifer thickness (because of the enlargement of the upper layer),
- or also the passage to a less permeable medium.

The variety of possible situations is huge in a heterogeneous medium. So this subject will indirectly be rediscussed in Chapter 3.

2.3 Local characterization and previous works

2.3.1 General aspects

The aquifer at Wilerwald was thought to consist of post-glacial Holoceoe sandy gravels, interspersed between alluvial sediments of low permeability and lacustrine sediments of variable thickness.
From the description of two boreholes (Wilerwald WIB01 [609520/222425], 500m distant, and Burgerwald WAB21 [610490/221440], 900 m distant), and the map of aquifer thicknesses (**WEA, 1981**), **Sansooi et al. (1987)** assumed that the thickness of the aquifer was quite regular (approximately 15 m), and that its hydraulic gradient decreased uniformely in direction of the north. Furthermore, it was assumed that the small dimensions of the test area meant it would be relatively homogeneous, although the opposite was already known to be true regionally. In fact, an error of scale was made.

The groundwater level lay at about -3 ± 0.5 m, with a northward gradient of about i = 4 $^{0}/_{00}$ (**Sansoni et al,1987**).

The construction of the piezometric map (1986) showed that this assumption wasn't totally correct, because some irregularities were found in the isohypsen map (**Fig. 8**). These irregulatrities were thought to be measurements errors and therefore ommited (**Sansoni et al,1987**), (see **Appendix 3. B, - Fig. 3B-1**).

Small-well pumping tests were carried out at Wilerwald (**Sansooi et al.,1987**). Because of the small diameter of the holes, 1 inch tubes were used, for maximal pumping rates of 100 to 110 l/min. The method used is described in **SNF (1984,)**. The pumping was performed in two steps: first was at the maximal discharge rate till the water level stabilized. Than the discharge was reduced approximately by half, till a second plateau was reached. Shortly after this, the pumping test was stopped. With the discharge, the head variation, the mean aquifer thickness, and the piezometer's radius and length, the following permeabilities were calculated, using the method described in **SNF (1984,)**. Therefore, some information about the permeability around each piezometer did exist, if one was ready to accept the assumption that the installation procedure by penetration did not compact the particles, which would have diminished the porosity around the walls of the piezometers.
These results were nevertheless insufficient to explain tracer behaviour, but already pointed out that the local degree of heterogeneity had to be investigated further.

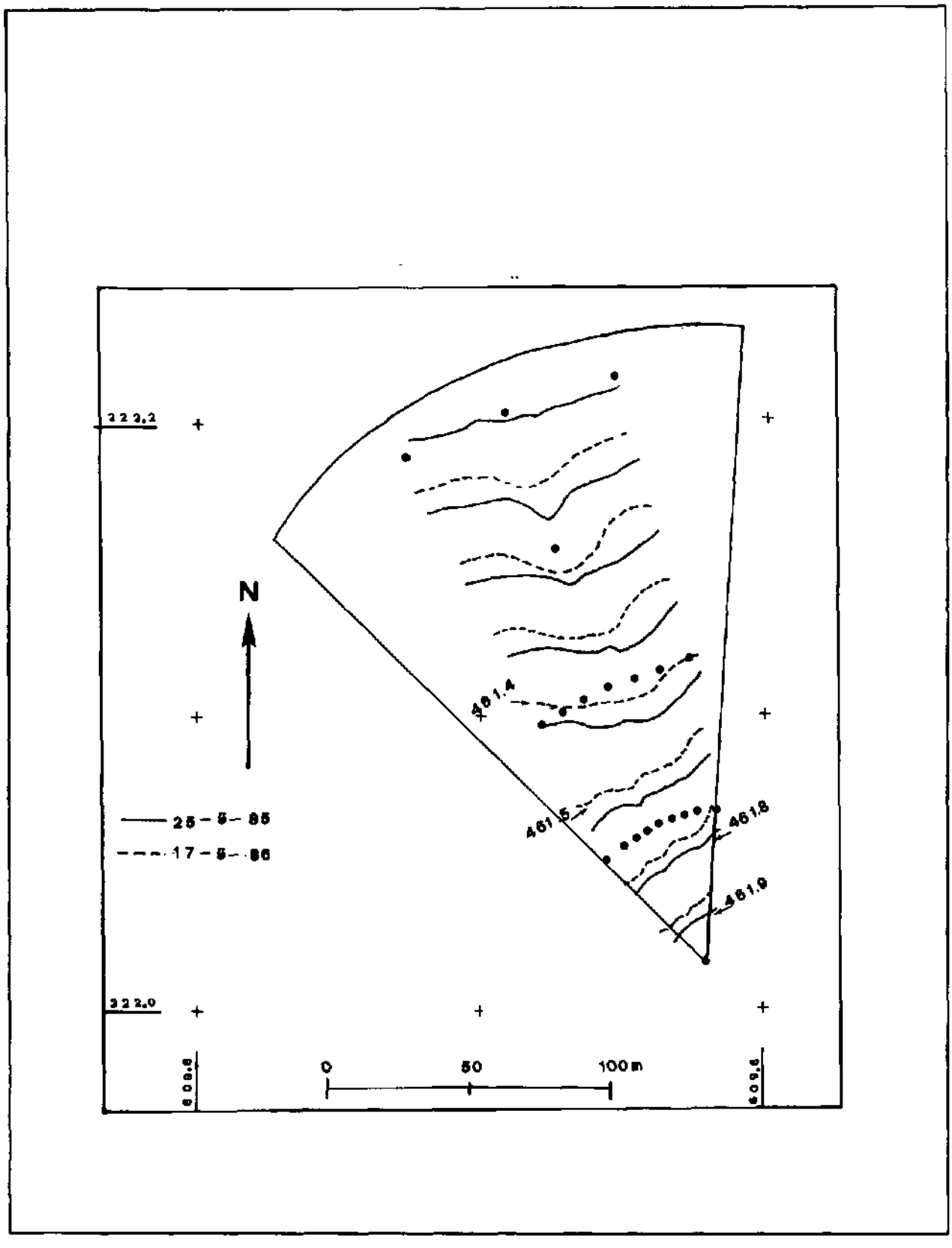

Fig. 8 1986 Piezometric map : indicating the main direction of flow towards NW and existence of small irregularities on the isohypsen, an indicator of heterogeneity.

The **Table 3** resumes the maio parameters that were calculated by **Sansooi et al. (1987)** for the aquifer. One must be aware that these authors concluded that the thickness of the aquifer was relatively constant over its whole area, a fact which the RMT-R and VLF-EM results did not confirm, since they revealed the existence of a paleochennal. It is probable that the driving in of the observation wells was halted whenever a sub-layer of finer material was reached, because of the information given by the literature.

The small diameters of the piezometers made it difficult to use other hydraulic techniques, such as flow meters, which could have given information about the vertical distribution of permeabilities.
After the pilot tracer-test, Sansoni et al. assumed for their modelling that the aquifer consisted of three distinct flow domains of constant thickness and specific hydraulic properties **(Maloszewski, 1981)**. So, they built the special sampling apparatus for collecting samples at three different depths that has already been described in **Fig. 4**.

Obs. wells designation	Coordinates		Thickness	Transmissivity		Permeability
	X	Y	[m]	[m2/s]	[m2/d]	[m/s]
EP1	609.781	222.017	9.31	5.78E-02	4995	6.21E-03
C0	609.783	222.066	9.75	4.33E-03	374	4.44E-04
C1	609.776	222.066	11.61	3.02E-02	2608	2.60E-03
C2	609.770	222.065	9.38	2.94E-02	2537	3.13E-03
C3	609.766	222.064	7.76	3.73E-01	32249	4.81E-02
C4	609.761	222.062	9.38	6.52E-02	5633	6.95E-03
C5	609.757	222.060	9.79	2.42E-02	2089	2.47E-03
C6	609.753	222.057	9.67	1.21E-01	10444	1.25E-02
C7	609.749	222.053	9.35	2.02E-02	1745	2.16E-03
C8	609.744	222.050	9.82	1.97E-02	1705	2.01E-03
CD (*)	609.749	222.083	11.00	1.74E-02	1503	1.59E-03
D7	609.720	222.095	9.77	2.54E-02	2195	2.60E-03
D6	609.727	222.099	9.86	2.53E-02	2189	2.57E-03
D5	609.734	222.104	11.53	1.35E-02	1166	1.17E-03
D4	609.743	222.109	9.88	7.71E-03	666	7.80E-04
D3	609.753	222.111	10	7.99E-03	690	7.99E-04
D2	609.762	222.113	9.95	6.23E-03	538	6.26E-04
D1	609.771	222.120	9.94	4.58E-03	396	4.61E-04
E4	609.724	222.155	13.99	3.06E-02	2647	2.19E-03
F2	609.746	222.210	10.35	4.20E-03	363	4.06E-04
F4	609.704	222.203	10.42	6.25E-03	540	6.00E-04
F6	609.669	222.186	10.29	1.69E-02	1458	1.64E-03

(*) determined in 1992 under the same method

Table 3: Hydraulic parameters determined by Sansoni et al, 1987.

The chemical composition indicated the water was hard. Table 4 shows some chemical data of Wilerwald water (Sansoni et al, 1987; Mägdefessel,J., 1990):

Parameter	Holzacker*	EP1
Total Hardness [^{0} f]	27.8	28.6
Carbonate hardness [^{0} f]	24.7	24.6
Ca^{2+} [mg/l]	104.6	-
Mg^{2+} [mg/l]	4.2	-
Cl^- [mg/l]	9	12.9
NO_3^- [mg/l]	21	-
SO_4^- [mg/l]	12	14.6
NO_2^- [mg/l]	< 0.0005	-
NH_4^+ [mg/l]	< 0.05	-
conductivity [µS/cm]	480	545
pH	7.14	7.2-7.3
Bakteriology	acceptable	-
* 200 SW EP1-drinking water - not performed		

Table 4: Chemical analyses performed at the test site Wilerwald

2.3.2 Tracer tests

A preliminary test was done in May 1986 in order to verify the assumptions made regarding the direction of groundwater flow and the flow velocity.
0,3 kg of uranine and 6 kg of naphtionate diluted in 70 l of water were injected simultaneously into the well EP1. The main direction of transport was thought to pass between C4 and C5, with the quickest arrival of the tracer at C4 and the bulk tracer transport at C5.
The horizontal and vertical heterogeneity was suggested by the considerable differences in the concentration distribution at each well and at different depths.

In the main test, the same authors wanted to compare uranine and naphtionate behaviour in field conditions, and at the same time study aquifer parameters. 1 kg of uranine and 20 kg of naphtionate dissolved in 90 l of water were injected into each of the assumed layers of the aquifer. The mixed tracer solution was injected simultaneously at the sampling levels of 5, 8 and 11 m (levels of the presumed layers) over a period of one hour (Leibundgut, 1992).

The assumption of a constant thickness and permeability for these three layers which would then result in layer-specific flow and transport was evidently wrong: the results of both tracers showed irregularly localized differences, not only between the piezometers, but also vertically. (Leibundgut 1992).

Furthermore, the tracer uranine and the results from -11 m were singled out for the following conclusions:

- They observed that the maximal concentrations occurred in the direction of C4, C5, C6, D5 and D6, while in the F range there was no significant maximum, presumably because the piezometers did not catch the principal direction of flow.
- they noticed in the east part of the field, namely in the D gallery, a remarkable delay in the flowing off of the tracer, with the occurrence of relatively high concentrations even after 30 days.
- they concluded that the direction of water flow was situated between C4 and C5 and between D4 and D5.

Mean values of the aquifer parameters, of the coefficient of dispersion, and dispersivity, as well as a comparison between both tracers can be found in Sansoni et al (1987). The utility of this information is rather questionable, considering the absence of foundations for their hypothesis and the complexity of the field.

2.3.3 Interpretatinn of tracer tests : modelling essays - Sansoni (1988) and Schneider (1991)

Initialty the Wilerwald test site was intended as a full-scale laboratory. In order words, an aquifer whose parameters were very well known, where different experiments using all kinds of tracers could be carried out, an ideal site whose border conditions corresponded perfectly to those needed when using analytical models.

After the first series of experiments, the authors (**Sansoni et al, 1988**) idealized the aquifer, dividing it into three distinct layers of constant thickness and specific hydraulic conductivities. The samples were taken at three levels and they modelled the data obtained correspondingly: the curve for each level was interpreted separately, assuming that the tracer flowed independently in three distinct layers (flow domains) with constant and individual transport parameters.

Three years later, **J. Schneider** (*in* **Leibundgut et al, 1992**) re-analised the experiment and criticised its authors for having by their pre-suppositions excluded the possibility of vertical changes of conductivity within each layer. She proposed another analytical model, with no predefined number or thicknesses of the layers. Instead, she assumed that if a tracer curve exhibited several peaks, each could be interpreted as a flow through a distinct but approximately parallel layers. Using the analytical solution developed by **Zuber (1974)**, she came however to a similar conclusion as Sansoni et al, namely the existence of three layers. She admitted nevertheless that her solutions should only be considered as approximations of the real situation.

The solution of an analytical model can only be formulated after having made some simplifying assumptions, in general very restrictive : it is usually necessary to postulate that the medium is homogeneous and isotropic, with a parallel flow of constant velocity, steady-state conditions and simple boundary conditions (infinite or semiinfinite media).

Wilerwald is anything but homogeneous, in all its aspects. In the course of this work, we discovered the existence of lenses of different material. It is therefore erroneous to speak of continuous layers. Instead the aquifer is composed of different pockets, containing varying proportions of finer sediments, and of paleochennals of virtually clean gravels. One observes situations where the aquifer seems to be confined or semi-confined , and others of free nappe. Different and constanlly changing hydraulic gradients exist within the site. The hydraulic mechanisms are therefore still far from understood.

It is always possible to create a model from a set of data. The validity of the model is another question. It is essential to start by investigating in depth the aquifer, its geometry, properties distribution and its hydraulic mechanisms. This is the subject of the following pages.

Part II : Regional studies

3. Regional studies

3.1 Identification and geometry of the aquifer

3.1.1 Literature Overview

3.1.2 Very Low Frequency Electromagnetic Surveys

3.1.3 Audio-Magneto-Tellury

3.2 Hydrodynamic aspects: piezometric observations

3.3 Hydrochemistry

3.4 Synthesis and conclusions

3. Regional studies

The aquifer has already been preseoted in general terms in Chapter 2, and its complexity discussed. In this chapter we will start by focusing on this regional aspect, with some investigation into the literature available (description of some boreholes), and of an electromagnetic survey (VLF-EM). After having examined the ideotification and geometry of the aquifer, hydrodynamic aspects will be discussed with the interpretation of daily observations of the water table evolution. Finally, some hydrochemical maps found in the literature which were considered relevant will be briefly mentioned (**WEA, 1981**).

3.1 Identification and geometry of the aquifer.

3.1.1 Literature overview

The principle units found in the Uoteres Emmental are manifold, as was shown in **Table 1.**
Those units that can constitute aquifers are the ones designated as **qs** (post-Wurmian Emme gravels), **q4vsB** and **q4vsW** (Wurmian gravels and sand, with the technical Swiss German name of Vorstossschotter), **q4st** (Wurmian gravels and sand known as Stauschotter) and finally **q3s-4s** (pre-Wurmian older Emme gravels). The permeability varies accordingly, the **qs** unit being much more permeable than the Vorstossschotter.

Considering this complexity, we thought it of interest to show two profiles surrounding the Wilerwald test site (**Fig. 9**). These profiles were adapted from **WEA (1981, vol III)**. The boreholes which were used to delimit them are also outlined. Because of the heterogeneity of the zone, they are obviously insufficient to allow conclusions about the geometry of the aquifer. So the information derived from these profiles may be erroneous and must be treated with caution. Nevertheless, they show the geological units referred to above and the extremely diverse development of these formations.

We thought instead that the presentation of single boreholes was much more suitable. Foreseeing their later use in the hydrodynamic studies, we represented only the boreholes of the **WEA** observation wells (**Fig. 10**). One observes that sometimes one is in presence of more than one sub-aquifer, (from the lithological point of view), as in the boreholes WAB 06, WAB 23, WAB 57. The unit designated by **qs** (Emme's gravels) is of irregular thickness, and sometimes is inexistant as in WAB 25, near the Oesch river.
The Molasse (m_1) is not always reached, such as in WAB 21 and WAB 23. Instead, WAB 21 and WAB 65 have the greatest development in **q4r**, the lacustrine unity, which acts as aquitard too. The groundwater level is also represented in each borehole core, revealing situations of free nappe (the great majority) and of confined aquifer (as by WAB 25 and WAB 57).

Also from the **WEA** is the Map representing the aquifer thicknesses (**Fig. 11**). This Map was responsible for the mistaken idea that the aquifer thickness was of about 10 meters at Wilerwald and at the site of implantation of the observation wells. It also provided a basis for the modelisatioo works done later on. And although the number of boreholes is not that small, if one considers the whole area they are however insufficient, in view of its heterogeneity. The information from this map should be used in parallel with geophysical surveys, such as those methods which don't homogeneize the medium and whose density of information is high : VLF-EM (Very Low Frequency - Electromagnetic Survey) and RMT-R (Radio-Magneto-Tellury).

3.1.2 Very Low Frequency - Electromagnetic Survey

Very Low Frequency - Electromagnetic survey was performed surrounding and southwards the Wilerwald test site. It was our purpose to search for preferential ground water pathways and become an image of the regional distribution of heterogeneities.

The continuous recording of the out-of-phase component by the VLF-EM technique was developed by **L Müller** (see **Appendix 1-A**). Its measuring device doesn't need any soil contact, so it was possible to be installed in a car. This allowed us to perform relative long profiles in a short period of time.

We used the fact that the out-of phase component is very sensitive to lateral changes of the electrical conductivity of the ground, in order to become a picture of the aquifer geometry and its filing. We based our

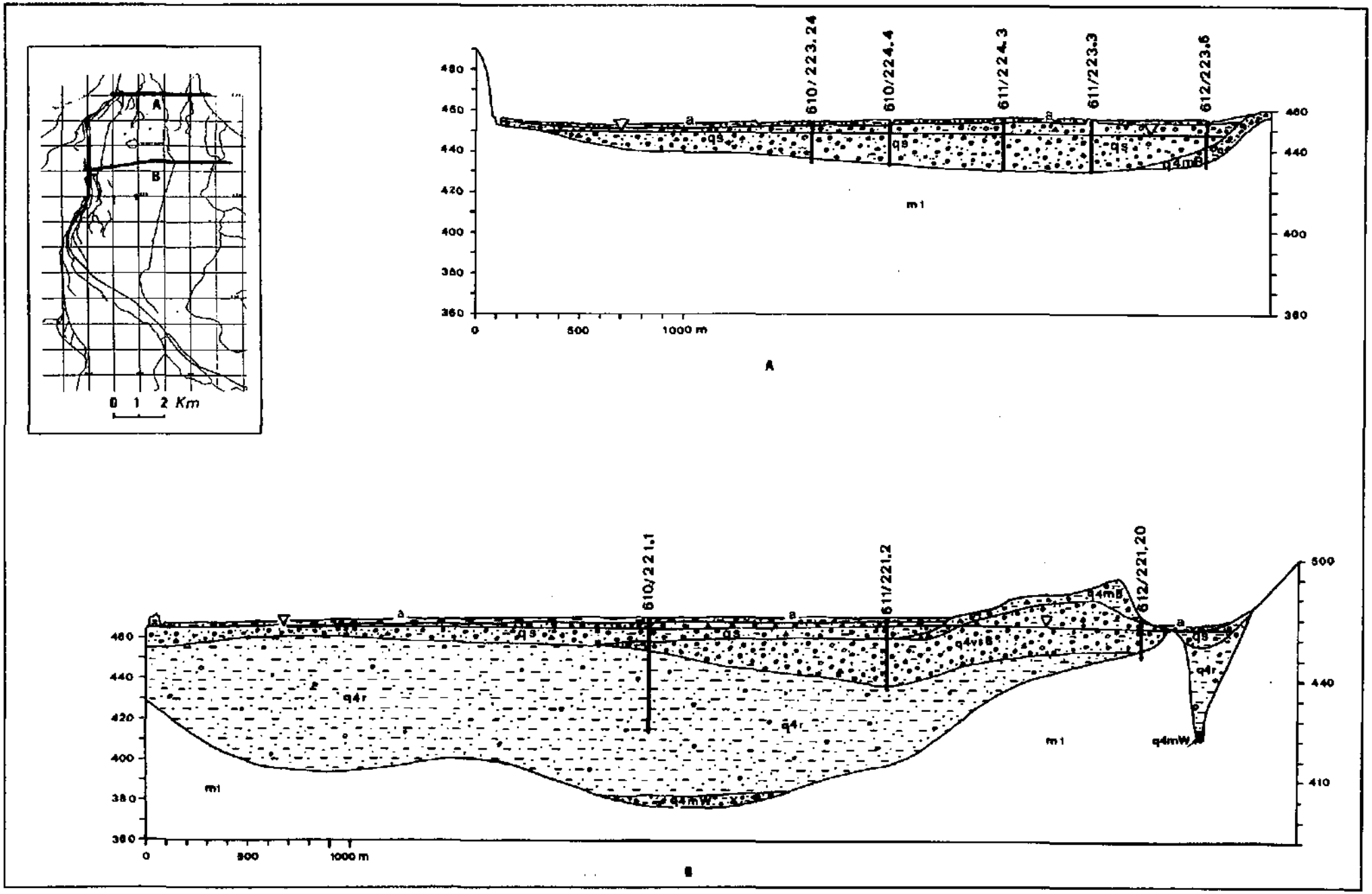

Fig. 9 Two geological profiles (after **WEA, 1981**) surrounding the site, showing the geological units mentioned in the text and the extremely diverse development of these formations (Window : location of the geological profiles and the test site)

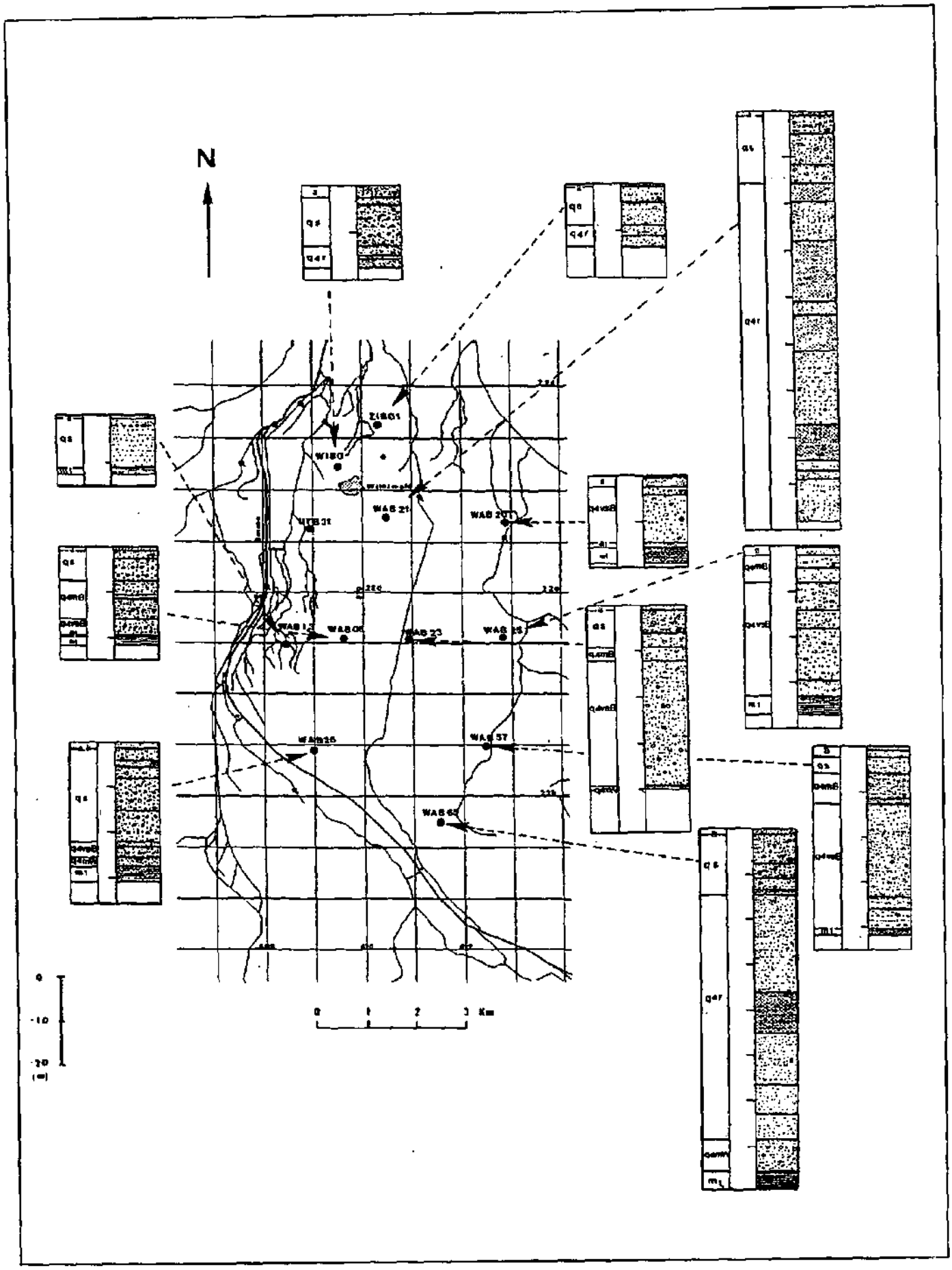

Fig . 10 Regional map with the location of the drill cores of the stations used for 1992 piezometric head level measurements (**WEA**) and drill cores logs (after **WEA, 1981**).

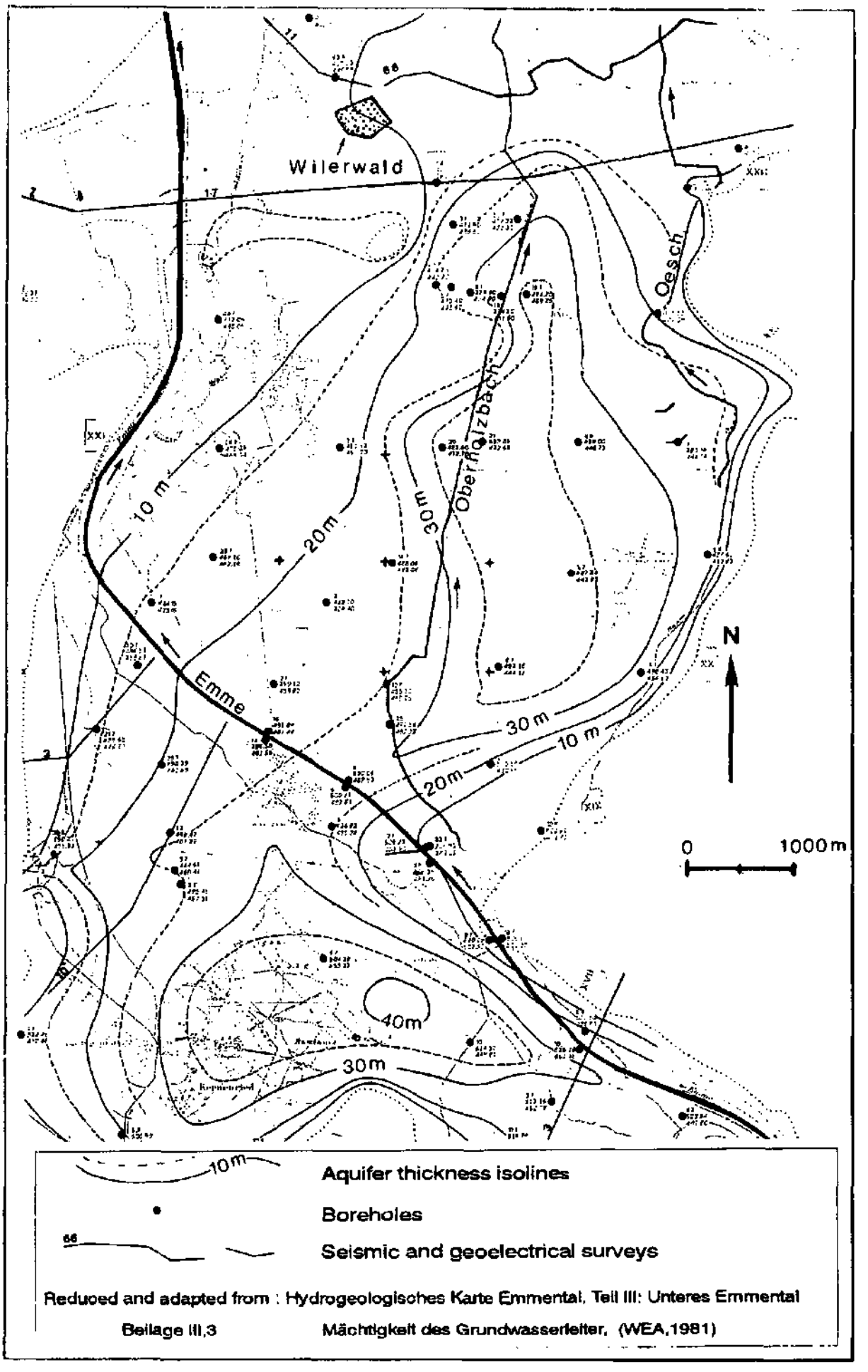

Fig . 11 Map of the isolines of the aquifer thickness **(WEA,1981)**

investigations on the assumption that the good correspondence betweeo VLF-EM profiles and the RMT-R conclusions would continue to exist in the surrounding area.

The next figure (**Fig. 12**) shows the designation and the localisation of the profiles in relation to the test site Wilerwald (shadow area). The map used as a basis is the geological map 1:25000. According to its author (**Ledermaon, 1977**) the Holocene gravels are covered by more than 2 meters of silt and silty clay sediments just northerly from Wilerwald (dotted area). Cover thicknesses of 1 meter were also found and are represented by pointed areas .

Exsurgences are signalised by a . Boreholes referring the molasse depth are plotted as bigger points • . Smaller points • ioclude only the drilling depth, when the molasse wasn't attained.
We can represent the VLF-EM surveys as graphic profiles, or we can create qualitative classes , in order to become a better idea of the regional heterogeneity distribution. **Fig. 13** represents both, the VLF-EM continuous recording of the out-of-phase overlaying a qualitative coloured map of classes, but also the altitude contour line. The limits of these classes seem to suit our purposes but they are quite arbitrary:

1. Values laying between -2 % and +2 %(represented with a white colour) seem to correspond to greater homogeneity. They are more developed in the N/NNE area. When the amplitude of the outphase vertical component has values very close to 0 % , this can be an intlication that a relative homogen region is been investigated, this can mean also that the underlying material has a predominance of fine sediments like the lacustrine silts. This is the case of a regioo located SSE of Wilerwald, as for instance at profile P-12. The description of the borehole Burgerwald, where 65 meters of lacustrine sediments underlay the aquifer, can be seen on the Map of **Fig. 10.**

2. According to test site observation, values situated below -2 % (blue and violet colours), seem to coincide with the presence of cbannels filled with gravels of big dimeosioos. This is the case of profile CD and Profile 11, situated southwards the test site, but mainly at P-19, where the values decrease below -4 %, having a great lateral extension (ancient Emme bed?). This fact could be linked to the existence of a glacial channel described by **J. Wanoer** (*in* **WEA, 1981, vol. III**), which once flowed parallel from Kirchberg in the direction of Koppigen, some kms eastward, because it is thinkable that the Emme did used these glacial pathways directions, at least at the beginning of its installation.
Another feature is remarkable and very important : it is very interesting to notice the correspondence of these paleochannels with the topographic lines. Looking at the lines contour, we can immediately observe that depressions and small valleys are localised in regions with oegative values of the out-of-phase component (high resistivities). This is even more outstanding considering the scale of the map and the fact that the slopes are very smooth. The actual surface is therefore still reflecting the ancieot ground of these paleochannels and these are still today preferential ground water pathways.

3. There are also values situated over + 2 % and + 4 % (brown and green colours). The physical meaniog of these values has to be proofed : it can probably correspond to the existence of areas where the totality of sediments are much finer. Or it maybe due to existence of a covering silty/clay deposits of much greater thicknesses.

It is to accent once more, how the aquifer varies laterally, in the scale of even less than teo meters. This emphasises the strong degree of heterogeneity, and points out how difficult it is to extrapolate any kind of information, if we simply possess a sparse and punctual information, as just some boreholes, without the complementary electromagnetic information.

Fig. 14 exemplifies a trial to interpolate aquifer thicknesses isolines by means of boreholes , in correspondence to the VLF-EM profiles. The picture is eloquent by itself. It is oot compatible the existence of deep paleochannels revealed by the VLF-EM survey, with the existence of a closed basin as it was once interpreted and which is found in WEA hydrogeological Map of the aquifer thickness.

3.1.3 Audio-Magneto-Telluric Survey

The Burgerwald borehole was the second place (the first was Wilerwald) where an AMT survey was performed. The borehole core description indicated a very thick layer (more than 65 m) of lacustrine sediments underlying

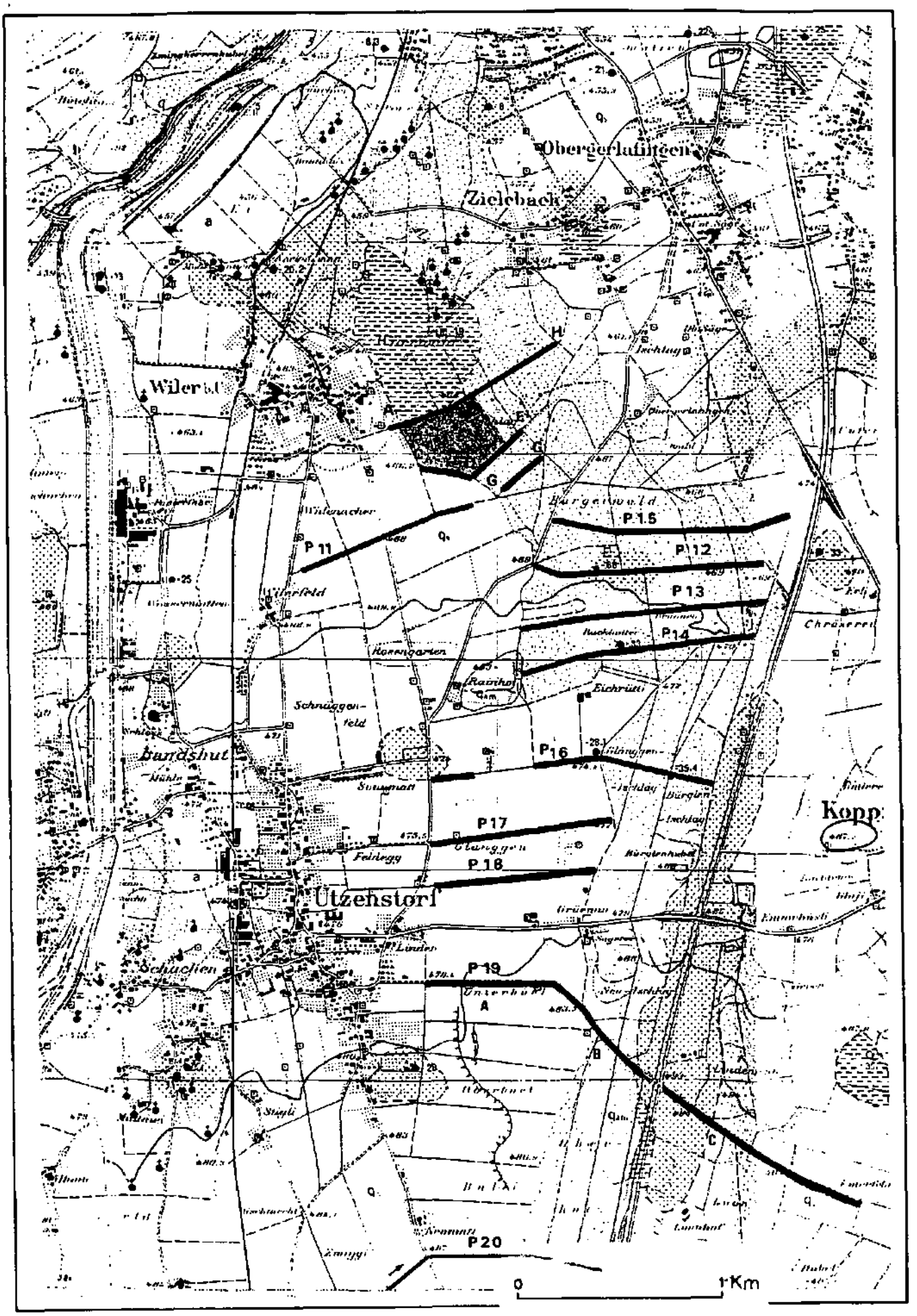

Fig . 12 Location of the VLF-EM profiles. The Wilerwald test site is represented by a shadow area. The map used as a basis is the geological map 1:25 000 (**Ledermann, H., 1977**).

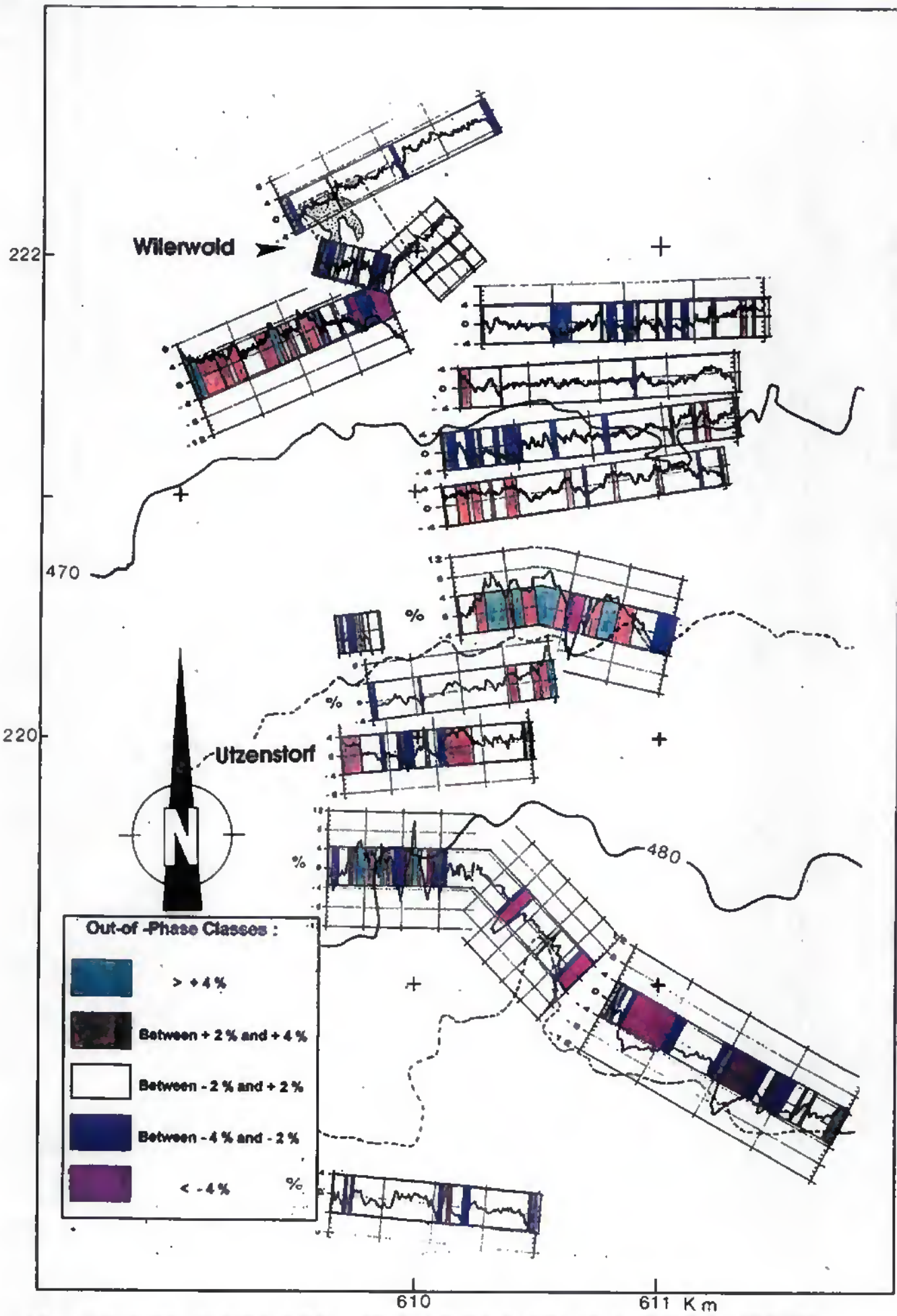

Fig . 13 Representing the graphic profiles, a qualitative division of classes, and the topographic contour lines. The site is represented by a dotted line. Only the paleochannel (chapter 4) is delineated at the site area (pointed area)

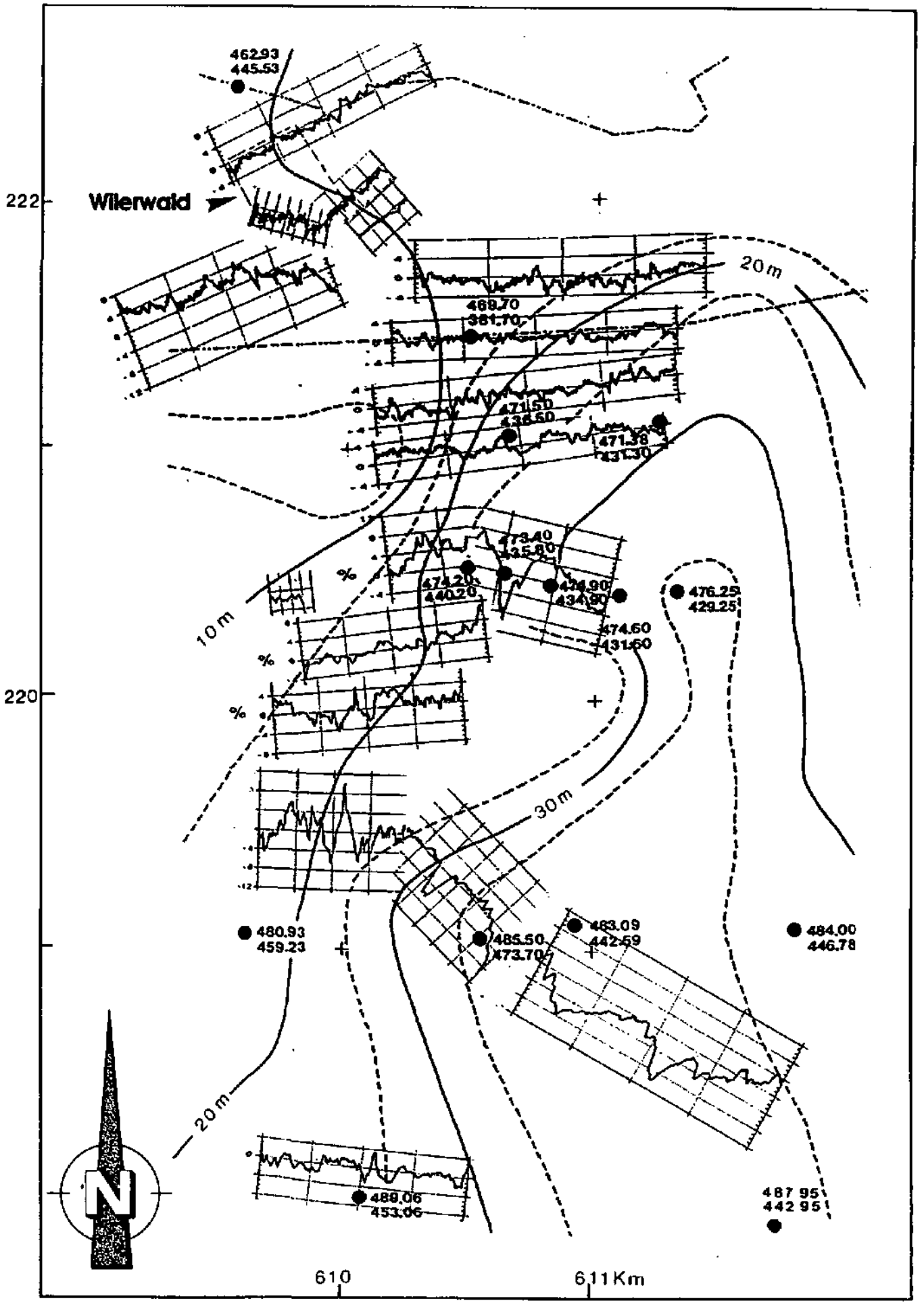

Fig . 14 Aquifer thickness isolines after WEA, 1981 and the VLF-EM profiles, illustrating the danger of interpolation using punctual and scattered information in a heterogeneous formation.

the aquifer. The molasse wasn't reached at depths of about 88 m. The fine sediments, along with the location of the site - far from industrialized areas - were thought to be ideal to test this method, which uses the pertubations of the Earth's natural magnetic field caused by tropical thunderstorms (see **4.1.1.D in chapter 4**, for more information). Nevertheless, the following information must be treated with care, as it is not very accurate because of all the interferences that are possible.
The AMT resistivity log suggests that underneath a thinner and more resistant layer (200 Ohm.m for the first 15 m) there is a relatively thick layer of less resistant material (from 70 Ohm.m to 36 Ohm.m). The Aquitanian could start at -130 m, coinciding to the very low values of resistivity measured there (18 Ohm.m). The same layer was detected at Wilerwald (see **Appendix 2A-1**).

3.2 Hydrodynamic aspects:

Groundwater level measurements were performed at the Wilerwald test site, first sporadically, but then quite intensively during the tracer test of November 1992. The daily changes and their relationship with the location of the observation wells and with the rainfall events observed there were so interesting that we tried to see how the regional net of observation wells responded during the same period and also in the coure of half a year.

One must be aware that the conclusions written below are based on the presuposition that the conditions are the same for all the measurements. That all the observation well tubes are perforated along their whole length, and that mean poteotials are being compared. If this is not the case, and the tubes are only open at their extremities, a variance in measurements depending on the depth of measurement and the heterogeneity may be observed.

The regional net data was kindly provided by Mr Bader from the Wasser u.- Energie Wirtschafstamt des Kantons Bern (**WEA**).

1992 was quite a rainy year. As one can see on the diagram below (**Fig. 15**), it is difficult to find a dry period longer than two weeks, except after the 13th of December, where a dry period lasted 24 days (19 days in December plus 5 more days at the beginning of January 1993). January 1992 presented 13 consecutive dry days, followed by April with 9 days. 8 continuous dry days were observed in May and July. This aspect is important for the interpretation of the aquifer's response to rain events. Most of all so as to differentiate the sudden variation of the groundwater level after precipitations from the cumulative one.

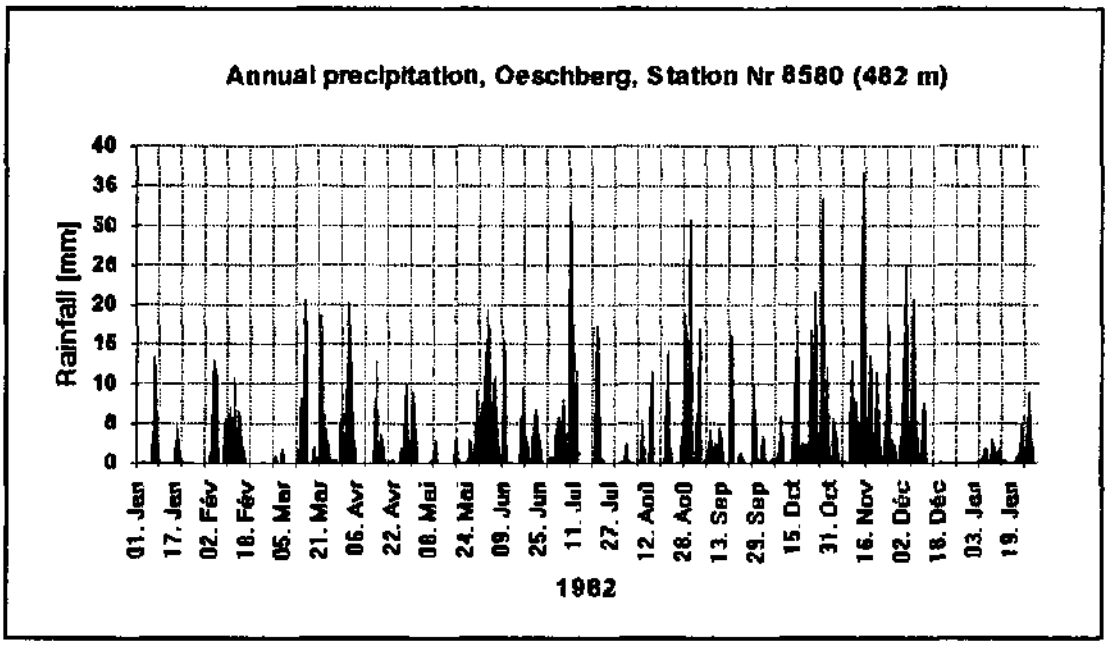

Fig. 15. Annual Precipitation from January 1 1992 to January 31 1993, measured at the Oeschberg Station.

The Map of **Fig. 16** presents the regional observation net, the geological logs and the delta h calculated between the groundwater's maximal level of November 9 1992 and the levels measured from the 9th of November till the 16th of December 1992. The map also includes the information about the ground altitude, the day when the

maximal level occurred, the exact diffference in cm and the minimal depth reached by the groundwater. The Table 2B-1 (in **Appendix 2B**) gives all the levels during the period mentioned.

Minimal variations seem to be linked to exfiltration zones, as for instance at ZIB 01 and WAB 13. A central area in the region where the deltas were higher than 100 cm appears. This includes the observations wells designated as WAB 21, WAB 23, WAB 06, WAB 25 and WAB 65. A remarkably high response of 2.78 m was observed at the piezometer WAB 57. It is also interesting to see that the date of the maximal level varies accordingly. For deltas over 100 cm the maximal level occurred between the 12th and the 16th of December. The nearer the observation wells are to the Emme river, the later the maximal level seems to have been reached.

Fig. 17 gives the delta h of the observation wells situated nearest to Wilerwald and that of WAB 57, from Nov. 9 to Dec. 16 1992. ZIB 01, which is the well situated on the exfiltration zone called Zielebach, presents the curve with the greatest variation. It seems to respond very quickly to rainfall, but the dissipation is also quick (better transmission). On the contrary, WAB 57, presents a curve with a cumulative aspect. Looking back to the map of **Fig. 16** where the geological logs are plotted, it is clear that this piezometer is the one with a situation of confined aquifer. On the other hand,the literature states that its permeability was low or even impossible to determine. Another situation of confined aquifer is found at WAB 25 (h = 161 cm).

A possible reasoo for the higher deltas observed in the central part is that this region constitutes the main drainage of Emme infiltration (**WEA, 1981**). This could explain the observations made in piezometers WAB 23, WAB 26 and WAB 06. There the aquifer is constituted of more than one lithological unity (sub-aquifer?).

Another possible reason for the higher delta h is the generally lower permeability that some observation wells show with respect to others (ex. WAB 21, WAB 57). The groundwater of the Unteres Emmental is very much influenced by the Emme infiltration. Some regions being less permeable than others, the energy will dissipate more slowly there. The incoming Emme infiltrate will be less easily transmitted, and consequently a cumulation is observed. **Fig. 18** presents the groundwater level evolution of the piezometer WAB 57 in comparison with the rainfalls registered at Oeschberg. This illustrates the cumulative aspect clearly. In more permeable regions, or near exfiltrations zones, the incoming energy will instead be dissipated more rapidly.

A possible explanation for the later date of maximal level which seems to characterize observation wells lying near the river, could be the increasing discharge of the Emme (with the increasing discharge of its tributaries). Unfortunately there is no surperficial water station functioning in the vicinity.

3.3 Hydrochemistry

No chemical data was available for 1992. So only a small resume of the **WEA**'s conclusions is presented here.

The importance of the Emme water infiltration can be clearly seen in the **Appendix 2C** (maps of **Fig. 2C-1,a) & b)**) , corresponding to the conductivity isolines during a dry period and after a rainfall. The main infiltration of the Emme described above, occurring in the central part of the zone, is made obvious by the lowering of the conductivity values after the rain period.

The contribution of the Emme infiltration decreases with the increasing distance from the river. This is also evident on the map of **Fig. 2C-2** in **Appendix 2C**, where the mean annual oscillation of temperature is plotted.

3.4 Synthesis and Conclusions

The literature overview made it clear that we are in the presence of a very complex aquifer, with extremely variable geometry and lithology. It also pointed out that the Emme plays an important role in the chemical balance of the groundwater, and that the zone of influence of its infiltration is irregularly distributed. This is due to differences in permeability.

Regional piezometric observations showed the different responses of the aquifer to rain events. Higher amplitude variations, and correspondly delays in reaching the maximal level, seem to correspond with lower permeabilities. Observation wells situated in exfiltration zones have small amplitudes and very quick responses.

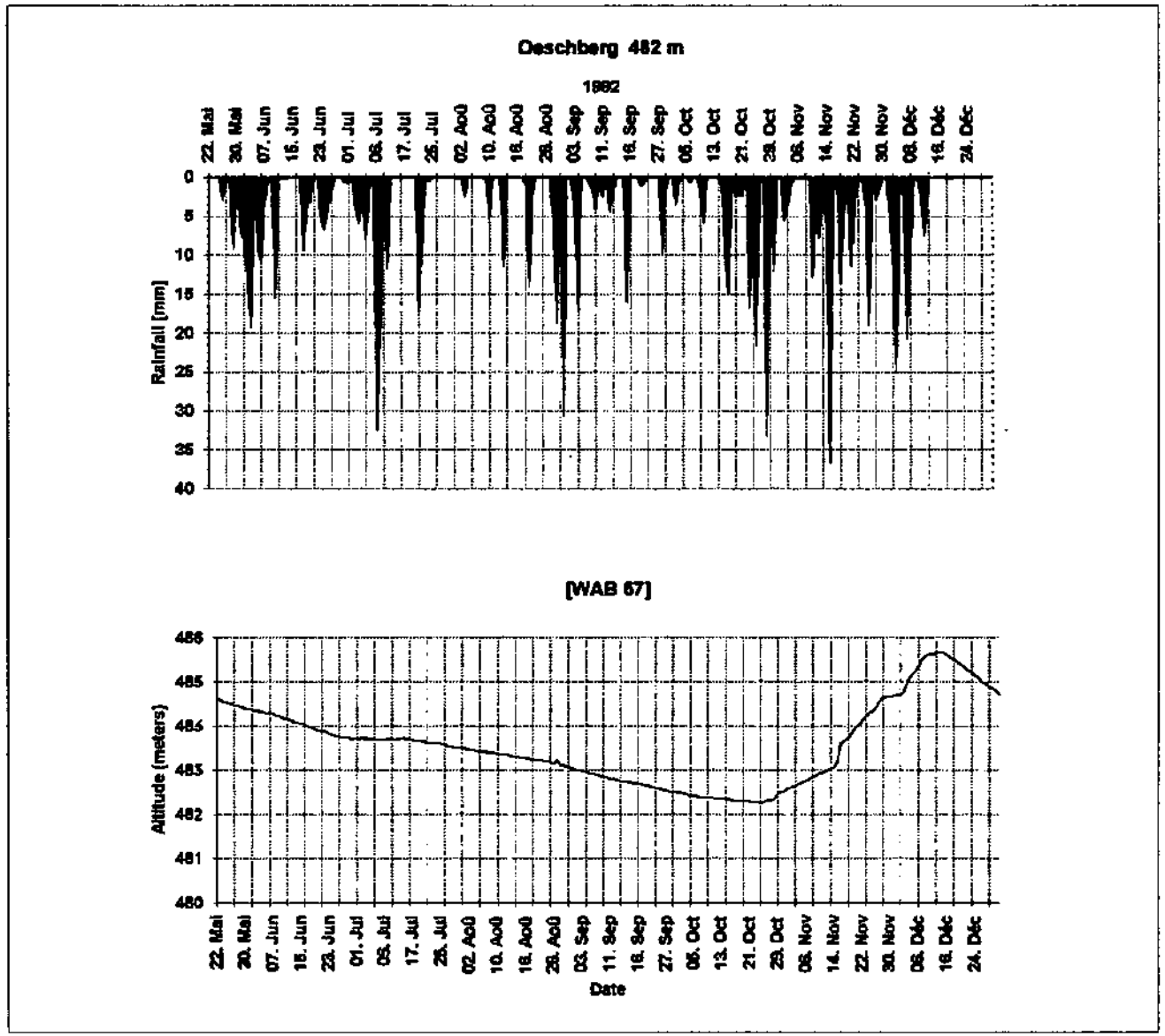

Fig . 18 Groundwater level evolution during about 6 months (May 22 .1992 - Dec.31. 1992) for the observation well WAB 57 - exemplifying the cumulative aspect referred above.

Due to the great heterogeneity of the zone, it is better to avoid interpolations based only on puntual information. Geophysical techniques which don't homogeneize the medium, such as the electromagnetical VLF-EM and RMT-T are therefore a good complement.

About 10 VLF-EM surveys were made very rapidly (half-a-day), regionally and around the Wilerwald test site. These continuously registered out-of-phase variations confirmed the extreme lateral variability of the quaternary deposits. They also allowed to delineate preferential groundwater pathways - paleochannels filled with coarse gravels. The location of these paleochannels corresponds to the actual topographic lines. The present surface still reflects the ancient lie of the paleochannels.

Part III: Local studies, field experiments and analyses

4. Identification and geometry of the aquifer

4.1 Geophysical Methods:

4.1.1 Electromagnetical methods

A RMT-R

A.1 Results

A.2 Methods of interpretation

A.2.1 Application of Kriging

A.2.2 Interpretation based on raw data

A.2.3 Interprretation based on MT. inversion

B multidirectional RMT-R

C VLF-EM

D audiomagnetic tellurics

4.1.2 Electrical method: Schlumberger configuration

4.1.3 Seismic surveys

4.2 Geological Aspects

4.3 Syothesis and conclusioos

Part III : Local studies, field experiments and analyses.

This section describes all the experiments performed on the Wilerwald test site. Starting with those undertaken in order to describe the aquifer, its geometry and distribution of properties, we will then focus on the hydrodynamic aspects determined by periodical readings of the piezometric surface and pumping tests. Next, the chemical analyses will be discussed, and finally the tracer tests that were performed in 1988 and 1992. To interpret RMT-R raw data a new approach was used, based on the indirect relationship between resistivities and grain size distribution. This is a rapid method for determining both the horizontal and vertical distribution of heterogeneities. It differentiates the vertical distribution of layers and resistivities, and also defines the influence of the upper conductive layer on the resistivity data.

4. Identification and geometry of the aquifer

4.1 Geophysical methods

Electromagnetic methods constitute an indirect approach for estimating hydrogeological aquifer parameters (lithology, thickness, permeability). Two complementary electromagnetic methods were used to reveal the aquifer's heterogeneity and its structure at the local scale :

1) - RMT-R which uses the same principle as the VLF-R (Very Low Frequency-Resistivity) method, but is extended to higher frequency ranges (240 kHz),
2)- and VLF-EM (Very Low Frequency - Electromagnetic).

The principles of the methods are given in **Appendix 1-A.**

4.1.1 Electromagnetic methods

A. - RMT-R (Radio-Magnetotelluric-Resistivity):

The great advantage of the RMT-R method is that it allows to make as many measurements at any place and time one thinks important, and this very rapidly and for a minimal cost. We thought that the variability of the quaternary formation mentioned in the literature would also be found on the small scale of the Wilerwald test site area. So as to be able to map it, about 600 RMT-R multifrequency and RMT-R multidirectional soundings were made (see **Fig. 19-a**).

A.1 - RMT-R results

The site was divided into 30 profiles perpendicular to the main direction of waterflow, as shown in **Fig. 20.**

The soundings were separated by 5 to 10 meters on average. (see **Table 3A-1** *in* **Appendix 3**)
Three, sometimes four, frequency ranges were used: 183 kHz, 70 kHz (60 and 77.5), 19 kHz and 12 kHz. The transmitters are all oriented approximately in the same direction (N150°). The electrodes that measure the electric component (see Appendix 1-A) were also aligned in this direction. The simultaneous use of different frequencies, each one penetrating to a different depth, enables among others the calculation of actual resistivities and of the local thickness of the aquifer, using the MT. Inversion procedure (**Fischer et al, 1981, Thierrin, 1990**).

A lot of information can already be obtained simply with the analysis of the raw data:

The direct use of the apparent resistivity data allows the construction of Contour Maps, which give a good picture of the structure of the aquifer. These maps were first drawn by hand (**Fig. 21**), when the number of points measured was not too large and then by computer, using the kriging method of interpolation (see **A.2.1** in this chapter).

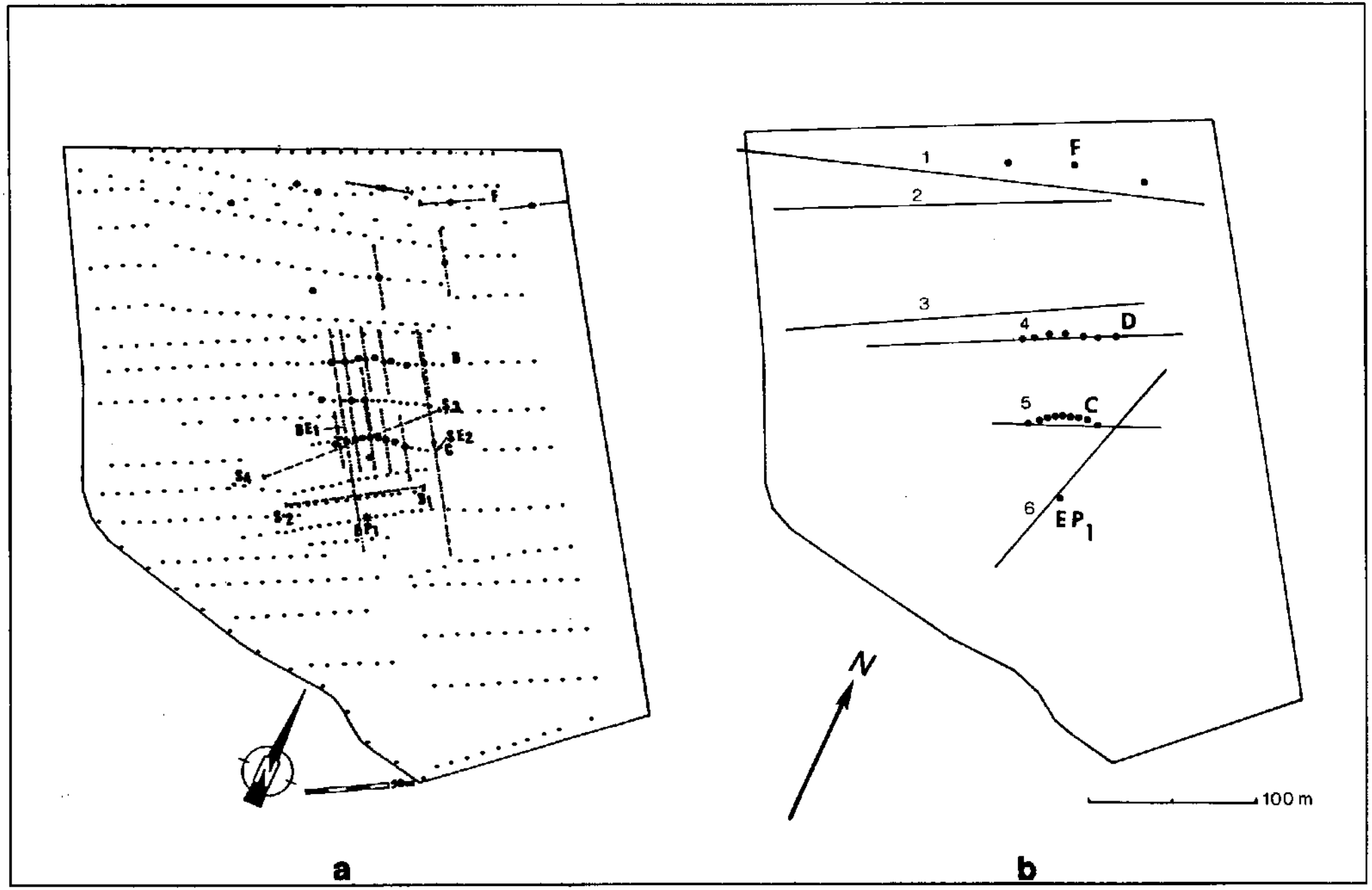

Fig. 19 Location of the geophysical observation net : **(a)** · RMT-R measuring points; —·—·—·— Schlumberger soundings ; – – – – – seismic profiles (S1..S4); **(b)** VLF-EM surveys: C, D & F = galleries.

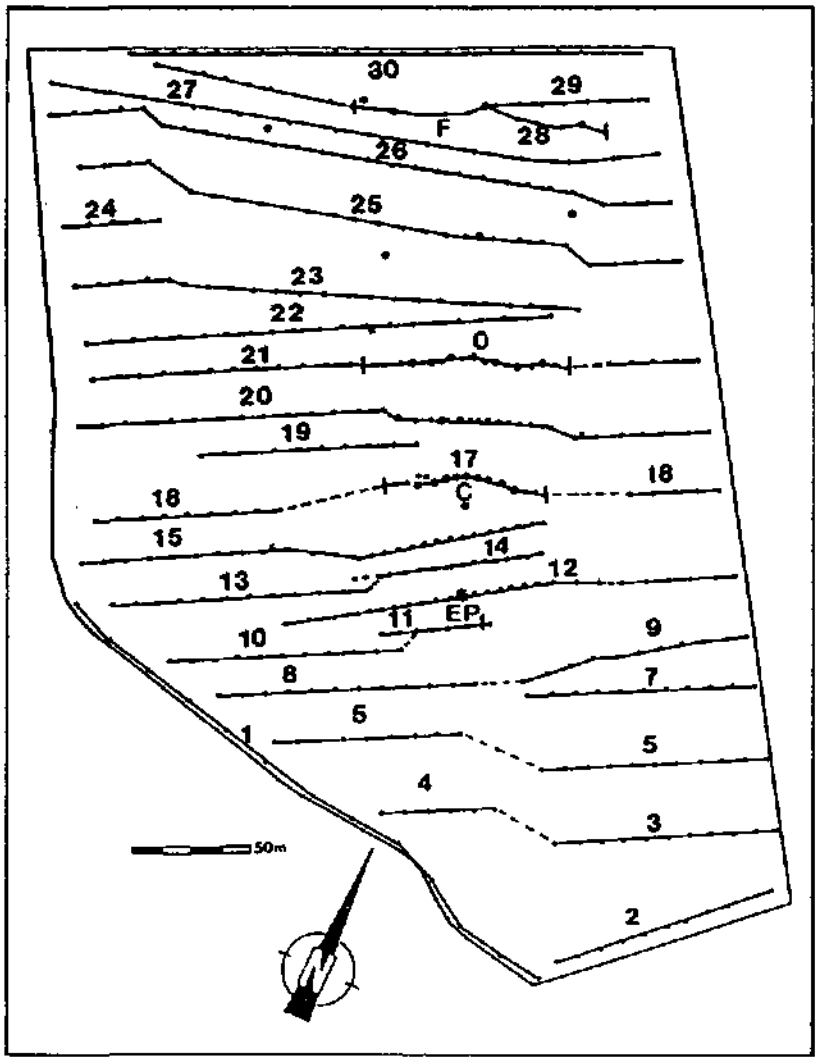

Fig. 20 Location of the RMT-R profiles mentioned above : • = RMT-R measuring points; 1...30 Profile number; **C, D, F** gallery names; $\mathbf{EP_1}$ = Iojection borehole .

The higher the resistivity values in unconsolidated sediments, the more permeable those should be. Bearing this in mind, a "channel" of a "meander"-like shape appears on the hand-drawn 183 kHz contour map. A quick look of the map permits us to localize the piezometers concerned by this structure:

- C7 and C6 in the channel zone,
- F4, F2 in a less permeable region, which circles the NE area of the test site
- and the injection point lyiog in a not so permeable zone...

The maps done by kriging (**Fig. 22**) complete the image : on the 183 kHz one, the channel is seen to be confluent with another one, but its contour diffuses to a greater depth and, at 19 kHz, the higher resistivity values are to be found mainly on the southern edge. The conductive zone, situated at the north-east end, is well individualized (Rho approx. < 50 Ohm.m at 183 and 70kHz, and < 100 Ohm.m at 19 kHz). This suggests a sedimentatioo environment of lower energy, quite different from that of the deposits in the rest of the zone.

Not only does the apparent resistivity supply valuable ioformation concerniog the structure, but so do the dephasing values.
Contour maps of the dephasing values were also drawn. Their interpretation is unfortunately not so easy.
For instance, on the 183 kHz dephasing maps, it is clear that there is some kind of a structure, with lower phase values, oriented northwards and stretching diagonally across the map. It then appears fragmented on the 60 kHz phase map and clearly moves north at deeper levels (19 kHz).

This structure, since it interrupts the paleochannel, seems contradictory with the other evidence of its existence. This is difficult to understand. Besides, also considering at the Rho ap. values, it is clear that the regioo located NNE is quite different (much lower values of resistivity) than the one S, and shouldn't be grouped with it.

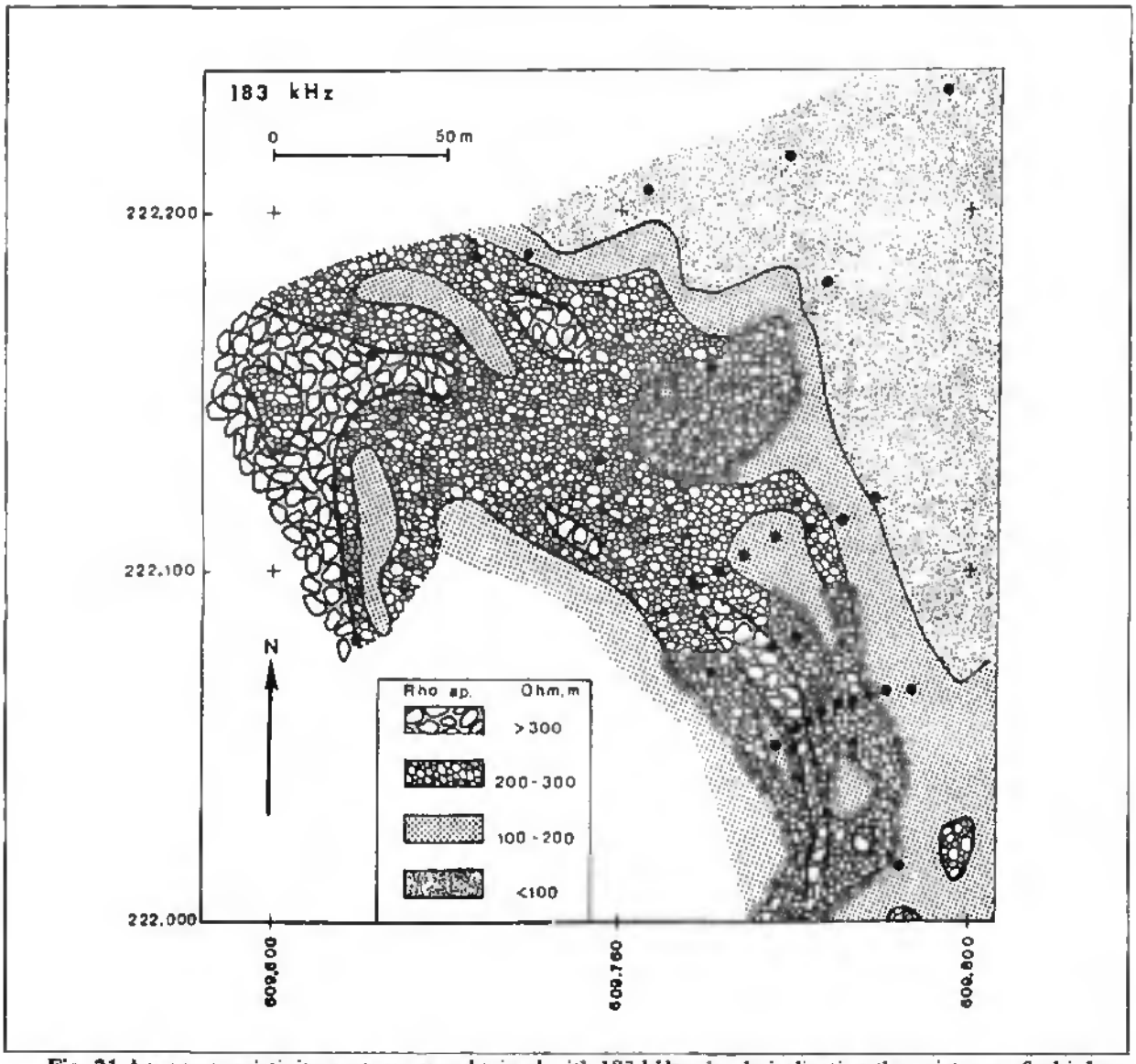

Fig. 21 Apparent resistivity contour map obtained with 183 kHz, clearly indicating the existence of a higher resistant channel (Rho >300 Ohm.m) and its disposition relative to the net of observation wells.

The combined used of both parameters for the interpretation of RMT data (Rho ap and Phases) seemed to be the most suitable. Therefore, all 30 profiles mentioned above were redrawn, with the Rho apparent data (Y1 axis) and the dephasing values (Y2 axis) plotted simultaneously. **Fig. 24** shows three of these profiles, through the C, D and F galleries. The scale of the Rho values is not logarithmic, as is usually done, but normal, starting at 0 Ohm.m, and the dephasing values are represented from 0 to 60 degrees. This was done on purpose, to be able on one hand to show the variability of the Rho values (that would be smoothed by logarithmic scale), whilst avoiding a superposition of the curves which would make the profiles more difficult to read.

These profiles do very clearly show the situation observed on the apparent resistivity maps, concerning the localization of the observation wells in regard to the channel. C7 and C6 (C gallery) as well as D7 and D6 (D gallery) have very high 183 kHz values of apparent resistivity. C8, D1, F4 and F2 (F gallery) have lower values and are all, except C8, in the NE area referred to above.

The phases are always lower than 45 degrees at 183 kHz, become clearly higher than 45° at 19 kHz, and have an oscillating behaviour around the 45° line at 60kHz. This situation indicates the existence of three layers (C/R/C): a conductive surface layer, of variable thickness, a resistive and uniformely thicker intermediate layer and a bottom layer, once again conductive.

It is also interesting to observe that the 183 kHz resistivity values are not always smaller than the 70 kHz values - this may indicate the non-existence, or the presence, of a rather thinner conductive upper layer. This is the case for the points situated in the paleochannel and its vicinity. This will be discussed in the next sub-chapter.

A.2 - Methods of interpretation

A.2.1.- Application of kriging to Wilerwald

At Wilerwald kriging was used only as an interpolation method for the drawing of contour maps. The different variograms function were calculated for the resistivity at each frequency, for the logarithm of the resistivity values and for the phases. The variograms calculated for the four main directions were similar for all variables.

The theoretical model which fitted the experimental variogram was a spherical one. As there also was a nugget effect, the following equations will define the variogram function:

$$\gamma(h) = \omega[\frac{3}{2}\frac{|h|}{a} - \frac{1}{2}(\frac{|h|}{a})^3] + C \qquad h \leq a$$

$$\gamma(h) = \omega + C \qquad h > a$$

$$\gamma(0) = 0 \qquad h = 0$$

where,
C = the nugget value
ω = the sill
a = the range.

Wilerwald	Statistics		
183 kHz	Rho ap.	Log Rho ap.	Phase
Variance	6584.76	0.05	24
Sill	8000	0.075	26
Range	0.3 Km	0.26 Km	0.15 Km
Nugget	3000	0.01	11
Std. Dev.	81.15	0.224	4.880
Sample Size	475	475	475
Min.	41	1.613	20
Max.	541	2.733	47
70 kHz	Rho ap.	Log Rho ap.	Phase
Variance	6819.79	0.0346	29
Sill	8100	0.049	33
Range	0.25 Km	0.33 Km	0.15 Km
Nugget	4000	0.015	1
Std. Dev.	82.58	0.186	5.410
Sample Size	475	475	475
Min.	62	1.792	30
Max.	805	2.906	57
19 kHz	Rho ap.	Log Rho ap.	Phase
Variance	3295.64	0.028	10.100
Sill	4000	0.045	12.200
Range	0.3 Km	0.45 Km	0.22 Km
Nugget	2000	0.015	2
Std. Dev.	57.41	0.167	3.170
Sample Size	475	475	475
Min.	36	1.556	45
Max.	427	2.630	60

Table 5 main characteristics of the kriging interpolation function

The table above (**Table 5**) shows the main characteristics of the interpolation function. As the range varies between 150m and 300m, the distance between sampling points shouldn't exceed these values. At Wilerwald,the measuring points were 5 to 10 meters apart on average along each profile and up to 30 meters distant between profiles, which seems very adequate. The standard errors (reliability of the estimation) are

Fig. 22a Apparent resistivity map (183 kHz)

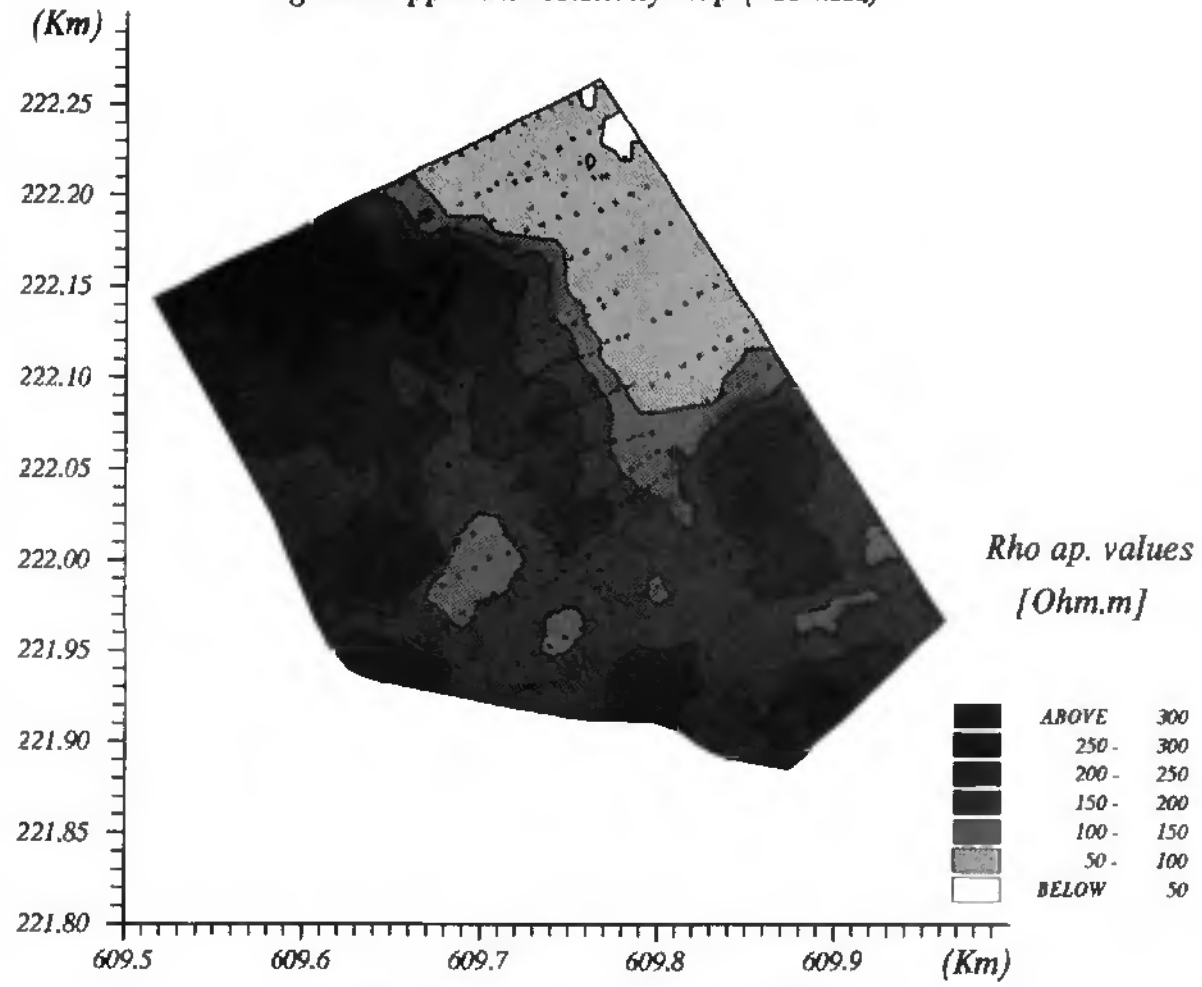

Fig. 22b Standard errors map (183 kHz)

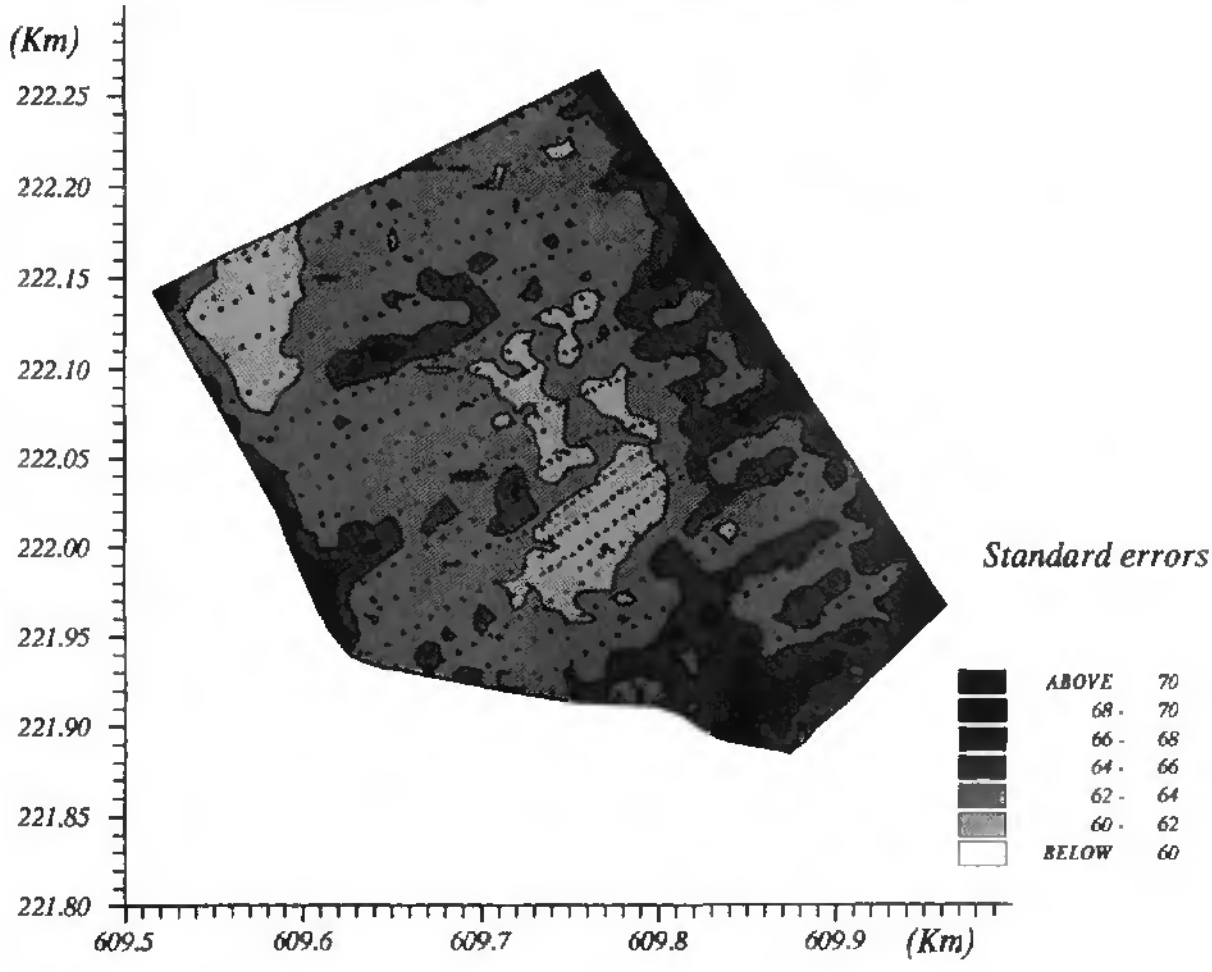

Fig. 23a Phase map (183 kHz)

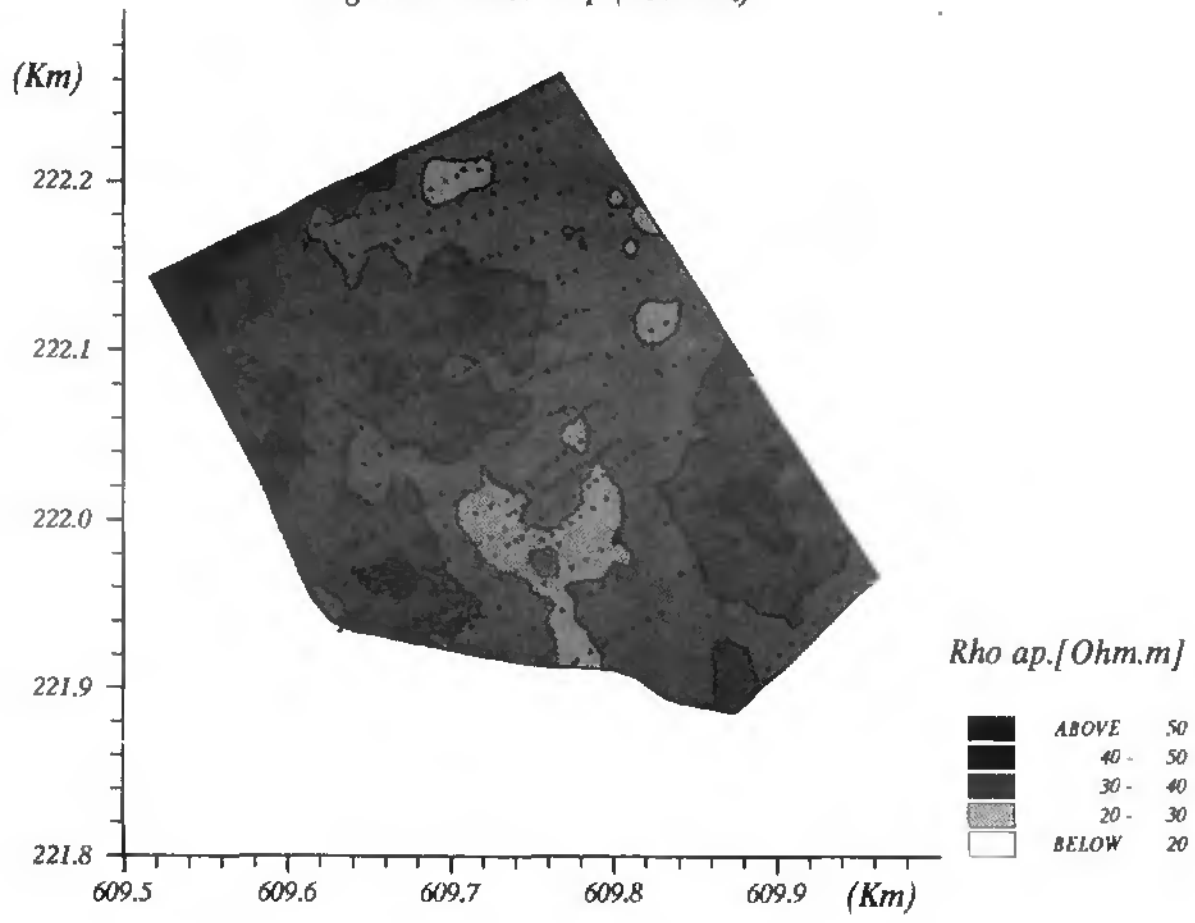

Fig. 23b Standard errors map

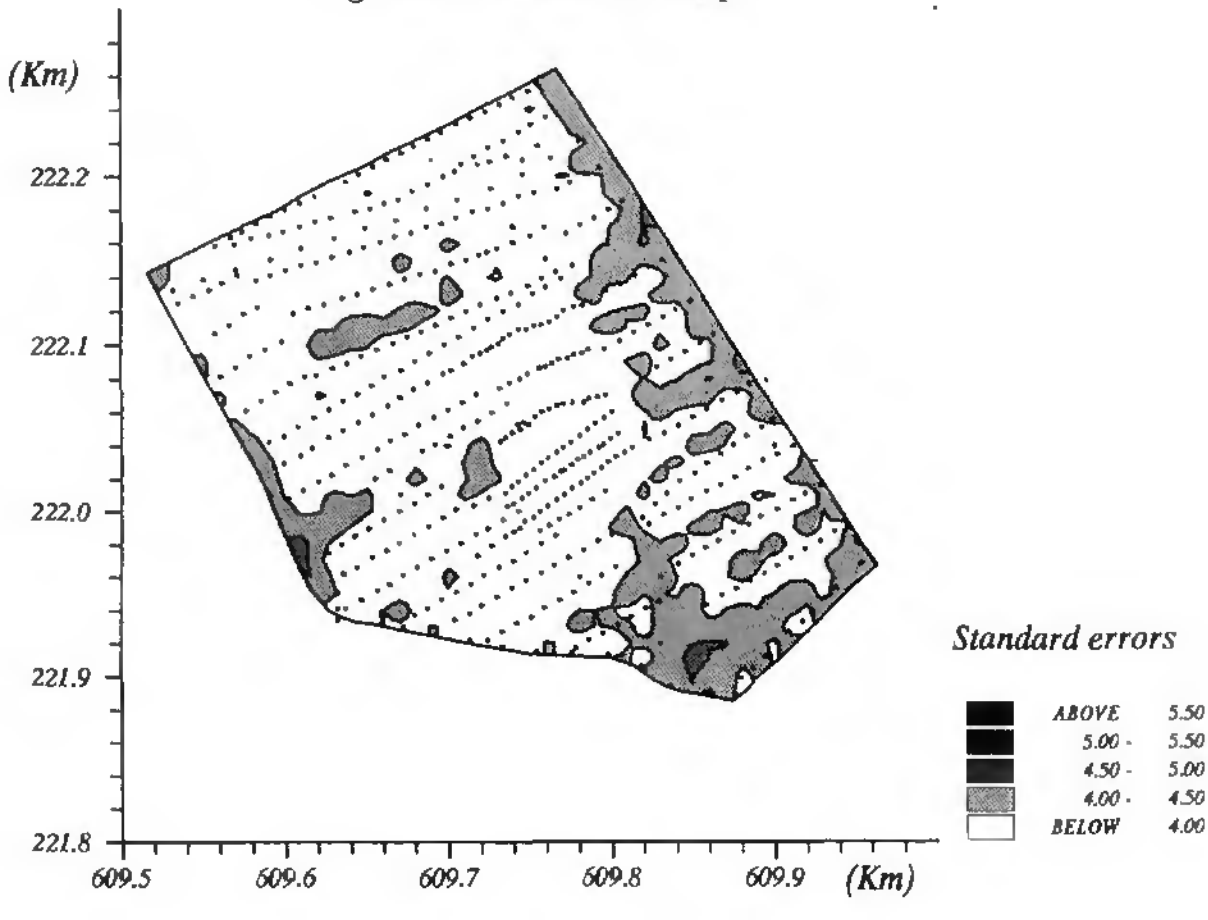

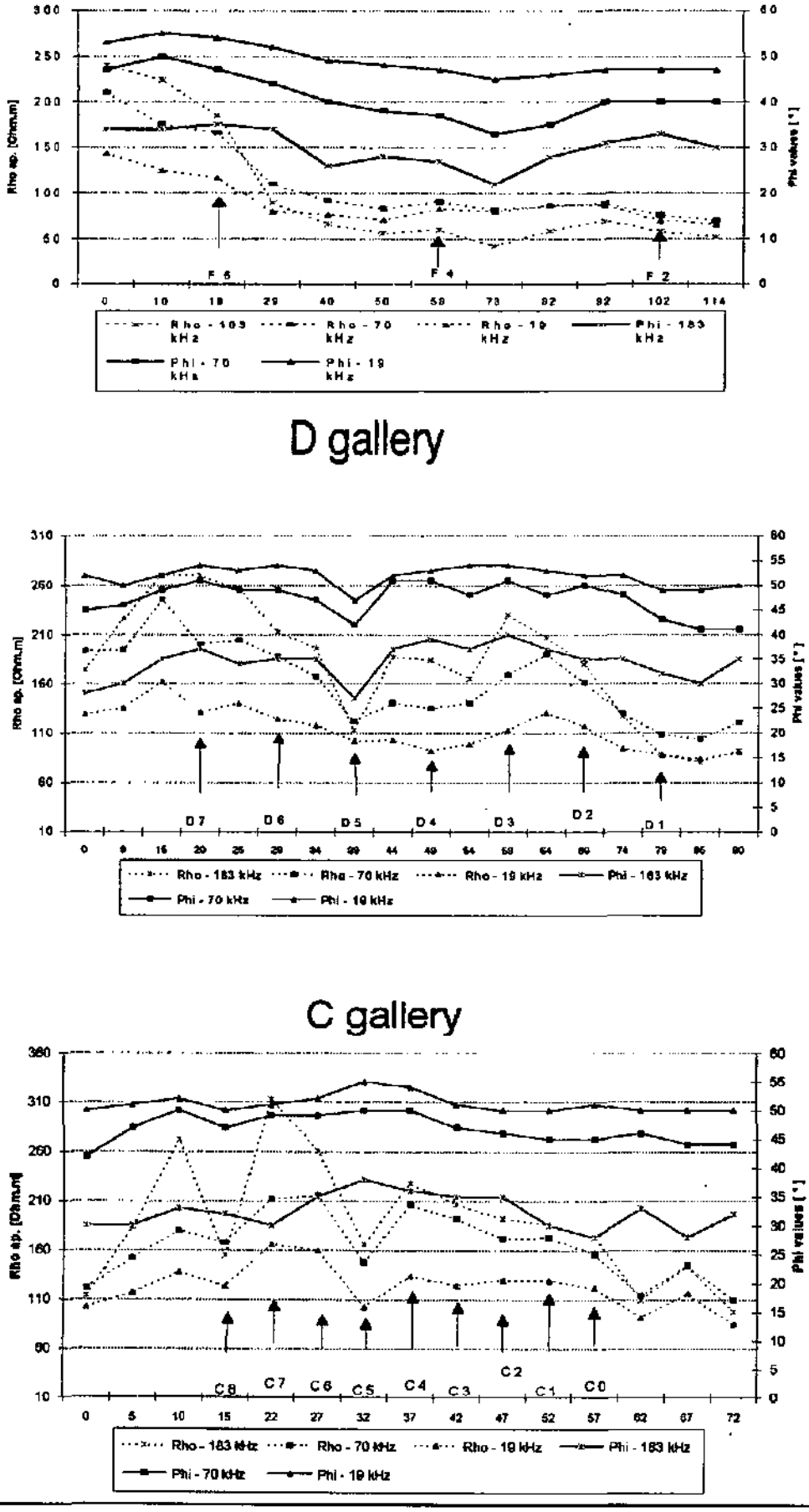

Fig. 24 Profiles passing through the C, D and F galleries, representing the Rho apparent values at Y1 (left axis) and the phase values at Y2 (right axis).

generally low, and the maps constantly show the same pattern - the highest standard errors are to be found at the test site borders and they are function of the sample density. The presence of a nugget is maybe due to measurements errors but also due to the limitations of the RMT-R method, which is unsensitive to micro-structures, therefore indicating again, that one is in the presence of a highly heterogeneous aquifer.

The **Table 3A-2 in Appendix 3** resumes the equations of the spherical functions.
With these functions Kriging Maps described in A.1 were drawed.

A.2.2 - Interpretation based on raw data:

The idea was to see if it was possible to establish plausible spatial relationships within the RMT-R raw data. The aim was to infer about the environment of deposition, by exploring the features referred to this in A.1, such as, the structural character of the phase information and the existence or not of an upper conductive layer, which influences the values of the Rho ap., etc.

This was done in several steps:

First, all the values of the resistivity logarithms,histograms were plotted for each frequency. The results can be seen in **Fig. 25**. The effect wasn't as clear as had been hoped for, except for the higher frequencies, where a bimodal distribution appeared (more so at 183 kHz than at 70 kHz). It was also possible to gather some information about the modal class (the most frequent one), about the number of classes (which indirectly reflects the degree of selection in a population), and about the symmetry of the class distribution. Unfortunately the form of a histogram varies with the limits of the class interval that is chosen, making its utility limited.

The spatial distribution of resistivities is correlated with the sediment distribution. Besides, resistivities are also indirectly related to the grain size distribution.
We made use of this similitude, trying to apply to the distribution of data measured by RMT-R the methods used in grain-size analysis, which give a lot of information about the environment of deposition and its energy. The aim was to see if it was possible to find a coherent method of analysis for the raw data, specially for field cases like Wilerwald, where not much direct information is available.

In sedimentology, there is a well known method for studying a sediment sample, considered a priori to be heterogeneous, using a very simple statistical treatment. The sediment is divided into artificial classes by means of sieves of different diameters. Than, the weight of the population retrieved in each sieve is noted. Histograms are seldom used in grain size analysis. Instead, they are transformed into cumulative percentage curves, which offer greater advantages. A cumulative curve always has the same form, independently of the class limits chosen. Furthermore, a lot of information can be extracted from such a curve. According to the selection degree (homogeneity), the form of the curve will vary from almost vertical to nearly horizontal. The modal class will be situated on the steepest part of the curve (see the example in **Fig. 26**). Irregularities, expressed by means of the curve's inclination, indicate secondary modal classes.

In this way, it is possible to conclude about the environment of deposition. A sample of dune sand, for instance, having a high degree on selection, will present an almost vertical shape, which would be expressed by very small values of standard deviation. An environment of higher energy could also present a very good selection, but the curve would be clearly displaced towards much larger diameters. Therefore, the difference with the dune distribution would be reflected by a higher value of mean diameter. The asymmetry of a heterogeneous sediment would signify the predominance of higher or lower values of diameters (also an environmental indicator).

Mean and standard deviation, asymmetry, etc., are calculated graphically from the cumulative curves. There exist a lot of procedures to calculate these parameters. The one given by **Folk and Ward (1957)** was preferred here, because it takes into account not only the central part of the curve, but also the tails, and that is very important, considering the heterogeneity of the values.

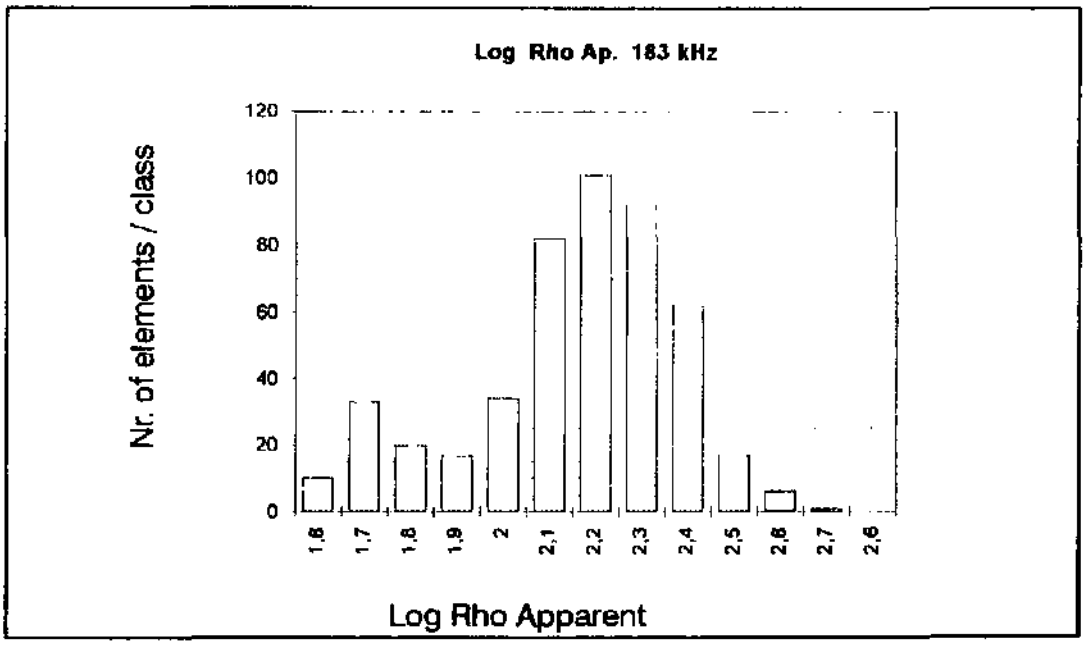

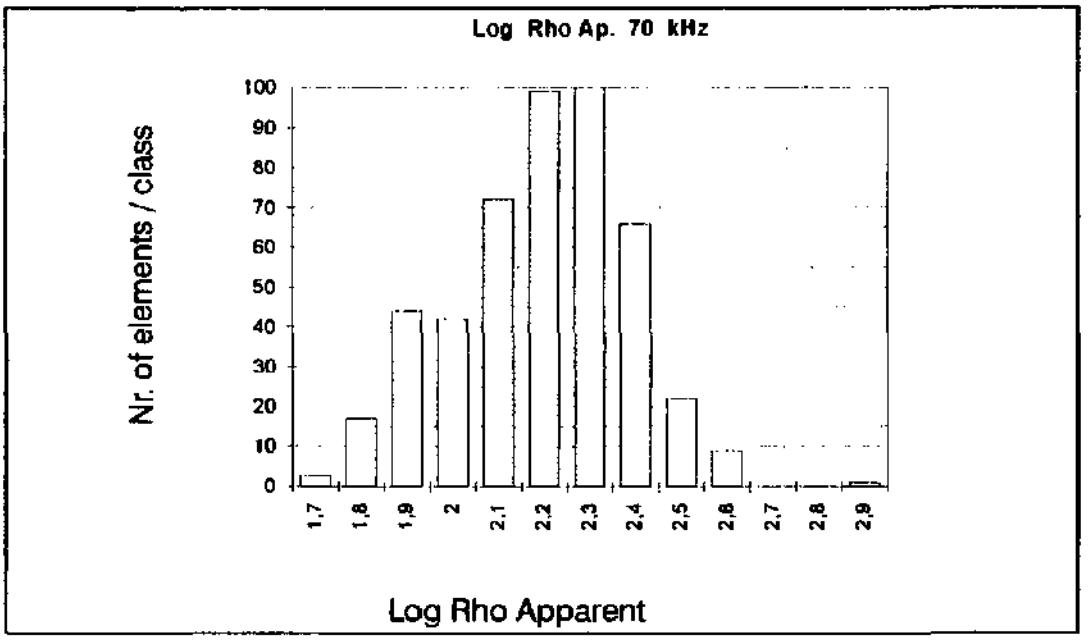

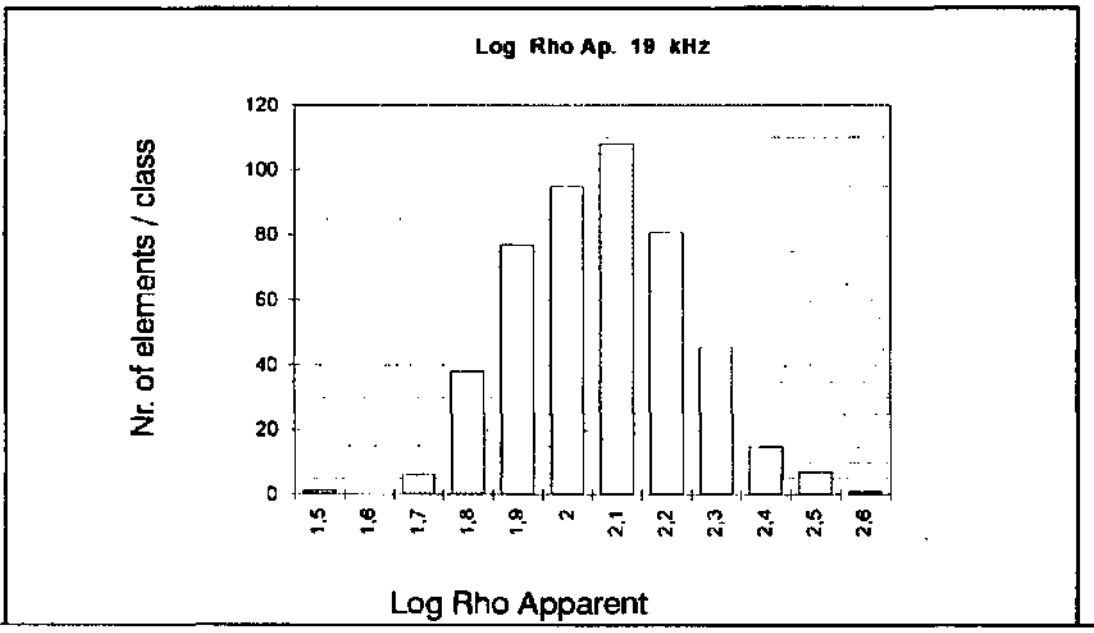

Fig . 25 Histograms of the Rho ap values (transformed into logarithms) - a bimodal distribution at 183 kHz.

Some of the Folk and Ward parameters (Suguio, K.,1973) are listed below:

The mean diameter: Mz

$$Mz = \frac{\phi 16 + \phi 50 + \phi 84}{3}$$

The standard deviation:

$$\sigma I = \frac{\phi 84 - \phi 16}{4} + \frac{\phi 95 - \phi 5}{6.6}$$

where, according to values, the sediment is classified, as following, if a ϕ scale ($\phi = -\log_2 d$, d =diameter in mm) is used :

σ_I	Selectioo Degree io a grain size analysis
< 0.35	very good selected
between 0.35 and 0.50	good selected
between 0.50 and 1.00	fairly selected
between 1.00 and 2.00	poorly selected
between 2.00 and 4.00	very poorly selected
> 4.00	extremely bad selected

Table 6 Selection degree in a grain size analysis after **Folk and Ward (1957)**

and the asymmetry: SkI

$$Sk_I = \frac{\phi 16 + \phi 84 - 2\phi 50}{2(\phi 84 - \phi 16)} + \frac{\phi 5 + \phi 95 - 2\phi 50}{2(\phi 95 - \phi 5)}$$

The following qualitative scale is used to describe the sediment:

Sk_I	Asymmetry Degree
between -1.00 and -0.30	very negative asymmetry
between -0.30 and -0.10	negative asymmetry
between -0.10 and +0.10	approximately symmetric
between -1.00 and +0.30	positive asymmetry
between +0.30 and +1.00	very positive asymmetry

Table 7 Assimetry degree in a grain size analysis after **Folk and Ward (1957)**

As explained above, the idea was to adapt these priociples to the RMT-R data.

The next figure (**Fig. 26**) shows three hypothetical distributioo curves of Rho data treated in this way, as well as the information that can be deduced from the form of the curves.

The next step was to define classes of facies among the RMT-R data (475 measuring points, and three frequencies), just as in sedimentology. If in a coastal sediment it is relatively easy to find facies of dune, beach or lagoon for iostance, at Wilerwald, due to the heterogeneity of the fluvio-glacial deposit, the situation was more complicated. Besides, the RMT-R data not only give two dimeosional spatial informatioo about the distribution of the resistivity data but also have a vertical component which must be taken into account.

Definition of facies and classes: just as for a grain size analysis, the cumulative distribution curves of the resistivity data (475 points) at each frequency were plotted on the same figure (**Fig. 27**).

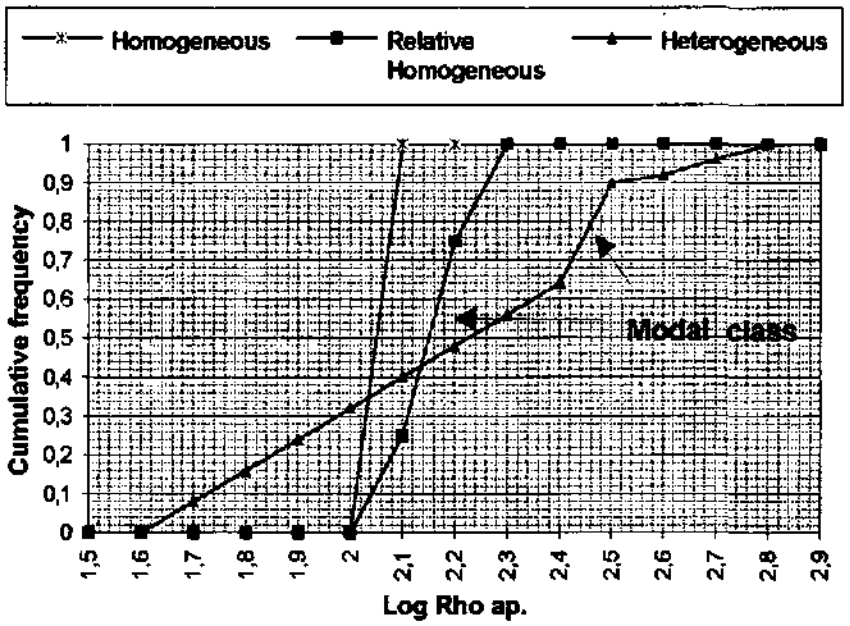

Log Rho ap.	Homogeneous	Relative Homogeneous	Heterogeneous
1,5	0	0	0
1,6	0	0	0
1,7	0	0	0,08
1,8	0	0	0,16
1,9	0	0	0,24
2	0	0	0,32
2,1	1 ←	0,25	0,4
2,2	1	0,75 ←	0,48
2,3	1	1	0,56
2,4	1	1	0,64
2,5	1	1	0,9 ←
2,6	1	1	0,92
2,7	1	1	0,96
2,8	1	1	1
2,9	1	1	1

Modal class indicated by : ←

Fig. 26 Hypothetical cumulative distribution curves of apparent resistivity values, representing:
1) an extremely homogeneous sediment where all the values are the same,
2) a situation of symmetrical distribution with a modal class, the case of a relatively homogeneous deposit,
3) a very heterogeneous deposit, where practically all classes are represented.

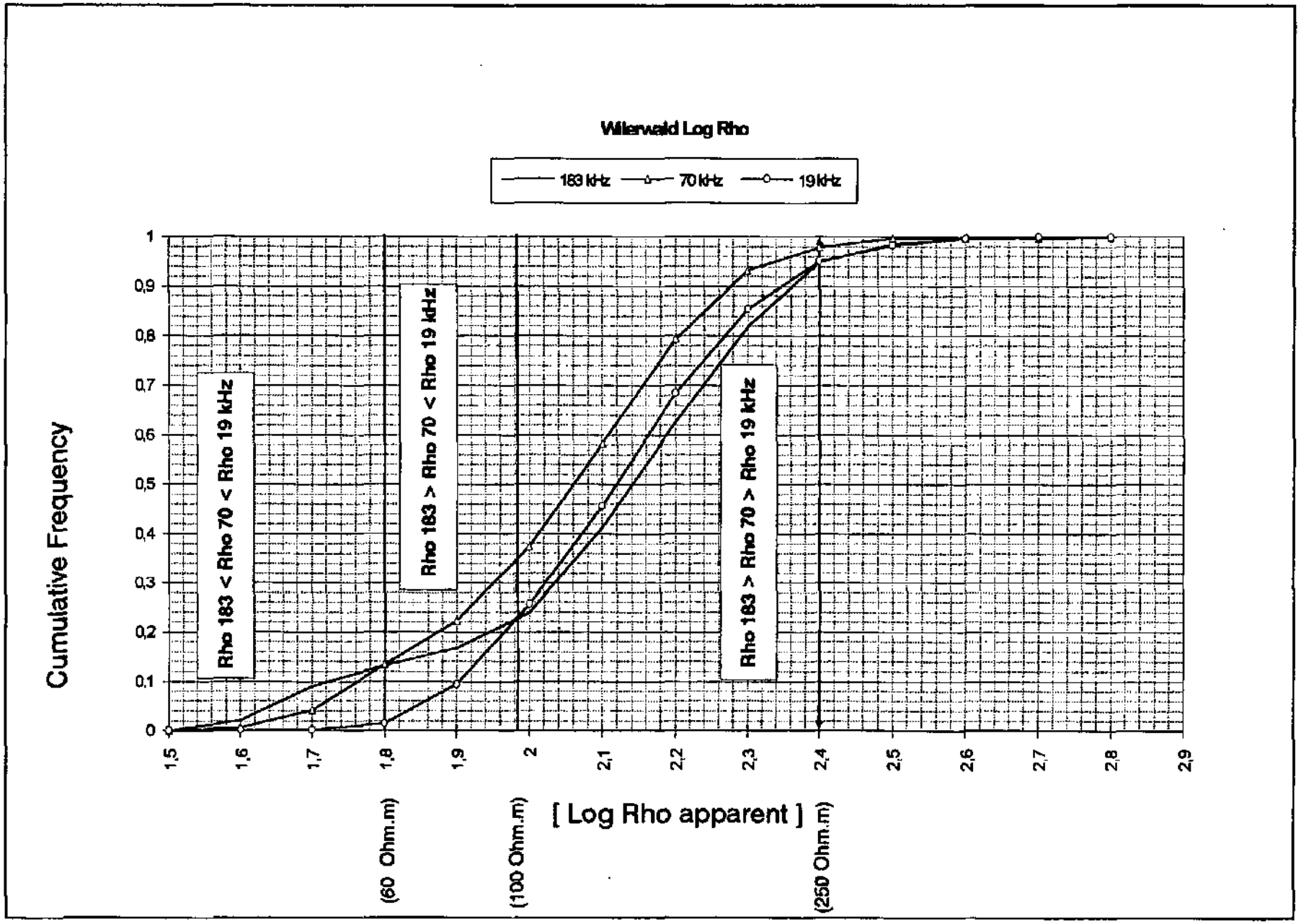

Fig. 27 Cumulative percent distribution curves. For the explanation of the separation domains, please see text.

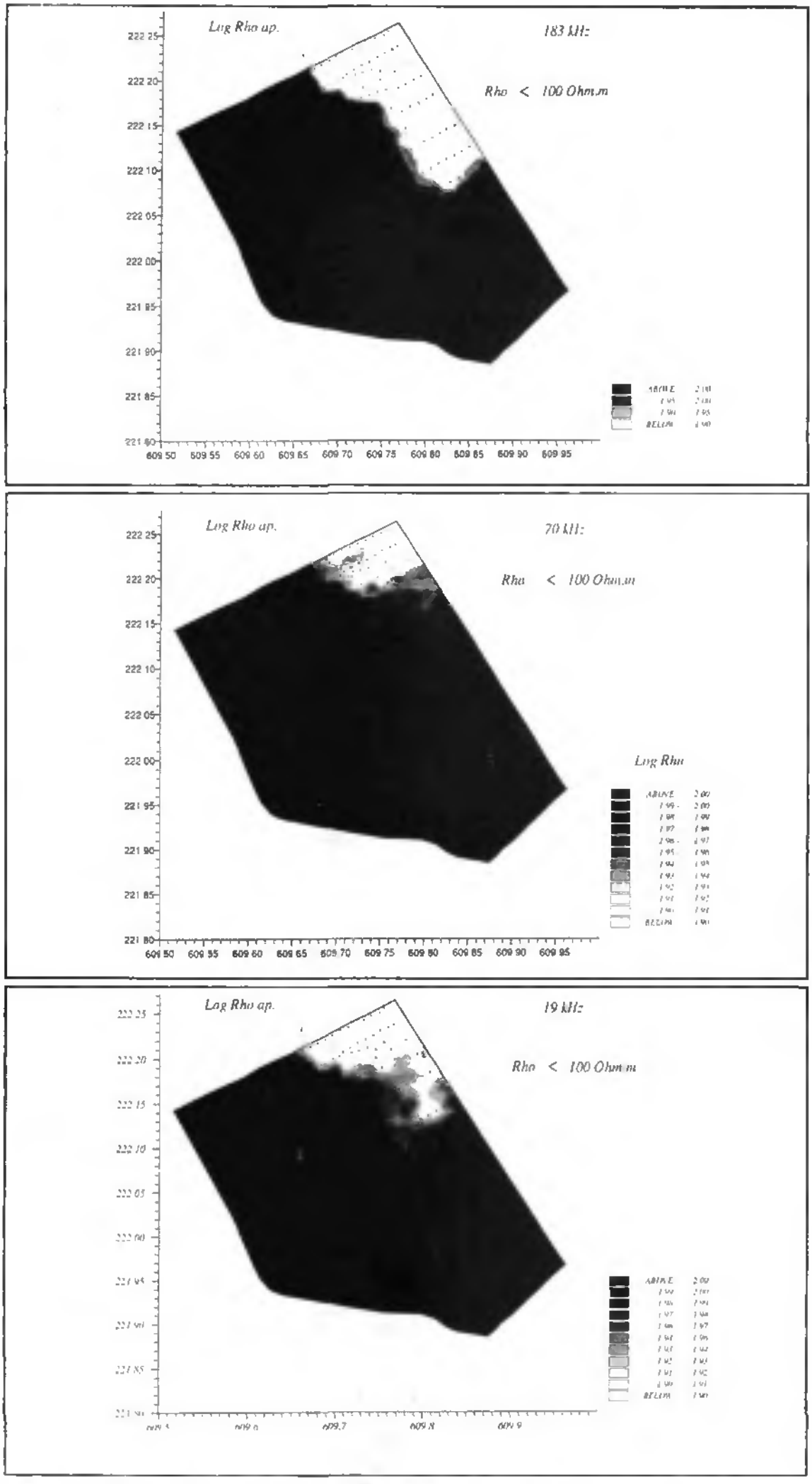

Fig . 28 100 Ohm.m separating borderline, separating the more conductive NNE region. detectable at all frequencies.

Observing **Fig. 27** it is obvious that the 183 kHz measurements are the ones which change the most. One can distinguish 3 main zones:

- the left tail of the curves, values lower or equal to 1.8 (log 60 Ohm.m (log 60 Ohm.m ≈ 1.8), where Rho values for 183 kHz are the lowest ones: Rho 183 < Rho 70 < Rho 19.
- then follows an intermediate zone, where Rho ap. values for 183 kHz are lower than 70 kHz values and higher than 19 kHz ones (in the 1.8-2 ≈ 60-100 Ohm.m interval): Rho 183 < Rho 70; Rho 183 > Rho 19.
- and finally on the right tail, the 183 kHz values are clearly higher than the others, till about 2.4 (≈ 250 Ohm.m), where the Rho values for 183 kHz are more or less equal the Rho ones for 70 kHz: Rho 183 > Rho 70 > Rho 19.

To find the physical meaning of the 60 Ohm.m, 100 Ohm.m and 250 Ohm.m, the kriging maps for the 3 frequencies were drawn. These revealed that 100 Ohm.m was definitely a frontier line, separating the NNE region from the rest at all frequencies, and could also be used as a class separator (**Fig. 28**). For 250 Ohm.m, the result wasn't as clear, except that, when used, it contributed to delimit spots where gravels are very clean (with a very high porosity) and relatively big (pebbles and cobbles).

Using these limits, the following classes were created:

Class 1 - Rho 183 kHz < Rho 70 kHz < Rho 19 kHz < 100 Ohm.m
Class 2 - Rho 183 kHz < Rho 70 kHz < Rho 19 kHz > 100 Ohm.m
Class 3 - Rho 183 kHz < Rho 70 kHz > Rho 19 kHz
Class 4 - Rho 183 kHz > Rho 70 kHz > Rho 19 kHz < 250 Ohm.m
Class 5 - Rho 183 kHz > Rho 70 kHz > Rho 19 kHz > 250 Ohm.m

Within each class many situations can exist. Possible situations corresponding to these classes are represented in **Fig. 29.** And their spatial distribution can be seen on the Map of **Fig. 30**.

Class 1: The values of the resistivity in the 200 kHz range are lower than in the other ranges. This is the same as in class 2, only they are lower than 100 Ohm.m. As, for example, in the case of 92 Ohm.m,43°; 77 Ohm.m,50°; 89 Ohm.m,50°, it is also a C/R/C situation. A very thick conductive upper layer is followed by a resistive layer of smaller dimensions (sand, or sand and silt with small gravels ?).

Class 2: this class is characterised by a very thick upper layer, which causes the resistivity and the phase values to diminish in the 200 kHz range (for instance 150 Ohm.m,28°). Sometimes a higher resistivity value in the 20 kHz range appears, indicating an increase of gravel dimensions with depth.

Class 3: This is the typical case of the three layer C/R/C mentioned in A 1. An example would be: 225Ohm.m,39°; 292 Ohm.m,47°; 140Ohm.m,54°.

Class 4: This class diverges from the 5th class because the Rho values at 183 kHz are lower than those at 250 Ohm.m, meaning either that the dimensions of the gravels are smaller [for instance 125 Ohm.m and 43°], or that there is an upper conductive layer which lowers the values [as in 150 Ohm.m; 30°].Two situations are possible in this case.

-Either the resistivity values at 70 kHz are smaller than the ones at 19 kHz, indicating the possible existence of an intermediate conductive layer and an increase in size of the gravel at bigger depths. An example would be: 172 Ohm.m,32°; 170 Ohm.m,37°; 212Ohm.m,51°;
-Or else, the 70 kHz resistivity values are higher than the 19 kHz ones. This could be explained by the absence of the intermediate layer.

Class 5: Clean gravels, pebbles and cobbles. The resistivity given at 183 kHz is high , and the phases very near to 45°(absence of an upper conductive layer) . The depth penetration in the 200 kHz range is deep ,≈ 20meters. At the range of 70 kHz it extends to about 32 meters and the phase 51°, indicates that the aquitard has already been reached. The resistivity value is lower because of that.

The classes were plotted on a map, in order to see if it was possible to delineate sub-regions.

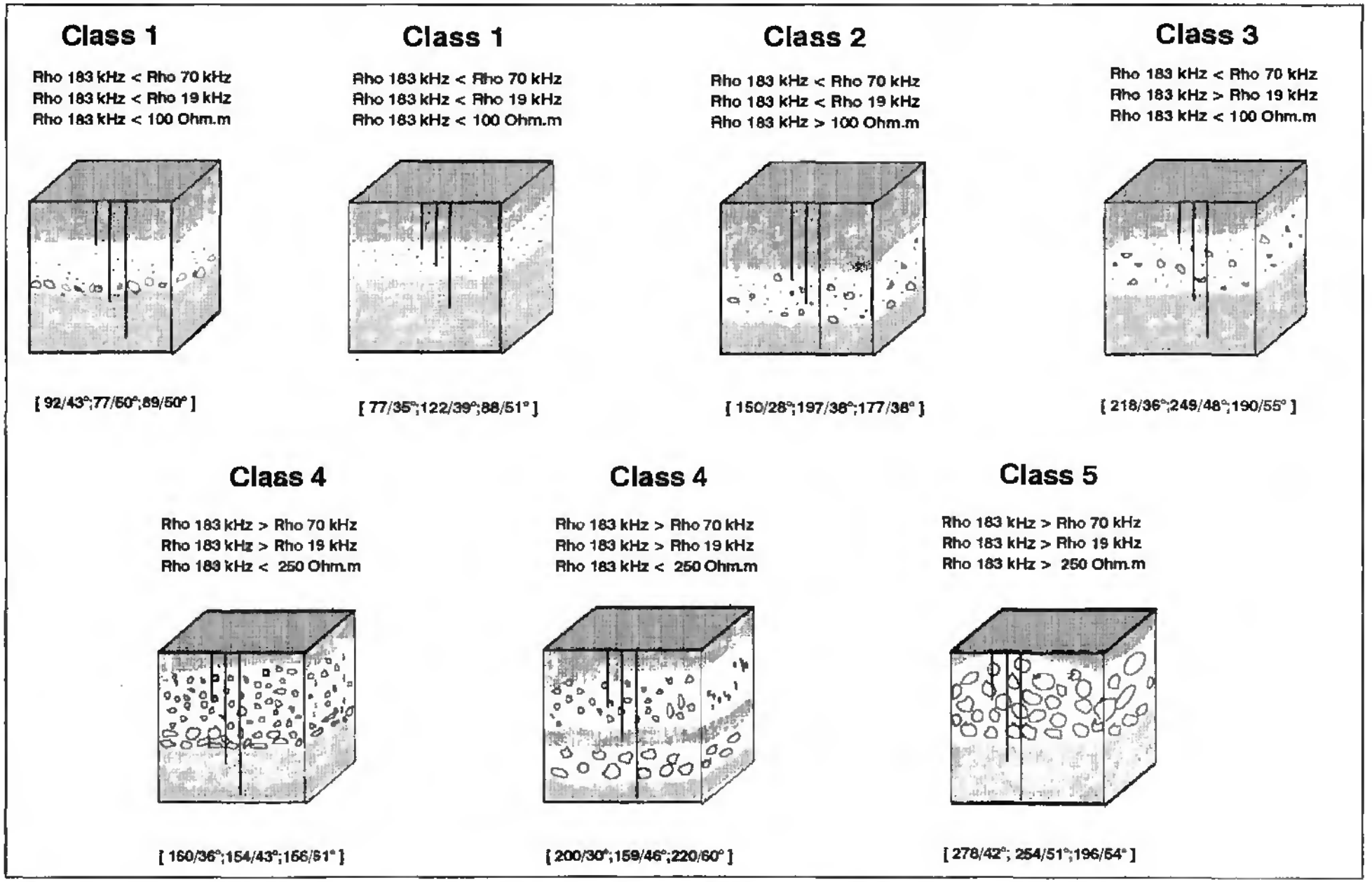

Fig . 29 Possible models corresponding to the 5 classes, illustrating that within each class, different situations can occur.

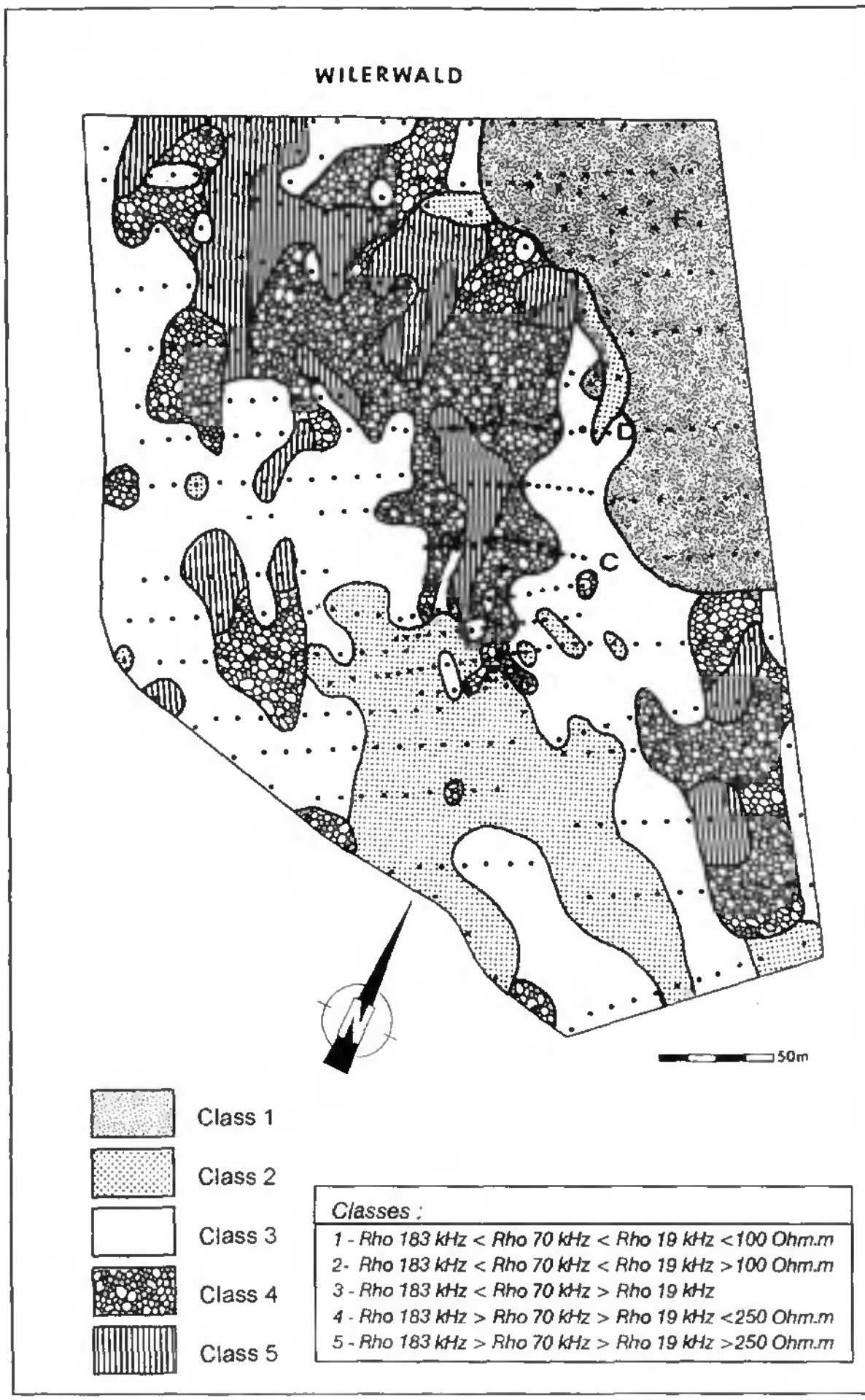

Fig. 30 Map of Classes : a trial to get a qualitative integrated information with the rho ap. values at three depths, simultaneously reflecting the influence of the structure and nature of the materials (see text).

Although the information of this map only has a qualitative value, it is interesting to note that class 1 appears distinct from class 2. Its values are much lower than those of class 2 (finer sediments), which reinforces the idea that they shouldn't be interpreted as grouped together, such as in the Phase Contour Map (**Fig. 23**).

Statistical treatment of the classes:

The cumulative curves of each class were plotted. The statistical information obtained by means of adapted Folk and Ward parameters as written below :

$$Mz = \frac{Rho16 + Rho50 + Rho84}{3}$$

$$\sigma I = \frac{Rho84 - Rho16}{4} + \frac{Rho95 - Rho5}{6.6}$$

$$SkI = \frac{Rho16 + Rho84 - 2\,Rho50}{2(Rho84 - Rho16)} + \frac{Rho5 + Rho95 - 2\,Rho50}{2(Rho95 - Rho5)}$$

Table 8 Folk and Ward parameters **Folk and Ward (1957)**

The next table (**Table 9**) resumes the **Folk and Ward** statistical parameters and the statemeots referred to above.

183 kHz	*Class 1*	*Class 2*	*Class 3*	*Class 4*	*Class 5*
Mean Log	1.678	2.10	2.153	2.247	2.466
Mean (Ohm.m)	59	155	177	177	292
Skewness	-0.435	0.207	-0.158	-0.076	0.252
Standard deviation	0.079	0.138	0.147	0.094	0.073

70 kHz	*Class 1*	*Class 2*	*Class 3*	*Class 4*	*Class 5*
Mean Log	1.832	2.218	2.212	2.192	2.391
Mean (Ohm.m)	88	204	204	156	246
Skewness	0.006	0.203	-0.133	-0.079	-0.146
Standard deviation	0.081	0.147	0.171	0.102	0.103

19 kHz	*Class 1*	*Class 2*	*Class 3*	*Class 4*	*Class 5*
Mean Log	1.808	2.153	2.033	2.063	2.225
Mean (Ohm.m)	79	177	134	116	168
Skewness	0.044	0.097	0.119	-0.036	-0.005
Standard deviation	0.077	0.149	0.161	0.109	0.122

Table 9 Statistical parameters of the Rho appareot values (logarithms) calculed after **Folk and Ward (1957)**

Skewness represents the deviation between the mean and the median of a variable. Where both coincide, there is no asymmetry. Positive asymmetries reflect the predominance of higher values of resistivity in the frequency distribution.
The classification intervals aren't the same as in a grain size distribution , so the quality of the information one can obtained from the parameters calculated, can only serve for comparison.

Observing the three diagrams of **Fig. 31** many considerations become apparent.

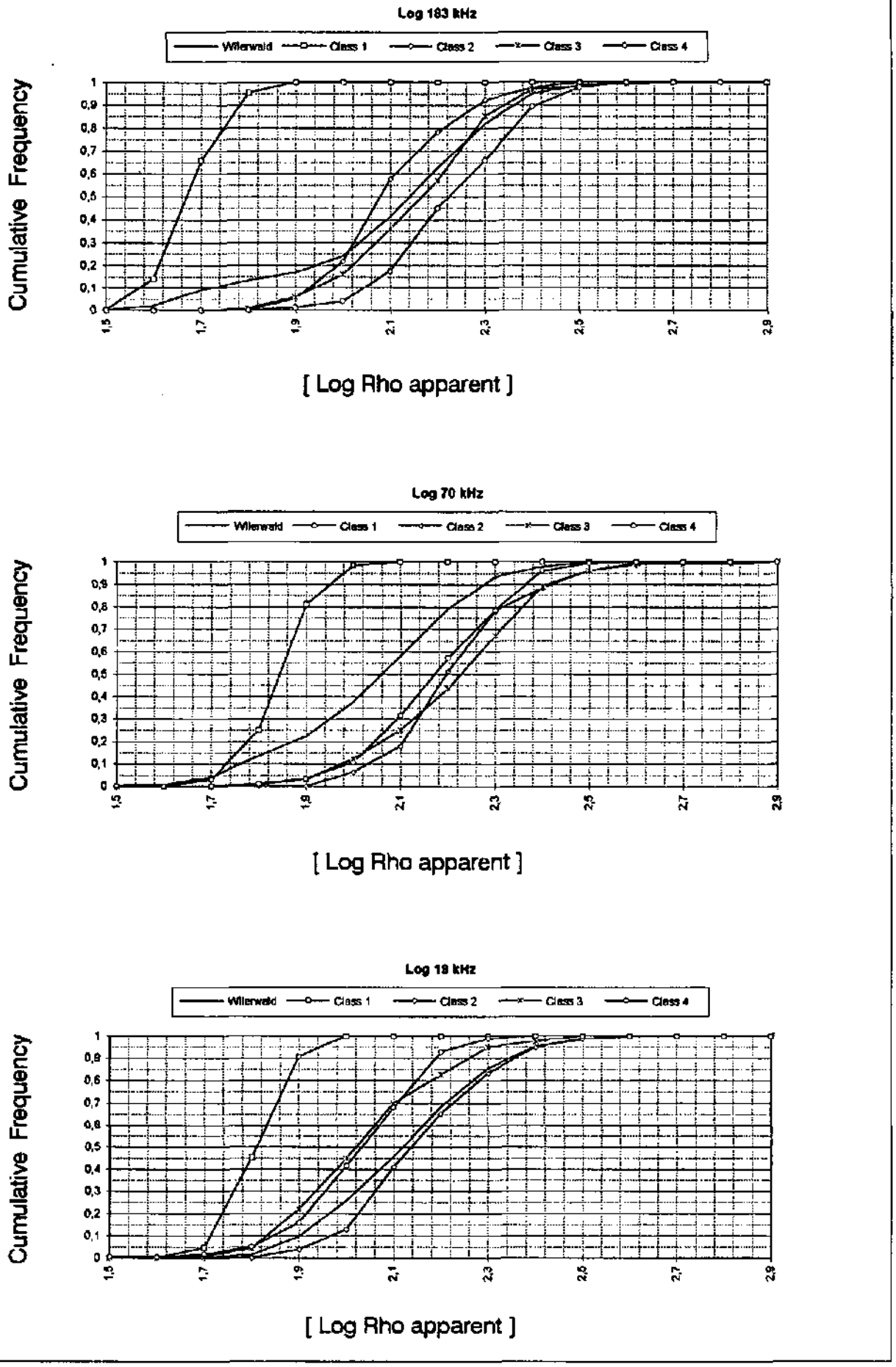

Fig. 31 Cumulative distribution curves of all Rho ap. values of the 5 classes at the three frequencies 183 kHz, 70 kHz and 19 kHz.

- Class 5 and 1 appear well individualised at 183 kHz and 70kHz, but only class 1 remains clearly apart at 19 kHz.
- Class 1 has the lowest standard deviation values, representing a fairly homogeneous sub-region of fine material (of deep lacustrine origin?).
- Class 5 is relatively well selected (clean gravels). So is class 4, though its dimensions seem to be smaller. Its distribution is almost parallel to that of class 5. And this situation is maintained at 70 kHz.
- Class 3 and 2 are not so well selected. Their dispersion of values is very similar, class 3 has slightly higher resistivity values than class 2 . Both classes increase their values at 70 kHz, approaching class 5, which may imply that the channel is larger and the energy of transport higher, or simply that the upper conductive layer no longer has any influence.
- At 19 kHz the situation changes, class 2 and 5 are nearer,class 2 having higher values. Class 5 is no longer so well selected. Class 1 seems to increase its values a little.
- It is interesting to see that the other classes are better differentiated at 183 kHz, practically coincide at 70 kHz (less influence of the upper layer) and than they become more separate again at 19 kHz. The possible reasons for this are:

    1. Either the 70 kHz data, representing older (deeper) sediments than the ones of 183 kHz, could correspond to a period of higher energy of transport. The distribution curves are displaced towards higher values of resistivity. The evolution of the curves also suggests that the bed of the channel has undergone several changes. At 19 kHz, the higher values of resistivity are to be found in class 2.

    2. Or the influence of the first conductive layer is greater in class 2 (thicker). The channel also becomes less and less detectable with the lower frequencies of measurement, because a)the wave has to cross more and more sediments, b) possible lenses of fine material exist and, the influence of the more conductive bottom layer increases.

The same treatment was applied to the phase values. It is interesting to see that class 2 is the one with lower phase values at 183 kHz. As stated above, one can connect this fact to the existence of a more developed conductive upper layer. Otherwise, all 4 classes present values characteristic of the C/R/C situation mentioned in A.1.

In short, from the observation of the cumulative curves following conclusions may be stated:

- If the different frequency ranges describe situations at different depths (that is different ages), they can be used as to express the evolution of the deposition environment.

Therefore one could infer that , there were two main regions at the beginning (at 19 kHz). One represented the more conductive NNE sediments. The other was not well differentiated at the time and included all the other classes.

Than, the classes began to be progressively accentuated. From the situation found at 70 kHz, where a higher energy of transport maybe existed, due to the enlargement of the channel as seen on the apparent resistivity map, till the situation reached at 183 kHz, where this higher energetic pathway (Channel) is restricted to class 5 .

These classes have the character of "sub regions". Within each one a large range of values is possible, reflecting micro-structures and small-scale heterogeneity.

- A totally different interpretation is also possible. The evolution of the classes would be related to the influence of the upper layers or to the fact that with deeper depths the RMT-R information becomes less accurate, because the wave has to cross more and more sediments and the influence of the bottom layer increases. This would make the channel, that was detected at 183 kHz, to disappear (interference of the bottom layer).

Unfortunately both interpretations are only speculative, because no physical proofs exist, since no drillings were made, to confirm.

A.2.3 - Interpretation based on MT. inversion:

With the help of a MT. inversion program (**Fischer & Le Quang, 1981**) (such as the FITVLF2 or a two-layer program), it is possible to calculate the true resistivity of the stratum(a) and the thickness of the layer(s). Both methods were used.

The FITVLF2 results were very complicated. They suggested several sub-layers, sometimes with no lateral continuity, because of the existence of an irregular upper layer and of lenses which are impossible to be detect with the RMT-R survey. Not having the possibility to calibrate the results, we used the two-layers inversion, knowing that this meant even more homogenisation was implicit.

An estimated true resistivity (Rho1) is obtained , using the values of Rho ap. and of the dephasing ϕ measured with the highest frequency. This value is than supplied to the program, along with Rho ap, a corrected ϕ value for the 20 kHz range (because it is known that the influence of the first layer diminishes the actual value of the dephasing) and finally, the lowest frequency used. The 1-D inversion method then calculates the true resistivity (Rho 2) of the more conductive bottom layer (aquitard) and the thickness of the upper layer (aquifer). It ignores the upper conductive layer.

The aim was to obtain an image of the geometry and a distribution of true resistivities for the saturated zone of the aquifer. And so the construction of several profiles (**Fig. 3A-2** in **Appendix 3**), and of a block diagram (**Fig. 3A-3 in Appendix 3**), a resistivity contour map (**Fig. 3A-5** in **Appendix 3**) (**Carvalho Dill**, *in* **Steiner et al,1992**) (**see also Fig. 74, in Chapter 10**), and an aquitard's depth contour map (**Fig. 3A-4** in **Appendix 3**) was possible.

These calculations are approximate because of several uncertainties, but useful when applied carefully (**Turberg,P.,1992**).
Unfortunately, only one drilling was performed at the test site. This does not really suffice to calibrate the calculations. Added to this, the drilling itself wasn't deep enough to conclude whether the silty-clay level found at the bottom was continuous downwards or not.

B. Multidirectional RMT-R

Multidirectional RMT-R is based on the anisotropy of the electrical properties of the sediment. (**Fischer et al, 1983**).

Its principles can be summarized as follows (**Fischer et al, 1983**).

- According to whether the alignement of a conductive body is perpendicular or parallel to the direction of the emitter, a measurement will be said to be respectively in **H-polarisation** or **E-polarisation**.
- In the presence of a conductive body and when the measurement is made in E-polarisation, the resistivity will increase and the phase decrease.
- If the measurement is made in H-Polarisation, the opposite effect is to be expected, i.e a decrease of the resistivity and an increase of the phase.
- In an isotropic medium all the measurements performed at the same point will be equal.
- If, instead of a conductive dyke, one has a resistive one filled by more resistant material (channel), mesurements made parallel to the dyke's direction will have the highest phase and lowest resistivities, just as in the H-Polarisation. And the opposite will happen when the measurements are made perpendicular to the channel's direction.

Directional anisotropies of the deposits that are detected will therefore also give information on the paleosedimentology. This was also tested at Wilerwald.
Emitters of the same frequency range (200 Ohm.m), situated in the following directions were used : N-S (183 kHz), N40 (153 kHz), E-W (162 kHz) N130 (198 kHz).

Wilerwald was quite a complex case and presented deviations from the simple cases described above. This is due to the fluvio-glacial character of these deposits. Parallel to the main direction of flow, elongated deposits of fine material alternating with ones of coarser sediments were once thrown up. The influence of these elongated lenses is apparently stronger than that of the coarser material, because the readings were often contrary to those expected: the highest values of resistivities and the smallest phases were obtained on measurements performed parallel to the channel.

Another aspect must be mentioned: a fluvio-glacial channel filled with loose sediments has a complicated structure. Instead of a clearly-shaped dyke, the pathways are tortuous, constantly changing direction. Therefore one can't really talk about E- and H-polarisation. The lowest phases are not always found with the highest resistivities, and vice-versa.

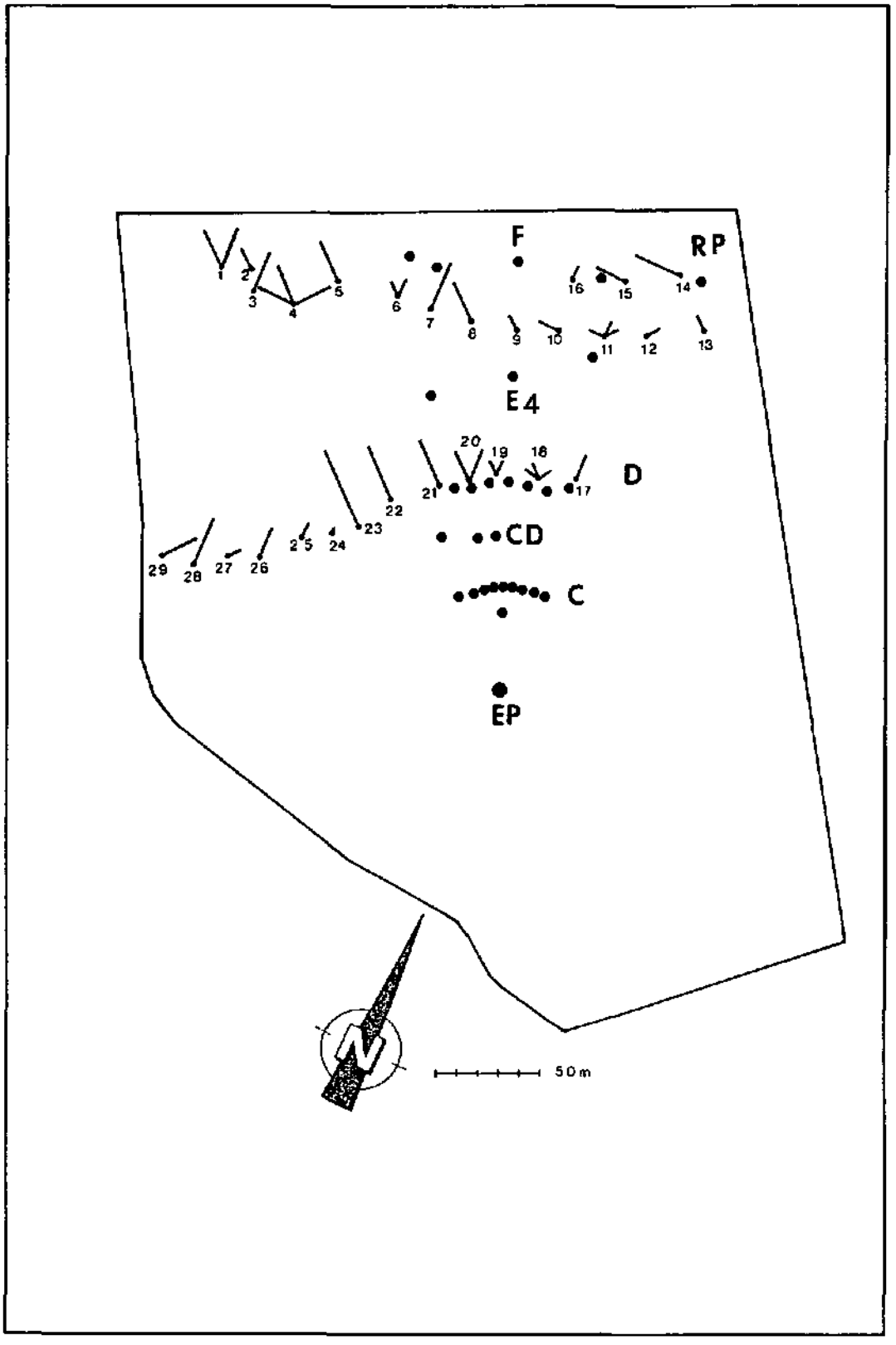

Fig. 32 Map with the results of RMT-R multidirectional.

- Observation wells
- RMT-R measuring stations

/,/ delta ϕ (for the exact value please see Tab.10)

These measurements are presented in **Table 10**. The important observation to make is that most of the stations are anisotropic. The fine elongated lenses do play a very important role in defining the electrical properties of the aquifer. Therefore one can infer its influence on the water flow and on the existence of anisotropies of permeability, not in accordance with the homogeneous laminar flow often said to be characteristic of porous media.

On the map of **Fig. 32** the differences between the highest and the lowest phase value were plotted in the direction of the lowest phase value. As one can see sometimes it corresponds to more than one direction (points 4, 18, 20,etc).

It is ioteresting to observe the D gallery, situated close to the confluence of the two channels, which is followed by strong anisotropies of convergent directions.

Direction	N S		N 40		E W		N 130		Delta Phi
Frequency	183 kHz		153 kHz		162 kHz		198 kHz		
Station Number	Rhoa	Phi	Rhoa	Phi	Rhoa	Phi	Rhoa	Phi	Phi max-Phi min
1	362	35	351	40	270	40	301	35	5
2	204	38	192	40	162	39	177	37	3
3	243	35	273	36	202	40	210	39	5
4	108	40	88	35	166	35	153	35	5
5	163	35	144	38	230	36	179	33	5
6	143	36	143	38	147	38	148	36	2
7	144	33	155	34	130	39	134	34	6
8	143	35	158	36	133	39	138	34	5
9	84	35	108	34	87	35	77	33	2
10	57	36	58	36	55	33	55	33	3
11	67	34	68	34	64	34	36	36	2
12	70	34	73	33	73	35	67	35	2
13	60	34	66	34	68	35	61	33	2
14	48	39	48	35	58	34	51	40	6
15	58	35	60	33	62	31	60	34	4
16	53	32	63	34	58	34	56	33	2
17	85	33	88	34	68	36	81	34	3
18	135	37	158	35	160	35	144	35	2
19	120	35	143	37	146	37	125	35	2
20	173	38	172	42	147	39	173	38	4
21	240	36	200	41	209	40	252	35	6
22	181	36	195	41	229	39	235	34	7
23	193	35	200	41	152	42	156	32	10
24	188	36	248	37	214	37	165	37	1
25	268	35	314	37	233	36	243	35	2
26	190	35	202	38	245	39	224	37	4
27	143	39	191	38	165	40	125	38	2
28	173	36	180	38	142	42	162	40	6
29	150	35	256	33	284	36	199	38	5

Table 10: multidirectional RMT-R data. The position of the stations can be seen on the Map of **Fig. 32**.

C. VLF-EM - Very Low Frequency - Electromagnetic survey

The continuous recording of the out-of-phase component by the VLF-EM technique was also tested by walking, on the Wilerwald test site. **Fig. 19b)** shows the VLF-EM profiles executed inside the testsite area. In **Fig. 33**, one can see the VLF-EM continuously recorded profiles and the RMT-R 183 kHz contour map.

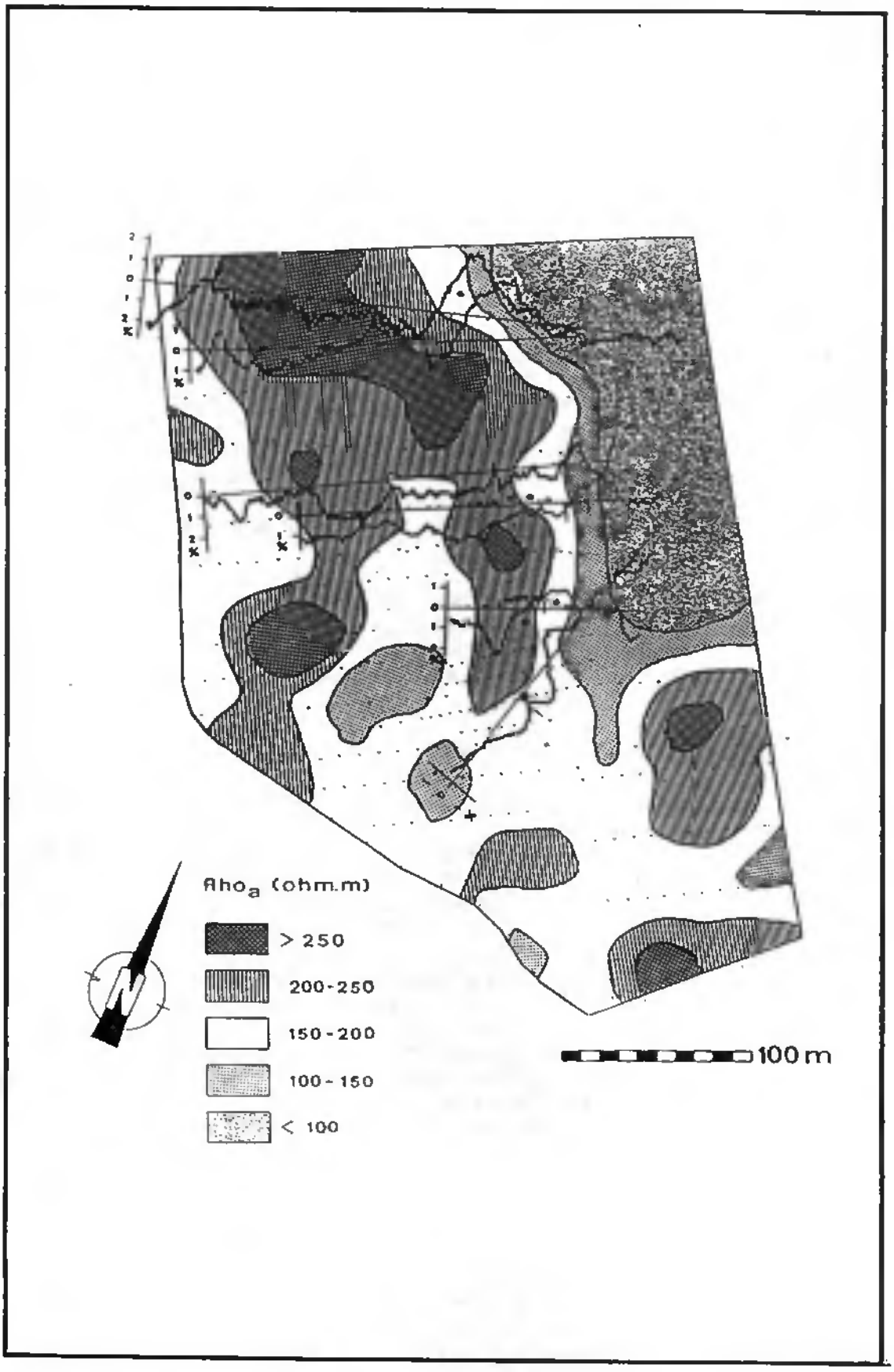

Fig. 33 Map showing the VLF-EM profiles inside the site, in correspondence with RMT-R results.

As one can observe, the channel is also detected very clearly with the VLF-EM method, since it represents a significant change in lateral electrical conductivity and layer thickness. The more conductive region is also detected - the out-of-phase component increasing towards the positive values. Comparing these profiles with the ones performed on the region (**Fig. 13**), we see that the channels belong to those anomalies referred to as class -2 and 0 This gives an idea of theorder of magnitude of the anomalies of class -4, found regionally near the railroad.

The Centre d'Hydrogéologie de l'Université de Neuchâtel now possesses modelling programs (**Steiner et al, 1992**) which allow the calculation of strata with different resistivities and thicknesses. However, we did not use these models. The main reason was the lack of direct information (no boreholes), making it impossible to calibrate the model. Secondly, the existence of lateral and vertical heterogeneities sometimes of metrical dimensions, would make any modelling unrealistic.

D. Audio magneto-telluric method:

Tropical thunderstorms cause perturbations of the Earth's natural magnetic field,creating electromagnetic currents of much lower frequencies than those used with RMT. These frequencies range below 12 kHz (at Wilerwald frequencies down to 35 Hz were used), reaching considerably greater investigation depths. Unfortunately, some restrictions to the use of this method exist in highly industrialized countries, because of the electromagnetical perturbations caused by the industries. One must to be located several kms away from such a region. The more conductive the sediments, the lower the perturbations. Wilerwald being far enough from an industrial area, the NNE area of the test site was selected for this investigation. The **Fig. 3A-1** in **Appendix 3** shows the evolution of the resistivity according to depth, calculated, as for the RMT-R, with the help of the automatic 1D-MT inversion (**Fischer et al, 1981**).
We can see that below a more resistant superficial layer (300 Ohm.m) the resistivity diminishes to less than 50 Ohm.m (up to 20 m). A unit with resistivity values of about 70-80 Ohm.m follows at 20 meters depth (q4r lacustrine sediments ?). According to the findings from boreholes drilled in the zone, the aquitanian follows - corresponding maybe to the next values, at over 130 metres depth. A plausible correspondence could be with marls (Rho values of about 20-40 Ohm.m), followed by sandstones (300 Ohm.m ?).

4.1.2 Electrical method : Schlumberger configuration

Schlumberger soundings were used to complete the gaps of the RMT soundings in the characterization of the upper layer formed of humus and silty, sandy clay.
The maximal distance between electrodes was 35,6 meters (AB/2 = 17,8 m) at the most of the soundings (See **Fig. 19a**), which thus allowed a detailed characterization of the first 6 to 8,5 meters depth. The two longer profiles SE_1 (C7) and SE_2 (25m east from C0) had AB/2 equal to 70 meters. The accuracy of the geoelectrical apparatus is better than 0.2 % of the resistivity value measured.

The true resistivities and the different depths of strata were calculated by inversion with a best-fit program which uses the Gosh filters. The results transformed into resistivity logs are plotted on **Fig. 34**. It is interesting to see that the thickness of the silty clay layer (Rho < 60 Ohm.m) clearly increased in the NNE area (F4,F2,R1,Rp, D1). It also shows the influence that this layer may have on the RMT-R measurements of the 1&3 kHz, considerably lowering the Rhoap and the phase values there. It also underlines the confined situation of the aquifer there, which will influence the interpretation of the measurements of the ground water level. The thickness of this layer diminishes towards the channel,where it is substituted by a sandy stratum (C7, D6). The thickness of the aquifer and the dimensions of the gravel, according to the higher values of resistivity, seemed to increase in that direction too.

4.1.3 Seismic Surveys

Two seismic surveys (profiles S1-S2 and S3-S4, in **Fig. 19a**) were carried out, in order to check whether the high resistance values were due to the existence of the loose-gravel channel. Similar values could be obtained in the presence of a changing of facies in sandstones (such as a tertiary paleochannel filled with Nagelfluh).

The seismic profiles were oriented perpendicularly to the channel.

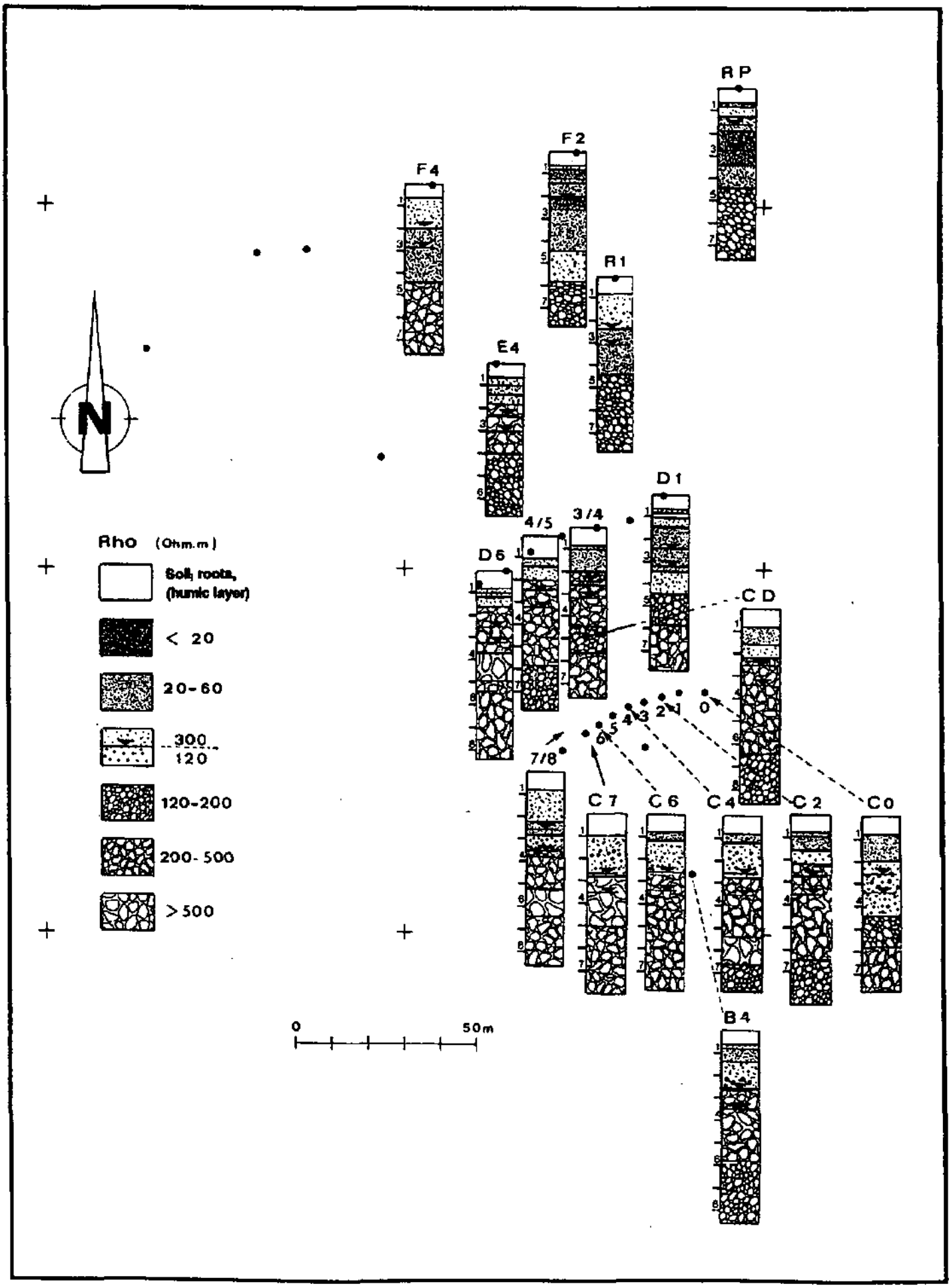

Fig. 34 Map of electrical soundings. The following features can be observed:
1) the situation of D1, R1, RP, F2 and F4 (confined);
2) the increased thickness of the silty clay layer in the east part of the site;
3) the aquifer thickness, greater in the channel (C7, D6), and also the increase of resistivity values increase of the gravel dimensions) there.

The existence of the channel was proven by the refraction survey S3-S4 (see **Fig. 35**): the channel effect can be seen by the loss of velocity up to the 12th geophone. The clean and coarser gravels have a higher porosity and a lower density (looser material), so they functions as a vertical dike, attenuating the velocity.

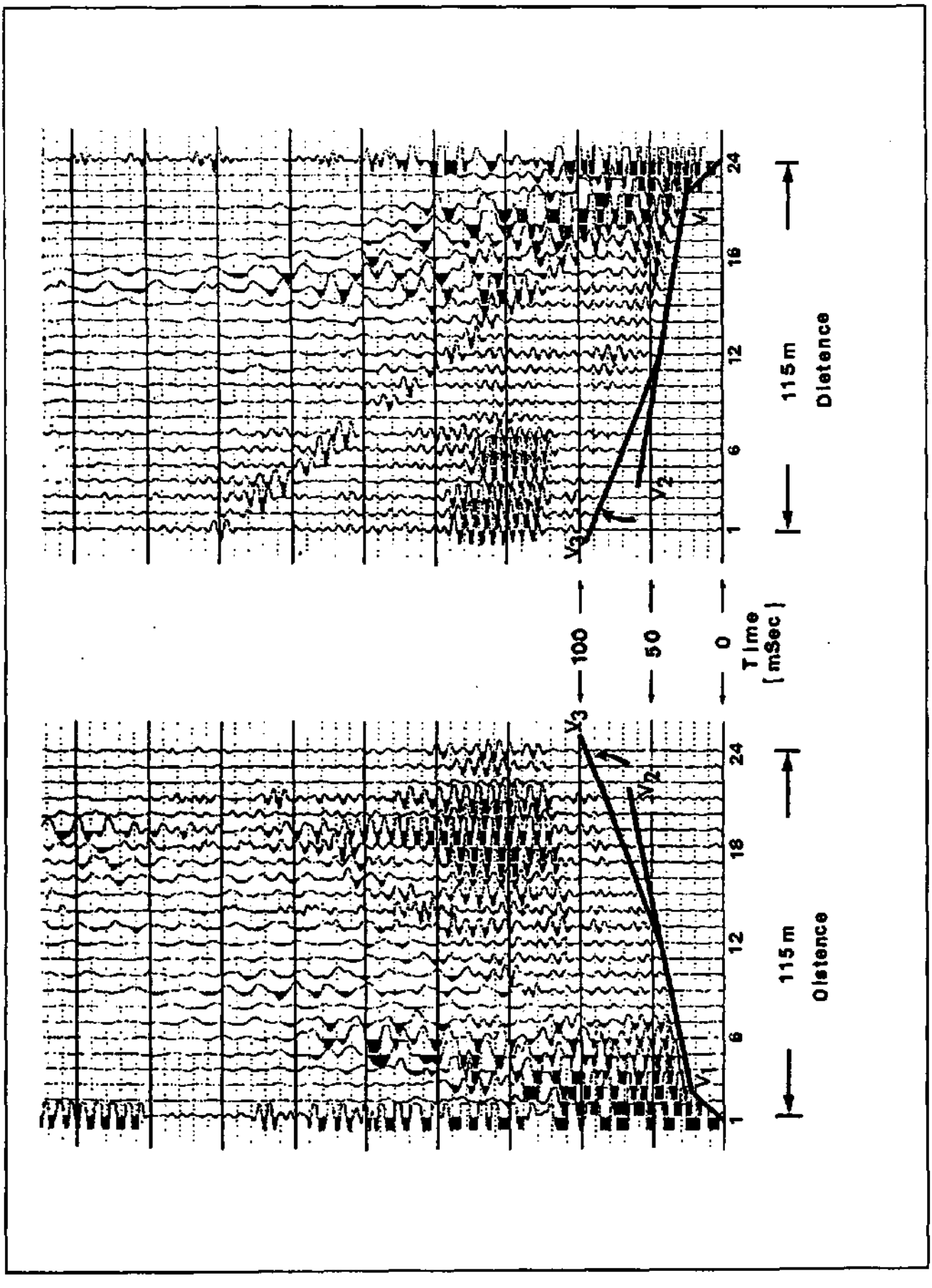

Fig . 35 Seismic results confirming the paleochannel.

4.2 Local geological aspects: Borehole CD and resistance to penetration.

Only one borehole was drilled at the Wilerwald test site - the borehole CD (**Fig. 3**). According to the RMT measurements it seems that the drilling reached the formation q4r (silt and clays). Nevertheless the possibility that it could be an intercalated finer lens cannot be excluded.

The drill core was submitted to a grain-size analysis. The samples were taken whenever a change in grain size or colour occurred. The grain size cumulative distribution curves of the aquifer samples are given in **Fig. 36**. The depth of each sample is indicated. After 80 cm of silt and humus, there are 80 cm of silty sand, followed by 60 cm of light grey silty sand. Two main sandy lenses are evident at 12 and 6 m depth. At 7 meters there is a sub-level distinct from the others (silty sand with gravels). The passage to the aquitard (?) begins at 14.5 m depth: the curve at 15 m is clearly displaced into the silt domain and possesses greater homogeneity.

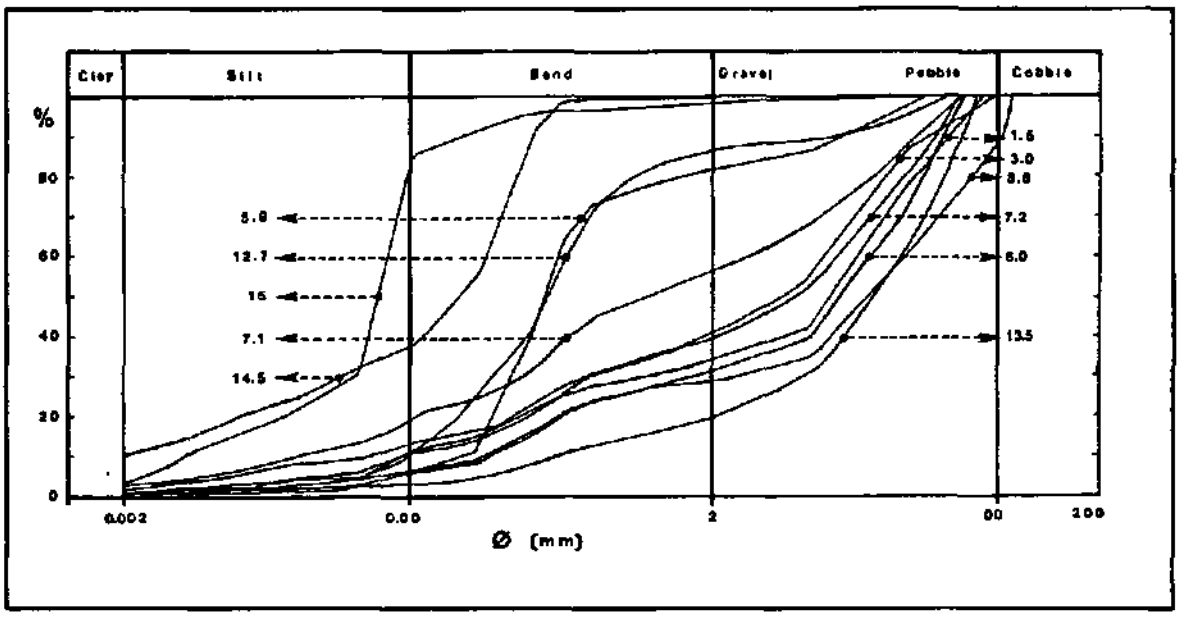

Fig. 36 Grain size cumulative distribution curves of the samples taken from the borehole CD. The depth of the sample is indicated and is in meters. One can observe that aquifer curves reflect the heterogeneity of the sediments (very inclined, almost horizontal curves). Some lenses have very distinguish curves reflecting the more percent on the sand fraction. The passage to the aquitard (?) can be clearly seen at 14.5 m depth. At 15 m depth the curve is dislocated toward the silt domain.

The **Fig. 37** shows the lithological log where all layers and lenses with their actual sizes are represented. At the borehole CD the largest gravels were found from 3.7-6 meters (see also **Fig. 36**, •→3.8)

It is also of interest to compare the lithological log with the Schlumberger log (**Fig. 38**). The higher resistivity values correspond to the same depths mentioned above, which is also an indication of the validity of the information given by the Schlumberger logs.

Six piezometers for measuring the groundwater level were installed in May 1992 (**Fig. 3**). These were metal tubes perforated with very small orifices and penetrating on average 6 meters below surface. The resistance to penetration during their installation was registered and can be seen in **Fig. 39**. It is interesting to see that the graphic of R5 (situated about seven meters from CD), situates the more resistant level (consequently the coarser one) between two and three meters deep, whereas at R4 (57 m downstream) the highest dimensions were found below 5 meters. The graphics only give a qualitative information. But clearly the small scale (order of magnitude 10^0 m) of this great vertical variability.

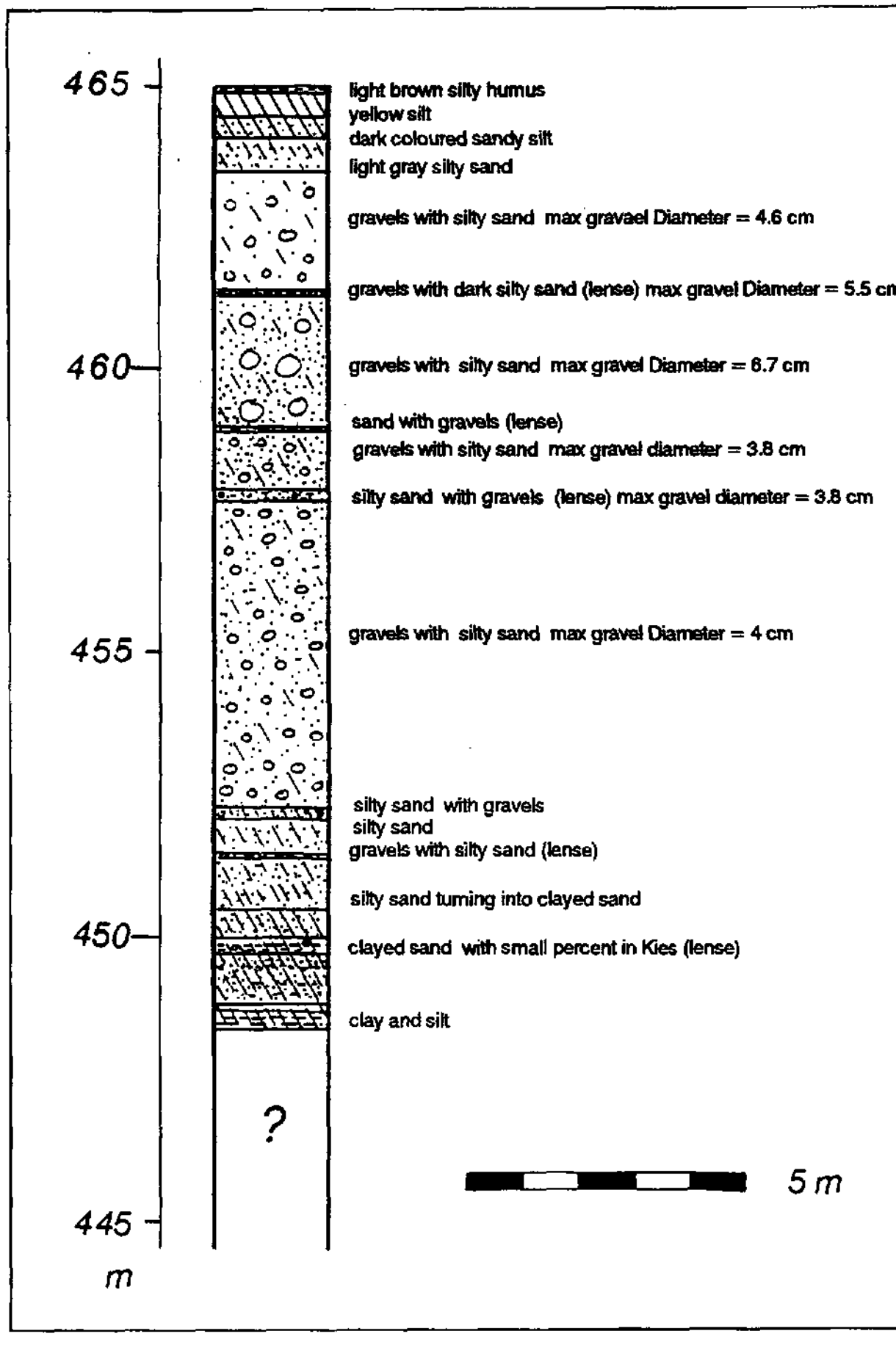

Fig. 37 Lithological log from the borehole CD.

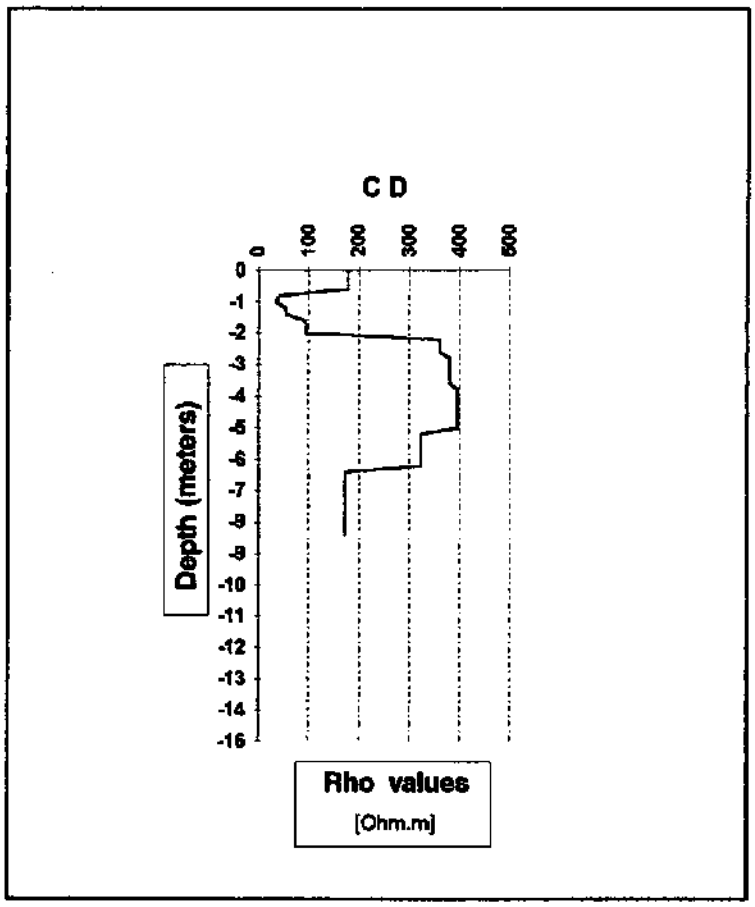

Fig.38 Schlumberger resistivity log of the borehole CD

4.3 Synthesis and conclusions

The carried out RMT-R soundings were ideal, and this because of the density of measurements (~ 500 in the test area), because of the its rapidity and versatility. At the same time the degree of information obtained is quite elucidative - it yields a good picture of the aquifer, about its geometry and about its resistivity distribution, related to permeability. We used manly three frequencies : 183 kHz, 70 kHz and 19 kHz.

Kriging was used to construct the apparent resistivity maps for the three frequencies. Since the investigation depth is a function of the frequency used and of the resistivity of the medium, we obtained a representation of the aquifer at three different depths. The map of 183 kHz showed the existence of a channel crossing the observation wells area and confluent to another nne situated further west. It affects the piezometers C7, C6, D7 and D6 more directly.

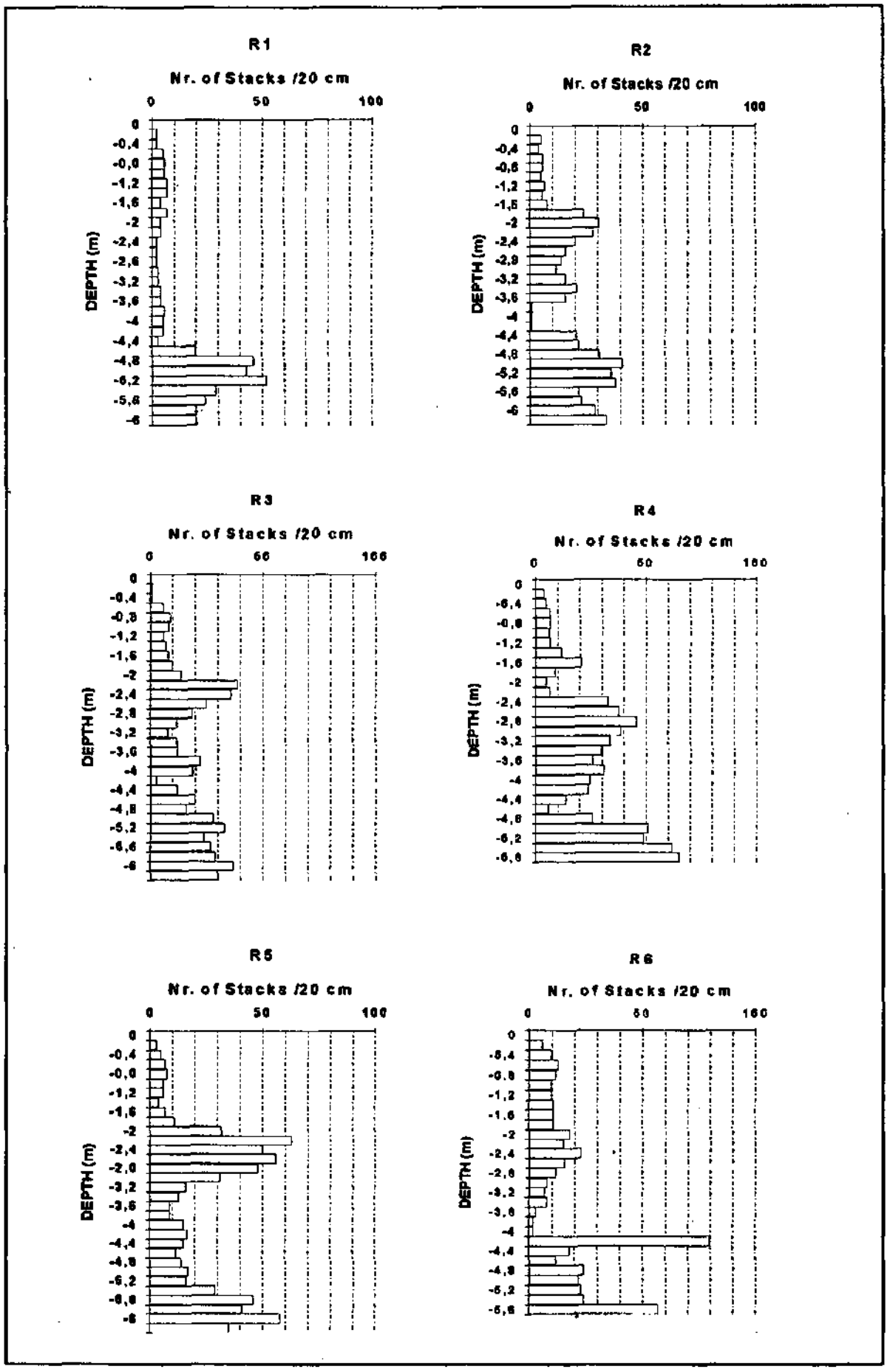

Fig. 39 Graphics representing the depth distribution of the resistance to penetration of the piezometers installed in May 1992 for groundwater level measurements. For the localisation of the piezometers please regard Fig. 3.

The interpretatioo of the RMT-R raw data with the help of a new approach was utilised, based on the indirect relationship between resistivities and grain size distribution, emphasize the beterogeneity. Instead of individualising "well defined uniformed" small classes I end up by emphasising all the possible situations within each class. We this method it was also possible to delineate the regions where an upper conductive layer (impermeable) exists, defining zones of captive aquifer.

RMT-R multidirectional soundings were carried out, revealing the anisotropy of the medium, conditioned by the existence of elongated deposits of fine material alternating with coarser sediments and parallel to the main direction of flow.

Very Low Frequency Electromagnetic (VLF-EM) surveys were done at the Wilerwald test area. The recording profiles were placed over the RMT-R 183 kHz map, allowing to establish a relationship between the RMT-R and the VLF-EM results.

Another electromagnetical method - AMT - was tested at the site .Because this method has great limitations in industrialised countries, due to all possible interferences, the results should only be regarded as possible and as a curiosity. Among them it seems that the very low resistant layer occurring at 130 m could correspond to the beginning of the aquitanian.

Schlumberger soundings were used to complete the gaps of the RMT soundings in the characterization of the upper covering layer of the aquifer. They revealed the confined situation of the piezometers D1,R1, RP, F2 and F4, the increase thickness of the upper silty-sand layer in the east part of the field and the increase on aquifer's thickness along the paleochannel.

Finally two seismic surveys confirmed the existence of the paleochannel.

The study of the single drill core CD allowed a detailed punctual sedimentological description. Together with the indirect information given by the resistance to penetration registered during the piezometers installation, we could determine the local existence of irregular lenses of finer material. These lenses seem to be irregular distributed, indicating, definitely that we cannot talk about the existence of parallel continuous layers mainly in fluvio-glacial sediments.

Part III : Local studies, field experiments and analyses

5. Local hydrodynamic aspects

5.1 Works performed

5.2 Conclusions about local hydrodynamic aspects

5. Local hydrodynamic aspects

5.1 Experimental work

The study of the piezometric surface and its evolution can yield a lot of information about the flow of the aquifer and the distribution of its properties. In order to avoid misinterpretations, it is important that the conditions be the same in all the observation wells, so that their information be comparable. In a heterogeneous aquifer it is also important that the observation well penetrates the whole thickness of the aquifer and that the tubes be perforated along their whole length. Only so can one obtain a comparable mean potentials. This problem will be re-examined later on.

Another important lesson learned at Wilerwald was the tremendous importance of the frequency of measurements. At the beginning, we thought that a periodical observation of the groundwater level would be enough. Not expecting great changes, we started with readings every 15 to 30 days. These results can be seen in **Appendix 3 - Fig. 3B-2**. The Figure speaks for itself. Nothing can be said about the evolution of the groundwater level with these measurements. One could erroneously infer the existence of a trend and than try to see if any law of reaction could be stated that would agree with the existent heterogeneity. However, comparing the data with the rain events (graphic above) one comes to the conclusion that a lot of information was lost.

The idea to measure almost every day if possible came during the last tracer experiment. We had planned to take readings every week in order to control the local directions of water flow. (**Fig. 40**). Fortunately it rained a lot. When after the first week very significant changes were observed, we realised that it was important to measure them as frequently as possible.

It is interesting to see that the piezometer which varies a lot and presents one of the greatest amplitudes of variation is Rp, the one situated in a less permeable region (D1 had the greatest amplitude). Remarkable also is the comparison of the water-level situation of this piezometer between **Fig. 3B-2 in Appendix 3** and **Fig. 40**. From the lowest position (June-Sept.) it moves to an intermediate one, although it is situated downstream from R4 .

Fig. 41 presents the difference between the maximal and minimal values at all the piezometers from June to Sept., and in Nov.-Dec. Both C0 and D1 are very conspicuous in the two graphics, but Rp only in Nov.-Dec. One possible explanation is to relate the greater amplitudes to the less permeable piezometer - i.e., slow dissipation of energy because of the impediment to the water flow (see **Chapter 3.2**). Could the opposite reason be valid for D7? Being the main drainage the volume of water flowing is greater. But in this case, why do C7 and D6 not present similar profiles?So as to open up new possibilities of explanation, the main information from the Schlumberger survey was plotted with the groundwater amplitude. It is clear that the piezometers D1, R1, F4, F2 and Rp are in a confined situation. This should also play a role on the values obtained, specially if the observation well doesn't traverse the whole aquifer.

The conditions in the observation wells are not all the same at Wilerwald. The six piezometers installed in May 1992 do not penetrate enough into the aquifer, as do the others. They reach circa 3 to 4 meters below the groundwater level, so that one cannot be sure whether the water-head always corresponds to the groundwater level and if it is in equilibrium with the atmospheric pressure. In an heterogeneous and anisotropic aquifer the potential measured at different levels will be different (**Bouzelboudjen,1991**). In order to check the importance of this factor, the maximal and minimal depth of water level of all observation wells were plotted. Six piezometers stand out: R2, F6, F4, F2, RP and R4. F6, F4 and F2, are complete observation wells, bridging the whole breadth of the aquifer. R2 and F6 lie in a region whose surface is particularly depressed, no wonder that it is the one with the water level nearest the surface. The others are in confined situations.

As for using other methods, it has already been hinted that the small diameter of the observation wells limited the possibilities of performing pumping or flowmeter tests etc. at Wilerwald.
On the other hand, these same small diameters can become an advantage, if one seeks to reproduce the natural situation of the flow field, because the convection flux within the piezometers will be lowered.

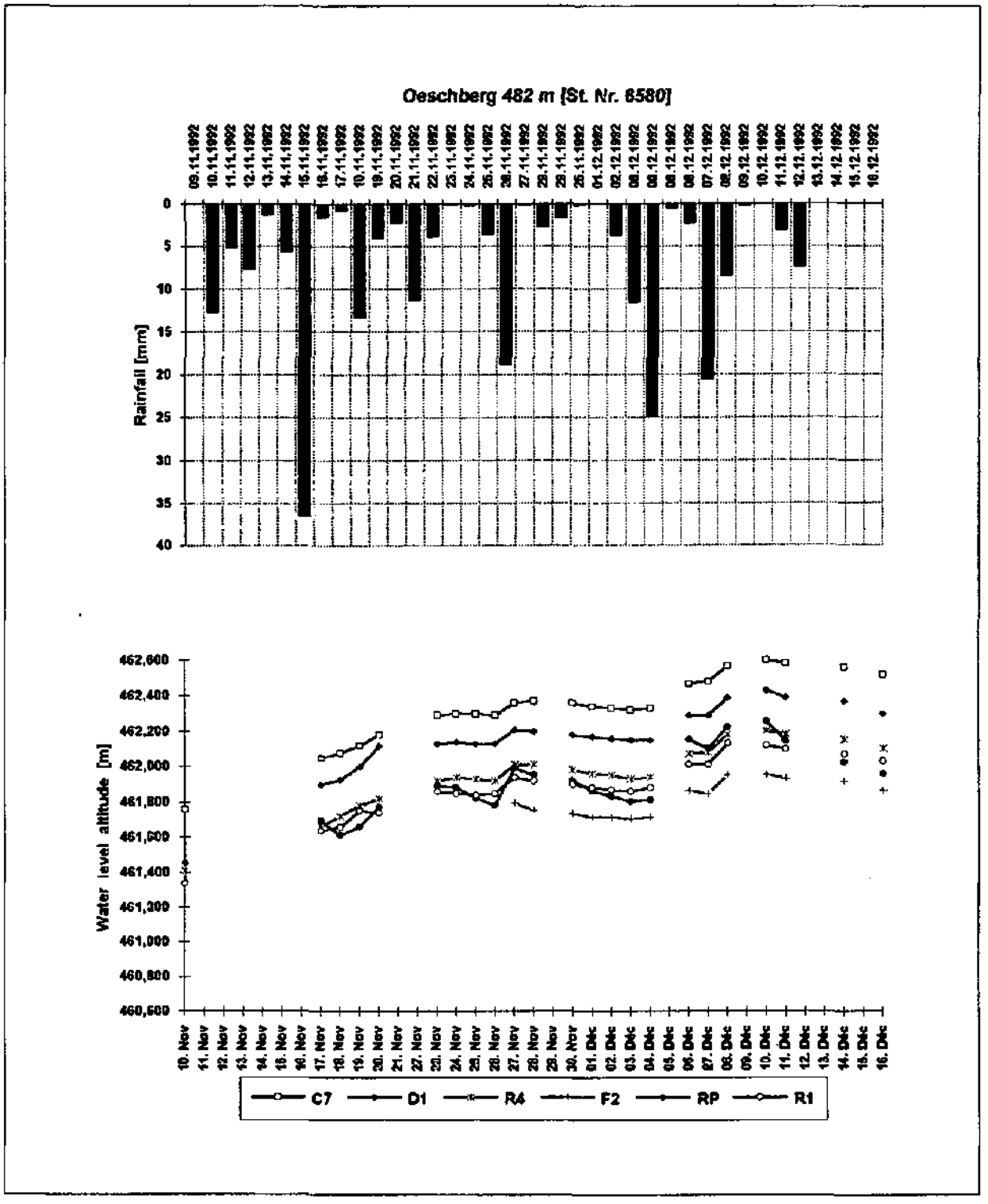

Fig. 40 Groundwater level measurements performed during the 1992 tracer experiment (graphic below). The rain fall events and their magnitudes are plotted on the graphic above (Station Oeschberg).

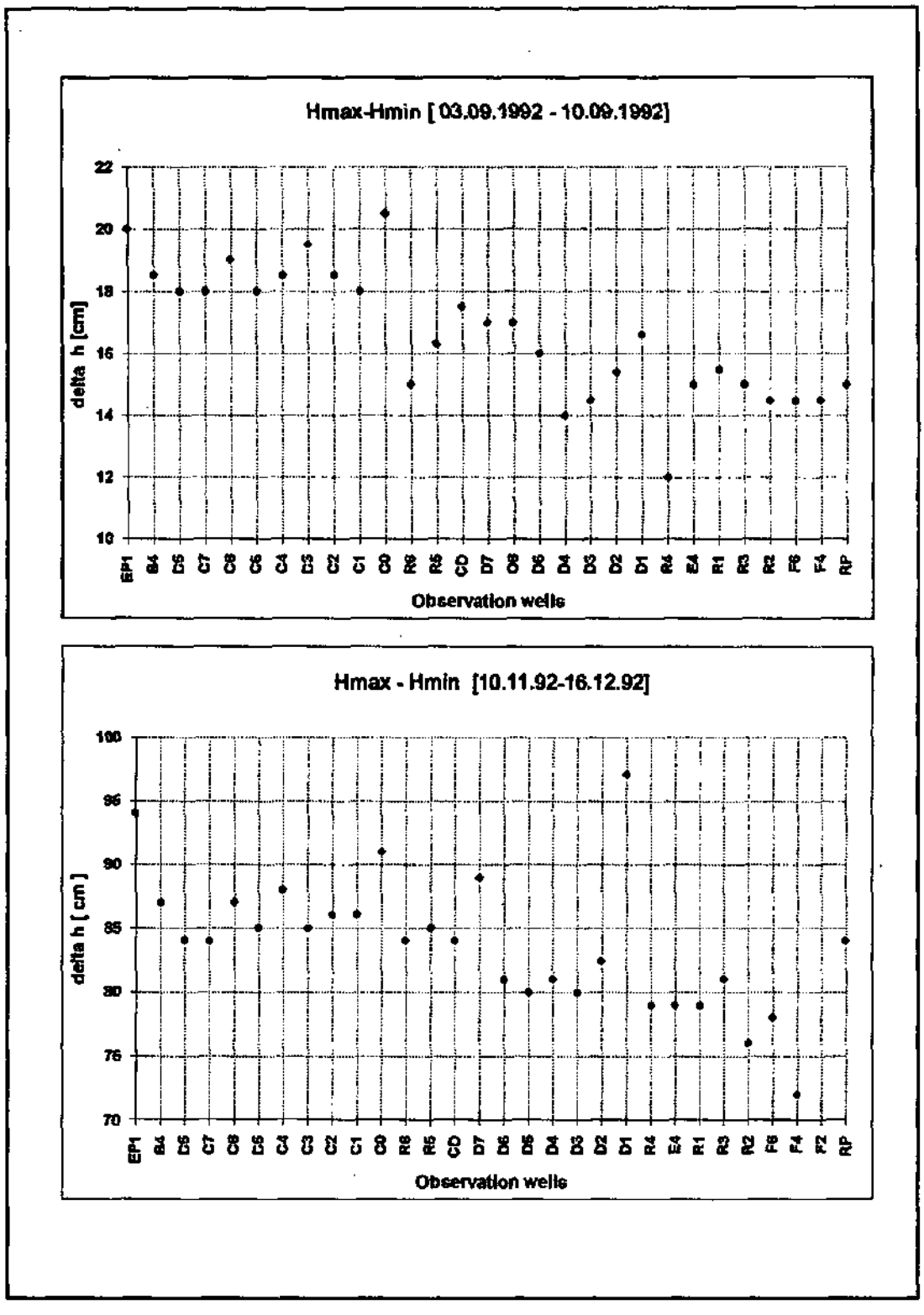

Fig. 41 Differences on head maximal and minimal values, for the periods of June-Sept. (sporadic measurements) and Nov.-Dec. 1992 (almost daily measurements, during one month).

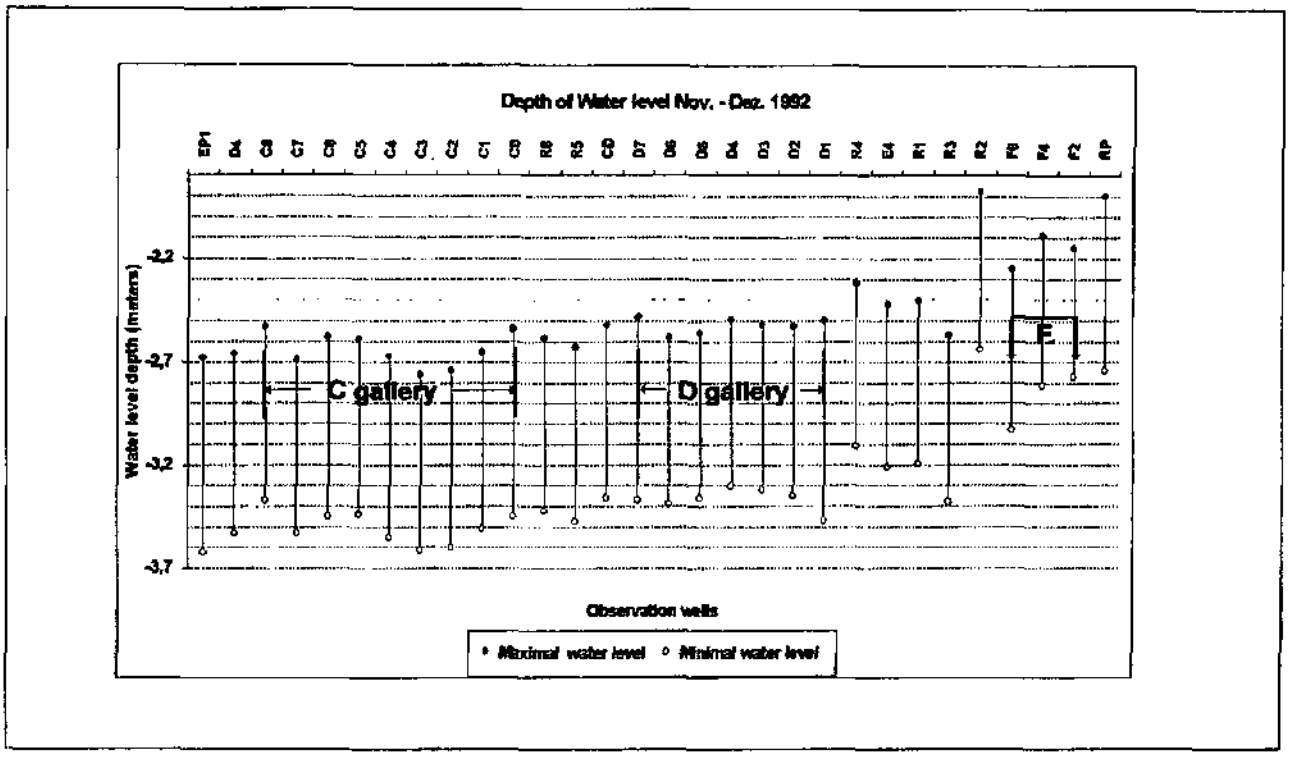

Fig. 43 Depth of the groundwater level at each observation well.

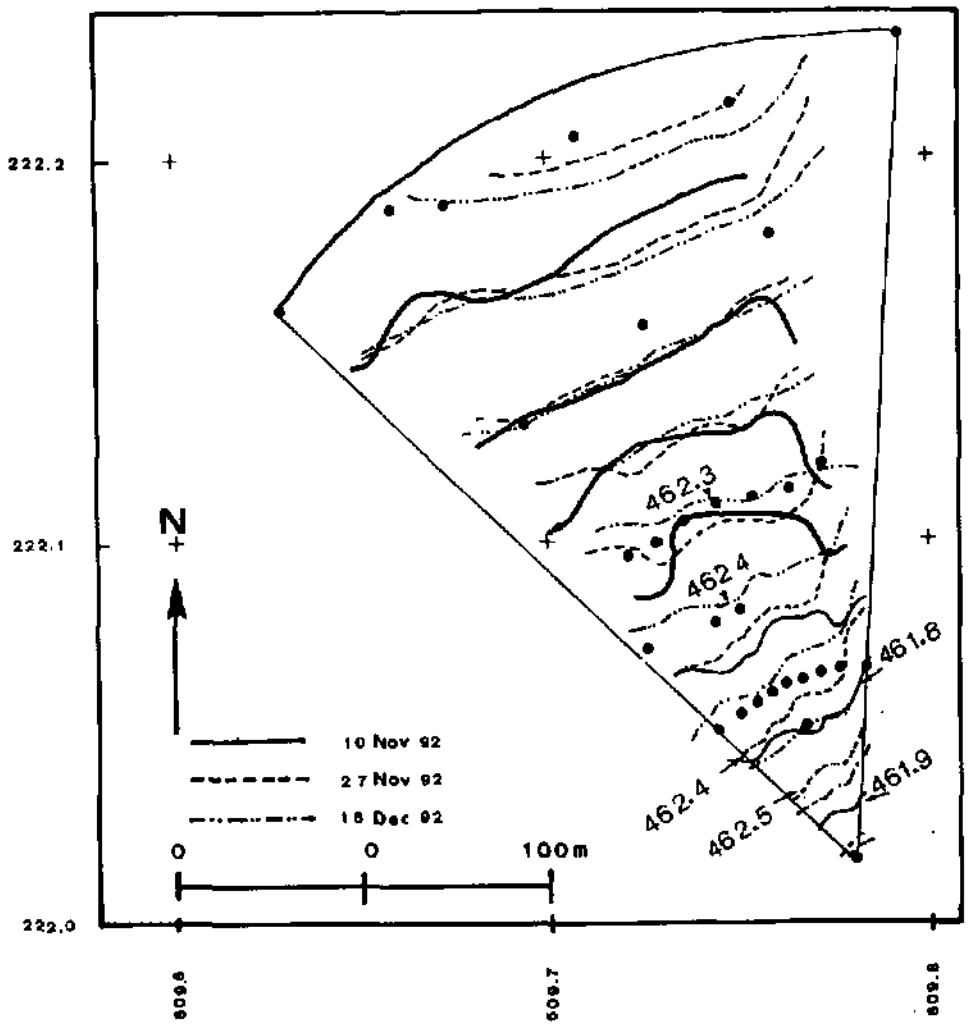

Fig. 44 Piezometric maps representing the three situations of the isohypsen during the tracer experiment Nov./Dec 1992. 10 Nov. day of the injection; 16. Dec. last day of the experiment; 27 Nov. an intermediate situation.

5.2. Conclusioos

According to the piezometry, local variations of flow can be created. **Fig. 44** presents 3 situations observed during the tracer test : on the day of injection (November 10), at the end of the test (Dec. 16) and oo an intermediate day (Nov. 27). The depression observed around D1, at the beginning of the tracer test is remarkable. It will have an important influence on the data collected during the tracer experiment. This figure also suggests the existence of a time and space variability of the heads. Consequently, there are changes in the directions of flow, depending on the prevailing gradients. This important aspect which must be taken into account in studies of solute transport.

Finally, **Fig. 45** shows a longitudinal profile along the "main direction of flow", and how the groundwater levels vary constantly, illustrating the variability of possible situations, due to the specific conditions in each observatioo well.

In summary, the following main conclusions can be retired from what is written above:

1. It is very important to follow the evolution of the groundwater level very closely (at least daily), and to do so over a long period if one wants to be able to study the response of the aquifer to rain events.

2. Similar conditions should prevail in all the piezometers. One should not forget that in a heterogeneous anisotropic aquifer the hydraulic potential variation with depth is uneveo and this can also have an influence on the readings if the piezometer does not penetrate the whole breadth of the aquifer.

3. Higher amplitudes seem to be related to less permeable regions. However piezometers situated ia the channel presented sometimes similar variations.

4. At Wilerwald one can find situations of free nappe as well as from confined ones. This should also influence the readings made.

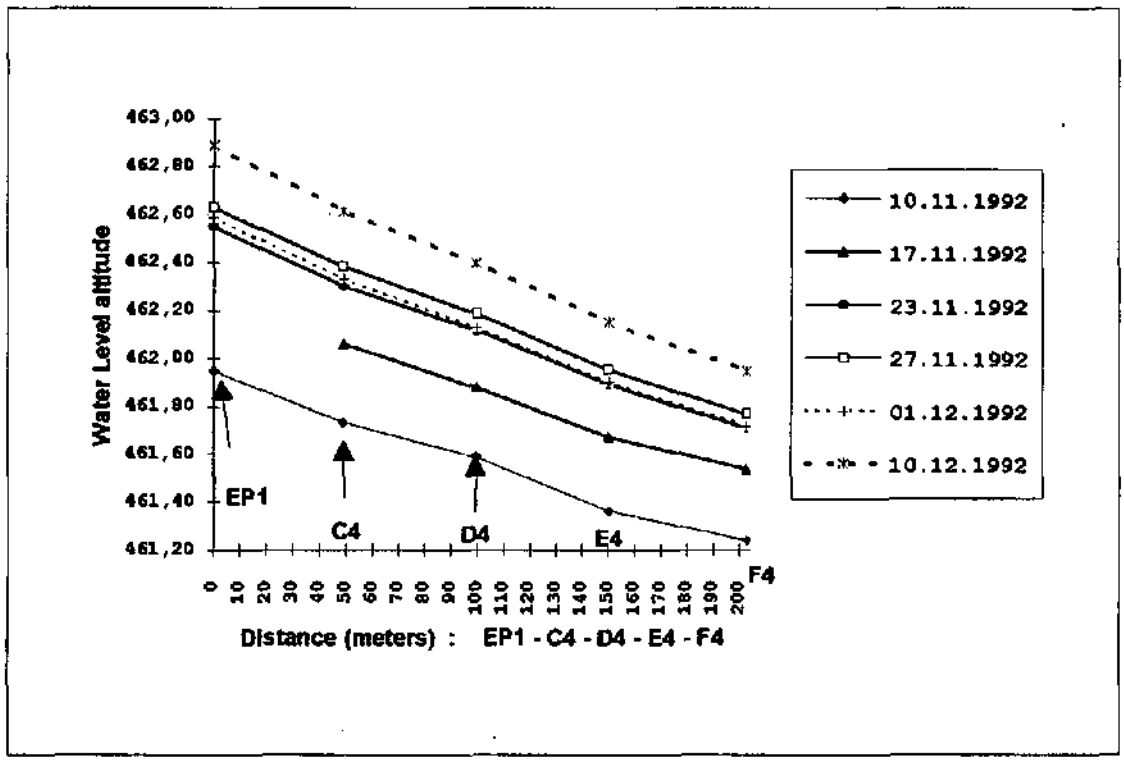

Fig. 45 Longitudinal profile along the once (1986) considered to be the main direction of water flow, showing the variability of the water level during one month.

Part III: Local studies, field experiments and analyses

6. Chemical analyses

6.1 Analyses performed

1- Conductivity (K)

2- Hardness

3- Nitrates

4- Chlorides

5- Sulphates

6- Temperature

6.2 Synthesis

6. Chemical analyses

In the summer of 92, chemical analyses were carried out in order to investigate the consequences of the heterogeneity on the chemical composition of the water.
We started with sporadical samplings, on the erroneous assumption that the groundwater composition wouldn't vary much over a period of 15 to 30 days. The results showed quite the contrary. Later, in winter of 92 (Nov./Dec.), during the last tracer experiment, daily measurements of the conductivity were carried out. We also intended to observe the changes in conductivity within each piezometer in correlation with the rainfall events.

We observed that each piezometer reacted differently; but the reasons for this have to be investigated further. The evolution of the values has a zigzag aspect. Nevertheless one must say that de daily delta values lay within the measurement error margins. An example of this would be a change of one to 10 microsiemens observed over a single day. But when this variation tends to grow, and after one week totalizes 27 microsiemens, then there should be some foundation for it(see **Fig 47(a)** by C2).
There are important variations in certain chemical parameters, specially the hardness values (increasing by 100 mg/l) and the concentrations of nitrates (values oscillating between 15 and 115 mg/l). This nitrate variation is even more important, since it far exceeds the established OMS norm (= 25 mg/l) and less so the Swiss one (=40 mg/l). It is obviously due to over-fertilisation. Each culture has its own fertilising period which varies from field to field. I observed that on the land distant circa 300 to 400 m from Wilerwald, a great area was fertilised at the end of May. **Table 11** shows the values measured in the summer of 1992:

Nitrates [mg/l]	11.06.92	20.07.92	06.08.92	19.08.92
C8	17.3	23.8	108.9	113
C7	25.7	24.7	108.9	118.3
C6	22.6	24.7	103.6	113.9
C5	25.5	25.3	-	113
C4	25.3	24.6	-	115.9
C3	26.2	24.9	110.5	108.2
C2	18.8	23.8	-	113.9
D7	24	23.8	111.3	111.9
D6	27.3	23.5	-	112.6
D5	25.1	24	112.3	113.9
D4	26.2	23.8	-	115.2
D3	21.7	23.7	-	116.6
D2	23.2	23.7	-	115.6
D1	17.3	30	108.9	110.9

Table 11: Nitrate content at the Wilerwald test site (summer 1992)

A possible future investigation at this site would be to use these nitrate increases as tracers. It would be interesting to follow the evolution of concentrations more systematically. The data about these observations is not sufficient to draw detailed conclusions. It is interesting however to note that there are observations which seem to agree with the geophysical ones. The nitrates arrived later in the piezometers lying in the less permeable part of the aquifer (D1). They reached those on the left side earlier, (except for C8, situated on a less permeable lense). Nevertheless, one must be prudent and not be too definite because it is clear that too much is missing, in particular continuous measurements and also information about the land uses and the fertilisers.
The content in nitrates of this aquifer (which is an important water reserve) is a serious problem that should be iovestigated further and controlled, because of the health problems it may create. According to **R. Blau et al. (1981)** (in "Grundlagen für die siedlungswasserwirtschaftliche Planung des Kantons Bern, Hydrogeologie Emmental, Teil III : Unteres Emmental. Wasser-u. Energiewirtschaftsamt des Kantons Bern. **(WEA)**), the Unteres Emmental was considered as having a low content in nitrates, between 19-28 mg/l, it being higher in the bordering

regions. Values situated over the established norms had already been measured, and associated with the use of fertilisers. The regions most affected were those where the groundwater is predominantly renewed by rainfall-infiltrated waters and by border-region tributaries. The influence of the Emme infiltration was considered beneficial, lowering the concentration. **Fig. 2C-3 in Appendix 2** shows the spatial distribution of nitrates, during the summer of 1971/72. Wilerwald was then situated between the 15 and the 20 mg/l isoline.

The chemical measurements were done over too short a period. One comes therefore to the same conclusion as in chapter 5: so as to be able to infer something about the groundwater reaction towards rainfall events, daily measurements over a longer period of time should have been made.

6.1 Analyses performed

The composition of the water in Wilerwald is typical of a groundwater of the Alp-foreland sedimentary basin. It is a hard water (Carbonate hardness ≥ 150 mg/l of $CaCO_3$), with an accentuated mean mineralisation, the conductivity values oscillating between 400 and 600 μScm^{-1} (at 20°C).

The physico-chemical parameters studied were: the conductivity, the temperature, the hardness and the chemical contents in nitrates, sulphates, and chlorides. pH measurements were also carried out in situ, but because of the discrepancies observed (due to a failure of the measuring devices). They are not included here.

1- Conductivity (K) [μScm^{-1}]:

The conductivity was measured *in situ* with a conductimeter. It reflects the totality of the dissolved ions in the water solution, and depends on the water temperature. In order to make a comparative study, all the values were corrected to the reference temperature of 20° C, according to the following formula (**Thierrin,1990**):

$$K_{20} = K_{Tmes.} \cdot \frac{1}{1 - 0.022 \cdot (20 - Tmes)}$$

where,

$T_{mes.}$ = is the temperature of the measurement [°C]
K_{20} = the conductivity corrected at 20°C

Figs 46 a & b present the values of the conductivity measured at each observation well. The rainfall events are also plotted, but for the whole year. It seems that there is a connection between the latter and the increase of the values which is admissible. The direct infiltration of the rainwater is linked to an increase in dissolved ions. If the salt content of the land surface rises due to fertilisation, this will be even more pronounced. The delay between the rainfall event and the increase of the values is not that evident. Besides, one is dealing with a phenomenon which is not punctual but irregularly distributed over a surface. Therefore one should observe a cumulative aspect: a local infiltration of the rainwater and the lateral arrival of groundwater. This actually complicates the interpretation.

Figs 47 a & b present the daily observation of the conductivity values of mean samples of water at each observation well. As stated at the beginning of this chapter, different responses at each observation well were observed. The reasons are not yet clear. Other factors can influence the values. One is that the observation wells are not impermeable to rainwater. This fact is visible in the conductivity profiles. An example is given in **Fig. 48 *b2*** and ***b3*** showing the same profile at different scales. 150 µS/cm was the value found at 3 meters depth for the piezometer B4.

Other conductivity profiles are given at the end of this chapter. They show the irregular distribution of the conductivity, a consequence of the vertical heterogeneity. Different pathways with different permeabilities may result in differences of temperature and chemical composition.

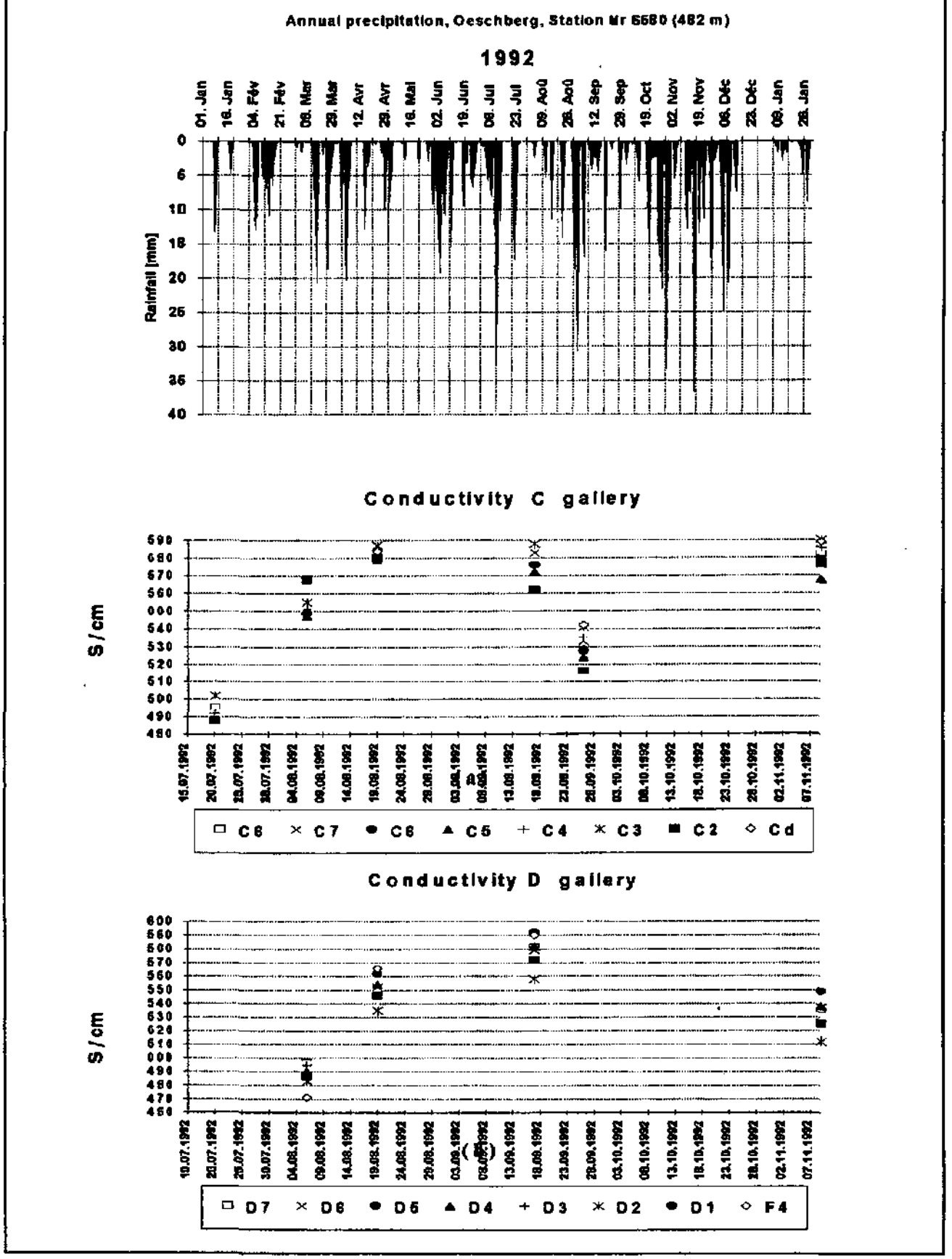

Fig. 46 Conductivity values for the C **(a)** and D **(b)** galleries with simultaneous representation of the rainfall events during 1992.

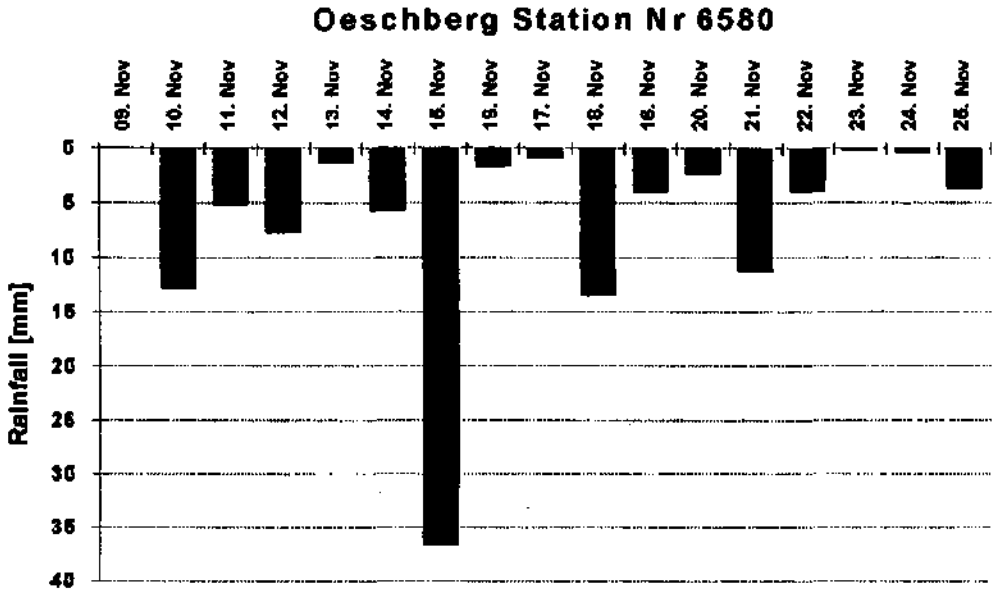

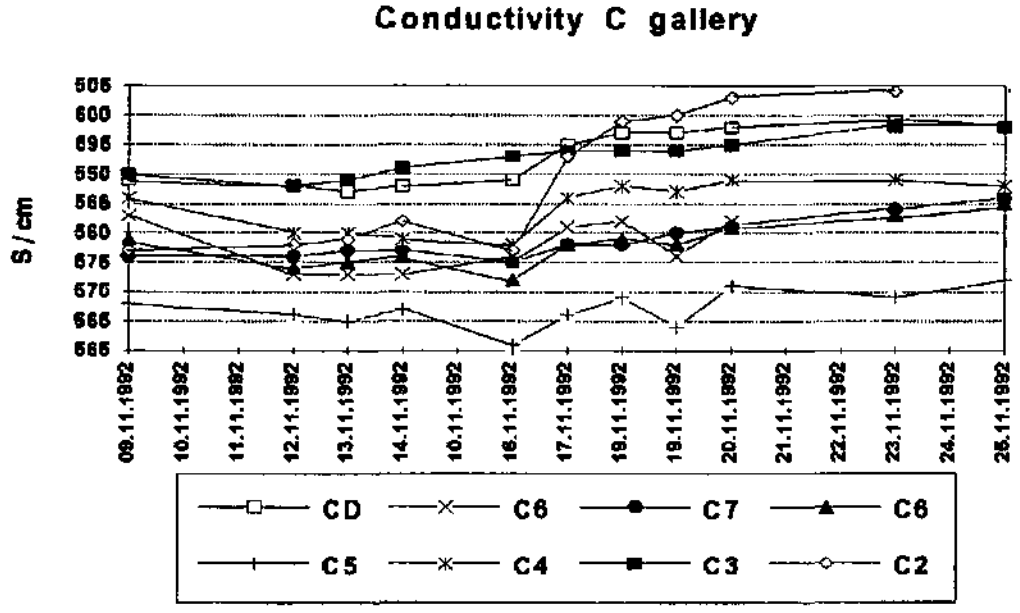

Fig. 47a Conductivity values for the C gallery with simultaneous representation of the rainfall events during the tracer experiment at Nov. 1992.

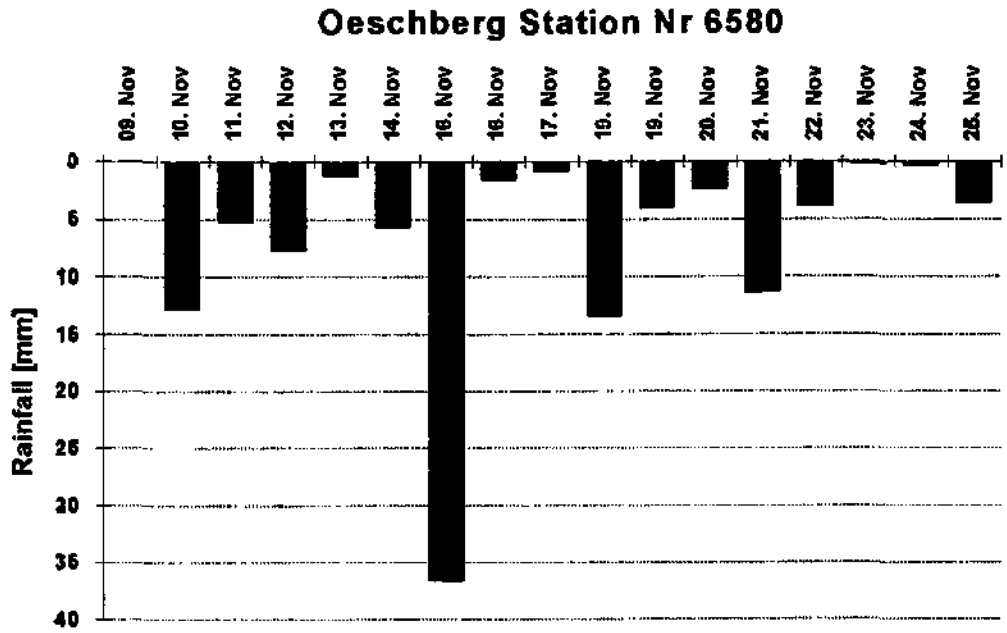

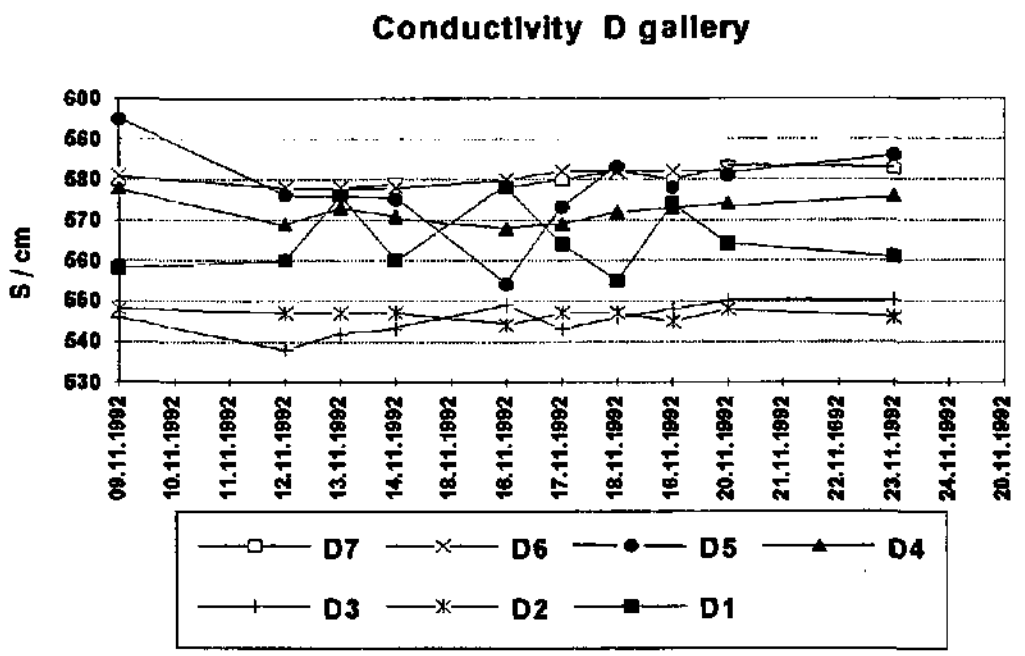

Fig. 47b Conductivity values for the D gallery with simultaneous representation of the rainfall events during the tracer experiment at Nov. 1992.

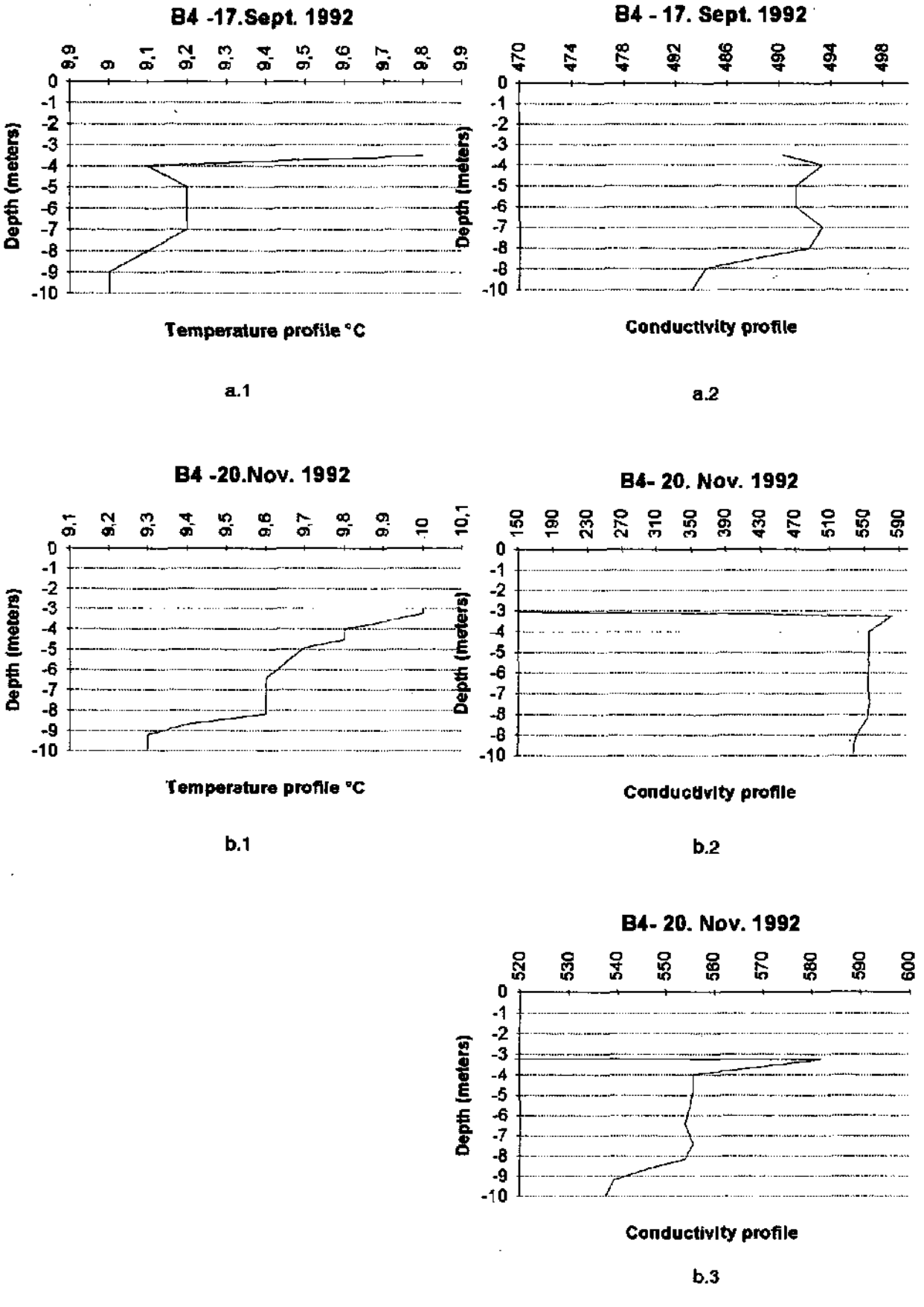

Fig. 48 Conductivity profiles for the observation well B4 measured in Sept. 1992 **(a)** and Nov. 1992 **(b2+b3)**. The profile **b2** is the same as **b3**, with only a different scale.

2- Hardness

The hardness of a water represents the sum of the concentrations in metallic cations (excepting the hydrogen ion and the alkaline metals).

Different kinds of hardness can be defined (**Rodier,1984**):

Total hardness (Dto) or hydrotimetric titer (T_H) - the sum of calcium and magnesia concentrations.
Calcium hardness (Ca^{++})- expressing the global content in calcium salts.
Magnesium hardness (Mg^{++})- corresponding to the global content in magnesium salts.
Carbonate hardness- the content in calcium and magnesium bicarbonate and carbonate. This hardness is either equal to T_{AC} if T_H is greater than T_{AC}, or equal to T_H if T_{AC} is greater than T_H.
Note: T_{AC} is the complete alkalimetric titer, i.e. the total content of hydroxides, alkaline and alkaline-earth carbonates and bicarbonates.

When the hardness is essentially due to the presence of Ca^{++} and Mg^{++}, because the content of the other bivalent cations is lower than 0.02 mval/l and its contribution lower than 0,5 %, the following relation holds valid (after **Thierrin, 1990**):

$$\text{Dto [mg/l } CaCO_3\text{]} = 2.497 \bullet Ca^{++}\text{ [mg/l]} + 4.117 \bullet Mg^{++}\text{ [mg/l]}$$

The total and carbonate hardness the Wilerwald water samples were calculated in the laboratory by complexometric titration with EDTA. Sometimes it was possible to determine the calcium and magnesium hardnesses. The hardness values can be seen in **Tables 3C2-3a, 3C2-3b, 3C2-3c and 3C2-3d** (Appendix 3).

Fig. 49 shows the temporal variation of the total hardnesses. As was written for the conductivity, there is an increase in hardness and it seems to be linked to the infiltration of raiowaters. This may be explained by a local factor. The decomposition of the vegetal cover (the site is situated in a forest) can liberate carbon dioxide in great quantities. The rain reacting with it, produces carbonic acid which will then dissolve the carbonate rocks during its infiltration (**Rodier,1984**), and thus contribute to the variations observed. Another possibility could be the use of acidifying fertilisers which would also dissolve the carbonate sediments below, and cause the values to increase.

3- Nitrates

All the forms of nitrogen, ammonia and nitrite can be oxidised into nitrates. Great changes in groundwater content are often observed in intensely cultivated regions.

As **Fig. 50** shows, a great increase was observed soon after the July rain period, possibly linked to the use of fertilisers. As written above, these nitrates inputs could be used as a tracer. The few results which were measured do probably reflect the geophysical observations, because the times of arrival seem to correspond with the permeabilities indirectly inferred from the geophysical measurements.

The determination of the nitrate content was done with specific ionic electrodes (**Orion Research, 1982**).
The results can be seen in **Table 11** at the beginning of this chapter.

4- Chlorides

The chloride content was low, oscillating between 8 and 18 mg/l at the time of its measurement. **Fig. 51** shows the temporal variation of rainfall and of chloride content for the galleries C and D.
Like the nitrates, they seem to increase after the rain period. Nevertheless the variations are not so significant, the values lying far below the OMS norms (250 mg/l for the Cl^-). The European Community recommends a maximal content of 25 mg/l for a water of good quality.
The chloride determination was done using a specific ionic electrode too. **Table 12** shows the results of themeasurements.

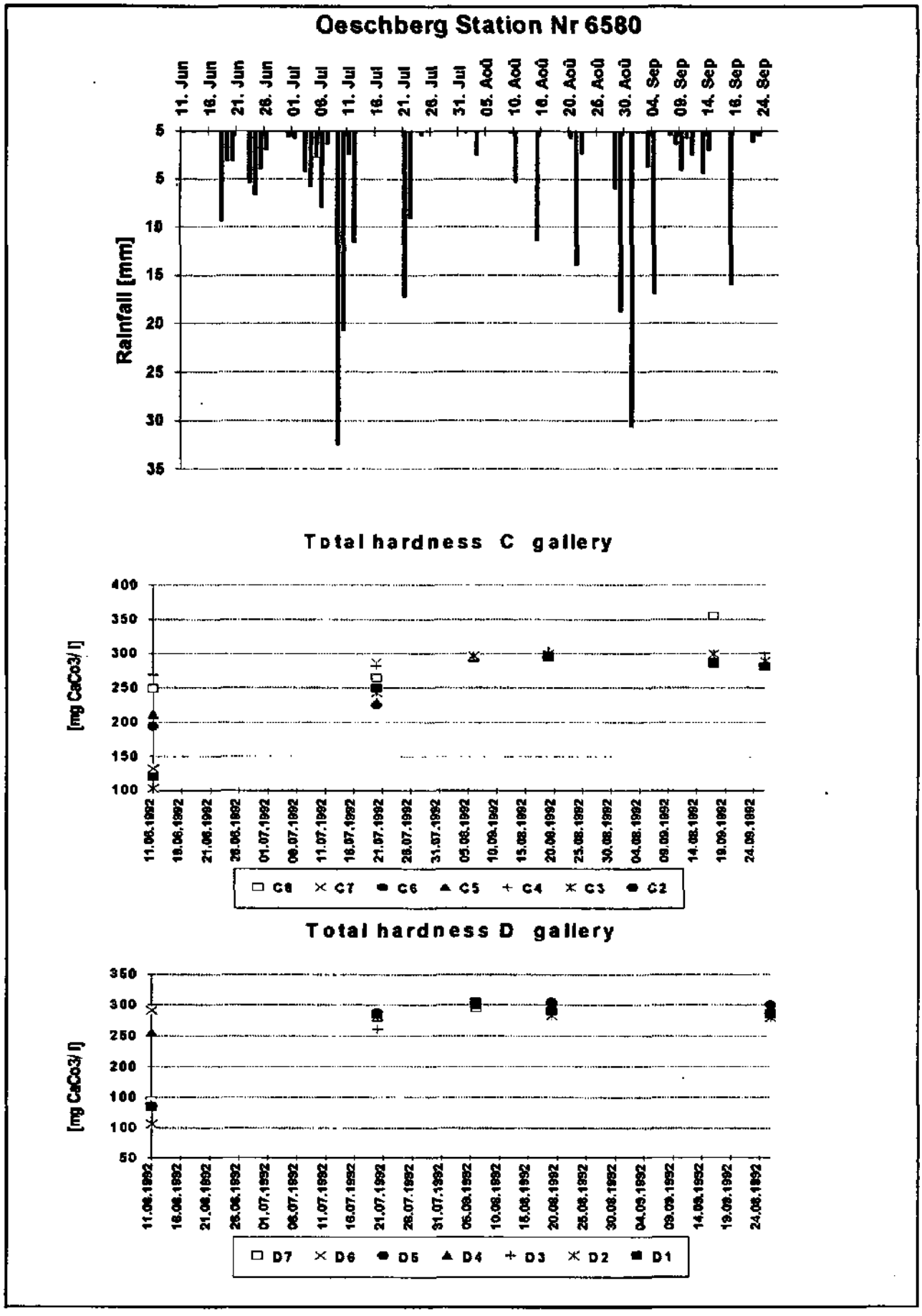

Fig. 49 Total hardness values (Dto) measured during June and September 1992.

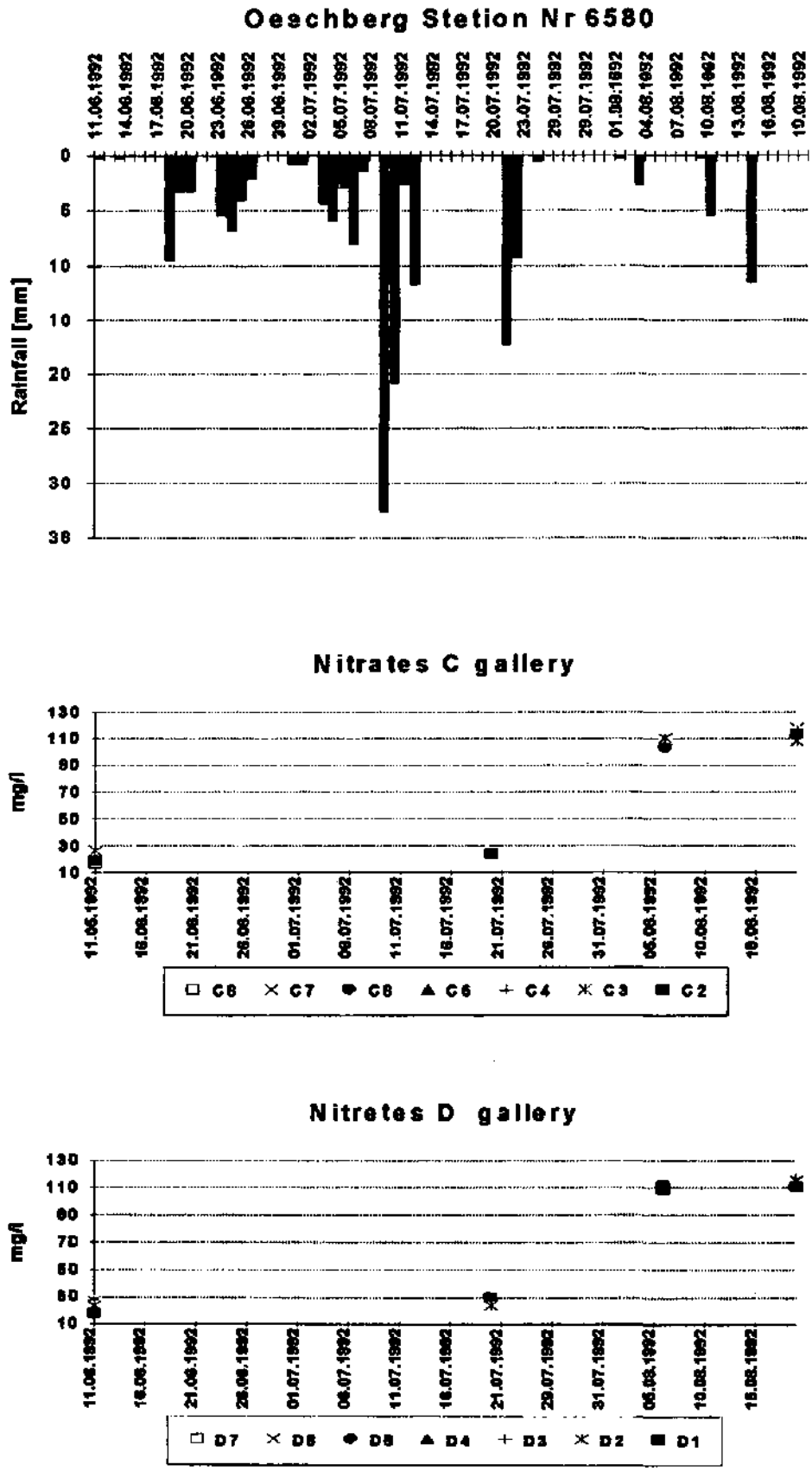

Fig. 50 Nitrate values for the C (a) and D (b) galleries with simultaneous representation of the rainfall events.

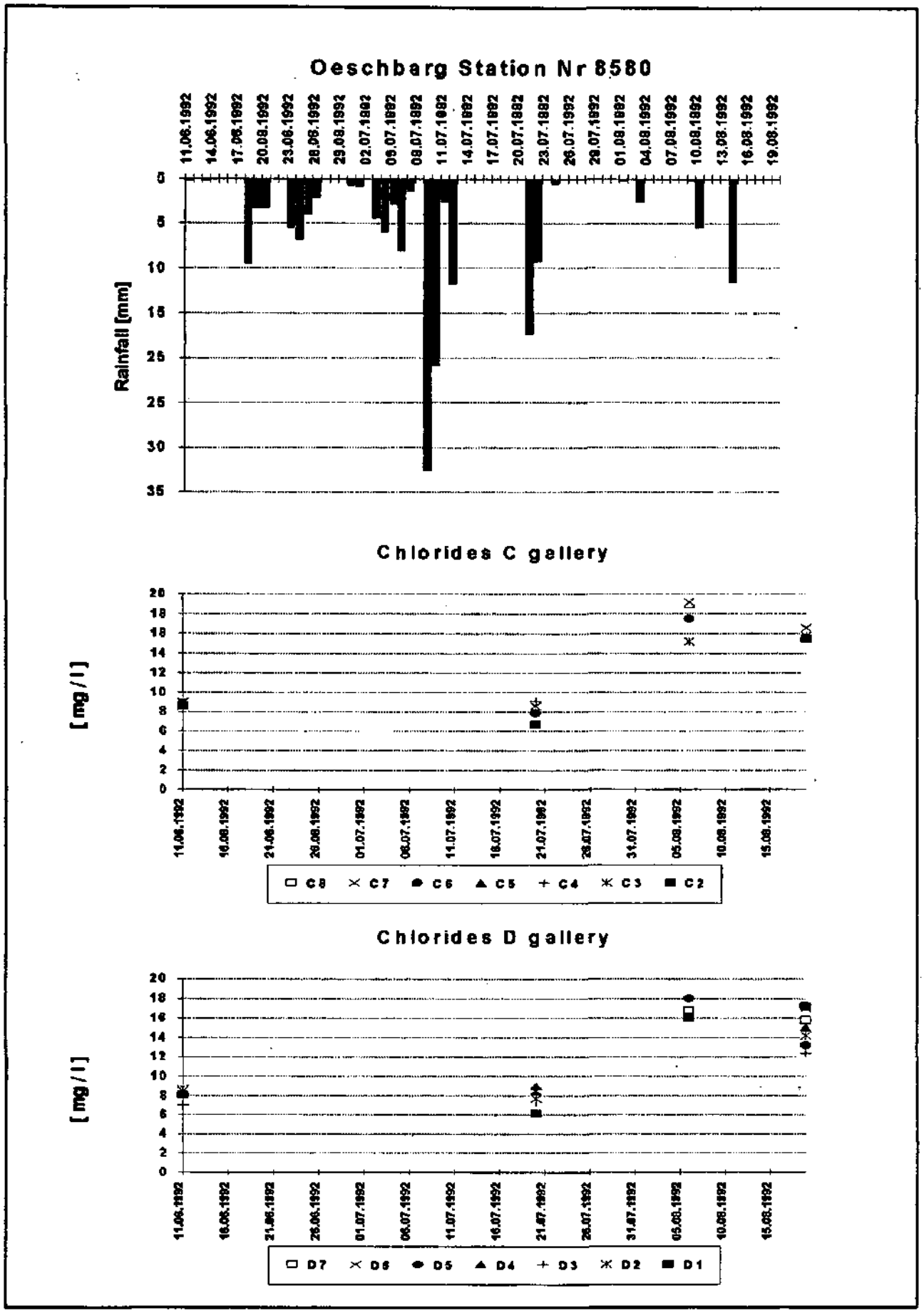

Fig. 51 Chloride values for the C (s) and D (b) galleries with simultaneous representation of the rainfall events.

Chlorides [mg/l]	11.06.1992	20.07.1992	06.08.1992	19.08.1992
F4	8.6	8.8		12.3
F6	8.6	7.9		13.2
E4	8.6	6.7		13.1
D7	8.7	7.7	16.8	15.8
D6	8.7	8.5		17
D5	8.6	8	18	13.2
D4	8.5	9		15
D3	7	7.3		12.4
D2	8.5	7.7		14.2
D1	8.1	6.1	16	17.2
CD				16.5
C8	8.7	6.7	19	15.8
C7	9	8.8	19.2	16.6
C6	8.9	7.9	17.5	15.5
C5	8.7	8.6		15.5
C4	8.7	9.1		15.5
C3	8.5	8.6	15.2	15.8
C2	8.6	6.7		15.5
Emme	3.8	5.5	8.5	11
Zielebach	8.5	8.5	14.2	11

Table 12 Chlorides concentrations

5- Sulphates

Sulphates [mg/l]	11.06.1992	20.07.1992	06.08.1992	19.08.1992	17.09.1992	26.09.1992
F4	4.26	6.52		9.67		
F6	3.81	7.95		8.84		
E4	6.21	7.01		7.39		10.5
D7	3.87	6.81	9.14	8.71		10.8
D6	7.11	7.36		8.76		11.2
D5	4.65	6.84	10.3	8.81		10.9
D4	6.69	7.43		8.54		10.9
D3	4.04	6.28		8.11		10.4
D2	3.51	6.31		7.55		10.7
D1	4.81	7.59	10.5	10		11.8
C8	3.51	7.33	8.76	8.18	11.3	10.5
C7	6.89	7.71	9.6	7.82	10.5	10.3
C6	9.09	7.41	9.42	6.94	10.8	9.32
C5		6.79		8.13	10.8	8.49
C4	9.62	6.69		8.18	10.8	8.04
C3	7.75	7.77	9.65	9.11	10.7	8.93
C2	3.3	7.36		9.6	11.3	8.37
Emme	3.75	4.79	6.7	5.9	10.7	9.28
Zielebach	3.92	7.03	11.4	9.49		11.4

Table 13 Sulphate concentrations

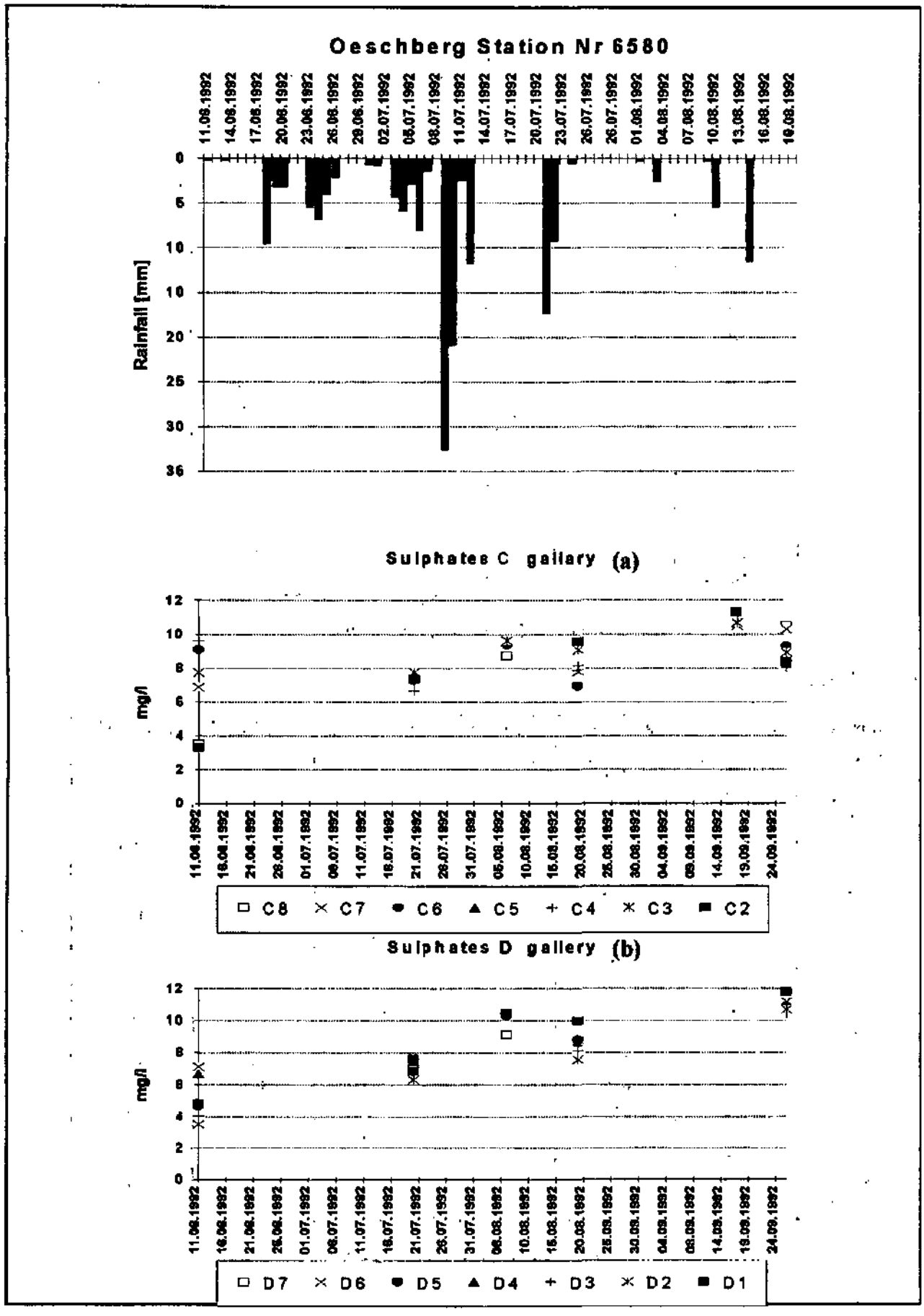

Fig. 52 Sulphate values for the C (a) and D (b) galleries with simultaneous representation of the rainfall events.

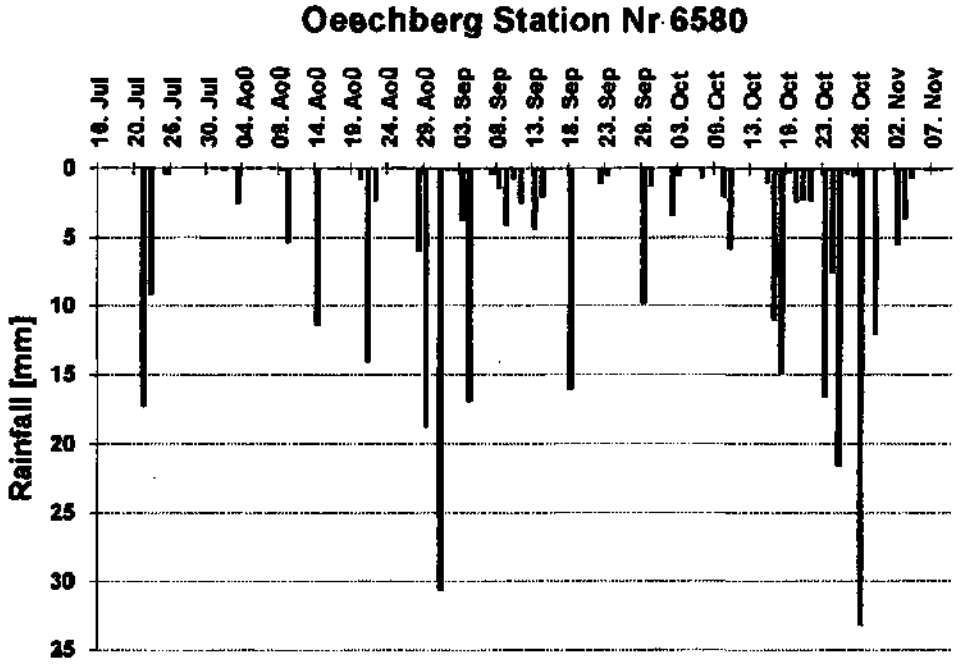

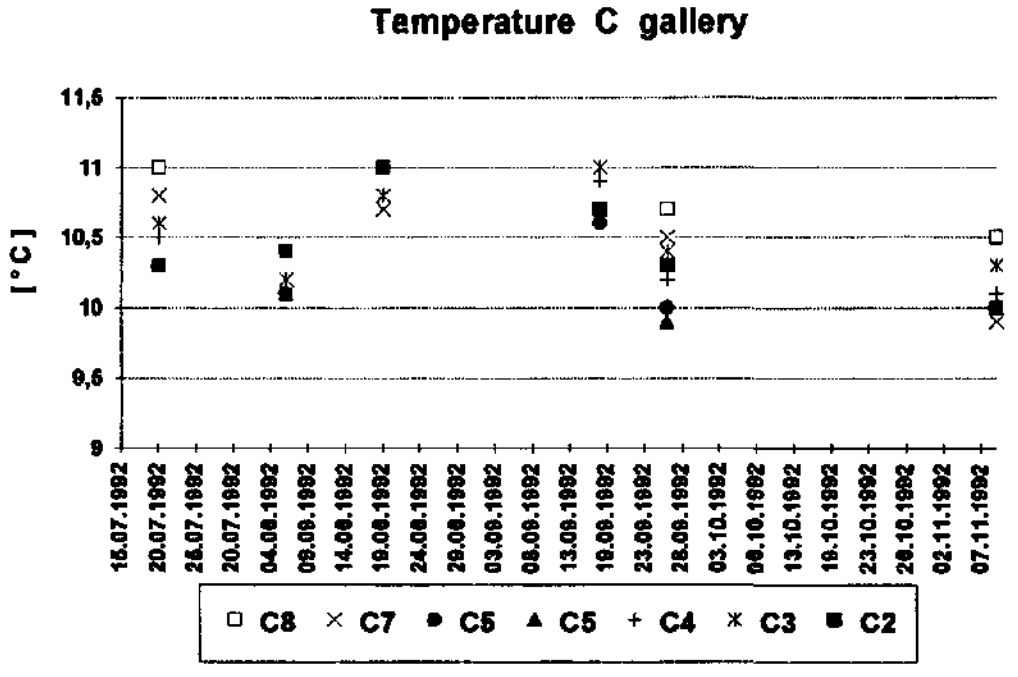

Fig. 53a Temperature values for the C gallery with simultaneous representation of the rainfall events from July till Nov. 1992..

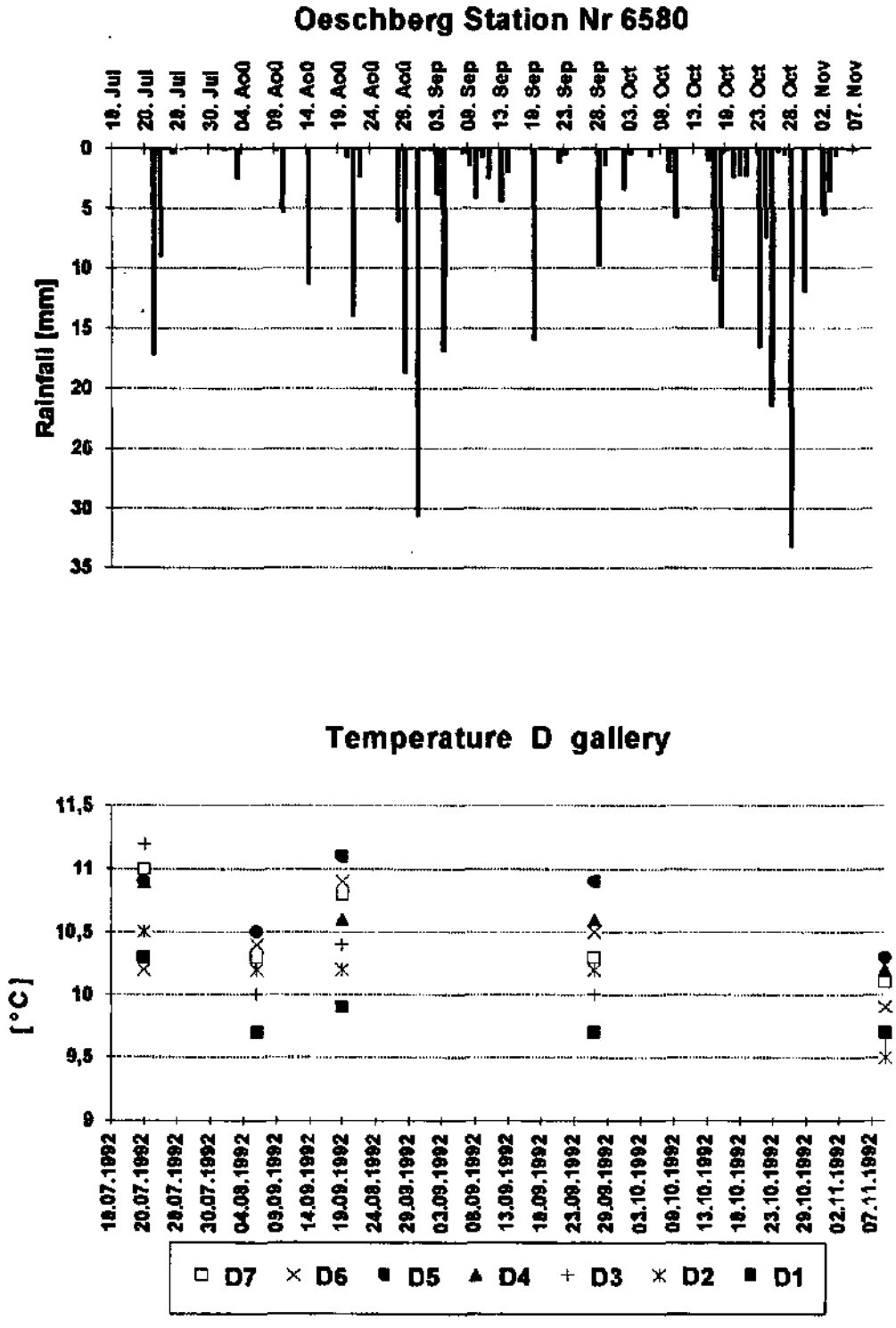

Fig. 53b Temperature values for the D gallery with simultaneous representation of the rainfall events from July till Nov. 1992..

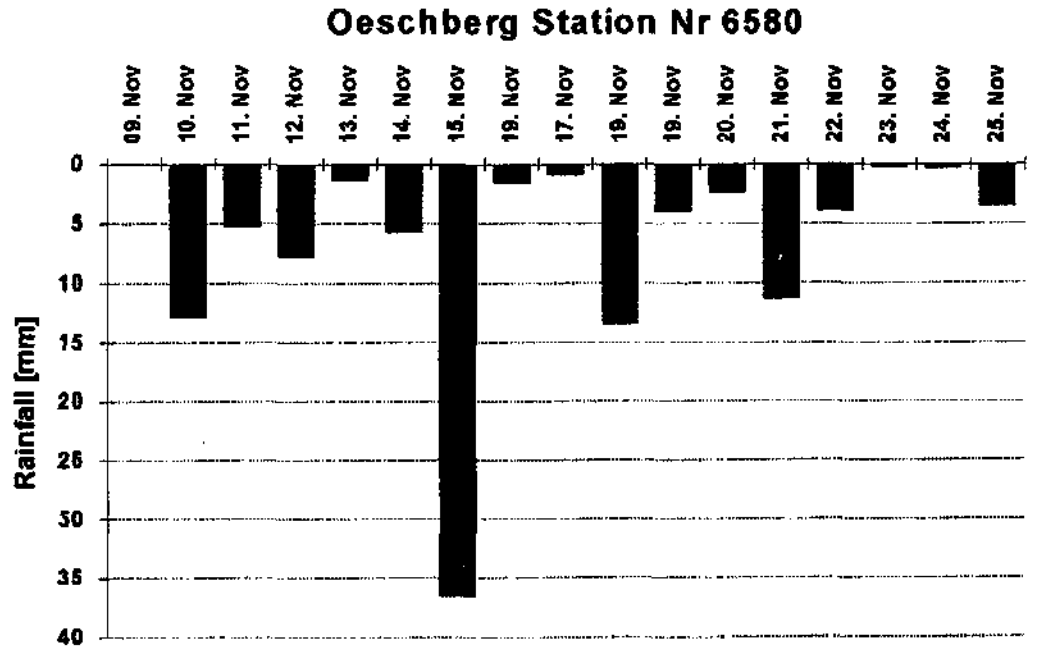

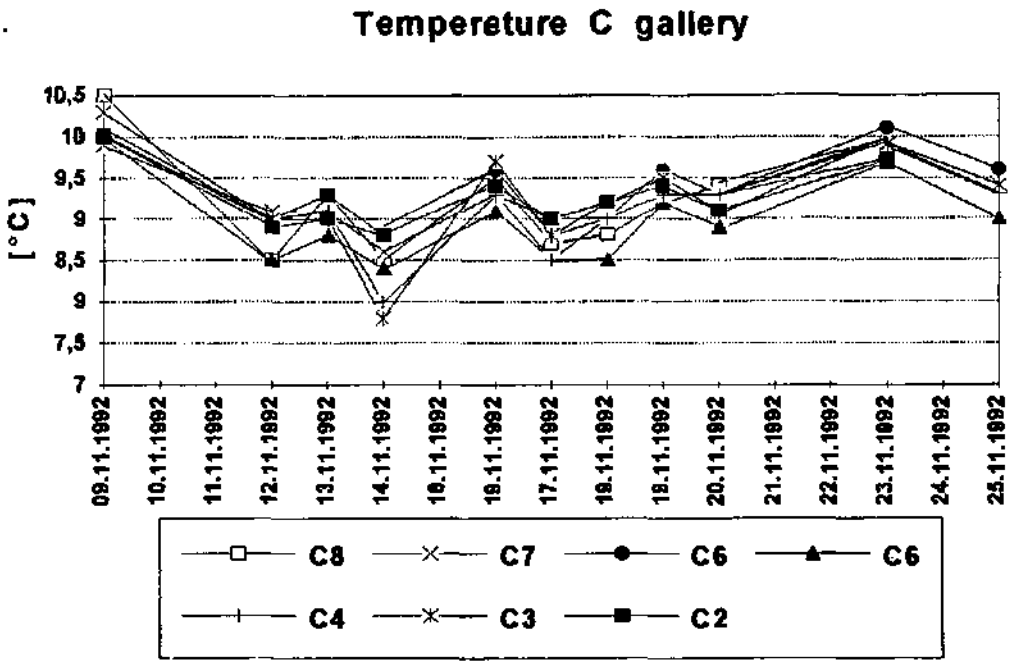

Fig. 54a Temperature values for the C gallery with simultaneous representation of the rainfall events during the tracer experiment at Nov. 1992.

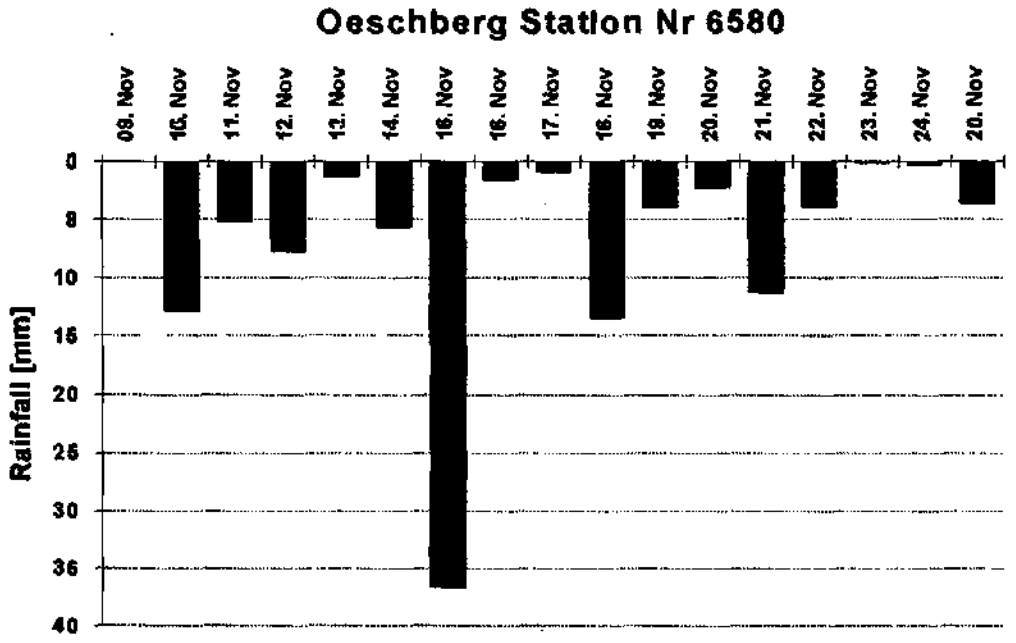

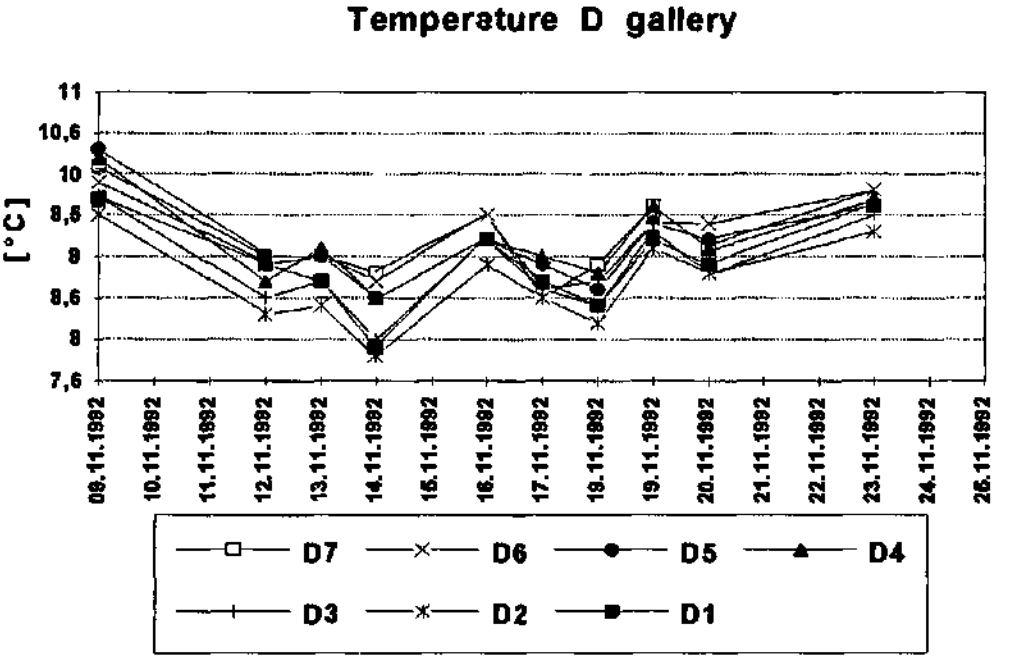

Fig. 54b Temperature values for the D gallery with simultaneous representation of the rainfall events during the tracer experiment at Nov. 1992.

The concentrations in sulphates are low in the region. The small variations seem also to be linked to the rainfall infiltration (**Fig. 52**).
They were determined by the turbidometric method. The concentrations observed can be seen above in **Table 13**.

6- Temperature

Temperature measuremeots were performed at the same time as the conductivity measuremeots, allowing the same graphics and profiles to be built. In general the groundwater temperature is lower than the air temperature in summer and higher in winter. Oscillations in groundwater temperature can therefore have different origins. Mean annual temperature oscillations and the influence of the Emme, were discussed in Chapter 3 (**Fig. 2C-2** *in* **Appeodix 2**). Wilerwald lay between the 3° and the 5° isodelta line.
As **Figs. 53(a) & (b)** and **54(a) & (b)** show, the temperature oscillation in summer was relatively small (maximum 2 degrees), and seems to be linked to water infiltration too. once more, one must keep in mind that these values are punctual and sporadic. Oscillations of 4° were observed during the daily observations performed in winter. Here the effect of the infiltrated rainwater seems to be the opposite, contributing to the loweriog of the groundwater temperature. There are specific reactions within each piezometer, though they are not easily interpretable.

Temperature profiles can be seen at **Fig. 48** and in the **Appendix 3C2-4 till 3C2-11**. The differences io temperature are nevertheless low (1 degree), this also lies within the measuremeot error.

6.2 Synthesis

A highly heterogeneous aquifer, studied on such a small scale, needs more detailed data, and long-term and very frequent investigations. The chemical analyses performed were rather restricted, both in number and io observation time. They were nevertheless very interesting.

They showed that the whole system is very complex, and that many factors may play a role. Lateral and vertical inputs exist. The influence of the particular situatioo around each piezometer is great (existence or not of an impermeable cover layer, local distribution of permeabilities, ...). And the role of the regional frame is all but secondary.

It would be interesting to follow the evolution of theses chemical parameters during a longer period of time. However, some of the observation wells should be then impermeabilized, in order to avoid the mixture with direct rainwaters.

The results of the chemical analyses revealed two important aspects:

1. A local specified response at and within each piezometer, which is due to the local heterogeneity. The number of observations is to small to build any theory.

2. An important infiltration of rainwater which can periodically deteriorate the quality of the water. This worsening seems to follow rainfalls occurring after fertilisatioo of the neighbouring lands.

The results of the nitrate analyses revealed that the system is in potential danger, considering the increase in values observed. On the other hand, the nitrates can be used as a tracer. It seems that the increase follows a logical distribotion sequence, convergent with the geophysical observations - the quickest arrival observed io the piezometers lying in or near the paleochannel (C7 and D6).

The convergence of the different methods used in this study is again a very important conclusion.

Part III : Local studies, field experiments and analyses

7. Isotope hydrology in Wilerwald

7.1 Tritium (^{3}H)

7.2 Oxygen-18 (^{18}O)

7 Isotope hydrology in Wilerwald

Stable and radioactive isotopes are well established tools to investigate the hydrological system (**Fritz & Fontes,1986, IAEA,1987**)

In the Wilerwald area two isotopes of the water molecule were used, the radioactive tritium and the stable isotope oxygen-18. Since these isotopes are build into the water molecule, they trace the surface and the subsurface water flow, in a more or less ideal manner.

The purpose of the isotope measurements was to get an estimation of the subsurface residence time (radioactive tritium) and to obtain additional information about the contribution of the local infiltrated rainfall and of water from the Emme river (with the help of oxygen-18).

7.1 Tritium (^3H)

The radioactive tritium has an half life time of 12.43 years. Its concentration is usually given in TU (Tritium Units; 1 TU = one Tritiom atom in 10^{18} hydrogen atoms.

Natural tritium is produced by the interaction of cosmic rays with oxygen and nitrogen atoms at the higher levels of the atmosphere. This natural production is latitude dependent. Before 1952, the found annual production was less then 10 TU, in the mid latitudes of the northern hemisphere . Tritium concentration levels in the atmosphere, increased during the period of nuclear weapon tests, between 1952 and 1963, where they reach maximum values up to 6-thousands TU. Some nuclear industries, reactors and military labours can also contribute to the atmospheric level of tritium.

The study and interpretation of tritium converges mainly on the possibility to calculate the mean residence time of water. The common model hypothesis used for this purpose is the one that admits an exponential age distribution (**Siegenthaler, 1972**), where

$$g(T)=\frac{1}{T_0}e^{-T/T0}$$

g(T) = relative abundance of water of age T

T_0 = mean residence time of water

The model is based on the assumption that:

- the mixture of the rain infiltrating water and aquifer water is instantaneous and perfect,
- the aquifer permeability is uniform and input equals output,
- there is no by-pass in the systems, i.e. there are no different water components such as mixtures of surface and groundwater.

Allowing for these considerations, the mean age of a groundwater can be obtained by comparing the integrated input concentrations of precipitation with the output concentrations of a spring or well water. The solution of the equation then is:

$$A(T) = \int_{t=0}^{t=\infty} 1/T_0 \bullet e^{-T/T0} \bullet A0(T-t) \bullet e^{-\lambda t}$$

where,

A(T)= Tritium activity relative to a date T in the aquifer output
$A_0(T-t)$= Tritium activity in raiowater
$\lambda = \ln(2)/T^{1/2}$ = radioactive disintegration-rate constant
$T^{1/2}$ = half-life of tritium (12.43 ± 0,5 years).

The model is limited *a priori* by its own presuppositions. Natural conditions are always too complex to fit the theoretical considerations, and a porous aquifer is almost always very heterogeneous, with highly variable permeabilities. This is even accentuated in the case of the Emme aquifer (and therefore Wilerwald), because of its fluvio-glacial origin. A non-captive (free nappe) aquifer like in the Unteres Emmental is therefore a complex system. Waters mix: direct rainfall infiltration, with infiltration of Emme water, and of other surface waters. This made the discrimination of the different contributions difficult. Even surface waters represent mixtures of water: direct rainwater precipitated over the whole basin and of older ground waters.
Also, depending on the basin, industrialised regions may contribute to the tritium inputs (**Schotterer et al, 1993**).

The qualitative information given by the exponential model nevertheless constitutes an important complement to the hydrological studies. The comparison of residence times of the different water components can be used as an indicator of the heterogeneity, pointing out the areas drained fastest, or those where the rainfall infiltration represents an important factor. It may also indicate the areas that should be investigated more closely in the future.

In **Fig. 55a** are plotted the mean yearly tritium values of some sites in Switzerland from 1985 to 1992, (**Schotterer et al 1993**). These values are not affected by industrialised tritium and represent the depletion of the stratospheric tritium reservoir filled by the nuclear weapon tests. The difference in concentrations north and south of the Alps (Säntis, Guttanen and Locarno) can be explained by the higher content in direct marine moisture containing very little tritium on the southern side.

In **Fig.55b** the mean tritium values of the waters of the investigation area are plotted in the context of the theoretical output based on the exponential model for different residence times. The input data for the exponential model are taken from the IAEA Isotope in Precipitation Network (**IAEA, 1992**) and from 1972 onwards from Stations in Switzerland, sampled and measured at the Physics Institute of the University of Bern.

Based on these assumptions the mean age is situated between 6 and 8 years, the surface water having the shortest residence time, and the water from the observation wells the longest. The age distribution of the different water types seems reasonable, though the range of ages must be seen as an upper limit.

Besides, one must not forget to take into account the seasonal variation of the precipitation (from 10 to 30 TU). A direct influence of summer rainfall could therefore be mistaken for a higher residence time.

The following general statements can be made.

The river Emme is the youngest water. It is a mixture of young surface water and older groundwater, mixed in varying quantities, depending on the hydrological situation at the moment of the sampling.

Zielebach has a slightly higher residence time than the Emme but is younger than the groundwater. This is possibly due to the fact that Zielebach represents probably a drainage system of the Emme river, situated on the continuation of a paleochannel, where the water passes relative quick. A direct connection to the Emme could not be proven yet. In addition, some admixtures of surface water cannot be excluded.

The groundwater within the site, sampled at various piezometric wells (see **Table 3C3** *in* **Appendix 3**) has generally higher tritium values which indicates also a higher age distribution. It is interesting to see again that the piezometers C7 laying on the paleochannel has in the mean lower tritium values and seems younger than D1, for instance. Depending on the existence and distribution of a loamy and more impermeable covering layer, the local rain waters will move slower or faster into the groundwater, leading to differentiation in age. This irregular distribution and development of the loamy layer is supported by the Schlumberger soundings (**Fig. 34**). For instance, the aquifer is covered by a thick impermeable layer at D1, which probably represents a barrier, hindering the local infiltration of rainwater. On the other hand, the electromagnetic methods suggest a generally lower permeability there, which could be associated with slower drainage, and consequently with the older age found there.

Schlumberger soundings and RMT results (**Fig. 21**) revealed the existence of a paleochannel at C7 (faster drainage). Added to this, it seems that the aquifer is covered by coarser sediments (sand layer) there. The tritium values suggest an increasing residence time from C7 in the direction of D1. One must not forget that these conclusions are based on values close the margin of error, though they seem logical and repeat the pattern of the chemical and geophysical conclusions.

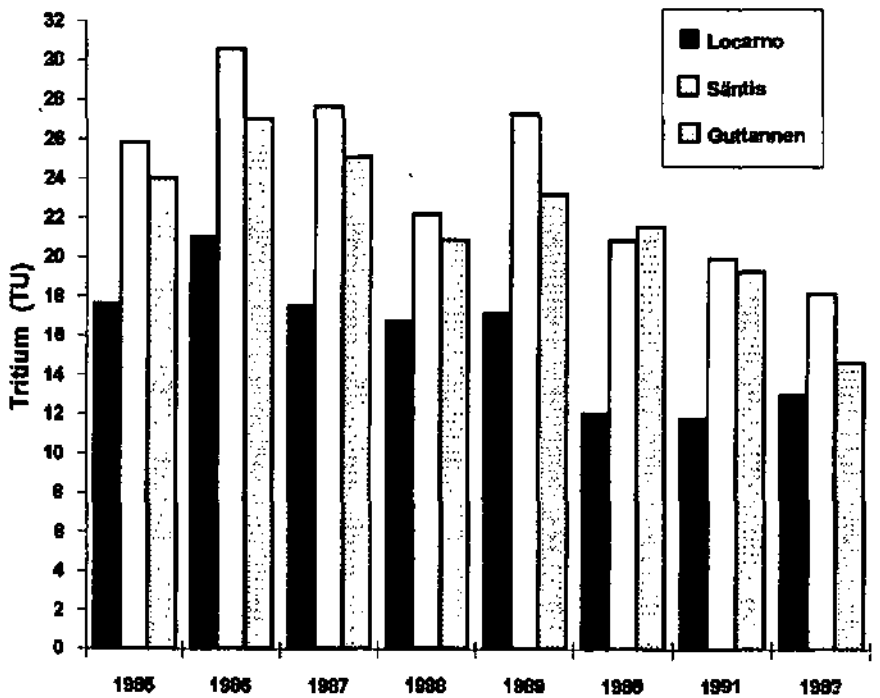

Fig .55a Tritium in Precipitation

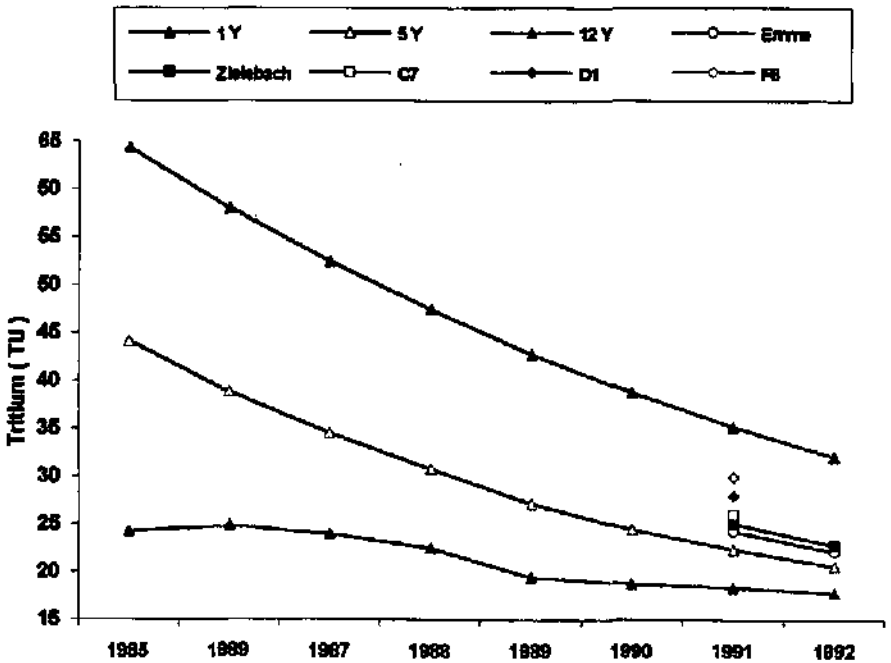

Fig. 55b.- Tritium in the investigation area and exponential model output.

As was stated in Chapter 6, a prolonged study of the daily variations at chosen observation wells would bring more information and this we suggest as a follow-up investigation.

7.2- Oxygen-18 (^{18}O)

The relative abundance of $^{18}O/^{16}O$ varies today between 188-202·10^{-5}. Measurements of this isotope are expressed as relative deviations from the standard mean ocean-water value (SMOW) in per mile -^{18}O:

$$\partial^{18}O[\%0] = \frac{^{18}O/^{16}O(\text{Sample}) - ^{18}O/^{16}O(\text{SMOW})}{^{18}O/^{16}O(\text{SMOW})} \times 1000$$

The $^{18}O/^{16}O$ relation is of first order, linked to temperature. In the seasonal course of a year, positive air temperatures lead to more positive $\partial^{18}O$ values in precipitation, lower air temperature leads to more negative values.

Because of the different molecular weight of $H_2{}^{18}O$ and $H_2{}^{16}O$, a fractionating occurs whenever evaporation or condensation takes place: the sea water vapour content is lower than that of the sea water itself; while rainwater is richer in ^{18}O than vapour from which precipitation occurs, due to the condensation. Successive condensations of the same moisture source result in a lowering of its isotope content : an oceanic mass of vapour will be more and more depleted in its isotope content by rain out, as it moves towards the continent. This is called the continental effect.

The temperature dependence of $\partial^{18}O$ can be used for hydrological purposes. Since the temperature is related to the altitude, one can estimate the mean altitude of the recharge area of aquifers, by the oxygen-18 content of a spring , for example. The altitude gradient in the Swiss Plateau is today ~ 0.2 ‰ /100 m. In this context, one must also to be aware that the monthly mean values in precipitation vary by up to 15 ‰. It is equally important to note that the yearly changes in oxygen-18 are very often 1 to 2 per mil. Changing climate conditions, such as the increasing air temperatures of the eighties led to a higher oxygen-18 content. Groundwater was then traced by its increasing oxygen-18 content which would reflect the changing climatic condition (**Schotterer, 93, IAEA**).
This is illustrated in **Fig. 56a** and **Fig. 56b** : the variation of oxygen-18 due to changing atmospheric conditions is reflected also in spring water.

One must take this fact into account in the case of the measurements made in the Wilerwald area. In **Fig. 56c** Oxygen-18 in the monthly precipitation at Burgdorf is plotted with the values from the Emme and the Zielebach. Several facts can be noted:

The seasonal variation in oxygen-18 seen in the precipitation is displaced by several months in the Emme river. This time-lag is interpreted as mainly due to the contribution of the snow melting in the higher regions.

In the water of the Zielebach these seasonal variations are practically absent. The general trend towards lower values in oxygen-18 is due to the fact that this system contains older water components from the precipitation of the years before - another proof for the longer residence time compared to the river Emme.

In figures **57a** and **57b** this situation is enlarged. Zielebach and all the groundwaters at Wilerwald generally have higher Oxygen-18 values than the river Emme, since the recharge area of the latter is about 400 to 500 m higher on average. This should be reflected in the local groundwater by an oxygen-18 value about 1 ‰ higher (corresponding to an oxygen-18/altitude ratio of about 0.2 ‰ per 100 m in altitude difference of the recharge area).

Since the investigated water components have different residence times and therefore contain different portions of past precipitations, one cannot calculate the proportion of the Emme water and of the local groundwater exactly from the present data. In addition, the aquifer should be very well mixed to allow such calculations. Nevertheless, the comparison of the values within the site, with the ones from the Zielebach, the Emme and the

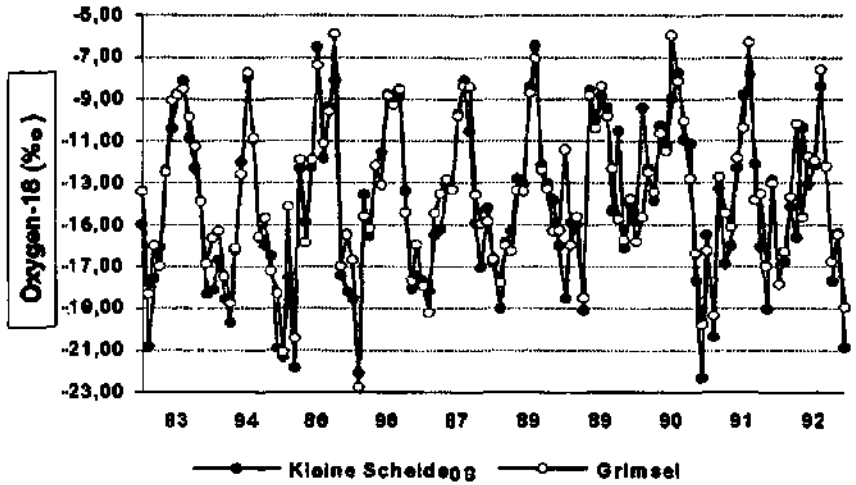

Fig.56a Oxygen-18 in Kleine Scheidegg and Grimsel (Schotterer et al. 1993)

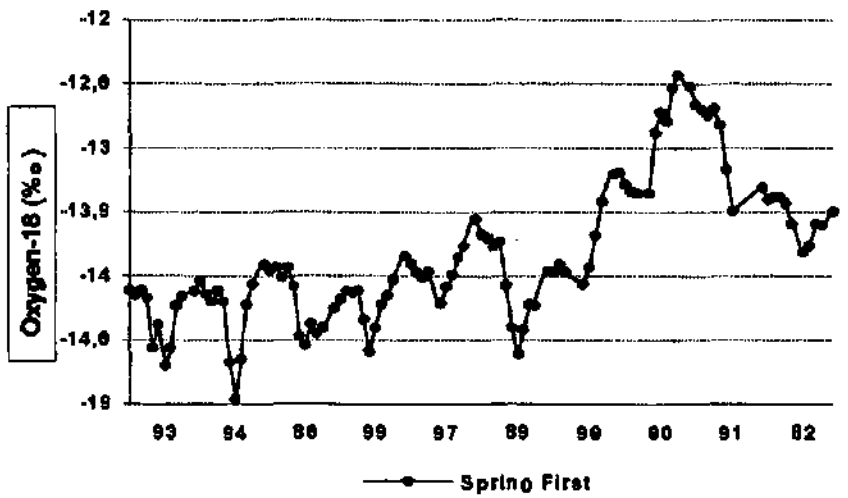

Fig.56b Oxygen-18 in spring water (2-4 years subsurface residence time).

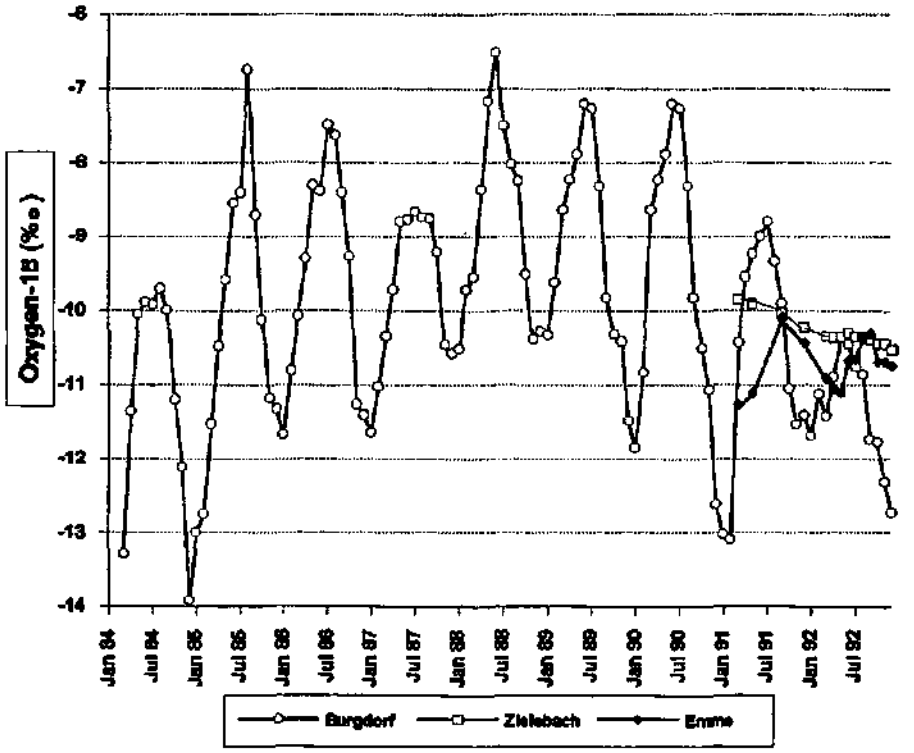

Fig.56c Oxygen-18 in precipitation Burgdorf (six months gliding means, 1984-1992), Emme and Zielebach.

Fig. 57a Oxygen-18 in surface water in the investigation area

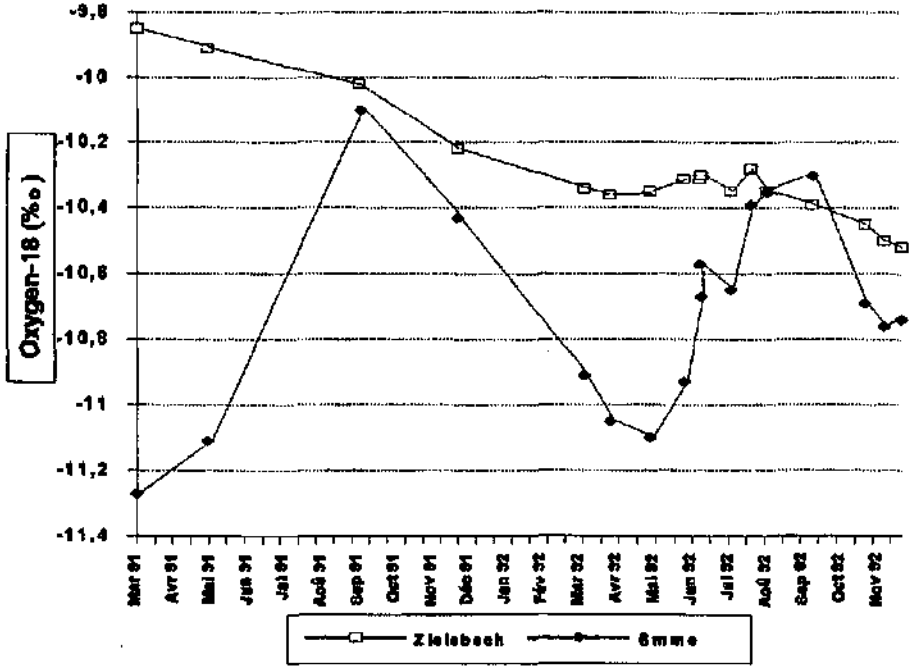

Fig. 57b Comparison of Oxygen-18 in ground and surface water in Wilerwald

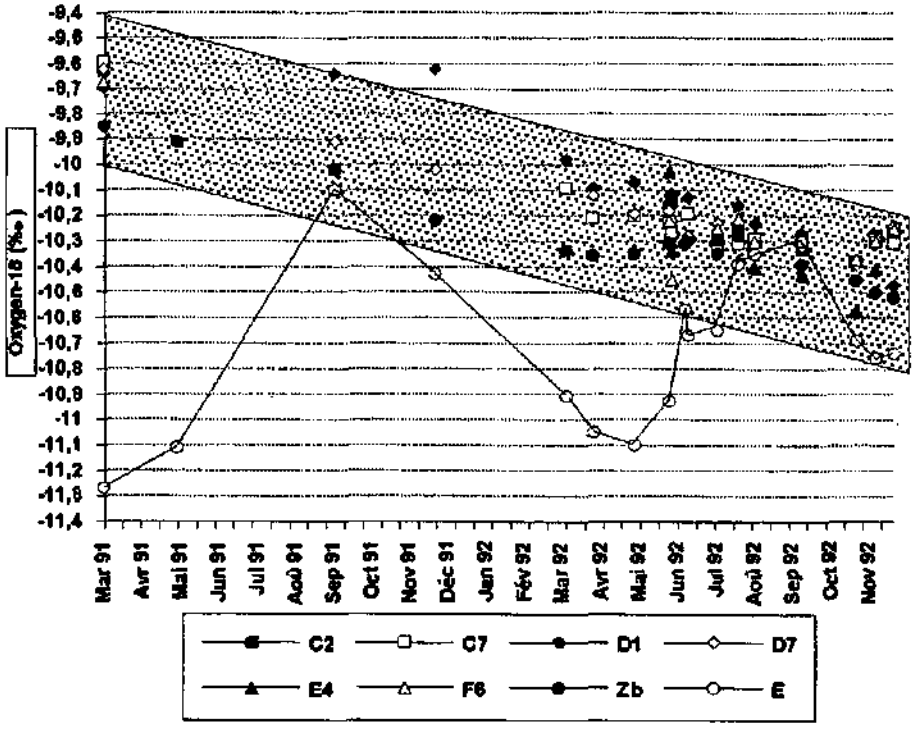

rainfall (local waters) allows rough estimations based oo a local $\partial\ ^{18}O$ content of ~9.6 ‰ and ~ 10.6 ‰ for the Emme river respectively .

From this, one can estimate Zielebach contains 40 % Emme water and this amount decreases for to ~ 20 % in the low permeability regions. Nevertheless one should be aware that the reliability of these calculations is restricted by the assumptions mentioned before.

Zielebach seems to be nearer to the Emme water. If this corresponds to a higher proportion of Emme water this would support the hypothesis written above, i.e. that the Zielebach represents a possible drainage system of the Emme river, situated on the continuation of a paleochannel, where the water moves relatively quickly.

On the other hand, groundwater samples always gave higher values, mainly in the regions with low permeabilities (D1). This could mean that the proportion of local water is greater than the proportion of Emme water. But also that the residence time (according to the general trend towards lower values in O-18 observed in the last years) is greater and changes from piezometer to piezometer - another argument for the great variability of this porous formation.

Part III: Local studies, field experiments and analyses

8 Artificial tracers: experiments performed in 1988 and 1992. Differences and analogies

8.1 1988 Tracer test

8.2 1992 Tracer test

8.3 Conclusions about the tracer results of 1992

8 - Artificial tracers: experiments performed in 1988 and 1992. Differences and analogies

8.1. - Tracer test of 1988

The disparity of the results obtained by Sansoay et al (1987), led us to choose another criterion for comparison. Instead of the sampling at each level, we tried to compare each observation well at just one level of the aquifer - the 8m one (between the former 6 and 10 meters sampling levels). The injection borehole was also prepared in order to allow injection at that level. Only the wells C6, D2, D4 and E4 were also sampled at the three levels. The 8-meter level sampling was done automatically with the help of a programmable sampling device. At the beginning, right after the injection, samples were taken every half-hour, then, after the peak, progressively less frequently.

In November 88, 0.5 Kg Uranine, 9.9 kg Sulforhodamine B and 25 kg of Lithium chloride were diluted in 60 l of water and 20 l of ethylenglycol and injected. The injection rate was of 1,2 l per mioute. 60 l of water were used for the spill.

With such quantities, the experiment was necessarily a long-term one, with all the problems this involved. Not only did the heterogeneity play a important role in the results obtained, but also the hydrodynamic situation, which changed a lot during the experiment. This resulted in non-stationarity conditions, which complicated the calculations once more.

Uranine and Sulforhodamine B were analysed with a fluorescence spectrometer (Perkin Elmer model 3000). Lithium was analysed by Mr. W. Käss (Umkirch , Germany), with a Zeiss flame-absorption spectrometer.

The results were quite different from the first series. C7 was the well reached fastest by all the tracers. All three concentration peaks were measured on the day of the injection.
The highest concentrations were detected in C4, C6, D6 and D7. In the F gallery, F6 received ten times more tracer than F4.
There was also a vertical difference in the concentrations measured at three levels, but with no obvious trend: C6 and D4 showed higher concentrations at 4 meters, the others at 11 meters.

Lithium was not always present in the samples. It did not reappear in F4, D1 and D5 at all, showing another important feature influencing solute transport: the nature of the tracer and its interaction with the substrate.

Fig. 58 shows four chosen observation wells and the breakthrough curves for the three tracers injected. It is difficult to imagine such discrepancies without having to admit a permeability difference due to an unequal distribution of finer sediments. This could explain the difference between D1 and D7, separated by 50 meters. But it is more difficult to explain the differences between C7 and C8 which are only set 7 meters apart.

Tracers are used for the study of the water flow, to calculate mean residence times of water, and to determine aquifer parameters such as porosities, permeabilities, etc. The analytical interpretations are based on models which admit the homogeneity and the stationarity of the system. This constitutes an *a priori* limitation of these methods. Furthermore, it is perhaps not absolutely correct to assume that the equation of dispersion which was determined in the laboratory holds under field conditions, considering both that the big difference in the dispersion coefficients determined at either scale, and the huge variability of the natural medium.

That is why one is often faced with the question of which model is best suited or calculates more significant aquifer parameters, and finds oneself incapable of answering it. Table 14 shows a trial made to calculate transport parameters using the conservative tracer Uranine. It is useless to try and interpret such results, or decide which method is most suitable, if one's knowledge about the aquifer is very limited.

For the numerical model, knowledge about the aquifer's properties, geometry and boundary conditions are important, and nothing can be done before one is in possession of this information.

However, tracers are a powerful tool for the study of the aquifer, revealing important aspects which influence solute transport. They are a priori good indicators of its heterogeneity and anisotropy. The performance of the RMT-R surveys contributed to validate this point of view. The correspondence between the tracer

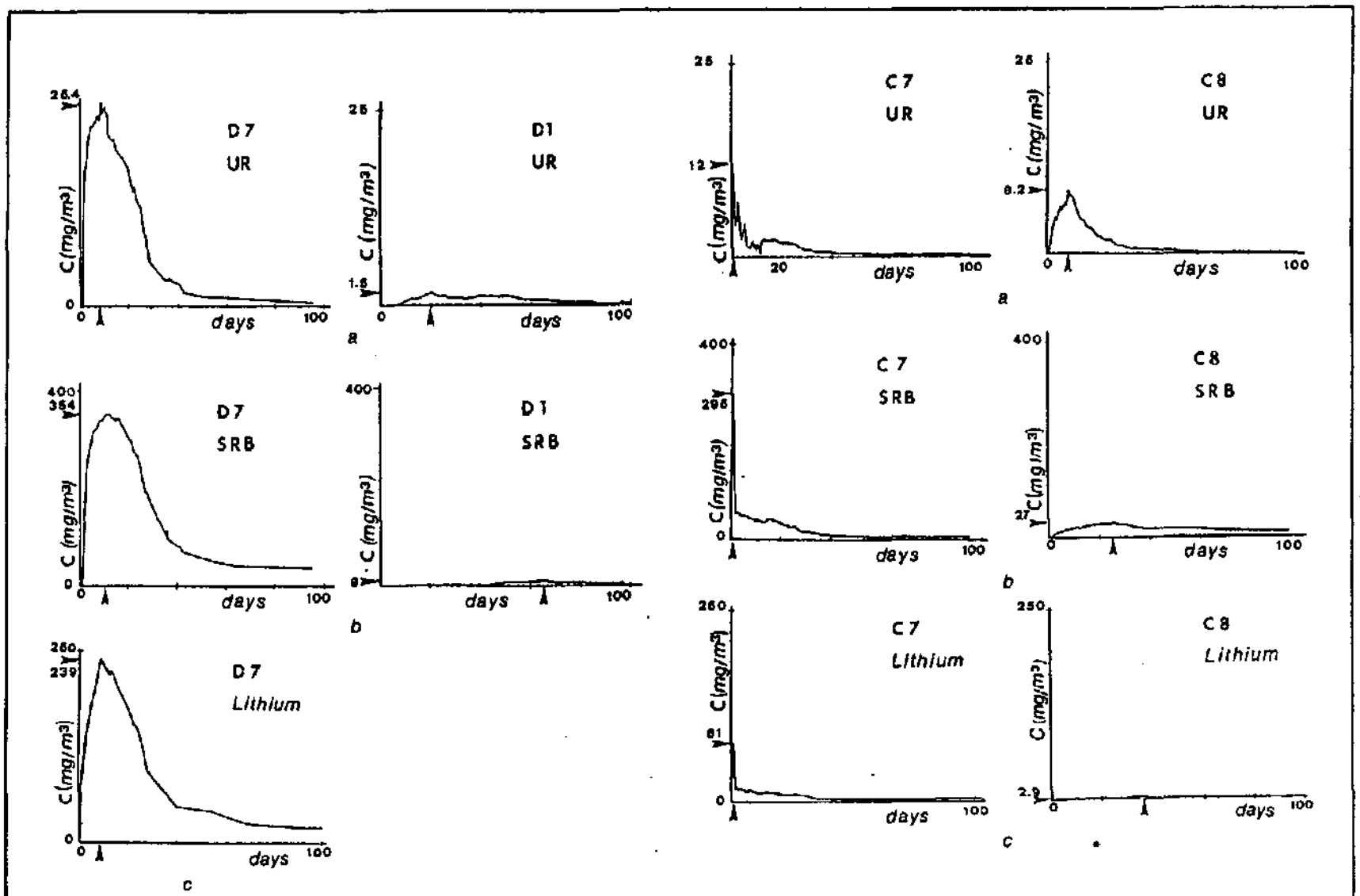

Fig. 58 Uranine, Lithium and Sulforhodamine-B breakthrough curves at four chosen observation wells, D1 and D7, set 50 meters apart (D gallery) and C7 and C8, separated by only 7 meters (C gallery). The contrasts between C8 and C7 are outstanding.

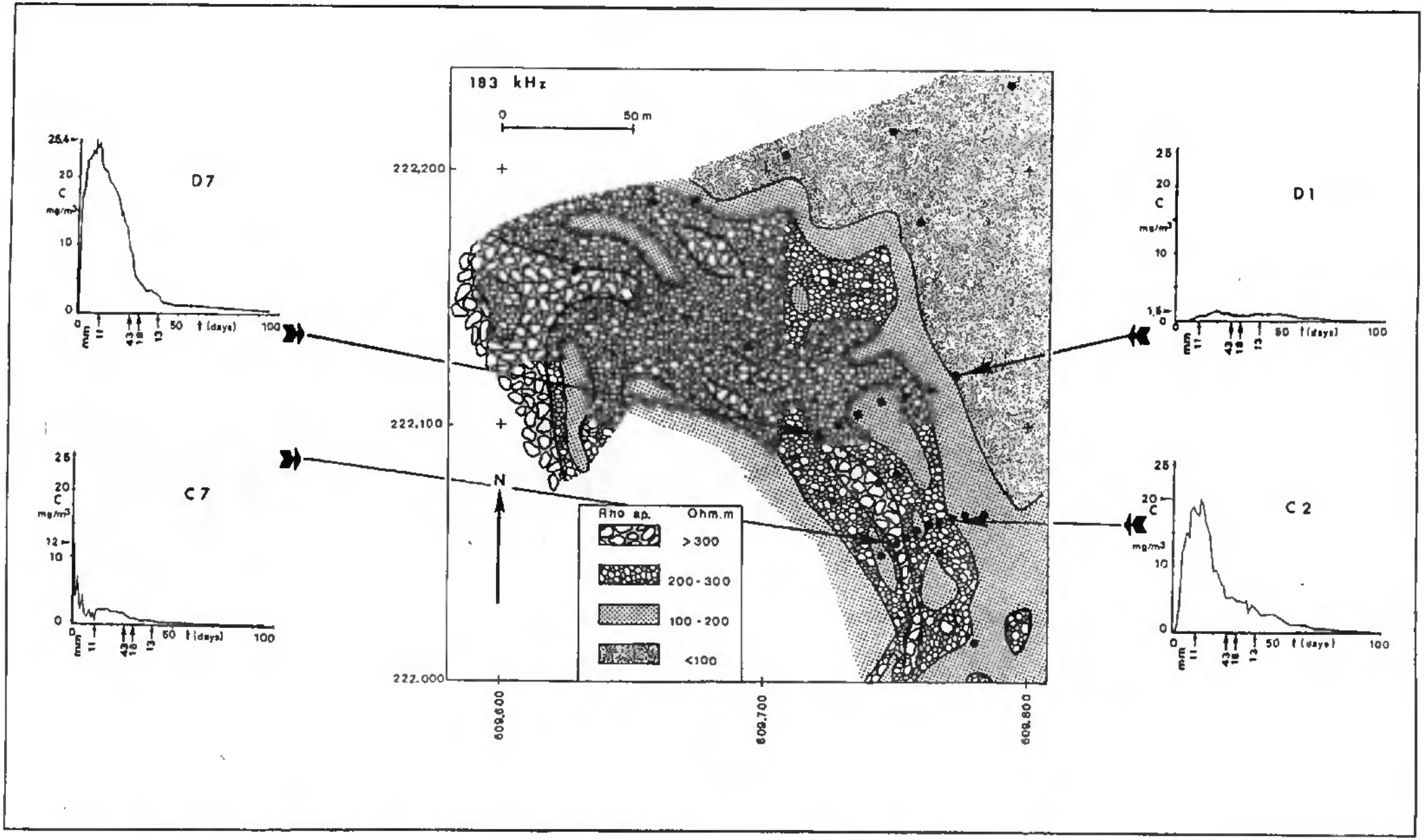

Fig. 59 Hand-drawn apparent-resistivity map and the Uranine breakthrough curves of four observation wells.

breakthrough-curves and the distribution of structure and resistivities (an indirect measure of the permeability) revealed by the RMT-R survey is remarkable (**Fig. 59**).

Because of what has been said above, only maximal concentrations and their corresponding times are given in **Table 15**, as a simple comparative criterion between observation wells.

8.2. - Tracer test performed in 1992

Following the conclusions of the 1988 tracer experiment, another strategy was tried for the last experiment.

Two simultaneous injection points were used, so as to study the influence on the results, both of the location of the injection point, and of the distribution of permeabilities. The tracers were injected in the well B4, which is 12,5 meters distant from the C gallery, and 62,5 m from the D gallery. This injection lasted 20 minutes. The second injection was made at EP1, over one hour. The following tracers were used:

-At B4:

Naphtionate (1 Kg diluted in 10 litres of water),
Amidorhodamine G (300 g diluted in 3 litres),
Bacteriophage f1 (960, ml at a concentration of $1 . 10^{11}$ Ph/ml),
Bacteriophage T7 (2.280 litre of a $3.9 . 10^{10}$ Ph/ml)

-At EP1:

100 g of Uranine,
2260 ml of the Bacillus subtilis phage PM7a ($7.7 \cdot 10^{9}$ Ph/ml),
2340 ml of phage VH5a of the marine bacteria Vibrio harveyi, ($3.2 \cdot 10^{10}$ Ph/ml).

For both injections the method developed by Mr **W. Käss (1992 & 1993)** was used. Water is pumped at the injection point from a depth of 0.5 m below the water table. It is mixed with different tracers aboveground and re-injected at a depth of 9 meters.

Instead of just one fixed sampling-level, we tried to obtain mixed samples of the whole water column at each well. This was done because we knew from the geophysical surveys (see **chapter 4**), that the vertical distribution of permeabilities was specific to each well.

Every well was therefore equipped with a 10 m-long PVC tube connected to a small vacuum pump. Each tube was weighted at its extremity. The tube was lowered regularly by hand, till the maximal depth was reached. The regularity of the procedure was controlled by maintaining an equal level within the PVC tube while pumping. As soon as the bottom was reached, the pump was turned off, the tube removed and its content emptied into a plastic container. Each observation well was equipped with its own container. This operation was done twice, in order to rinse the sampling apparatus and stir the water before taking the sample.

With the withdrawal of the three-level sampling device, it became possible to make parallel measurements of the piezometric level. As already written in chapter 5, we were surprised by the variability of situations which occurred during the experiment, simultaneously influencing the local directions of flow and transport.

Another important aspect of this experiment was the simultaneous injection of bacteriophages, with unexpectedly higher comparative velocities of migration (**Rossi, P. et al, 1993**).

Nevertheless, it is not yet possible to answer the questions asked or present a transport model. It rained a lot and very irregularly during the whole experiment. This non-stationarity aspect made it once more impossible to use analytical transport models, and too complex the use of a numerical one. However, the positive aspect is that it emphasised the multitude of possible hydrodynamic situations conditioning the solute transport.

Another problem must be mentioned. Except for the injection, when we were helped by Mr **W. Käss** (Umkirch, Germany), the team consisted only of two persons - Mr **P. Rossi** (Lab. de Microbiologie, Uni Neuchâtel) and myself. The sample procedure was quite slow, and a complete series of samplings (about 15 observation wells) became a two-hour procedure. This was certainly a disadvantage at the beginning of the experiment. I am convinced that we probably missed the Uranine peak at the observation well C7. If one observes its breakthrough curve (**Fig. 60b**), one notices that this observation well received only a very small quantity of

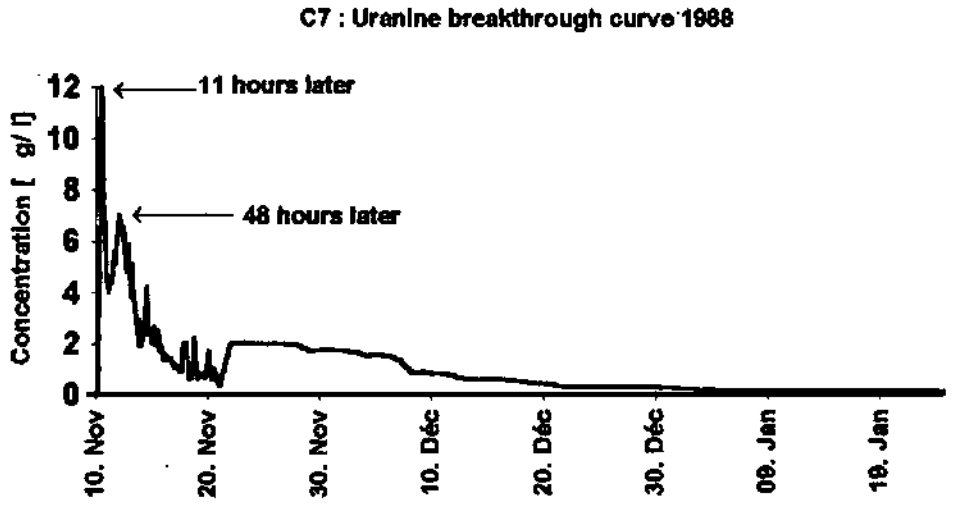

a

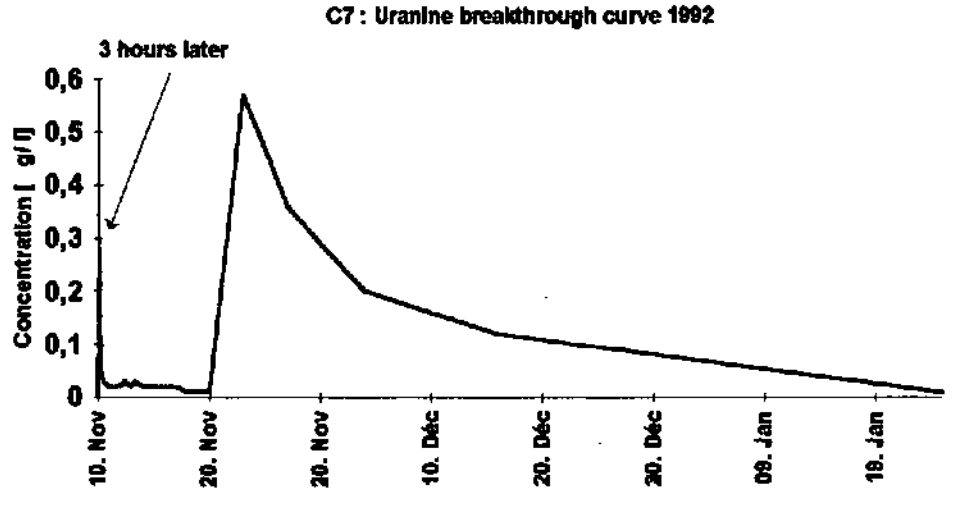

b

Fig. 60 Uranine breakthrough curves in 1988 (a) and 1993 (b). Both injection were done on November the 10th.

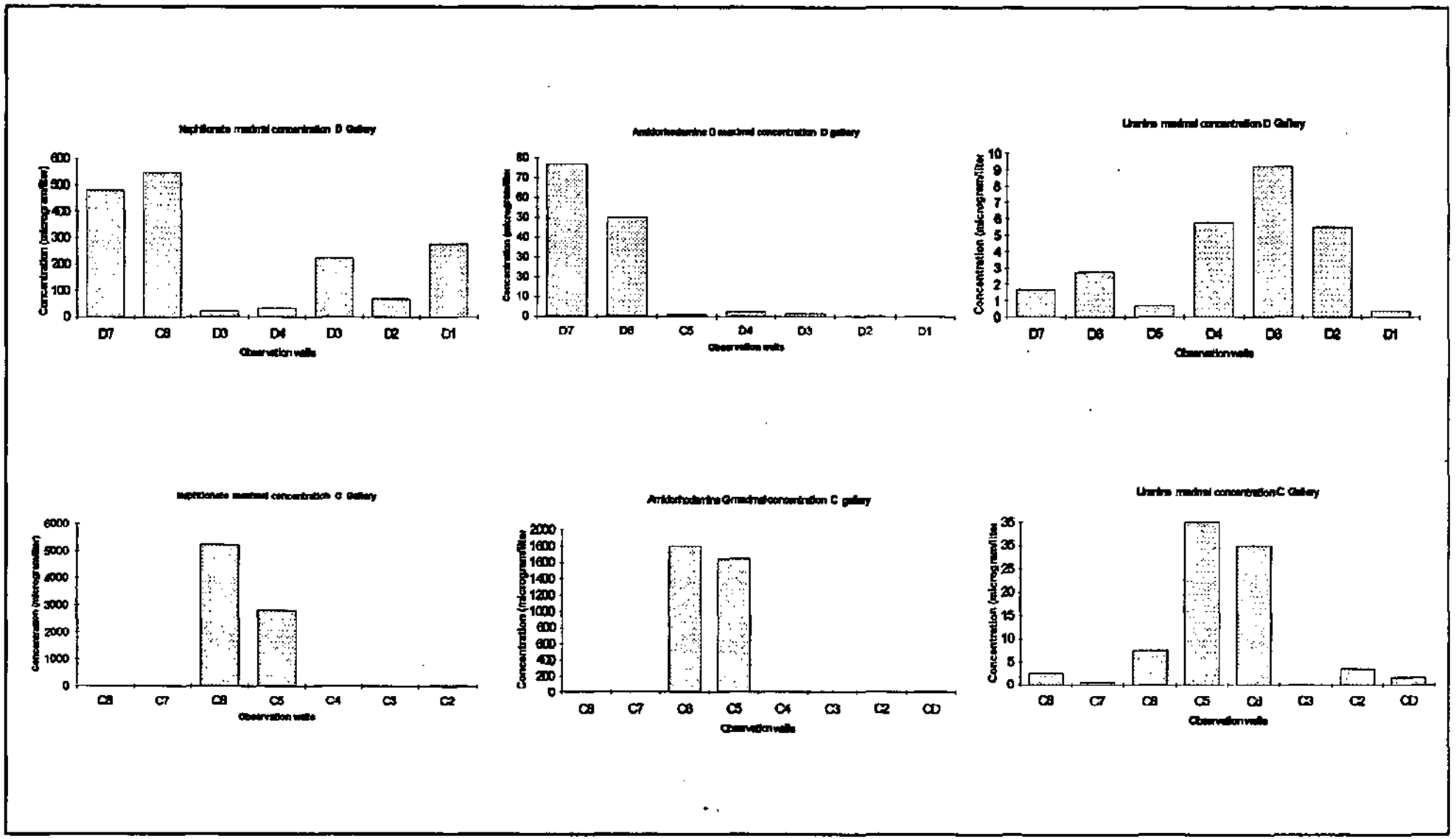

Fig. 61 Peak concentrations in different observation wells - 1992 tracer experiment.

tracer, but it was the one where the tracer arrived first (first detection 3 hours after injection). Another peak occurred ten days later. This theory is also supported by the piezometric map of the 10th of November (**Fig. 44**)
It is curious to compare this breakthrough curve with the one from the experiment of 1988 (**Fig. 60a**), where the sampling was carried out every half-hour at the beginning. I am almost sure that one is in the presence of a similar pattern, admitting the differences in concentrations (there was also a difference in injection concentration), the missing in-between samples and, of course, the difference in the hydrodynamic conditions.

In general, the higher concentrations of Naphtionate and Amidorhodamine G measured at C6, C5, and further down at D6 and D7, confirmed that the tracer tends to be deflected towards the west side of the field. This was also the case for the bacteriophages (**Pierre Rossi et al, 1993**). Another feature was also discovered: a particular piezometric situation existed in the east part of the field on injection day, mainly at D1, where an head "depression" was detected. This depression could be easily interpreted as a measurement error, but the detection of a surprisingly high concentration of the tracer Naphtionate (less sorptive than the Amidorhodamine G),(**Carvalho Dill *in* Pierre Rossi et al, 1993**), and also of bacteriophages , confirmed that it was not a mistake. This situation influenced the tracers injected at B4 the most, since that well is nearer, and is particularly evident for the Naphtionate. By the time the Uranine arrived, the situation was probably different, more in the direction of D3, if one considers the results obtained there.

Fig. 61 shows the histograms of the higher concentrations (peaks) in the C and D galleries. **Figs. 62a & b, 63a & b and 64a & b)** present all the tracer breakthrough curves in the two galleries. Table 16 shows the peak concentrations and corresponding times for each piezometer.

8.3.- Conclusions about the tracer results of 1992

Tracer transport seems to be conditioned by the distribution of permeabilities revealed by the RMT-R survey. This means that there is a heavier transport towards the paleochannel. The tracer is "pushed" in that direction and its path inflects towards NW. In this experiment the piezometers C6 and C5 as well as D7 and D6 received the greatest quantity of Amidorhodamine G and Naphtionate injected at B4. This effect of the channel was also observable in the experiment of 1988, where the fastest peak occurred at C7 and great quantities of tracers reached D6 and D7.

Permeability is directly linked to the grain-size distribution and the selection degree of a sediment. In the channel (where the degree of selection is higher and there is a lower percentage of fine material) the sorption of tracer is practically inexistent. In the eastern part of the site, which has a higher proportion of fine sediments, the interactions between tracers and the substrate are greater. This is clearly shown by the very low concentrations of Amidorhodamine, (**Fig. 63**) detected in the eastern observation wells (C2,D1,D2). And it was already noticeable with the Sulforhodamine and Lithium during the 1988 experiment (**Fig. 58**).

The nature of the tracer is very important, just as the differences between the different tracers injected. Naphtionate, the least sorptive tracer, was nevertheless detected at D1 (the least permeable well) emphasising another factor as important as the permeability distribution: the role of the particular hydrodynamic condition (in this case the head depression that was also measured at D1). Hydrodynamics are also related to the permeabilities distribution. But in this case the coincident depressions detected at C7 (paleochannel) and D1 (less permeable) are apparently contradictory, and serve to underline the complexity of the phenomenon.

The choice of injection point plays an important role. We observed a seemingly contradictory result - the tracer Uranine did arrived in great quantities at the piezometers C5 and C4 but also at D3 (!), followed by D4 and D2. This is certainly due to the piezometric situation mentioned above. The paleochannel being farther from the piezometer EP1 than from B4, its influence is not as great and the tracer injected at EP1 was deflected more towards the eastern part of the field. Because of the distance, it reached the D gallery days after the Naphtionate and Amidorhodamine did, probably when the "depression" at D1 did not exist any more.

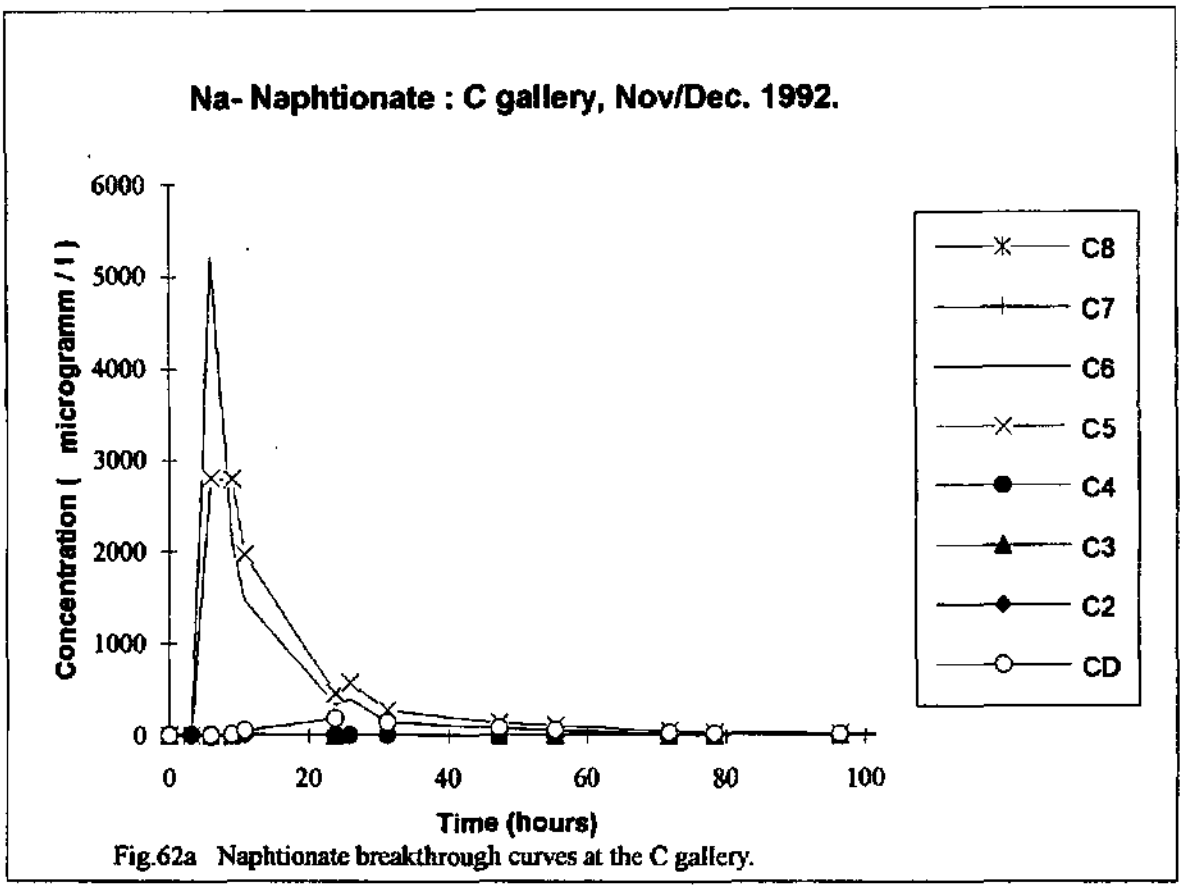

Fig.62a Naphtionate breakthrough curves at the C gallery.

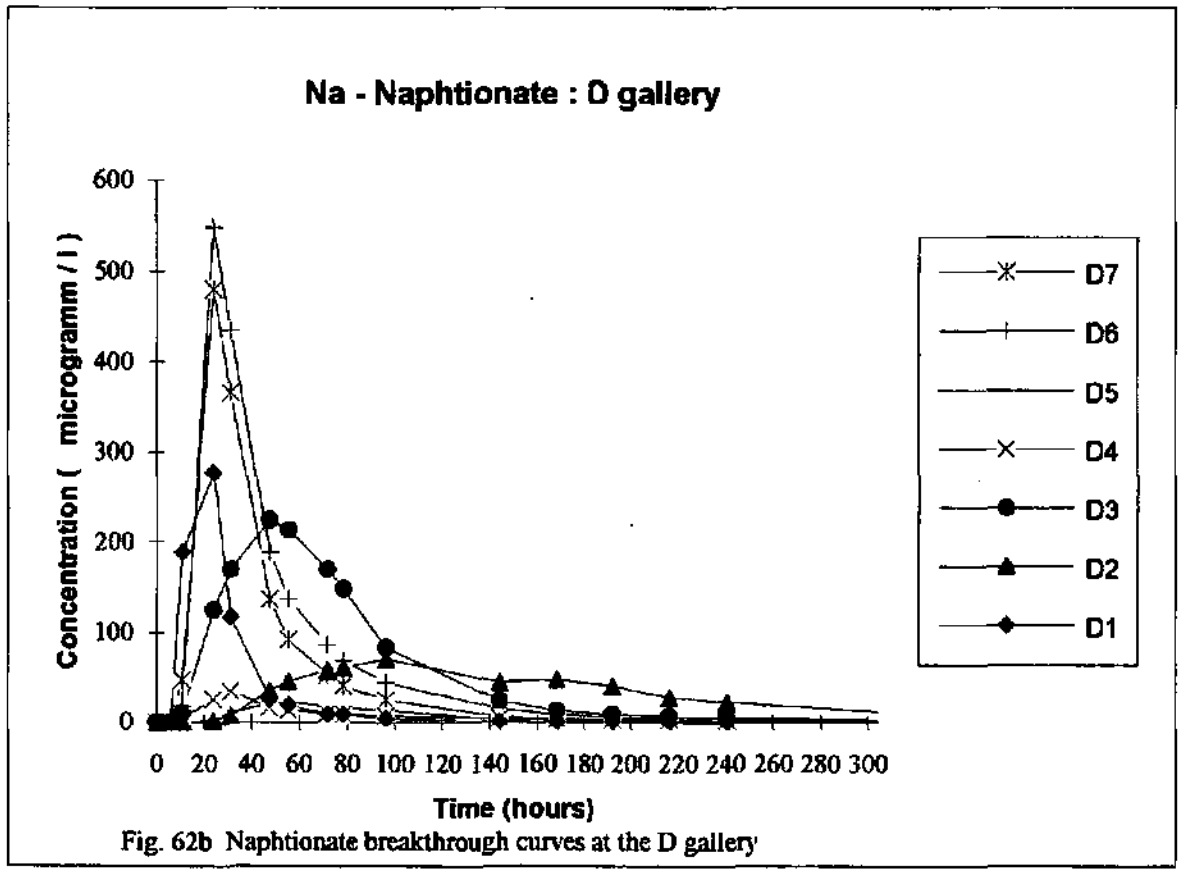

Fig. 62b Naphtionate breakthrough curves at the D gallery

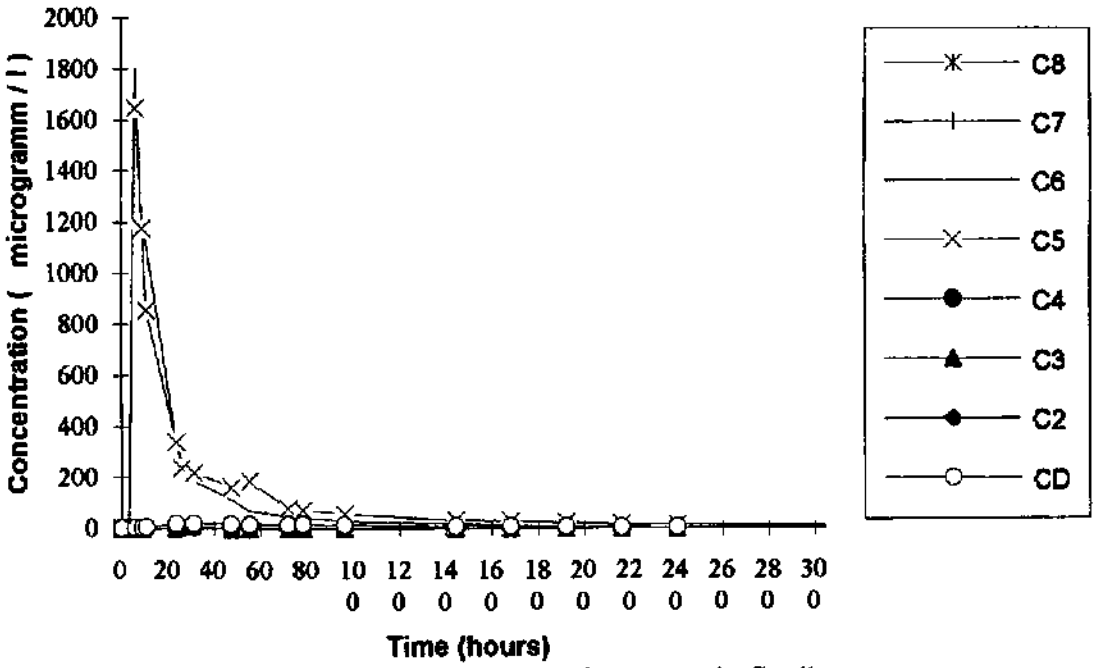

Fig. 63a Amidorhodamine G breakthrough curves at the C gallery.

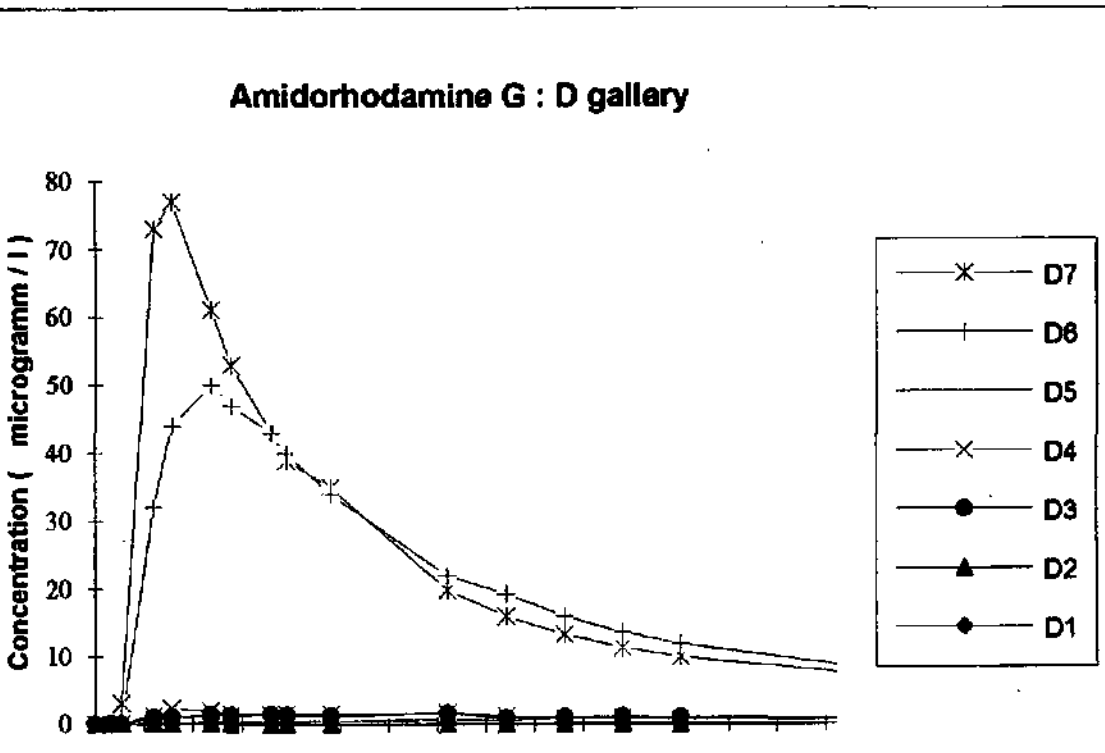

Fig. 63b Amidorhodamine G breakthrough curves at the D gallery

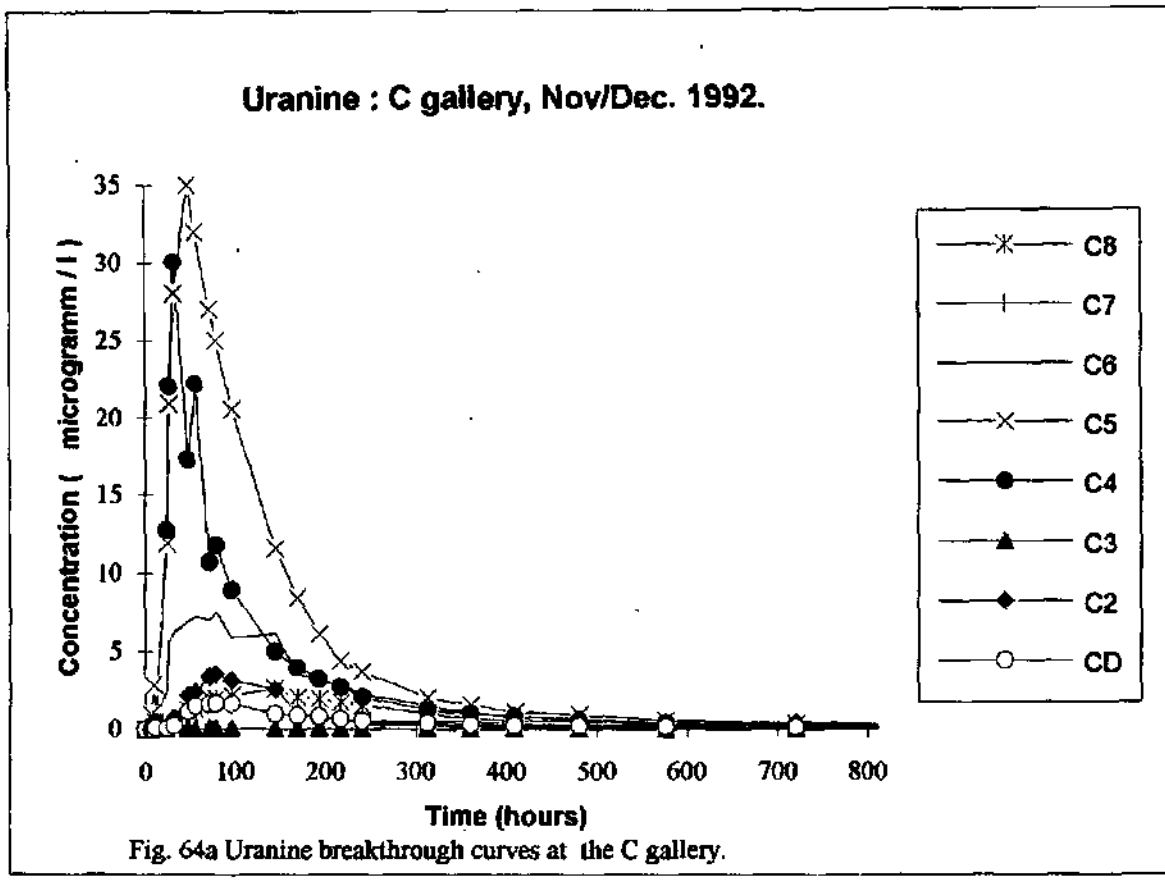

Fig. 64a Uranine breakthrough curves at the C gallery.

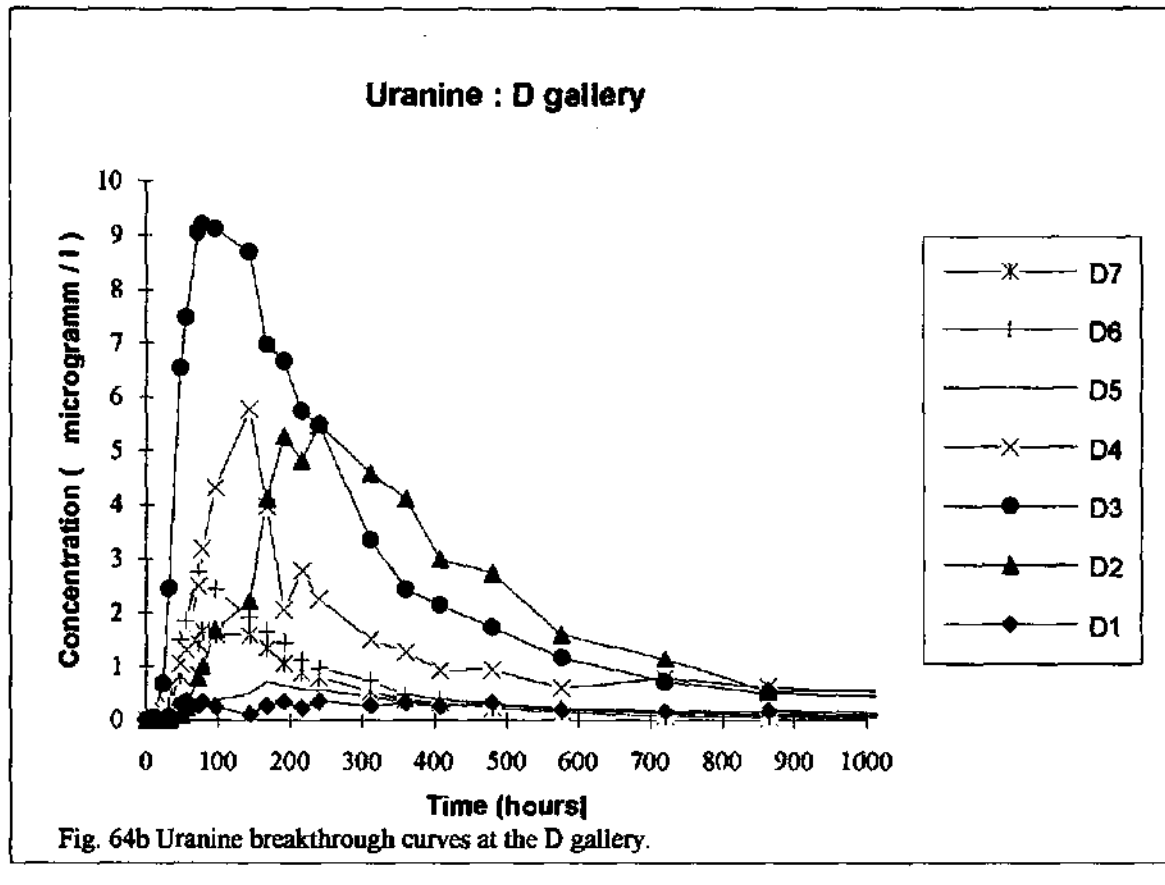

Fig. 64b Uranine breakthrough curves at the D gallery.

In summary, we can conclude that the experiment of 1992 emphasised the following main aspects :

1- the role of the distribution of permeabilities, detected by the radiomagnetotelluric surveys.

2- the variability of the hydrodynamic situations in space and time, that condition the direction and velocities of flow and transport over short periods of time.

3- the influence of the tracer's nature and of its interactions with the medium. A particularly curious and unexpected transport result must be pointed out - the bacteriophages injected simultaneously were transported more rapidly than the chemical tracers (**Pierre Rossi et al, 1993**). Like the chemical tracers, they were also selectively pushed towards the west part of the field at very great velocities. Forwards investigations are being carried out by Mr. Pierre Rossi.

URANINE																												
			C gallery										D gallery												E4		F gallery	
							C6							D2				D4										
Obs. well (sampling depth)		B4 (8m)	C2 (8m)	C3 (8m)	C4 (8m)	C5 (8m)	C6 (4m)	C6 (8m)	C6 (11m)	C7 (8m)	C8 (8m)	CD (8m)	D1 (8m)	D2 (4m)	D2 (8m)	D2 (11m)	D3 (8m)	D4 (4m)	D4 (8m)	D4 (11m)	D5 (8m)	D6 (8m)	D7 (8m)	E4 (8m)	E4 (11m)	F4 (8m)	F6 (8m)
distance (m)		37.12	49.3	49.0	49.15	48.89	48.47	48.47	48.47	48.55	49.12	74.0	103.79	98.50	98.50	98.50	98.30	99.37	99.37	99.37	99.05	97.68	99.19	149.82	149.82	202.56	202.15
Cmax (mg/m^3)		101.9	20	11.1	90.9	36.8	67.9	66.0	60.8	12.0	6.2	24.5	1.47	15.3	17.9	21.5	14.6	-	7.12	89	3.29	30.7	25.4	3.84	3.18	0.75	6.70
t(Cmax) (h)		43.7	289.4	57.2	44.4	53.2	75	59.2	120	11	199.5	167	482.3	336.8	252.5	336.8	212.5	-	107.0	2448.5	204.5	268.5	204.5	726.5	490.7	231.7	434.3
Va (m)	S	2.98	3.01	3.46	6.98	3.82	3.76	3.67	4.03	2.98	3.98	4.62	2.4	3.49	4.75	5.03	5.65	-	6.71	0.82	6.91	5.99	6.61	3.73	7.25	8.23	6.61
	M	1.91	2.13	2.56	3.90	2.08	2.84	2.56	2.82	2.08	2.55	3.45	2.2	2.92	3.45	3.82	3.85	-	4.21	0.79	4.61	4.41	4.78	3.36	5.73	6.08	5.18
	C	-	1.94	-	-	-	-	-	-	-	2.58	-	-	5.38	-	3.88	-	-	-	-	3.51	2.3	-	-	3.28	-	2.88
DL (m^2/h)	S	92.3	66.7	97.4	283.6	257.4	76.6	97.2	146.3	105.6	97.9	166.5	41.4	81.8	206.1	193.9	315.5	-	546.3	0.8	348.9	228.3	230.6	98.9	404.9	734.8	429.6
	M	41.5	41.5	62.9	185.7	68.7	66.2	72.2	65.5	66.2	73.3	93.0	38.0	53.2	115.3	100.3	174.7	-	252.4	1.46	241.7	204.7	250.8	66.8	234.5	434.0	290.8
	C	-	34.04	-	-	-	-	-	-	-	42.6	-	-	14.4	-	97.2	-	-	-	-	178.0	117.0	-	-	248.8	-	291.5
α (m)	S	31.0	22.1	26.1	40.6	67.4	20.4	26.5	36.3	35.4	24.6	36.0	17.2	23.4	43.4	38.6	55.8	-	81.5	0.97	50.5	38.1	34.8	26.5	55.9	89.3	65.1
	M	21.7	19.5	24.4	46.9	33.0	23.3	28.0	23.3	31.8	28.7	27.0	17.3	18.2	33.4	26.2	45.3	-	59.9	1.89	52.4	46.4	52.5	19.9	41.0	71.4	56.2
	C	-	17.6	-	-	-	-	-	-	-	16.5	-	-	2.68	-	25.0	-	-	-	-	50.6	50.7	-	-	76.0	-	101.3
D/vx	S	0.84	0.44	0.56	0.81	1.35	0.41	0.53	0.73	0.71	0.49	0.48	0.17	0.23	0.43	0.39	0.56	-	0.81	0.01	0.51	0.38	0.35	0.18	0.37	0.45	0.33
	M	0.58	0.39	0.49	0.95	0.66	0.47	0.56	0.46	0.64	0.57	0.36	0.17	0.18	0.33	0.26	0.45	-	0.60	0.02	0.52	0.46	0.53	0.13	0.27	0.36	0.28
	C	-	0.35	-	-	-	-	-	-	-	0.33	-	-	0.03	-	0.25	-	-	-	-	0.51	0.51	-	-	0.51	-	0.51
t_0 (h)	S	299	398.6	346.8	177.8	322.2	319.1	326.5	297.8	402.8	301.5	389.6	1000	687.7	502.3	477.1	424.8	-	357.8	2926.8	347.3	400.6	363.1	965.1	496.6	583.2	726.2
	M	465.4	563.8	468.1	307.7	576.5	423.2	464.8	426.1	576.2	470.2	522.3	1092.2	822.3	695.5	627.7	622.8	-	569.7	3048.5	520.4	543.8	502.5	1072.7	628.5	789.7	927.5
	C	-	619.4	-	-	-	-	-	-	-	464.6	-	-	446.0	-	618.0	-	-	-	-	628.5	1042.5	-	-	1099	-	-

Table 14 Comparison of the transport parameters calculed by different methods using the conservative tracer Uranine (The calculations were done with the help of programs installed at Geographishes Institut, Uni Bern).

C max = peak concenuration ; t(Cmax) = time of the peak

S = Summenkurve (cumulative distribution curve) ; va = va_{med} = t(50 %) (Fried, 1975)

M = Moment method (Maloszewsi,1985); C = Cmax /0.5 Cmax Method (Maloszewsi,1985).

DL - Longitudinal dispersivity

t_0 - the mean transit time of water t_0=x/v

α = dispersivity ; D/vx = dispersions parameter

URANINE

		C gallery										D gallery												F gallery	
						C6							D2				D4						E4		
Obs. well (sampling depth)	B4 (8m)	C2 (8m)	C3 (8m)	C4 (8m)	C5 (8m)	C6 (4m)	C6 (8m)	C6 (11m)	C7 (8m)	C8 (8m)	CD (8m)	D1 (8m)	D2 (4m)	D2 (8m)	D2 (11m)	D3 (8m)	D4 (4m)	D4 (8m)	D4 (11m)	D5 (8m)	D6 (8m)	D7 (8m)	E4 (8m)	E4 (11m)	F4 (8m)	F6 (8m)
distance (m)	37.12	49.3	49.0	49.15	48.89	48.47	48.47	48.47	48.55	49.12	74.0	103.79	98.50	98.50	98.50	98.30	99.37	99.37	99.37	99.05	97.68	99.19	149.82	149.82	202.56	202.15
Cmax (mg/m3)	101.9	20	11.1	90.9	36.8	67.9	66.0	60.8	12.0	8.2	24.5	1.47	15.3	17.9	21.5	14.6	-	7.12	89	3.29	30.7	25.4	3.84	3.18	0.75	6.70
t (Cmax) (h)	43.7	289.4	57.2	44.4	53.2	75	59.2	120	11	199.5	167	482.3	336.8	252.5	336.8	212.5	-	107.0	2448.5	204.5	268.5	204.5	726.5	490.7	231.7	434.3

Sulforhodamine B

		C gallery										D gallery												F gallery	
						C6							D2				D4						E4		
Obs. well (sampling depth)	B4 (8m)	C2 (8m)	C3 (8m)	C4 (8m)	C5 (8m)	C6 (4m)	C6 (8m)	C6 (11m)	C7 (8m)	C8 (8m)	CD (8m)	D1 (8m)	D2 (4m)	D2 (8m)	D2 (11m)	D3 (8m)	D4 (4m)	D4 (8m)	D4 (11m)	D5 (8m)	D6 (8m)	D7 (8m)	E4 (8m)	E4 (11m)	F4 (8m)	F6 (8m)
distance (m)	37.12	49.3	49.0	49.15	48.89	48.47	48.47	48.47	48.55	49.12	74.0	103.79	98.50	98.50	98.50	98.30	99.37	99.37	99.37	99.05	97.68	99.19	149.82	149.82	202.56	202.15
Cmax (mg/m3)	939	189.7	226.3	692.3	258.2	1064.1	761.9	613.3	394.7	27.0	443.3	9.05	85.6	112.4	123.5	115.6	96.8	53.7	67.1	14.9	410.1	353.9	25.9	25.9	5.23	64.8
t (Cmax) (h)	57.3	482.0	65.2	75.2	120.7	75.0	87.2	288.6	12.5	605.5	289.5	1564.6	336.8	822.0	604.5	336.6	462.0	244.5	604.5	498.0	360.7	256.5	625.5	653.0	582.5	439.3

Lithium

		C gallery										D gallery												F gallery	
						C6							D2				D4						E4		
Obs. well (sampling depth)	B4 (8m)	C2 (8m)	C3 (8m)	C4 (8m)	C5 (8m)	C6 (4m)	C6 (8m)	C6 (11m)	C7 (8m)	C8 (8m)	CD (8m)	D1 (8m)	D2 (4m)	D2 (8m)	D2 (11m)	D3 (8m)	D4 (4m)	D4 (8m)	D4 (11m)	D5 (8m)	D6 (8m)	D7 (8m)	E4 (8m)	E4 (11m)	F4 (8m)	F6 (8m)
distance (m)	37.12	49.3	49.0	49.15	48.89	48.47	48.47	48.47	48.55	49.12	74.0	103.79	98.50	98.50	98.50	98.30	99.37	99.37	99.37	99.05	97.68	99.19	149.82	149.82	202.56	202.15
Cmax (mg/m3)	814	70.9	131.0	434.0	101.7	285.0	614.0	186.0	81.0	3.6	-	-	-	11.6	-	20.0	22.7	10.8	12.3	-	258.0	239.0	-	-	-	19.7
t (Cmax) (h)	59.2	434.0	91.2	57.2	96.7	678.5	79.2	147.5	13.0	1516.5	-	-	-	3047.5	-	510.0	626.5	594.0	528.0	-	260.5	252.5	-	-	-	1632.2

Table 15 Tracer test, 1988 : Main differences on peak concentrations and peak times.

Uranine (injection well: EP1)															
	C gallery								D gallery						
	C2	C3	C4	C5	C6	C7	C8	CD	D1	D2	D3	D4	D5	D6	D7
distance (m)	49.3	49.0	49.15	48.89	48.47	48.55	49.12	74.0	103.79	98.5	98.3	99.37	99.05	97.68	99.19
Cmax (µg/l)	3.54	0.115	30	35	7.51	0.57	2.62	1.68	0.36	5.47	9.2	5.76	0.7	2.74	1.67
t (Cmax) (h)	76.5	166.3	29.0	45.0	75.8	44.7	143.0	76.7	54.5	239.7	77.5	143.3	167.2	70.5	76.8
Amidorhodamine G (injection well: B4)															
	C gallery								D gallery						
	C2	C3	C4	C5	C6	C7	C8	CD	D1	D2	D3	D4	D5	D6	D7
distance (m)	14.48	12.34	12.04	12.62	14.29	17.03	22.76	37.45	68.90	62.36	61.39	62.25	62.30	61.72	64.37
Cmax (µg/l)	0.29	0.41	3.10	1645	1803	0.30	0.07	17.50	0.49	0.26	1.57	2.30	0.87	50.00	77.00
t (Cmax) (h)	7.2	4.1	6.8	3.7	3.4	0.5	8.0	28.2	239.8	191.7	143.5	27.8	191.2	45.9	27.5
Na-Naphtionate (injection well: B4)															
	C gallery								D gallery						
	C2	C3	C4	C5	C6	C7	C8	CD	D1	D2	D3	D4	D5	D6	D7
distance (m)	14.48	12.34	12.04	12.62	14.29	17.03	22.76	37.45	68.90	62.36	61.39	62.25	62.30	61.72	64.37
Cmax (µg/l)	9.10	0.75	20.40	2805	5220	10.50	1.90	187	278	70	224	34	22	548	480
t (Cmax) (h)	7.3	4.1	8.5	3.7	3.4	0.5	6.0	21.8	23.0	95.7	46.3	27.8	54.1	22.1	22.0

Table 16 Tracer test, 1992 : Main differences on peak concentrations and peak times

Part IV: Merdingen test site (Germany)

9. Merdingen

9.1 Description of the site

9.2 Geology and Hydrology

9.3 Electromagnetic surveys

9.3.1 RMT-R

9.3.1.1 Performance and Results

9.3.1.2 Interpretation based on raw data

9.3.1.3 Kriging at Merdingen

9.3.2 - VLF-EM

9.4 Synthesis and conclusioos

Part IV : Merdingen test site (Germany)

9. Merdingen

9.1 Description of the site.

The Merdingen test site is situated in the Upper Rhine Valley, some 15 km north-west of Freiburg, between the Kaiserstuhl and the Tuniberg (**Fig. 65**), where the Rhine once flowed.

It has been used as a test site since 1978 (**Käss,1990**). It is composed of two fields, with axes parallel to the direction of ground-water flow, oriented towards NE:
- a western field (A), the older one, where the observation wells, including 5 triple boreholes are disposed in half-circles, at a distance of 6.25, 12, 25, 50 100 and 200 meters from the injection borehole;
- an eastern field (B), circa 40 meters distant from the axis of field A, with boreholes arranged in rows perpendicular to its axis.

Today the site (**Fig. 66**) is also equipped with 130 flat wells less than 5 meters deep, made of rammed 1 1/2 ioches steeltubes, with perforations along their lower part. Only the five triple boreholes (site A) penetrate deeper (about 10 meters), with filter ranges of 1-2, 4-5 and 9-10 meters. Most of these wells were set up by **Mr.** and **Mrs. Käss**.

9.2 Geology and Hydrology

The Upper Rhine Valley is a Tertiary Rift System, where the Rhine has flowed since the beginning of the Quaternary. Up to the Pliocene young sediments of the Graben flanks filled the basin. After the breakthrough of the river Rhine, the deposits came form the Alpine area.

The Quaternary sediments began with sequences of sand and silt, followed by sand and gravels which have intercalations of a few silt and clay layers, responsible for the subdivisioo of the aquifer into sub-aquifers.

The upper aquifer is the one where the site is installed. It is composed of sands and gravels dating from the Pleistocene and the Holocene. Its thickness is about 20 to 25 meters. It is covered by one meter thick layer composed of dark clays, rich in humus and of lighter clays. Underneath the aquifer there is another clay layer. The permeability (k_f) varies from 5×10^{-3} up to 2×10^{-4} m/s. (**Carvalho Dill et al, 1992**).

A geoelectrical profile performed some 50 m east to the test field in S-N direction, detected an irregular stratification of the uppermost layer with a high resistivity, i.e. with a good permeability, between 300 and 900 Ohm.m. Downwards the resistivity of the layers diminished. The range of permeabilities < 100 Ohm.m may be the bottom layer out of strongly impermeable material rich in clay which rises towards north (NLfB 1981). The fields (mainly corn) two hundred meters upstream obviously influence the water quality on the site (for instance the nitrate concentrations have values varying from 100 mg/l, io the saturated zone to 500 mg/l in the unsaturated one).

Table 17 (page 109) , represents the hydrochemical data from the Merdingen test site (**Carvalho Dill et al, 1992**). The analysis were performed by **W. Käss**, the isotopes by **D.Rank**. It is a hydrogencarbonated water, with about 700 mg/l total amount of dissolved componeots.

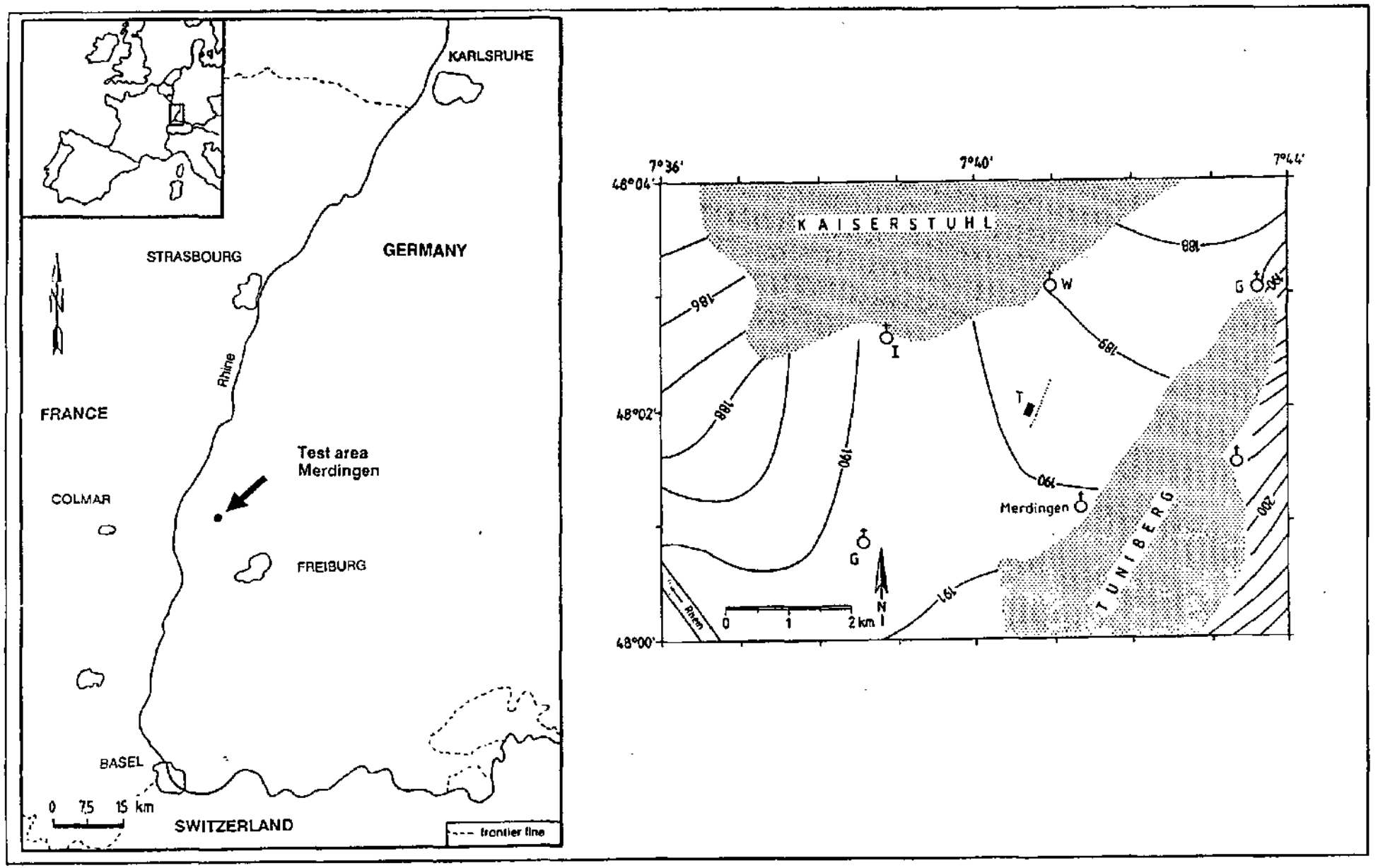

Fig. 65 Location of the Merdingen test site and contours of the water table in the environment of the test field Merdingen (MELU + MWMV 1977). Dotted line : geoelectric profile. (After W. Käss, in Carvalho Dill, A. et al. 1992).

Depth (m)	1–2	4–5	9–10	Rainwater
Temperature (°C)	12.0	12.2	11.9	
Conductivity (µS · cm⁻¹/20° C)	705	693	698	15.3
pH	7.19	7.19	7.24	6.91
Eh (mV)	509	514	529	
Hardness, total (meq/l)	7.51	7.44	7.44	
Na^+ (mg/l)	16.6	16.5	16.5	2.05
K^+ (mg/l)	2.11	2.58	2.37	2.28
Li^+ (µg/l)	4.7	4.9	8.6	
Sr^{2+} (µg/l)	271	266	275	
Cl^- (mg/l)	35.6	33.7	33.5	
NO_3^- (mg/l)	43	38	37	
SO_4^- (mg/l)	45.0	45.5	45.7	
O_2 (mg/l)	2.9	5.7	4.6	
O_2 (% saturation)	28	54	43	
CO_2 (mg/l)	20	22	22	
^3H (T.U.)	45.5	45.2	41.4	12.6
$\delta^{18}O$ (‰ SMOW)	–8.50	–8.56	–8.55	–11.41

Table 17 Hydrochemical data for the groundwater in the testfield Merdingen (extracted from **Käss** *in*, **Carvalho Dill et all,1992)**

The ground water table is situated at depths of 1.5 meters. Its gradient is of about 0.05 % towards NE. The lowest and highest level of the water were detected at 189,47 m on Sept.12, 1991, and at 190,87 m on May 30, 1983 respectively.

9.3 Electromagnetic surveys:

9.3.1 RMT-R

About 30 tracing tests were carried out from 1979 to 1992. These tests were mainly done to determine the applicability of different tracers in pore ground water. All these tracer experiments had something in common: the tracer cloud, did not disperse around the main direction of water flow, as theoretically it should. Instead a shift to the left was clearly seen at the very beginning of its transport, between the two injection points E and the 25 m profile line, followed by an inflexion to NE, which was observed at both sides of the field. Besides, the tracer seemed to vanish at the profile line 50 m, reappearing again at 100 m **(Käss,1992)**.

9.3.1.1 Performance and results

To investigate possible reasons for this mysterious behaviour, RMT-R surveys were performed. The 224 points measured were distributed along 21 profiles **Fig. 67**. The plotted resistivities (y1) and dephasing values (y2) were made as at Wilerwald, without transforming the resistivity values into logarithms. The first difference to be seen, if we compare **Fig. 68** with **Fig. 24**, is the constant parallelism of the resistivity lines, the values at 183 kHz being always higher than those at 70 kHz, and these always higher than those at 19 kHz. Already the values of the phases at 183 kHz are near 45° or even superior. This indicates a relatively small influence of the upper conductive layer which is thinner, and the presence of a resistant and relatively less heterogeneous layer than at Wilerwald which corresponds to the aquifer. The first frequency used practically travelled through the whole aquifer thickness (17 m). In the downstream profiles it seems that the thickness of the aquifer diminishes, as indicated by the phase values, which are of almost 50°. The values at 70 kHz are generally lower than those at

than those at 183 kHz, because of the influence of the conductive lower layer. The profiles suggest the existence of elongated alternating structures of low and high apparent resistivities.

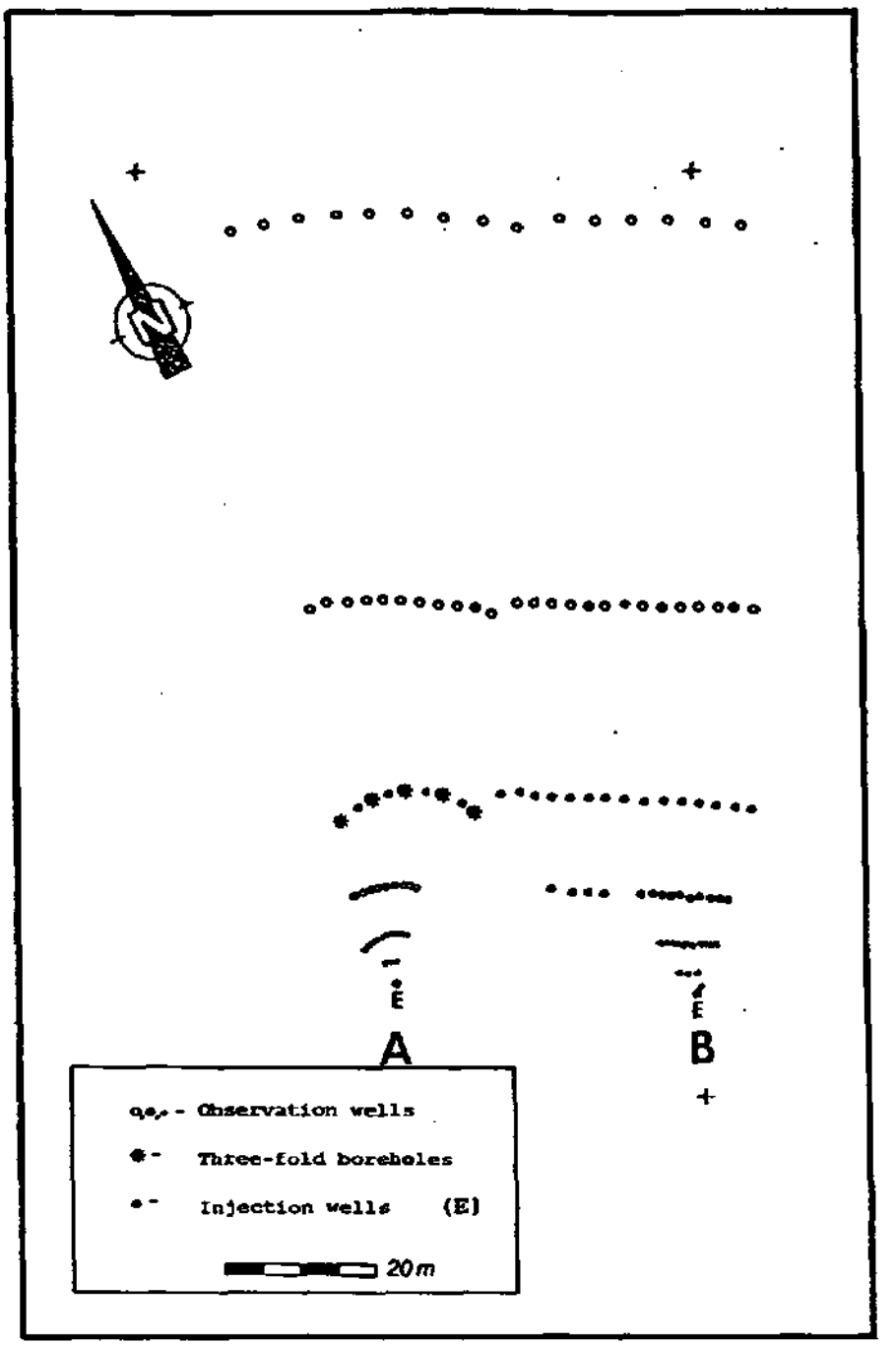

Fig. 66 Merdingen test area showing the two sub-sites A and B.

Like at Wilerwald , the construction of Contour Maps already give a good picture of the structure of the aquifer. These maps were first drawn by hand (Fig. 69). After a second campaign, interpolation using the Kriging method

was used to create six resistivity and phase maps, which will be discussed further on.

Looking at the hand-drawn 183-kHz contour map, one notices the marked elongated orientation of the resistivities. This could be the cause of the deflection of tracer transport at the very beginning of its movement, between both injection points (E) and the 25 m profile line, followed by an inflexion to the right, which can be observed at both sides of the field. This agrees with the results of the tracer experiments carried out at Merdingen since 1979.

The reasons for the disappearance of the tracer at 50 m is not clear. It is important not to forget that these resistivity values, and consequently the permeabilities, correspond to the whole soil column, and that the heterogeneous distribution of permeabilities with depth is not taken into account. Possibly the tracer is being pushed towards the higher permeabilities, plunging into deeper ground below the depth of the piezometers, and cannot therefore be detected. But the reappearance at lower depths would be another enigma. This subject will be discussed further on.

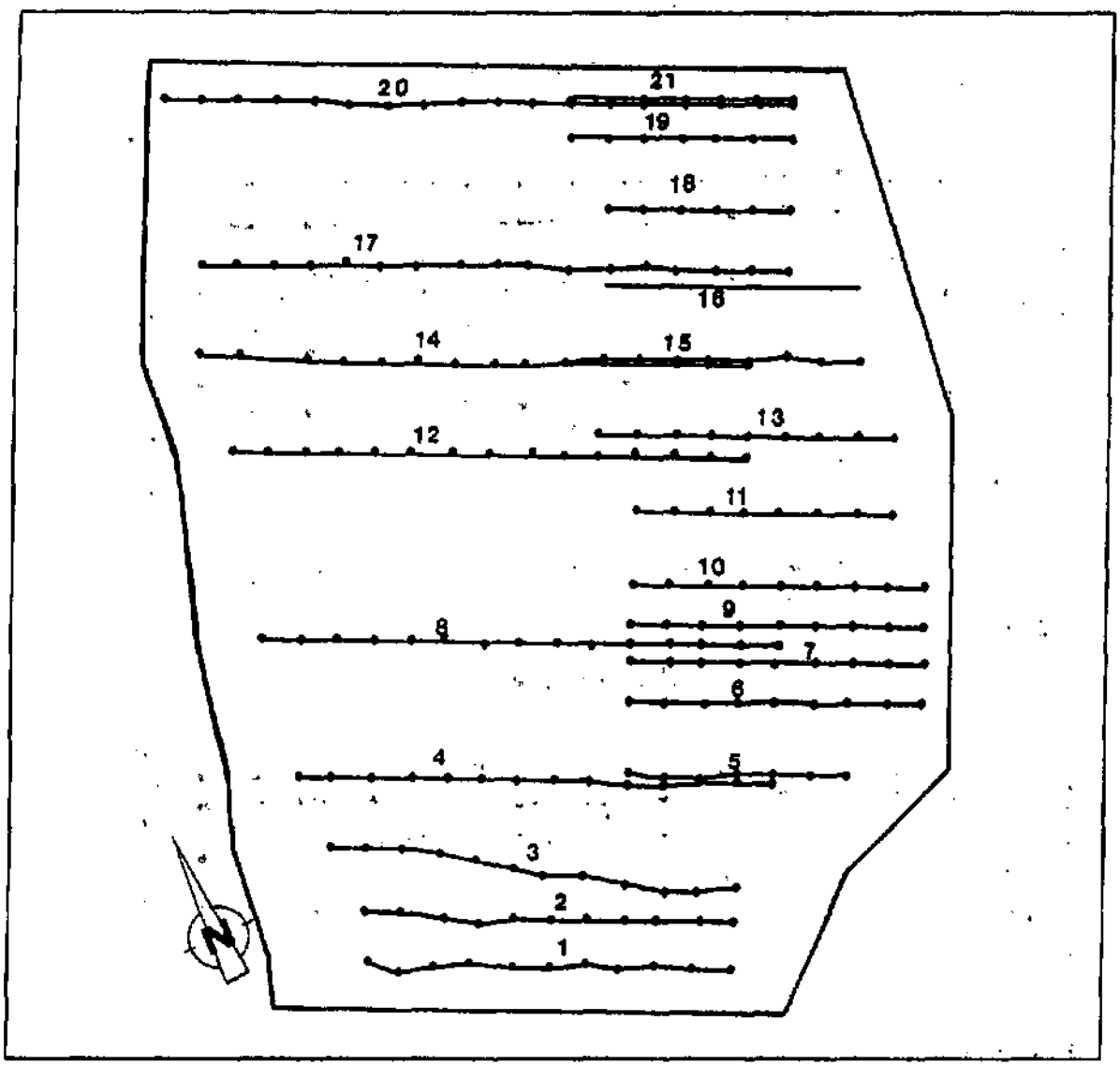

Fig. 67 Map representing the RMT-R profiles and the measuring points

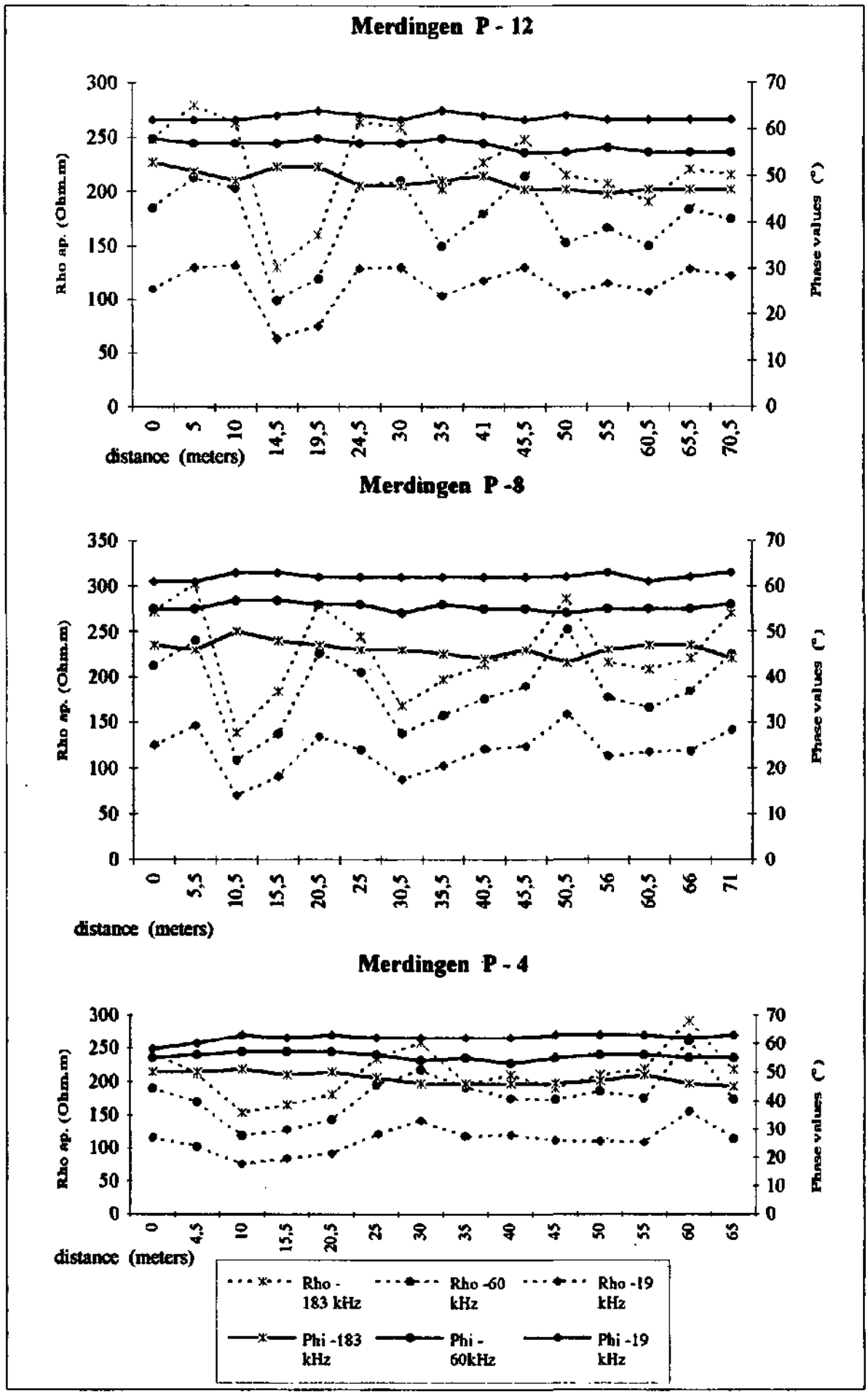

Fig. 68 Some profiles showing the Rho apparent values at Y1 (left axis) and the Phase values at Y2 (right axis). For the location of the profiles, please see Fig. 67 on page 111.

9.3.1.2 - Interpretation based on raw data :

The same method of interpretation of the raw data as at Wilerwald was tried.
First, all the values of the logarithms of resistivity, histograms were plotted for each frequency. The results can be seen in **Fig. 70**.
We can observe that with increasing depths of investigation, the apparent resistivity values become lower and the phases higher.

This fact was also confirmed when the cumulative frequency curves (**Fig. 71**) were drawn. The influence of the conductive bottom layer seem already to become apparent. The curves are obviously less tilted than the ones at Wilerwald, which is clearly a consequence of the higher selectivity of this deposit. This fact is in accordance with the genesis of this sediment - because the Rhine obviously had greater transport energy. This can be seen in the curves, and the lower values of the standard deviation (σ_l).

At 183 kHz, (depth of investigation ≈ 17 m), 45.5 % of the deposit have resistivity values between 200 and 250 Ohm.m. At 70 kHz, (depth of investigation ≈ 24 m), 40.6 % of the values are situated between 160 and 200 Ohm.m. The diminishing percentage maybe explained by the variation in depth of the bottom layer detected by the electrical profile (**NLfB 1981**). At 19 kHz ,(depth of investigation ≈ 36 m), 47 % of the values are situated between 80 and 100 Ohm.m. Comparing with Wilerwald, it is interesting to see that all the values belong to the 4th (79.5%) and 5th classes (20.5%), i e., Rho 183 kHz > Rho 70 kHz > 19 kHz, pointing out the higher degree of homogeneity and the fairly constant conditions of genesis.

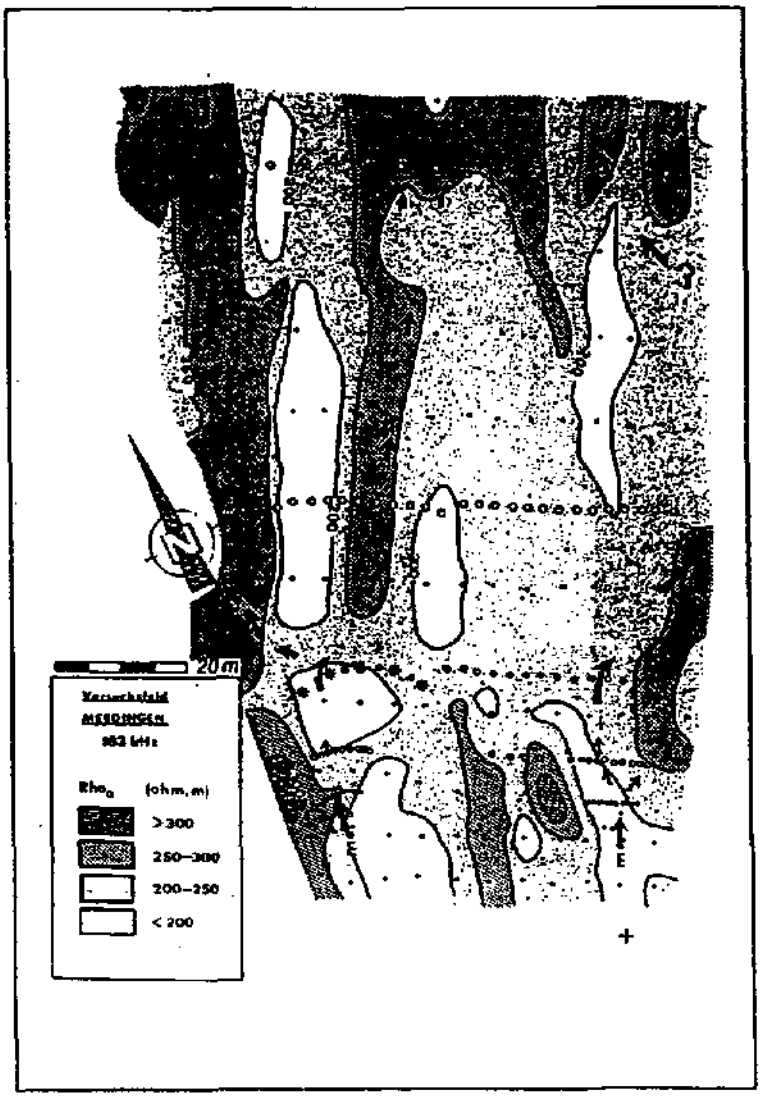

Fig. 69 Apparent resistivity contour map at 183 kHz, drawn by hand. The figure also shows: 1) the actual tracer path (arrows); 2) the piezometers which received the greatest amount of tracer.

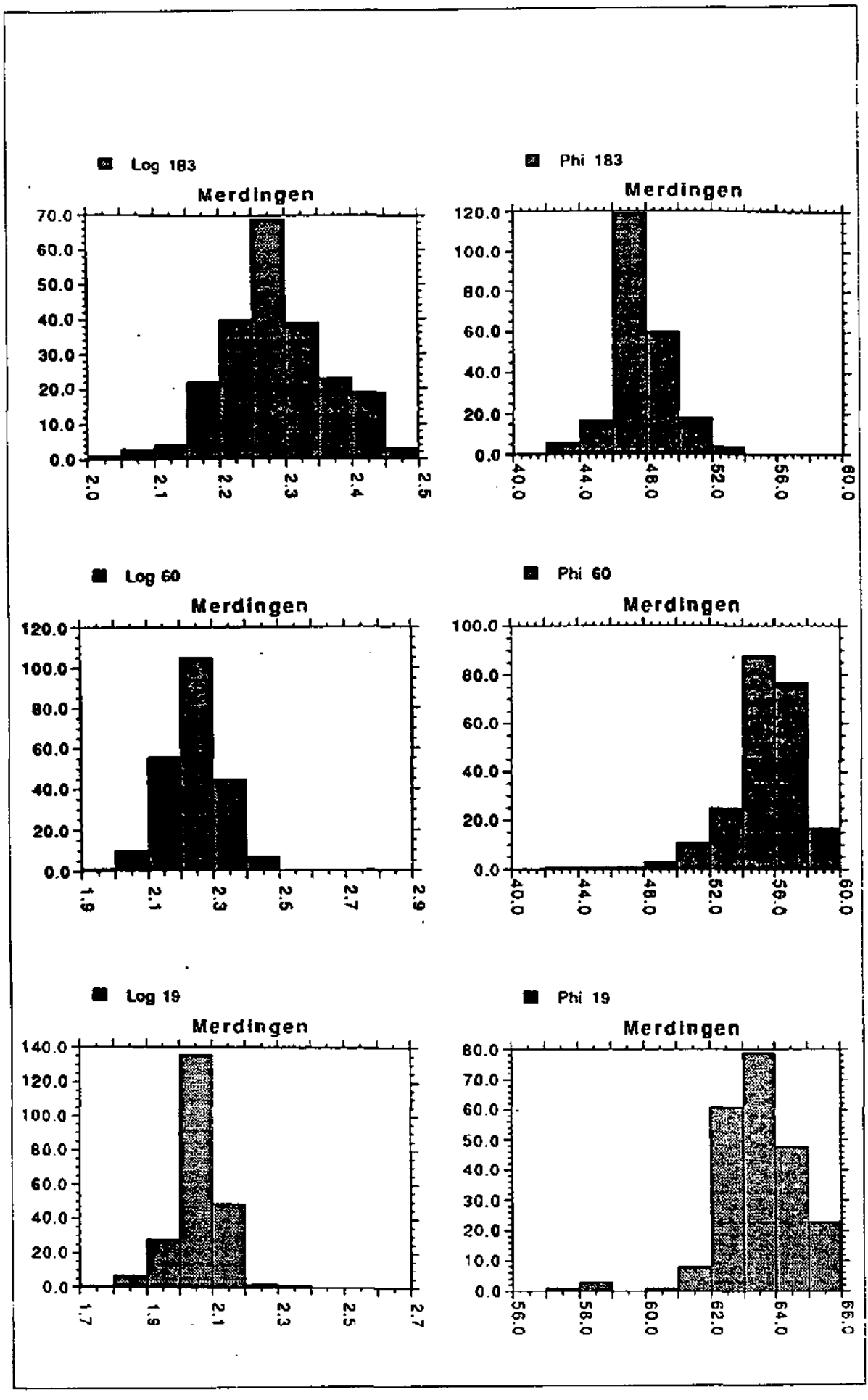

Fig. 70 Histograms of the resistivities transformed into logarithms and phase values.

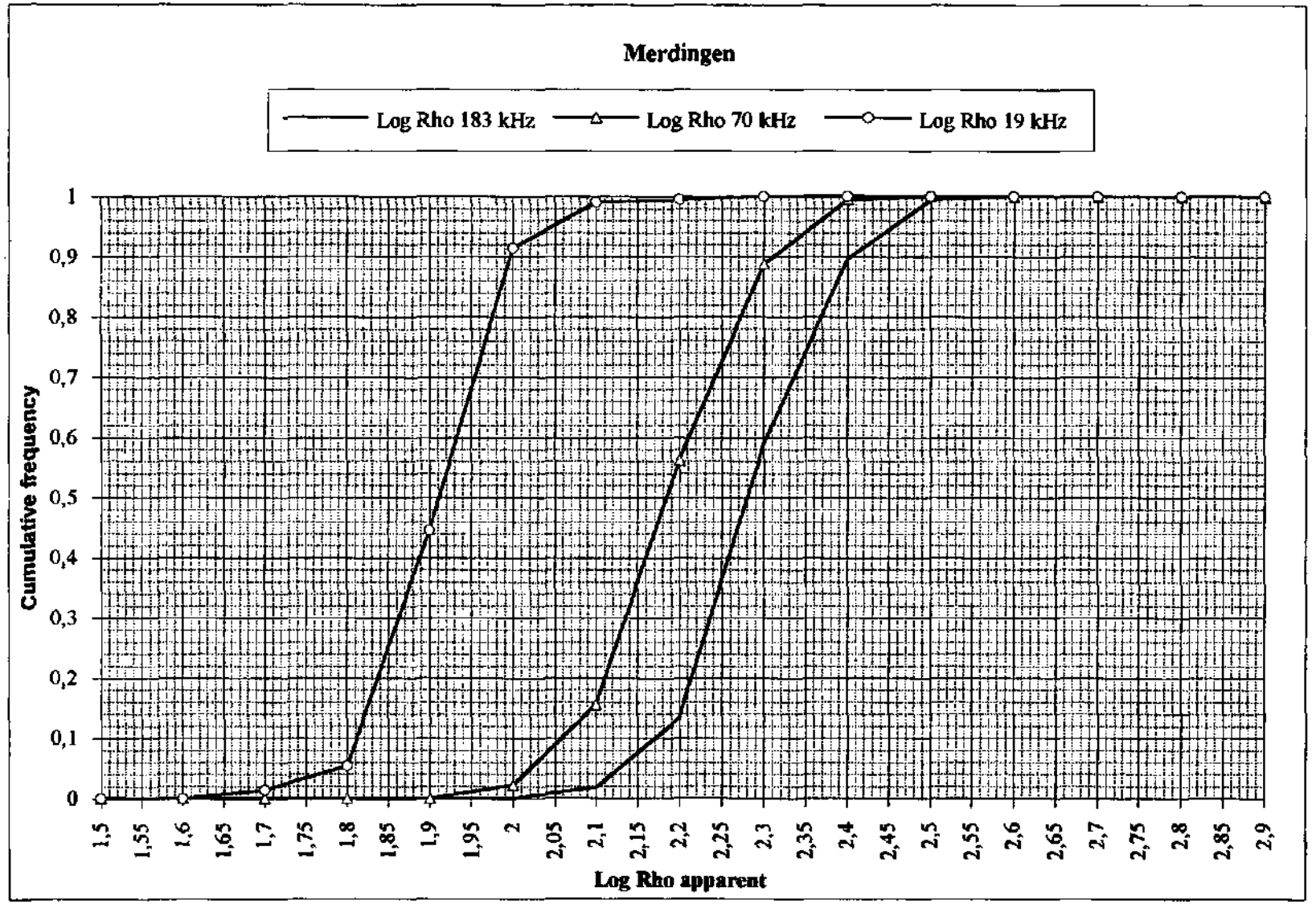

Fig . 71 Cumulative frequency curves (Log Rho apparent) at the Merdingen test site, illustrating the greater degree in homogeneity.

9.3.1.3 Kriging at Merdingen

The more homogeneous character of the Merdingen sediments is once more made clear by the values compiled from the variogram functions. The variogram functions at each frequency were estimated for the resistivities values and for the logarithm of resistivities. Comparing with Wilerwald, one sees that the range is practically the same, varying between 190 m and 300 m, but that the sample variance and consequently the sill (*a priori* variance) are particularly low. The almost total absence of nugget effect can be attributed to the greater homogencity already mentioned above.
Again, higher standard errors are found at the edges of the zone and in regions where the density of measurements is relatively low.

This homogeneity shows up very clearly in the contour maps of resistivities (**Fig. 72a & b**). All reveal the same structure of elongated and inflected domains of relatively higher resistivity. Only the lateral regions vary somewhat more (see also **Fig. 73a & b**). This seems to be related to the lower phase values observed, at 60 kHz for the right side and at 19 kHz for the left side, maybe due to the depth or nature of the aquitard - it seems that the aquitard is situated at lower depths at the right side.

This occurs in the vicinity of the 50 m piezometer-profile line (sub-site B), suggesting that the disappearance of the tracer could be linked to its deflection toward the left side of the area. At 100 m the resistivity values increase again, consequently the reappearance there is logical.

It is also interesting to see that the resistivity values at 200 kHz are generally higher than at 70 kHz, indicating that the humus cover layer isn't too important (relatively thin) and/or also that the aquifer is slightly shallower (20 m) than at Wilerwald. This is confirmed by the phase values which are already equal or higher to 45° in the 200 kHz range.

Merdingen		**Statistics**	
183 kHz	**Rho ap.**	**Log Rho ap.**	**Phase**
Variance	1609.55	0.00638	3.20
Sill	1900	0.008	5
Range	0.2 Km	0.25 Km	0.25
Nugget	900	0.0038	1.1
Std. Dev.	40.12	0.080	0.120
Sample Size	224	224	224
Min.	114	2.060	42
Max.	353	2.550	53
70 kHz	**Rho ap.**	**Log Rho ap.**	**Phase**
Variance	1214.52	0.00728	5.426
Sill	1600	0.009	6.6
Range	0.3 Km	0.3 Km	0.19 Km
Nugget	850	0.0055	3.4
Std. Dev.	34.85	0.0853	5.41
Sample Size	224	224	224
Min.	98	1.990	42
Max.	292	2.470	59
19 kHz	**Rho ap.**	**Log Rho ap.**	**Phase**
Variance	395.067	0.00538	1.58
Sill	430	0.0064	2.450
Range	0.2 Km	0.21 Km	0.265 Km
Nugget	320	0.004	0.5
Std. Dev.	19.88	0.073	1.260
Sample Size	224	224	224
Min.	63	1.80	57
Max.	227	2.360	65

Table 18 : main characteristics of the kriging interpolation function

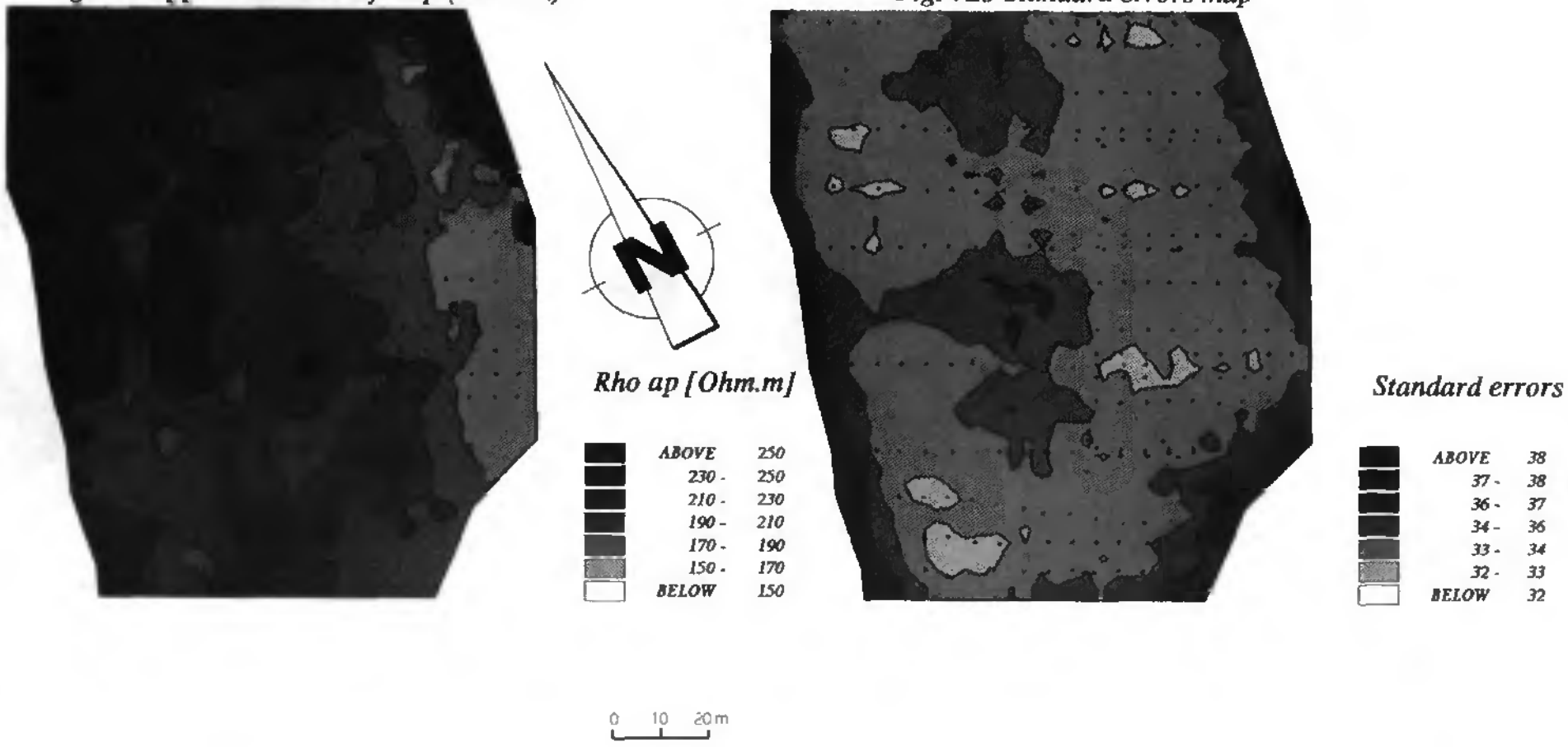

Fig . 72 RMT-Results : apparent resistivity map (183 kHz) **(a)** and standard error map **(b)** .

Fig. 73a Phase map (183 kHz)

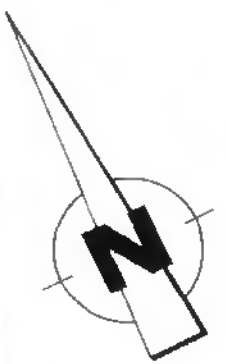

Phase values [°]

ABOVE	52
50 -	52
48 -	50
46 -	48
44 -	46
BELOW	44

Fig 73b Standard errors map

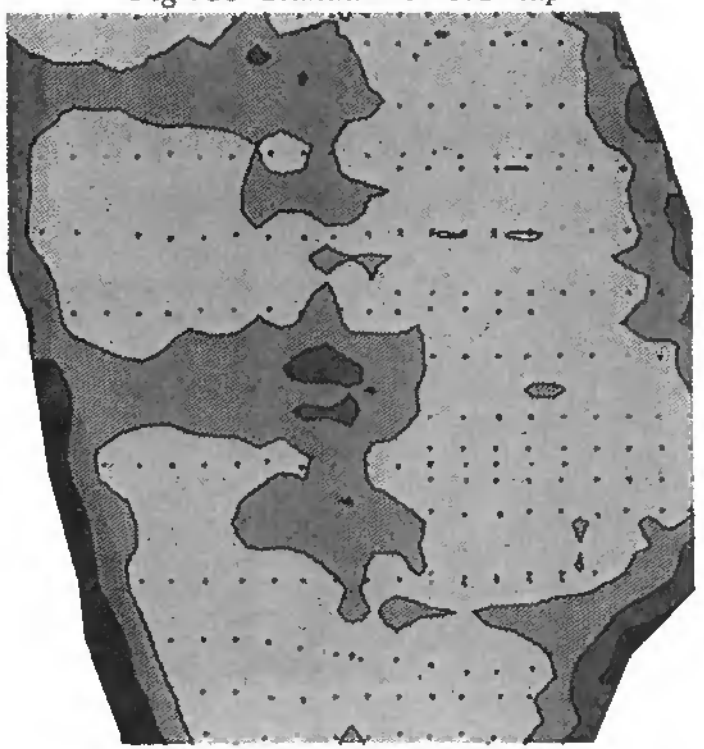

Standard errors

ABOVE	1.70
1.60 -	1.70
1.50 -	1.60
1.40 -	1.50
1.30 -	1.40
1.20 -	1.30
BELOW	1.20

0 10 20 m

Fig . 73 RMT-Results : phase map (183 kHz) **(a)** and standard error map **(b)** .

9.3.2 Very Low Frequency - Electromagnetic Surveys

The lateral changes in resistivities are not so strong here, so the continuous recording of the out-of-phase component of the VLF-EM technique did not show any remarkable regions. Only a trend is visible, a decrease towards the eastern part of the site and at the south, as well as some "depressions" whenever relatively higher values of resistivity exist.

9.4 Synthesis and Conclusions

With the electromagnetic survey performed at Merdingen it was our intention to find an explanation of the tracer behaviour - a deflection at the beginning of its transport, the disappearance at the 50 m piezometer-line and the reappearance at 100 m in field B.
Simultaneously the possibility to compare two test sites installed in porous sediments was at hand.

As to the tracers behaviour, the RMT-R results revealed the existence of more resistant elongated pockets inflecting towards the right in the vicinity of both injection points.
This aspect seems to be continuous at all depths, since it appears at all the frequency ranges.
The reasons of the tracer disappearance at 50 m in the field B could be the following. One notices on **Fig. 72**, that there is a general lowering of the resistivity values there, and that the phases maps (**Fig. 73**) revealed that the aquitard is deeper on the central right side. The apparent resistivity contour maps indicates that there is then again an increase of the resistivities values at 100 m. So it is possible that the tracer is deviated at 50 m towards the left side of the field, and later towards the right side. However, the other explanation, presupposing the existence of a thinner layer of higher resistivity (not detected by the RMT-R) at depths not reached by the observation wells and where the tracer would be channelled, cannot be totally excluded. Its reappearance at a greater/lesser depth would be then explained in terms of vertical upwards flow components.

Merdingen presents a higher degree of homogeneity than Wilerwald. This was revealed not only by the RMT-R surveys, but also by the VLF-EM. This fact is in accordance with the genesis of these sediments and greater transport energy of the Rhine.

Part V : Final Conclusions

10. Brief Overview

Part V : Final Conclusions

10. Quick overview

The Wilerwald aquifer was once considered to be a homogeneous porous medium. This small area was idealised, for modelling purposes, as having an uniform thickness of 10 meters, a mean hydraulic conductivity of ~ $2.4 \cdot 10^{-3}$ m/s, with a mean hydraulic gradient of 0.4 % oriented towards N and undisturbed. Like almost all porous media, its flow was considered to be laminar, with constant and low velocity.

Initially the Wilerwald test site was intended as a full-scale laboratory. In order words, an aquifer whose parameters were very well known, where different experiments using all kinds of tracers could be carried out. A site where the ideal border conditioos needed in the use of analytical models were available.

This work began with the issues involved in modelling. Modelling is of great demand in science today. Any model, is a simplified versioo of reality. Therefore the choice of simplifying assumptions will condition absolutely its capacity to simulate the aquifer behaviour, i.e., its validity.

The results of the first tracer tests, soon after the site's installation, pointed out that the use of analytical models was going to be problematical. Analytical models are in general very restrictive : they usually require a homogeneous and isotropic medium, with a parallel flow of constant velocity, steady-state conditions and simple boundary conditions (infinite or semi-infinite media).

Conceptually local scales require 3-D models.
A numerical model (a flow model or transport model) intends to simulate an aquifers behaviour by describing:

-the state of the system : its geometry (form and limits), its physical properties (permeability, transmissivity, storativity) and the boundary conditions,

-the state variables : (heads, chemical composition...),

-the laws linking these parameters and the system's reaction towards external action (by the resolution of differential equations which describes the water movement or solute transport through it).

Modelling techniques have improved a great deal in the past years, but old problems still remain to be solved. The quantification of the different parameters needed to define the system are subject to the uncertainties of the measuring techniques. Interpolating scattered and punctual data obtained from a very variable medium often does not reflect the heterogeneity of the medium.

This work is concerned with definiog the points listed above and points out some practical problems one is confronted with during the acquisitioo and interpretation of data.

Clearly, it is impossible to describe the geometry of the aquifer and study its properties in the site, without first acquiring some knowledge of its regional context.

The literature overview made it clear that we are in the presence of a very complex aquifer, with extremely variable geometry and litology. It also pointed out that the Emme plays an important role in the chemical balance of the groundwater, and that the zone of influence of its infiltration is irregularly distributed, due to differences in permeability.

Because of the great heterogeneity of the zone, interpolations based only on punctual information must be avoided. Geophysical techniques which don't homogenise the medium, such as the electromagnetical VLF-EM and RMT-T were therefore very suitable and helped the interpretation of values.

The VLF-EM method is very sensible to lateral changes in aquifer properties. About 10 VLF-EM surveys were made very rapidly, around the Wilerwald test site. The continuously registered out-of-phase variations confirmed the extreme variability of these quaternary deposits. They also allowed to delineate preferential groundwater pathways - paleochannels filled with clean coarse gravels (and also, pebbles and cobbles). It was also interesting to find that the location of these paleochannels corresponds to the depressions of the

actual topographic lines. Therefore it seems that the present surface still reflects the ancient lie of the paleochannels.

Piezometric observations in the region were related to the geological aspects and showed how differently the aquifer can react to rain events. Higher amplitude variations, and correspondingly delays in reaching the maximal level, seemed to coincide with lower permeabilities. Besides, a cumulative phenomenon appeared to occur in those wells. Observation wells situated in exfiltration zones generally had small amplitudes and very quick responses.

"Nature's fractal geometry" is the best way of describing what is to be expected in the small scale of Wilerwald. Had thisconcept been thought before, scale errors and false interpretation would have been avoided.

It is important to avoid interpolations based on scattered punctual measurements, even at the site scale. The RMT-R soundings were ideal, because of the density of measurements (~ 500 in the test area), and this because of the rapidity and versatility of the method. At the same time, the degree of information obtained is quite revealing - it yields a good picture of the aquifer, about its geometry and about its resistivity distribution, related to the permeability. Three frequencies allowing to investigate the aquifer at three depths were used: 183 kHz, 70 kHz and 19 kHz. They were a good complement of the hydrogeological studies carried out.

Kriging was considered the best method of interpolation to construct the apparent resistivity maps for the three frequencies. Since the investigation depth is a function of the frequency used and of the resistivity of the medium, the result is practically a representation of the aquifer at three different depths. The map of 183 kHz showed the existence of a channel crossing the net of observation wells area and confluent with another one situated further west. It affected the piezometers C7, C6, D7 and D6 more directly.

This channel's resistivity is situated between 250 and 500 Ohm.m. This, according to the water's electrical conductivity and to an empirical relationship, valid for the Swiss Plateau, seems to correspond to clean gravels, sometimes pebbles and cobbles with a permeability of 10^{-3} to 10^{-2} m/s. The existence in the north east part of a region of lower resistivities (and therefore of lower permeabilities) is detected at all frequencies. One is thus in presence of a very well individualised region of lower energy - according to the higher percentage of finer material.

To interpret RMT-R raw data a new approach was utilised, based on the indirect relationship between resistivities and grain size distribution. Sedimentologists usually infer about the environment of deposition of a sediment by analysing the grain-size distribution curves. The idea was to use a similar procedure. We hoped in that way to individualise small well defined and uniformed classes. Instead, we ended up emphasising the contrary, i.e., all the possible situations within each class, contributing to accentuate the degree of heterogeneity in Wilerwald once more. It also permitted us to delimit the regions where an upper conductive layer (impermeable) existed, creating zones of captive aquifer.

RMT-R multidirectional soundings were carried out, revealing the anisotropy of the medium, conditioned by the existence of elongated deposits of fine material alternating with coarser sediments and parallel to the main direction of flow.

Very Low Frequency Electromagnetic (VLF-EM) surveys were done in the Wilerwald test area. The profiles recorded were placed over the RMT-R 183 kHz map, so as to establish a relationship between the RMT-R and the VLF-EM results. Based on the hypothesis that this relationship would be valid for the regions around the site, we derived the above-mentioned regional conclusions.

Another electromagnetical method - AMT - was tested at the site and regionally. Because this method has great limitations in industrialised countries, due to all the possible interferences, the results should only be considered qualitatively and as curiosities. The layer of very low resistance detected at -130 m in both surveys could correspond to the beginning of the aquitanian.

Schlumberger soundings were used to complete the gaps of the RMT soundings in the characterization of the upper covering layer of the aquifer. They revealed the confined situation of the piezometers D1,R1, RP, F2 and F4, the increased thickness of the upper silty-sand layer in the east part of the field and the increase of the aquifer's thickness along the paleochannel.

Finally two seismic surveys confirmed the existence of the paleochannel.

The study of the single drill core CD allowed a detailed punctual sedimentological description. Together with the indirect information given by the resistance to penetration registered during the installation of the piezometers, we thus determined the existence of local lenses of finer material. These lenses seemed to be irregularly distributed, definitely indicating that it is wrong to think that fluvio-glacial sediments consist of mainly parallel continuous layers.

The study of the piezometric surface and its evolution yielded a lot of information about the flow within the aquifer. Sporadic measurements were not significant. Instead they can lead to false interpretations. It was essential to make them as frequently as possible. Similar conditions should prevail in all piezometers if one wants to interpret the readings correctly. We are dealing with a heterogeneous and anisotropic aquifer of variable thickness and vertical changes in permeability - the hydraulic potential can vary with the depth. Situations of free nappe and confined ones can also influence the readings.
The daily observations showed how the hydraulic potentials vary in space and time. After a rainfall , the response of each piezometer was slightly different and tended to increase in amplitude. In general, as observed regionally, the piezometers with a lower permeability, showed greater amplitude variations. This was interpreted as an accumulation due to a slower dissipation of energy. Nevertheless, some apparently contradictory features, at D7,C7 and D6, show that one is dealing with a very complex phenomenon, which needs more prolonged observations, before any definite conclusions can be written.

Depending on the prevailing heterogeneities, a regional flow system can thus be divided into local systems, each with a different flow-line pattern, a different residence time of the water, and consequently different chemical properties. The same applies to the test-site scale. Some chemical analyses (conductivity , nitrate, sulphate, chloride determinations and hardness) were carried out.
We started with sporadical samplings, on the erroneous assumption that the groundwater composition wouldn't vary much over a period of 15 to 30 days. The results showed quite the contrary. Later, in the winter of 92 (Nov./Dec.), during the last tracer experiment, daily measurements of the conductivity were carried out. We observed that each piezometer reacted differently; but the reasons for this have to be investigated further. Just as for the observations of the piezometric level, daily evolution was quite small, lying within the measurement error margins. However, these small variations can become significant, showing with time that they were founded.
There were important variations in certain chemical parameters, specially the hardness values (increasing by 100 mg/l) and the concentrations of nitrates (values oscillating between 15 and 115 mg/l). Both can have an agricultural origin. It is obvious for the nitrates. The carbonate values also, if acidifying fertilisers are used, dissolving the carbonate sediments below. Another possible explanation for the carbonate increase calls into play a local factor: decomposition of the vegetal cover (the site is situated in a forest).
The nitrate variation must be taken seriously because the values measured (over 100 mg/l) show that this important water reserve is potentially in danger.

The contents in the radioactive isotope tritium and the stable water- isotope oxygen-18 were followed at the test site, at the river Emme, at the natural source of the Zielebach and also in the precipitation over Burgdorf. The tritium made it possible to give a relative age to these systems. The mean age of the groundwater sampled at the site is higher than the one sampled at the source and clearly older than the Emme. The Emme has the youngest water, though it seems to correspond to a mixture of young surface waters and older groundwater, mixed in variable quantities, depending on the actual hydrological situation at the moment of the sampling. Within the site it seems that there is an increase of ages from C7 to D1. This agrees with the geophysical conclusions : C7 is the piezometer situated in the channel, covered by a sand layer. These observations are apparently confirmed by the oxygen-18.

All the tracer tests carried out indicated that the aquifer was very heterogeneous, since the very beginning. Like all the other hydrogeological observations, the interpretation of these experiments is impossible if one does not know anything about the aquifer, its geometry and permeability distribution and about the hydrodynamic situation. As a consequence of Wilerwald's heterogeneity and anisotropy, each experiment is a unique case.
However, some general statements may be made:

There is a tendency of the tracer to be deflect and pushed towards the paleochannel and to "avoid" less permeable regions.
This aspect is more pronounced if, depending on the character of the tracer, interactions with the matrix exist, - this explains the low concentrations always obtained at D1 and D2 with the more sorptive tracers.

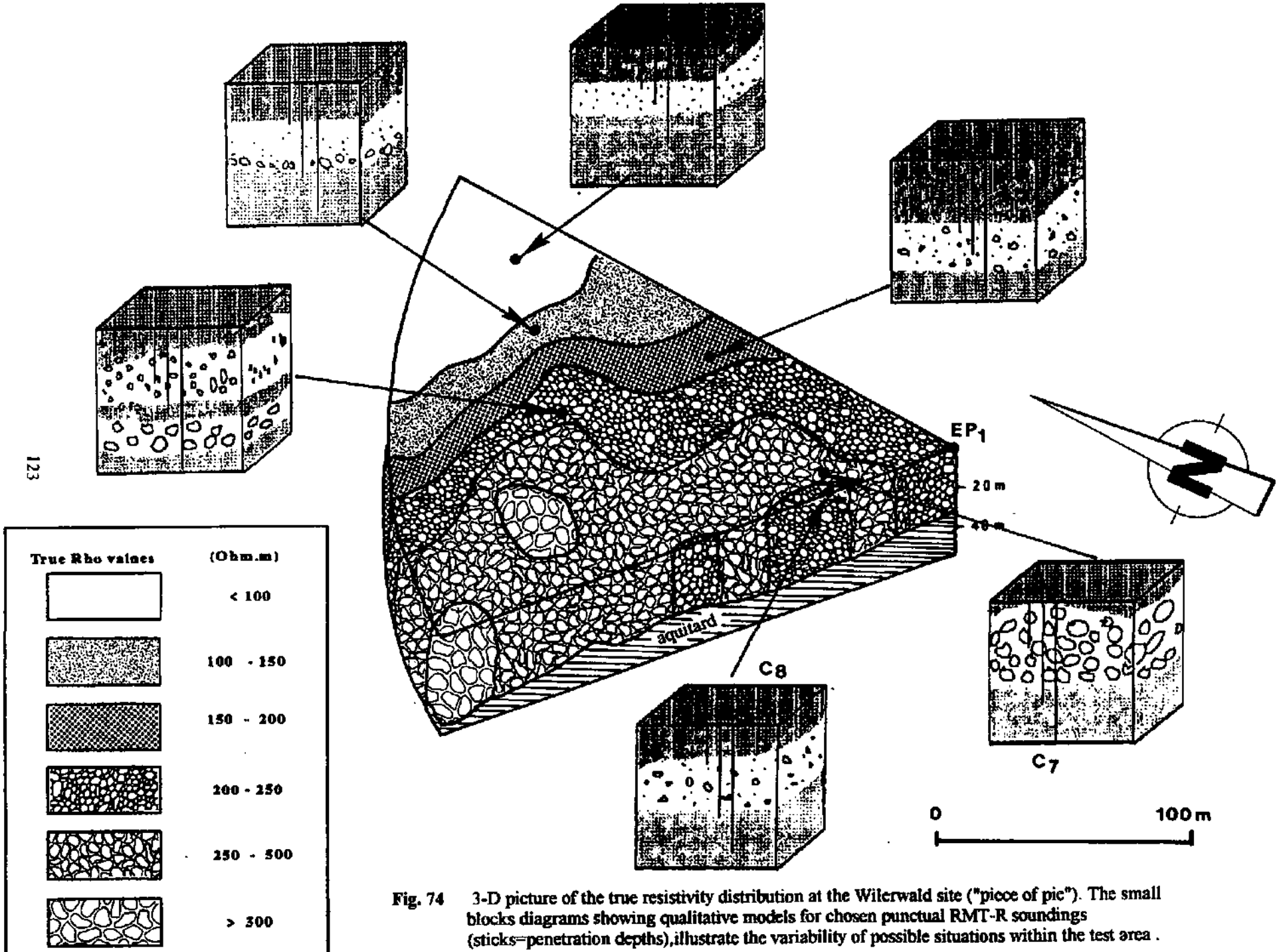

Fig. 74 3-D picture of the true resistivity distribution at the Wilerwald site ("piece of pie"). The small blocks diagrams showing qualitative models for chosen punctual RMT-R soundings (sticks=penetration depths),illustrate the variability of possible situations within the test area .

The hydraulic situation at the moment of the experiment is very important. Duriog the last experiment, daily observations of the piezometric level showed the response of the aquifer to rainfall events. Observed variations of gradients and flow directions pointed out how fundameotal these simultaneous measurements are, for the comprehension of solute transport.

In summary :

Two main aspects were revealed by this work.

The first concerns the ideotification of the aquifer and of its geometry at regional and local scales. Electromagnetical methods, were fundamental for the definitioo of the heterogeneity, though the detailed vertical individualisation of small lenses, was only possible with the help of the borehole and the resistance to penetration tests. Piezometry and tracers (natural, dyes and water chemistry) all contribute to the global knowledge of the aquifer, its heterogeneity and anisotropy.
Interpolations based on scattered punctual informatioo should always be avoided. Electromagnetical surveys (RMT-R and VLF-EM) are a very good complement and are fundamental for the interpretation of this data. - The utility of these methods was also confirmed at the Merdingen test site.
Besides, as one is dealing with highly variable media, more detailed information in space and time is needed. Small variations must also be taken into account, instead of considering then as useless because they might lie within the error margins.

The second aspect concerns the interconnections between all the methods used in this study for the comprehension of the aquifer. All of them yielded logical and convergent results, though sometimes within the "error margins". Two seem to be indispensable for the comprehension of the others : once again the electro-magnetical methods, because they define the geometry and distribution of some of the properties, and the piezometry, which translates the hydrodynamic situation conditioning the flow and transport.

It is clear that my work is just a small contribution to the knowledge of this system. All the elements I studied are still far from understood. Moch remains to be investigated, about the vertical distribution of hydraulic potentials, the permeabilities and about the border conditions, before one can model at this scale. For this, larger boreholes (of about 4 1/2 inches) and bridging the whole breadth of the aquifer should be installed. This would permit the use of flow-meters. It would be interesting to installed at least eight at the borders of the site - boundary conditions - , and a new injection borehole, for the knowledge of the conditions at the moment of the injection, and maybe situated direct in the channel.

The Wilerwald test site ended up being a true study of nature. It is anything but homogenous or isotropic (Fig. 74). Paleochannels with practically clean gravels coexist with elongated pockets of different permeabilities . The aquifer is sometimes free sometimes confined, with constant chaoges of hydraulic gradients, directioos and flow velocities. In short, it is a complex flow network.
A fascinating living system lies under the forest surrounding Wiler b. Utzenstorf, waiting for further investigation.

Bibliography

Bibliography :

Ababou, R., and Gelhar, L. W. (1989).- Implementation of the three-dimensional turning bands random field generator. Water Resour. Res. 25 (10), 2227-2243.

Abourifassi, M., and Marino, M. A. (1984).- Cokriging of aquifer transmissivities from field measurements of transmissivity and specific capacity. J. Int. Assoc. Math. Geol. 16 (1), 19-35.

Ahmed S., and de Marsily, G. (1987).- Comparison of geostatistical methods for estimating transmissivity using data on transmissivity and specific capacity. Water Resour. Res. 23 (9), 1717-1737.

Ahmed, S., de Marsily, G., and Talbot. A. (1988).- Combined use of hydraulic and electrical properties of an aquifer in a geostatistical estimation of transmissivity. Ground Water 26 (1), 78-86.

Ahmed,S., de Marsily,G. (1987b).- Multivariate geostatistical approach in estimating aquifer parameters, presented at Internat. Ground Water Conference at Kuala Lumpur, Malaysia.

Anderson, M.P (1979).- Using models to simulate the movement of contaminants throngh groundwater flow systems. CRC Critical Reviews in Environmental Control 9 (2),97-156.

Bertsch, W. (1978).- Die Koeffizienten der longitudinalen und transversalen hydrodynamischen Dispersion - ein Literaturüberblick. DGM 22, H.2, 37-46.

Bertsch,W, Reif,W., Schloz, W. & Zauter, S.(1972): Zur hydrodynamischen Dispersion im geschichteten porösen Medium bei gesättigtem Fließen.- Deutsche Gewässerkundliche Mitteilungen 16(5): 141-147, Koblenz.

Byers, E., and Stephens, D. B. (1983).- Statistical and stochastic analyses of hydraulic conductivity and particle size in a fluvial sand. Soil Sci. Soc. of Am. J. 47, 1072-1081.

Bouzelboudjen, M.,(1991).- 3-D Modelling of the Rhône aquifer at Visp (Valais, Switzerland). In : Computer Methods and Water Resources CMWR91 :1-8. 2nd Int. Conference Rabat, Morocco,7-11 Oct.1991.

Cameron, D. R., Klute, A. (1977).- Convective-dispersive solute transport with a combined equilibrium and kinetic adsorption model. Water Resour. Res. 13 (1), 183-188.

Carvalho Dill, A.; Gerlinger, K., Hahn, T., Hötzl, H., Käss, W., Leibundgut, Ch., Maloszewski, P., Müller, I., Oetzel S., Rank, D., Teutsch, G., Werner, A. (1992).- Porous aquifer- testsite Merdingen (Germany). Steir. Beitr. z. Hydrogeologie, 43, 251-280, Graz.

Carvalho Dill, A., Müller, I.(1992). Comparative results to structure analyses in the porous aquifer testsite Wilerwald (BE, Switzerland) with very low frequency geophysics : VLF-R, VLF-EM. in Tracer Hydrology, Hötzl&Werner (eds), 139-142.Balkema, Rotterdam.

Custódio,E., Llamas, M.R. (1983).- Hidrologia Subterranea. Tomo I e Tomo II. Ediciones Omega.

Dagan, G. (1967).- A method of determining the permeability and effective porosity on unconfined anisotropic aquifers. Water Resour. Res. 3 (4), 1059-1071.

Dagan, G. (1981).- Analysis of flow through heterogeneous random aquifers by the method of embedding matrix. 1. Steady flow. Water Resour. Res. 17 (1), 107-121.

Dagan, G. (1982a).- Stochastic modelling of ground water flow by unconditional and conditional probabilities. 2. The solute transport. Water Resour. Res. 18 (4), 835-848.

Dagan, G. (1982b).- Analysis of flow through heterogeneous random aquifers. 2. Unsteady flow in confined formations. Water Resour. Res. 18 (5), 1571-1585.

Dagan, G. (1989).- Flow and Transport in Porous Formations. Springer Verlag

Dagan, G., and Rubin, Y. (1988).- Stochastic Identification of recharge, transmissivity and storativity in aquifer transient flow: a quasi-steady approach. Water Resour. Res. 24 (10), 1698-1710.

Delhomme, J. P. (1979).- Spatial Variability and uncertainty in ground water flow parameters: a geostatistical approach. Water Resour. Res 15 (2), 269-280.

Dohr, G. (1981).- Applied Geophysics, Vol 1, 231 S. Ferninand Enke Publishers, Stuttgart.

Fasanino, G., Molinard, J. E., de Marsily, G., and Pelcé, V. (1986).- Inverse Modeling in gas reservoirs. SPE 15592, 1-15..

Fischer,G. Schnegg, P.-A., Peguiron, M. and Le Quang, B.V. (1981).- An analytical one-dimensional magnetotelluric inversion scheme. Geophys. J. R. astr. Soc., 67, 257-278.

Fischer, G., Le Quang, B.V., Müller, I. (1983).- VLF Ground Surveys, a powerful tool for the study of shallow two dimensional structures. Geophysical Prospecting, 31, 977-991.

Fischer, G. (1985) - Some remarks on the behavior of the magnetotelluric phase.Geophysical Prospecting, 33, 716-722.

Fischer, G., Schnegg, P.-A., Ma, J., Müller,I., & Burkhard, M. (1987).- Etude VLF-R du remplissage quaternaire de la Vallée de Gastern (Alpes Bernoises, Suisse). Eclogae geol. Helv., 80, 773-787.

Folk, R.L. & Ward, W.C. (1957).- Brazos river bar: a study in the significance of grain size parameters. J. Sed. Petrology, 38(1):5-12.

Fouquet, C., Beucher, H., Galli, A., and Ravenne, C. (1989).- Conditional simulation of random sets - application to an argilaceous sandstone reservoir. ed. M. Armstrong, in "Geostatistics", Vol 2, 517-530, Kluwer Academic Publishers.

Freeze, R.A., Cherry, J.A. (1979). Groundwater. Prentice Hall, Inc.

Fried, J.J.(1975).- Groundwater pollution.Theory,methodology, modelling and practical rules. Elsevier. Scient.publ. Amsterdam. Developments in water sc. 4.

Fritz, P.& and Fontes, J.C. (1980,1986): Handbook of environmental isotope geochemestry. Vol 1.- the terrestrial environment,A ;vol.2.- the terrestrial environment,B.- Elsevier Scient. Publ, X11,545 p.; 557 p.

Gelhar, L. W. (1984).- Stochastic analysis of flow in heterogeneous porous media. In "Fundamentals of Transport Phenomena in Porous Media", 673-720, (Bear, J., and Corapcioglu, M. Y. eds.), Martinus Nijhoff Publishers, Dordrecht, The Netherlands.

Gelhar, L. W. (1986).- Stochastic subsurface hydrology - Prom theory to applications-. Water Resour. Res. 22 (9), 1355-1455.

Gelhar, L. W., Axness, C. L. (1983).- Three dimensional stochastic analysis of macrodispersion in aquifers. Water Resour. Res. 19 (1), 161-180.

Gish, T. J., Zhnang, W., Helling, C. S., and Kearney, P. C. (1986).- Chemical transport under no-till field conditions. Geoderma 38, 251-259.

Gretillat,P.A., Bouyer, Y., Müller,I. (1987).- Un exemple d'utilisation de la geophysique electromagnetique (VLF et Bipole) pour l'etude de la fracturation au nord de la source karstique de la Noiraigue (Jura Neuchatelois). Bull. Centre d'hydrogeologie 7, 335-345.

Guillaume, A. (1977)- Analyse des Variables Regionalisées. Traitement du signal en Sciences de la Terre. Doin Editeurs,Paris

Hergold, P. C., Gilkeson, R. H., Cartwright, K., and Reed, P. C. (1979).- Aquifer transmissivity from surficial electrical methods. Ground Water 17 (4), 338-345.

Hubbert, M.K. (1940): *The theory of groundwater motion* . J. Geol., vol 48,785-944.

Huntley, D. (1986).- Relation between permeability and electrical resistivity in granular aquifers. Ground Water 24 (4), 466-474.

IAEA,(1987).- Isotopes techniques in water development: Proc. Intern. Symp. International Atomic Eoergy Agency Vienna, 30 March - 3 April 1987.- Vienna: International Atomic Energy Agency, 455-474.

IAEA, 1992- Statistical treatment of data on environmental isotopes in precipitation.Techn reports series nr. 331.

Isenbeck, I., Schröter, J., Taylor, T., Fic, M., Pekdeger, A., and Matthess,G. (1987).- Adsorption/Desorption and Solution/Precipitation Behaviour of Cadmium as influenced by the chemical Properties of Ground Water and Aquifer Material. Meyniana 39, 7-21.

Isenbeck,M., Schröter, J., Kretschmer, W., Matthess, G., Pekdeger, A., und Schulz, H. D. (1985).- Die Problematik des Retardationskonzeptes - dargestellt am Beispiel ausgewählter Schwermetalle. Meyniana 37, 47-64.

Journel, A., and Huijbregts, C. (1978).- "Mining Geostatistics." Academic Press New York.

Käss, W.(1990).- Chemiesorption als natürliche hydrologische Barriere. Z.dt. geol. Ges., 141, 225-231.

Käss,W.(1992).- Geohydrologische Markierungstechnik.Lehrbuch der Hydrogeologie Band 1. Gebrüder Borntraeger

Käss,W.(1993).- Hydrological tracing practice on underground contaminatioos. Environmental Geology, *in Press.*

Kelly, W. E. (1977).- Geoelectric sounding for estimating hydraulic conductivity. Ground Water 15 (6), 420-425.

Kelly, W. E., and Reiter, P. F. (1984).- Influeoce of anisotropy on relations between aquifer hydraulic and electrical properties. J. Hydrology 74, 311-321.

Kinzelbach,W.(1986).- Groundwater Modelling.An introduction with Sample Programs in Basic. Elsevier.

Kiraly, L.(1970).- L'influence de l'hétérogénéité et de l'anisotropie de la perméabilité sur les systèmes d'écoulement. Bull. Ver. Schweiz. Petrol.-Geol. u. -Ing., 37, 50-57.

Kiraly, L. (1985).- A three dimensional model for groundwater flow simulation. Technical report NTB84-49.Cédra.

Kiraly, L., (1992)- Introduction à l'utilisation des modèles en hydrogéologie. Bases téoriques à l'intention des hydrogéologues. Cycle Post-grad. en Hydrogéologie. CHYN (inédit).

Kjellbom, K., Moreno, L., and Neretnieks, I. (1989).- Case 1B - Preliminary evaluation of some uranium migration tests. KAT 89-08. Royal Inst. Technology, Stockholm.

Klotz, D. (1973).- Untersuchungeo zur Dispersion in porösen Medien. Z. dt. geol. Ges. **124**, 523-533.

Klotz, D. (1979).- Longitudinale Dispersionskoefflzienten für Einkornmaterialien und natürliche Kies-Sande. DGM **23**, H.2, 35-39.

Klotz, D. (1980).- Untersuchungen zur hydrodynamischen Dispersion in wasserungesättigten porösen Medien. DGM **24**, H.6, 158-164.

Klotz, D. (1982a).- Verhalten hydrologischer Tracer in ausgewählten Sanden und Kiesen. GSF-Bericht R **290**, 17-29.

Klotz, D. (1982b).- Abhängigkeit der longitudinalen Dispersion von Parametern des Grundwassers und des Grundwasserleiters. GSF-Bericht R 290, 309-321.

Klotz, D. (1982c).- Abhängigkeit der transversalen Dispersion von Parametern des Grundwassers und des Grundwasserleiters. GSF-Bericht R 290 , 340-349.

Klotz, D. (1982d).- Verhalten hydrologischer Tracer in ausgewählten fluvioglazialen Kiesen, Hangschuttkiesen und tertiären Kies-Sanden aus Bayern. in Beiträge zur Geologie der Schweiz-Hydrologie, Bd. 28, 245-256, Bern.

Klotz, D., Maloszewski, P., and Moser, H. (1987).- Mathematical modelling of radioactive tracer migration in water flowing through saturated porous media. in Int. Conf. on Chemistry and Migration Behaviour of Actinides and Fission Products in the Geosphere, Munich, 14-18 Sept. 1987, 1-21.

Klotz, D., Seiler, K.-P., Moser, H., and Neumaier, F. (1980).- Dispersivity and velocity relationship from laboratory and field experiments. J. Hydrology 45, 169-184.

Klotz, D.,und Moser, H. (1980).- Modelluntersuchungen zur longitudinalen und transversalen hydrodynamischen Dispersion von Tracerlösungen in porösen Medien. GSF-Bericht R 237, 76 S.

Koll, J. & Müller, I. (1989) - Elektromagnetische Very Low Frequency-Resistivity (VLF-R) Prospektion zur Erkundung von Grundwasserleitern im paläozoischen Mittelgebirge am Beispiel des Oberharzes. Steirische Beiträge zur Hydrogeologie, 40, 103-122. Graz 1989.

Kosinski, W. K., and Kelly, W.E. (1981).- Geoelectric sounding for predicting aquifer properties. Ground Water **19** (2), 163-171.

Kreft, A, and Lenda, A (1973).- A fortran program for the interpretation of porosity measurements by the two-well pulse technique. in report of the Nuclear Physics and Techniques, Academy of Mining and Metallurgy, Cracow (Nov. 1973), 1-20.

Langguth, H.-R., (1980).- Hydrogeologische Methoden. Springer Verlag

Ledermann, H. (1978): Erläuterungen zu Atlasblatt 72, Geologischer Atlas der Schweiz 1:25000, Blatt: 1127, Solothurn, Schweizerische Geologische Komission.

Leibundgut, Ch. (1981b).- Zum Adsorptionsverhalten von Fluoreszenztracern. Sonderdruck aus Festschrift J. Zötl, Graz, 111-129.

Leibundgut, Ch. (1982).- Stand und Entwicklung der Tracerhydrologie. in Tracermethoden in der Hydrologie. Beiträge zur Geologie der Schweiz - Hydrologie, Bd 28 I, 23-35, Bern.

Leibundgut, Ch., und Wernli, H. R. (1982).- Zur Frage der Einspeisemengenberechnung für Fluoreszenztracer. in Tracermethoden in der Hydrologie. Beiträge zur Geologie der Schweiz - Hydrologie, Bd. 28 I , 119-130, Bern.

Leibundgut,CH., Carvalho Dill,A., Maloszewski,P.,Müller,I. and Schneider, J. (1992).- Investigation of solute transport in the porous aquifer of the test site Wilerwald (Switzerland). Steir. Beitr. z. Hydrogeologie, 43, 229-250, Graz.

Lenda, A., and Zuber, A. (1970).- Tracer dispersion in groundwater experiments. IAEA-SM-129/37, Isotope hydrology, 619-641.

Luft, G. (1980).- Kennzeichnung der Fliessrichtung und der hydraulischeo Leitfähigkeit io schluffigeo Aquifereo mittels Uranin-Markierungsversuchen - Teil I. DGM 24, H.2, 37-42.

Luft, G. (1980).- Kennzeichnung der Fliessrichtung und der hydraulischen Leitfähigkeit in schluffigen Aquiferen mittels Uranin-Markierungsversuchen- Teil II. DGM 24, H.4/5, 128-132.

Luft, G. (1981).- Zur Schätzung der Parameter Abstandsgeschwindigkeit und Dispersionskoeffizienten aus Markierungsversuchen mit Uranin in schluffigen Aquiferen. DGM 25, H.1, 12-17.

Magdefessel, J. (1990).- Zum Fliessverhalten von Tracern und Schadstoffen im Porengrundwasser. Diplomarbeit, 1-109, Geographisches Institut Universität Freiburg i. Br.

Maloszewski,P. (1981): Computerprogramm für die Berechnung der Dispersion und der effektiveo Porosität in geschichteten porösen Medien.- (Mskr., GSF-Bericht R 269, München.).

Maloszewski, P.(1985).- Developmeot and applicatioo of mathematical flow models for interpreting tracer experiments in porous groundwater systems (with exercises). io Beilage 19 des " Weiterbildungs-kurs in Tracerhydrologie" 1985 , GIUB, Abt. Gewässerkunde. Bern.

Maloszewski, P. (1987).- Analytische Fliessmodelle in der Hydrologie : Sorptions- und Diffusionsmodelle. Vorlesung am GIUB, Abt. Gewässerkunde, Bern.

Mantaglou, A., and Gelhar, L. W. (1987).- Effective hydraulic conductivities of transient unsaturated flow in stratified soils. Water Resour. Res. 23 (1), 57-67.

Marsily, G. de, Lavedan, G., Boucher, M., and Fasanino, G. (1984).- Interpretation of interference tests in a well field using geostatistical techniques to fit the permeability distribution in a reservoir model. in "Geostatistics for Natural Resources Characterization", Part.2, 831-849, D. Reidel Publishing Company.

Marsily, G. de. (1986).- Quantitative Hydrogeology : Groundwater hydrololoy for Engineers. Academic Press London.

Matheron, G., Beucher, H., de Fouquet, C., Galli, A., Guerillot, D., and Ravenne, C. (1987).- Conditional simulation of the geometry of fluvio-deltaic reservoirs. SPE 16753, 591-599.

Matthess, G., Ubell, K. (1983). Allgemeine Hydrogeologie Grundwasserhaushalt. Lehrbuch der Hydrogeologie Band 1. Gebrüder Borntraeger.Berlin.Stuttgart.

Matthess,G. Frimmel,F.H., Hirsch,P., Schulz,H.D., Usdowski E. (Eds) (1992).-Progress in Hydrochemistry. Organics- Carbonate Systems- Silicate Systems- Microbiology - Models. Springer Verlag.

Mazac, O., Kelly, W. E., and Landa, I. (1985).- An hydrogeophysical model for relations between electrical and hydraulic properties of aquifer. J. Hydrol. 79, 1-19.

Moreno, L., and Neretnieks, I. (1989).- Case 5 - Preliminary evaluation of tracer test in Finnsjön. Radial convergent experiment. KAT 89-08. Royal Inst. Technology, Stockholm

Moreno, L., and Rasmuson, A. (1986).- Contaminant transport through a fractured porous rock: impact of the inlet boundary condition on the concentration profile in the rock matrix. Water Resour. Res. 22 (12), 1728-1730.

Moreno, L., Neretnieks, I., and Landström, O. (1989).- An evaluation of tracer tests performed at Studsvik. SKB Technical Report 89-09. Stockolm.

Moreno, L., Neretnieks, I., and Tryggre, E. (1985).- Analysis of some laboratory tracer runs in natural fissures. Water Resour. Res. 21 (7), 951-958.

Moreno, L., Tsang, Y. W., Hale, F.V., and Neretnieks, I. (1988).- Flow and tracer transport in a single fracture: a stochastic model and its relation to some field observation. Water Resour. Res. 24 (12), 2033-2048.

Müller, I.(1982).- Rôle de la prospection electro-magnétique VLF (Very Low Frequency): pour la mise en valeur et la protection des aquifères calcaires.- Annales scient. de l'Université de Besançon. 3ème Coll. d'hydrogéologie en pays calcaire.,1, 219-226.

Müller,I, (1983).- Anisotropic properties of rocks detected with electro-magnetic VLF [Very Low Frequency]. International Symposium on Field measurements in Geomechanics. Zürich, September 5-8, 1983.- special publ., 273-282.

Müller, I., Gibert, J., et Laurente, R, (1984).- Application des methodes geophysiques, electro-magnetique VLF (Very Low Frequency) et micro-sismique a l'etude du karst de Dorvan Cleyzieu (Jura meridional, France. Bull. Centre d'hydrogeologie 5, 145-162.

Müller, I., Schotterer, U. (1986).- Electromagnetic VLF-Resistivity Prospection in the region of Tripolis and the coastal area of Argos-Astros. Proc. 5. Int. Symp. Underground Water Tracing Athen:425-440.

Müller, I. (1992). Brief overview of the activity of ATH working-groups (tracing experiments, geophysics, mathematical modelling) in two porous groundwater test fields in Germany and Switzerland. in Proceedings of the 6th International Symposium on water tracing 1992- Karlsruhe.Rotterdam, Balkema.

NLfB-Niedersächsisches Landesamt für Bodenforschung (1982): Bericht über geoelektrische Untersuchungen bei Merdingen, Kreis Breisgau - Hochschwarzwald v. 8 April 1981.- Archiv-Nr. 88109, 4p., 3 Anl., 24 Sondierprofile, Hannover.

Oetzel, S., Käss, W., Reichert, B., & Botzenhart, K., (1991) : Field experiments with microbiological tracers in a pore aquifer.- Water Sci. Techn., 24(2),305-308.

Orion Research (1982).-Handbook of electrode technology. Orion Research Incorporated.

Parasnis, D.S. (1979).- Principles of applied geophysics. Halsted Press (div. of J. Wiley & Sons), N.Y., Third Edition.

Parker, J.C., and van Genuchten, M. Th. (1984).- Determining transport parameters from laboratory and field tracer experiments. Bulletin 84-3 , Virginia Agricultural Experiment Station, Blacksburg.

Peck, A., Gorelick, S., de Marsily, G., Foster, S., and Kovalevsky, V. (1989) .- Consequences of spatial variability in aquifer properties and data limitations for groundwater modelling practice. report by the"ICGW of the International Association of Hydrological Sciences" - IAHS Publication 175.

Rasmuson, A. (1986).- Modeling of solute transport in aggregated/fractured media including diffusion into the bulk matrix. Geoderma 38, 41-60.

Ravenne, C., and Beucher, H. (1988).- Recent development in description of sedimentary bodies in a fluvial-deltaic reservoir and their 3-D conditional simulations. SPE 18310, 463-476.

Ravenne, C., Eschard, R., Galli, A., Mathieu, Y., Montaglou, L., and Rudkiewicz, J. L. (1987).- Heterogeneities and geometry of sedimentary bodies in a fluvial-deltaic reservoir. SPE 16752, 115-122.

Reardon, E. J. (1981).- Kd's - Can they be used to describe reversible ion sorption reactions in contaminant migration ?. Grounwater 19, 279-286.

Reichert, B. (1991).- Anwendung natürlicher und künstlicher Tracer zur Abschätzung des Gefährdungspotentials bei der Wassergewinnung durch Uferfiltration.Dissertation.Schriftenreihe Angewandte Geologie Karlsruhe 13.

Ribeiro, L.T. (1982).- A Krigagem como novo instrumento de investigação hidrogeológica: uma introdução. III Semana de hidrogeologia. Faculdade de Ciências de Lisboa - Portugal,10-14 Maio 1982, 263-280.

Rice, W. A., and Gorelick, S. M. (1985).- Geologic inference from flow net transmissivity determination : three case studies. Water Resour. Res. 21 (6), 919-929.

Rodier,J. (1984): L'analyse de l'eau. Eaux naturelles, eaux residuaires, eau de mer. Ed.Dunod 1121 pp.

Rossi, P., Carvalho Dill, A., Müller, I. & Aragno, M. (1993)- Comparative tracing experiments in a porous aquifer using bacteriophages and fluorescent dye on a test field located at Wilerwald (Switzerland) and simultaneously surveyed in detail on local scale by Radio-Magneto-Tellury (12-240 kHz). J. Environmental Geology, in Press.

Russo, D., and Bressler, E. (1981).- Soil hydraulic properties as stochastic processes. I.- an analysis of field spatial variability.- Soil Sci. Soc. Am. J. 45, 682-687.

Sansoni, M., Schudel, B., und Wagner, T. (1987).- Tracermethodischer Beitrag zum Stofftransport im Porengrundwasser. Publikation Gewässerkunde Nr. 94 des GIUB, Bern.

Sansoni, M., Schudel, B., Wagner, Th. & Leibundgut, Ch. (1988).- Aquiferparameterermittlung im Porengrundwasser mittels fluoreszierender Tracer.., Gaz- Eaux - Eaux usées, 68 ème année, 3, 141-147.

Schmitt, H. W., and Stichcr, H. (1986).- Long-term trend analysis of heavy metal content and translocation in soils. Geoderma 38, 195-207.

Schotterer, U., Müller,1. (1986).- Investigation of Groundwater Flow Systems in a Quaternary-Sandstone Complex near Berne (Switzerland) by means of indirect methods of Enviromental Isotopes and Geophysiques. Proc. 5th Internat. Symposium on Water Tracing, 403-412 , Athens.

Schotterer, U., Fröhlich, K. & Trimborn, P. (1993).- Temporal variations of oxygen-18 and deuterium excess in precipitation, river and spring water in alpine regions of Switzerland. Proc. of Intern. Symp. on Applications of isotope techniques in studying past and current environmental changes in the hydrosphere and atmosphere.Viena, Austria, 19-23 April 1993 (*in press*).

Schotterer, U., Bürki, H. & Töngi M. (1993).- Messnetz des Bundes für die langfristige Beobachtung der Isotopenverteilung und -zusammensetzung im Wasserkreislauf.Zwischenbericht der Abteilung Klima und Umweltphysik der Universität Bern für die Periode Juil 1992 bis Juni 1993.

Schulin, R., Flühler, H., Mansell, R. S., and Selim, H. M. (1986).- Miscible displacement of ions in aggregated soils. Geoderma 38, 311-322.

Smith, L., and Schwartz, F. W. (1980).- Mass transport. 1.A stochastic analysis of macrodispersion. Water Resour. Res. 16 (2), 303-313.

Smith, L., and Schwartz, F. W. (1981a).- Mass transport. 2.Analysis of uncertainty in prediction. Water Resour. Res. 17 (2), 351-369.

Smith, L., and Schwartz, F. W. (1981b).- Mass transport. 3.Role of hydraulic conductivity data in prediction. Water Resour. Res. 17 (5), 1463-1479.

SNF (1984).- Quantitative Erkundung von Lockergesteins-Grunwasserleitern am Beispiel Emmental. Handbuch Nationales Forschungsprogramm Nr. 2 "Grundlegende Probleme des Schweizerischen Wasserhaushaltes", Teilprogramm 2 "Grundwasserdargebot, quantitative und qualitative Aspekte". Schweizerischer Nationalfonds, Sonderdruck Nr 1056 aus Gas-Wasser-Abwasser, 1984/5.

Souma, G.A.R. (1989).- Trans3: Modèle numérique d'un transfert de masse et d'énergie conductif-advectif par élements finis en une , deux et trois dimensions. (Programme d'ordinateur en Fortran77). Thèse présentée à la Faculté des Sciences de l'Université de Neuchâtel.

Steiner,T., de Carvalho Dill, A., Szarka, L. & Müller, I.(1992).- Comparative studies of VLF-R and VLF-EM geophysical methods; 1-D and 2-D numerical modelling at the tracer test-field Wilerwald (BE, Switzerland) - Bull. du Centre d'hydrogeologie de l'Université de Neuchâtel, 11 *(in Press)*.

Stumm, W. (1986).- Coordinative interactions between soil solids and water - an aquatic chemist's point of view. Geoderma 38, 19-30.

Suguio, K. (1973).- Introdução à Sedimentologia. Ed. da Univ. de São Paulo.

Telford, W.M., Geldart, L.P., Sheriff, R.E., Keys, D.A. (1976).- Applied Geophysics, 860 S. Cambridge University Press, USA (reprinted 1985).

Thierrin, J., Müller, I. (1988).- La méthode VLF-Resistivité Multifrequence, un example d'exploration hydrogeologique dans un synclinal Crétace a la Brevine (Jura Neuchâtelois). *In*: Annales Scientifiques de l'Univ. de Besançon, Geologie, Memoire Hors Serie n°6 (Quatrième Colloque d'hydrogeologie en Pays Cal-caire, Sept 1988), 17-25.

Thierrin, J. (1990).- Contribution à l'étude des eaux souterraines de la region de Fribourg (Suisse Occidentale). Thèse présentée à la faculté de Sciences de l'Université de Neuchâtel. CHYN.

Tóth, J. (1962): A theory of groundwater motion in a small drainage basins in Central Alberta, Canada. J.Geophys. Res.,67, 4375-4387.

Tóth, J. (1963): A theoretical analysis of groundwater flow in a small drainage basins. J.Geophys. Res.,68, 4795-4812.

Turberg, P. (1991). Note brève- Modes d'utilisation de la prospection géophysique électromanétique "very low frequency-resistivity" (VLF-R 12 - 240 KHz). Bull. du Centre d'hydrogeologie de l'Université de Neuchâtel, 10: 28-33.

Turberg, P., Müller, I. (1992).- La méthode inductive VLF-EM pour la prospection hydrogéologique en continu du milieu fissuré. Ann. Sci. de l'Université de Besançon, Geologie, Memoire Hors Serie N° 11, 207-214.

Turberg,P., Müller,I. & Flury, F. (1993)- Hydrogeological investigation of porous environments by Radio Magnetotelluric Resistivity (RMT-R 12-240 kHz). Geoexploration, *(in Press).*

Van der Zee, S. E. A. T. M., and Van Riemsdijk, W. H. (1986).- Sorption kinetics and transport of phosphate in sandy soil. Geoderma 38, 293-309.

Wang, H., Anderson, M.P. (1982).- Introduction to groundwater modelling. Finite difference and finite element methods. W.H.Freeman. San Francisco.

Werner, A., Wanner, J. (1981): Grundlagen für die siedlungswasserwirtschafliche Planung des Kantons Bern, Hydrogeologie Emmental, Teil III : Unteres Emmental. Wasser-u. Energiewirtschaftsamt des Kantons Bern, (WEA).

Zahn, M.T. (1988) - Die Ausbreitung von Schwermetallen und Anionen im Grundwasser der quartären Kiese aus dem Raum München (Dornach) - Ergebnisse von Labor- und Geländeversuchen. (Dissertation). GSF-Bericht 26 / 88.

Zahn, M.T. (1989) - The migration of As, Hg and Cd in groundwater of the Quaternary gravels in Dornach near Munich. in "Contaminant Transport in Groundwater", Kobus & Kinzelbach (eds), Balkema, Rotterdam.

Appendix

Appendix 1:

A : Geophysical methods used:

Electromagnetic methods: RMT-R, VLF-EM; seismic and electric methods

B Applied geostatistic :

Theory of the regionalized variables
Variogram
Kriging

Fig. 1A-1 Principles of the electromagnetic methods : **(a)** VLF-EM , **(b)** RMT-R.

Fig.1B-1 Some models of variograms after **Delhomme,(1978).**

A. Methods used :

1. Geophysics

The following description concerns the electromagnetic methods used io this work, since they are quite exclusive and barely known. A complete description of the seismic and electric methods can be found at **Telford & all (1976)**, **Parasnis (1979)**, etc.

1.1 Electromagoetic methods :

Two electromagnetic methods were applied in Wilerwald testsite : Radio Magnetotelluric-Resistivity (**RMT-R**)and **VLF-EM** (Very Low Frequency-Electromagnetic). The radio-magnetotelluric method is an extension to higher frequencies of the VLF-R traditional method (**Fischer et al,1983,1987**; **Keller & Frischknecht, 1976**; **Parasnis ,1979** and **Telford et al, 1976**). These methods were developed by **Mr LMfiller (1982,1983,1984,1992)** and the measuring devices are prototypes constructed by **Mr L Müller** and **J. Dupperex**.

Both methods use VLF emitters **Fig. 1A-1a) & b)**, powerful radio antennae transmitting in a low frequency range: 12- 24 kHz. The RMT-R Method had extended its frequencies to higher levels up to 240 kHz.

Those waves travel not only through the air but also currents flow in the ground inducing there secondary electromagnetic fields. At any point in space , the total electromagnetic field is the sum of the primary field and the secondary field. Therefore, the resultant field, differ from the primary field in intensity, phase and direction.

The principle of both methods consists of measuring these induction effects. Both methods differ io the process of measuring them.

1.1.1- VLF-EM

The VLF-EM method measures 3 parameters of the VLF magnetic field **Fig. 1A-1a)** :

1. The horizontal amplitude vector Hy (primary field), which is perpendicular to a line joining the receiver and the VLF station;
2. The amplitude of the component of the vertical resultant field vector, which is 90° out-of-phase (vertical) with the horizontal vector;
3. The amplitude of the vertical field vector which is in-phase with the horizontal vector.

The vertical components are expressed as a percentage of the horizontal vector and are very sensitive to conductive anomalies. Thus it indicates lateral changings in conductivity.

The VLF-EM technique allows the continuous recording of the out-of-phase component which is very sensitive to lateral changes of the electrical conductivity of the ground. The method is relative new, for hydrogeological survey. It was developed by **Mr. LMüller**.

The measuriog device is composed by two orthogonal coils, functioning as a T - Antennae. One coil is kept vertical (the longest one) and measures the vertical component which is in-phase and out-of-phase. The other coil catches and measures the horizontal amplitude vector H_y, the reference primary field.

A description of the method , as well as program for modelling, allowing the calculation of strata with different resistivities and thicknesses, can be found in **Steiner et al,(1992)**, and **Turberg,(1992)**.
Technical data can be seen at 1.1.3 (*2. **Magnetic device***).

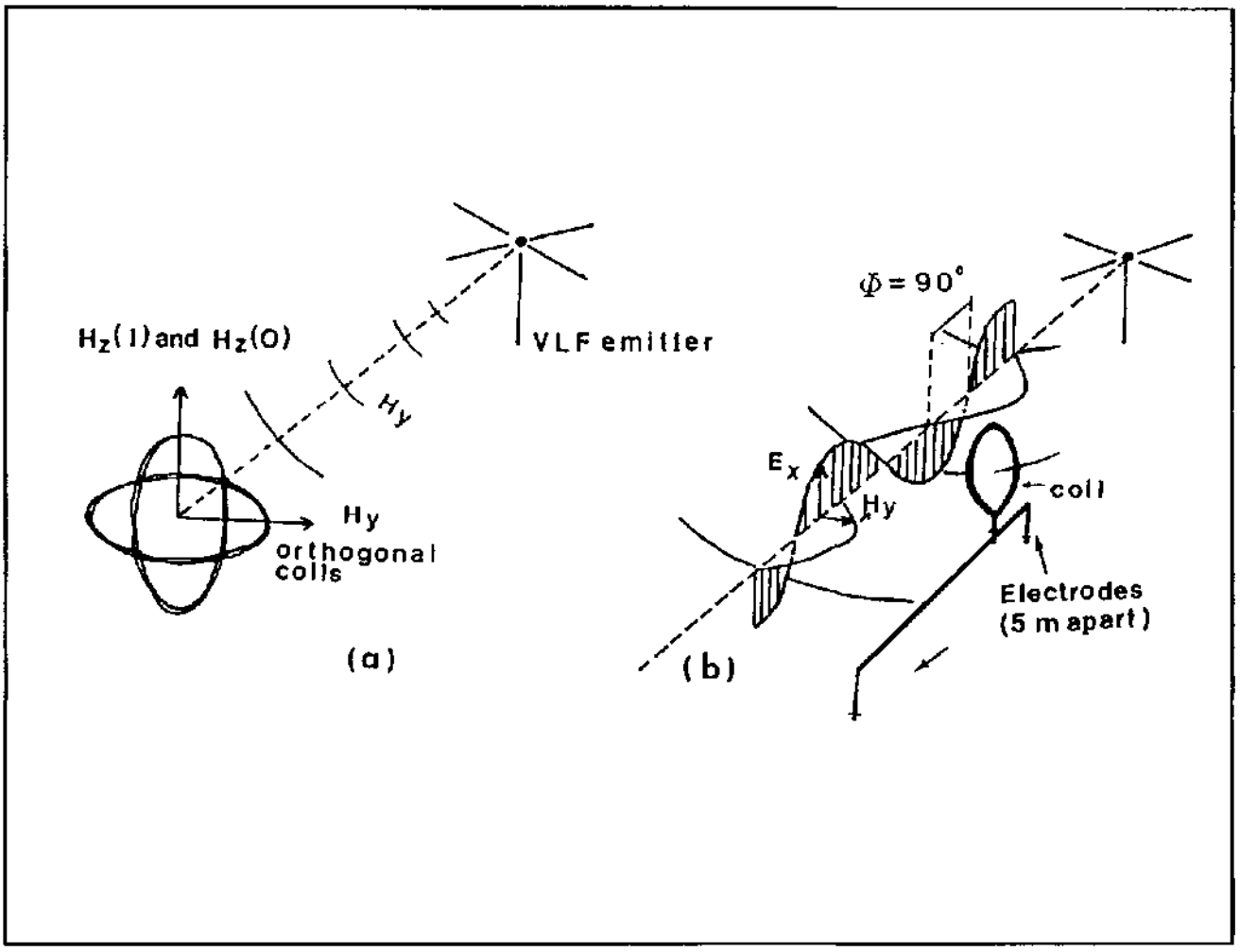

Fig. 1A-1 Principles of the electromagnetic : methods : **(a)** VLF-EM , **(b)** RMT-R

1.1.2- RMT-R

The resultant electro- magnetic field to be measured has two components: a magnetic and an electric component. The magnetic component is measured with a coil **Fig. 1A-1b)** and compared with the electric component measured between two ground electrodes spaced 5 meters. These are placed perpendicularly to the magnetic field, i. c in the direction of the emitter. Technical data can be seen at 1.1.3 (*1. Resistivity device*).

The apparent resistivity (ρ_a) of the strata between the two points serving to measure E_x can be obtained, according to the following relation:

$$\rho_a = \left(\frac{Ex}{Hy}\right)^2 . \frac{1}{2\pi F \mu o}$$

where,

- ρa apparent resistivity, is given in ohm meters
- Ex the electric component of the resultant field, given in volt/meters
- Hy the magnetic component of the resultant field, given in ampere/meters
- F (emitter's frequency) is given in Herz(Hz)
- μo (electromagnetic permeability of the vacuum) is given in henry/meters.

Each type of sediment possesses different electrical characterist. The resistivity is therefore a good indicator of the type of sediment we want to investigate.

The dephasing is the second parameter to be measured and it complements the information of the resistivity because of it structural character. At the air, the electric and the magnetic fields are orthogonal and the dephasing therefore equal to 90°. The electric component of the resultant field, leads the magnetic one (Fischer, 1985). At the interface of the an homogeneous half-space the phase of the electric field leads the phase of the magnetic field by 45°. If instead of the homogeneous half-space, we have a stratified formation, following situations may occur:

- If we have the situation of a conductor sheath lying over a resistant one , the dephasing will be less than 45°.(see example at Wilerwald, Cap. 4)
- If we have the inverse situation, a resistant layer over a conductor, the dephasing will be greater than 45° (ex. Merdingen, Cap. 6).

Because of the finite conductivity of the sediments, the incident wave is absorbed, and the amplitude of the waves decreases exponential (Parasnis) in traversing the conductors. Another magnitude can be defined : the skin depth. It is the depth at which the amplitude of the electromagnetic signal is attenuated by a factor of 1/e (=0.368).

$$P = 503\sqrt{\frac{\rho a}{F}}$$

Where,

P = skin depth or penetration depth, in meters,
ρa = apparent resistivity (ohm.m)
F = frequency used (Herz)

The investigation depth is therefore a function of the resistivity of the strata and of the frequency used.

Knowing the apparent resistivity and the dephasing it is possible to estimate the true resistivity and the thickness of the strata, using any classical MT. Inversion (Fischer et al, 1981).

1.1.3 Technical description of the elctromagnetic devices

The devices used in this work are prototypes. Because they are very adequate for scientific investigation, and particularly for hydrogeology I thought to be of interest to include an overview of the technical characterists of the devices.
The technical description were kindly yield by **Mr. L Müller.**

Complete VERY LOW FREQUENCY ELECTROMAGNETIC system :

Technical Description:

The system measures with two separate devices both VLF-magnetic and electric field parameters: horizontal amplitude, vertical inphase component, vertical quadrature component, apparent resistivity and phase angle.

1. Resistivity device:

Manual tuning in the range 12.0 to 240 kHz, with a bandwidth of 100 Hz. Four frequencies can be preselected by keyboard for sequential measurements. Very good signal filtering with narrow bandpass, low pass and sharp cut -off high pass filters. Minimal received field is better as 50 nA/m.

Accuracy is ± 1 % of the measured apparent resistivity and ± 0.2 % of the phase angle, by manual nulling of the signal in the earphone.

Output for recorder or datalogger 0–200 mV. Simultaneous digital display of the resistivity and phase.

Three resistivity range : 0–200 Ohm.m; 0–2000 Ohm.m; 0–20000 Ohm.m. Two capacitive electrodes. Electrode spacing 5 m. Magnetic sensor diameter 40 cm.

Power : 1 external 12 V DC rechargeable sealed lead-battery, 2 Ah. Weight : Console with magnetic sensor and electrodes 7 kg. Operating temperature range : –5° C –+ 50° C.

2. Magnetic device:

The measured magnetic field components are : horizontal amplitude, vertical inphase component and vertical quadrature (outphase) component. Permanent and simultaneous digital display all these parameters. Vertical components are displayed as a percentage of horizontal component and are related in phase to the horizontal component.

The range is ± 150 % with exceptional good resolution of 0.1 % Output : Simultaneous permanent recording of all parameters are possible on analog chart recorder or datalogger (0–200 mV). Airborne, waterborne possibility with permanent recording of data.

Two (orthogonal) receiver coils detect the horizontal vector of the primary VLF field and the vertical components of the secondary field.

Weight: 8 kg. Operating temperature range and power supply is the same as by the resistivity device.

Table 1A-1 Technical description of the electromagnetic devices **(I. Müller)**

B. Geostatistics - Kriging and Variogram analysis for RMT-R raw data

To be able to judge about the spatial variation of the RMT-R parameters at different depths of penetration, contour maps where drawn using the kriging method as an interpolator tool.

Kriging is considered the best linear unbiased estimator and it is very often used when outlining contour maps. To use this technique, one needs information about the spatial distribution of the variable (the data) and about its structure. This method was developed by the mining industry **G. Matheron** and later adapted to hydrogeology by **Delhomme**.

Kriging is based on the following considerations:

All earth variables have a double and complementary nature: they possess a great spatial variability (local random erratic behaviour), but, at the same time, this variability is not accidental - these variables have a a spatial correlation. In other words, the phenomen is said to be structured.

Because of this structure, they were called "Regionalised variables" by **Matheron**. The details of the theory and the developments of kriging equations can be found in **Matheron (1971)**, **Journel and Huijbregts (1978)** and Guillaume (1977). The applications of the regionalised variables in Hydrology are to be found in **de Marsily (1981)**, **Delhomme (1978 and 1976)**, **Ahmed (1987)**, etc.

The structural model needed is the co-variance function or the variance of the increment between two points. This is called the variogram.

This essential tool for the structural analysis of a variable gives information about the structure. The variogram assumes the second order stationary for the increment (h) (the distance between two points x_1-x_2), i.e.:

The increment $Z(x+h)-Z(x)$ has an expected value equal to zero and a variance independent of x.

This is given by the following equation:

$$\begin{cases} E[Z(x+h)-Z(x)] = 0 \\ var[Z(x+h)-Z(x)] = 2\gamma(h) \end{cases}$$

The semi-variogram $\gamma(h)=\frac{1}{2}$ var$[Z(x+h)-Z(x)]$, therefore represents the average of the quadratic increment between two points, separated by the distance h.

The behaviour of a variogram function must be studied around the origin (small distances) and at infinity (big distances).

At the origin it is important to see whether there is a discontinuity. If would mean the existence of micro-structures smaller than the distance between the measuring points, or measuring errors. This is called the *nugget effect*.
A pure nugget effect corresponds to a purely random case, or total absence of structure: there is no correlation, whatever the distance.
It is also important to see whether the variogram is derivable (the graph is then parabolic at the origin, like a regular variable) or continuous (corresponding to a less regular variable).

At infinity the variogram may increase unlimitedly, or it may stabilise around a limit called *sill*. The sill value is, *a priori*, equal to the data value variance. The *range* can be defined as the distance at which the correlation reaches zero.

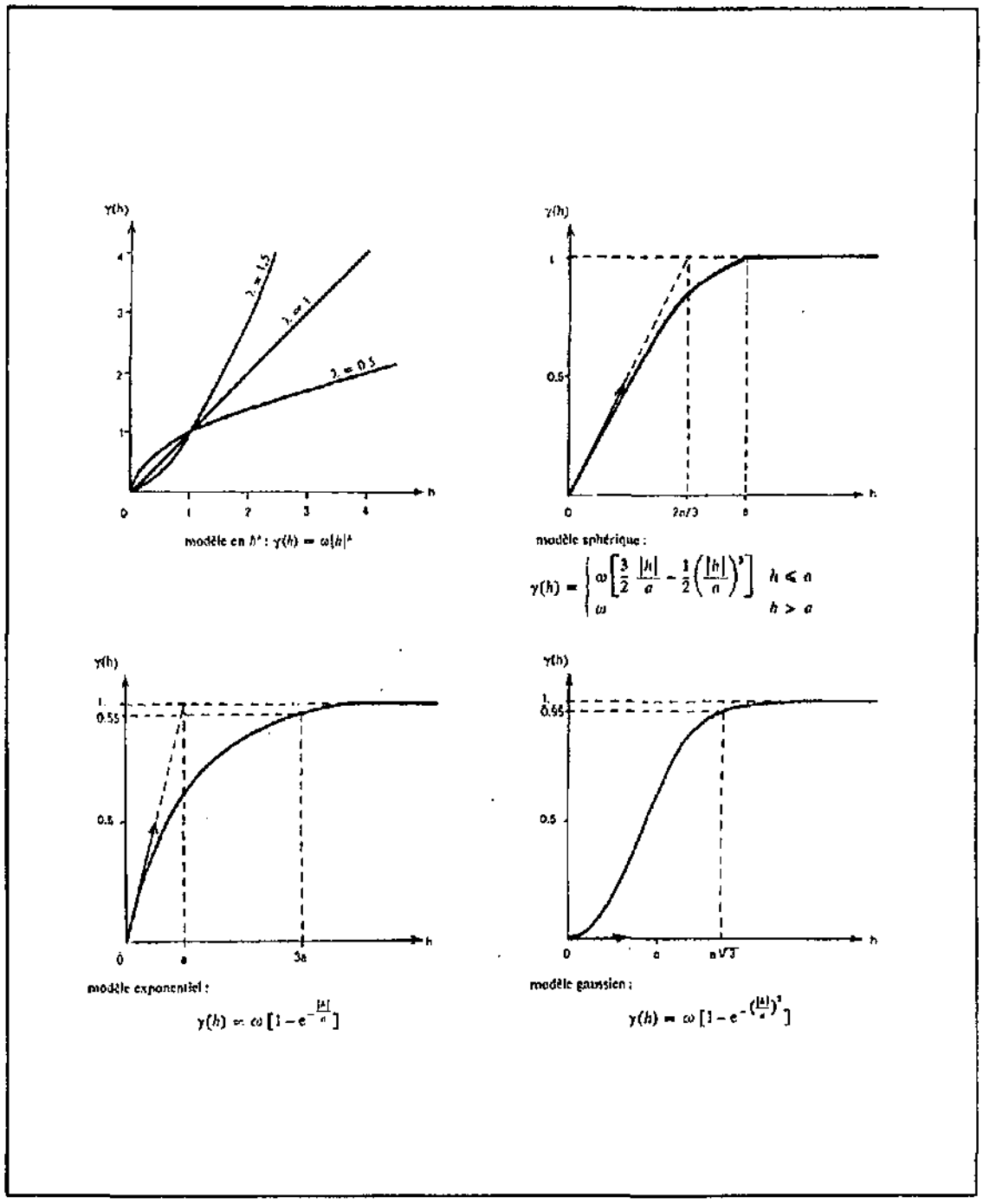

Fig.1B-1 Some models of variograms after **Delhomme,(1978).**

In practice one starts by estimating the experimeotal variogram of the data sample. After this, a model - linear, exponential, gaussian or spherical - with well-defined equations (**Delhomme,1978**) must be fitted to the variogram. This is done by trial, introducing different sill, range and nugget values, or the slope and exponent of a linear function, etc. This operation provides the equations of the variogram function.

Variograms can also be used to check the anisotropy of the phenomena. This is done by comparing the variogram's behaviour in different directions.

Once the variogram function has been defined, it may be used for interpolation purposes (kriging methods). Kriging is an exact interpolator and has the great advantage of informing about the reliability of the estimation, therefore standard-errors maps should always accompany the contour maps calculated.

Appendix 2: regional

Fig. 2A-1 Log of the AMT true resistivities at the Burgerwald borehole, determined with MT inversion.

Fig. 2B-1 Map with the distribution of permeability (**WEA, 1981**) and the location of Wilerwald test site

Fig. 2B-2 Map with discharging and recharging areas (**WEA, 1981**).

Fig. 2C-1 Map with distribution of conductivity adapted from **WEA (1981)** for the dry period (7.12.1978) and after rain fall event (21.2.1979).It is visible the importance of the Emme water infiltration lowering the conductivity values mainly in the region where the main infiltration takes place.

Fig. 2C-2 Map of distribution of the middle annual temperature oscilation isolines, taken 0,5 m under the ground the water level, for the period 1976-1979,adapted from **WEA (1981)**.

Fig. 2C-3 Nitrate distribution map (1971/1972) retired from **WEA (1981).**

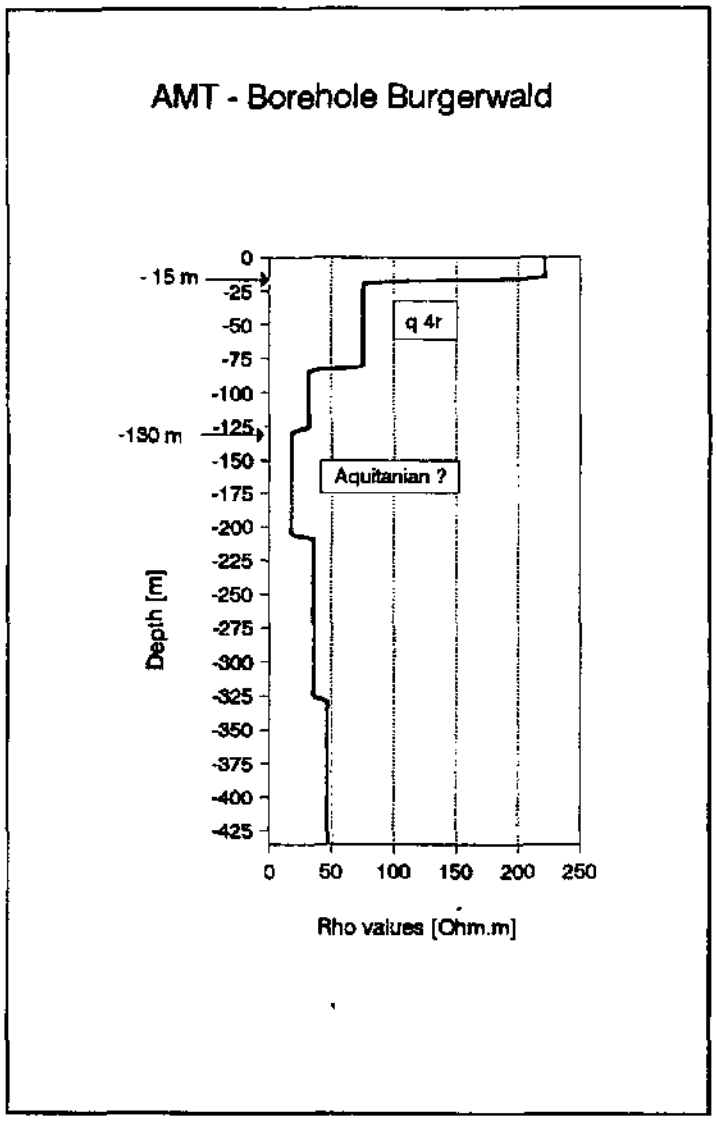

Fig. 2A-1 Log of the AMT true resistivities calculed with MT at the Burgerwald borehole .

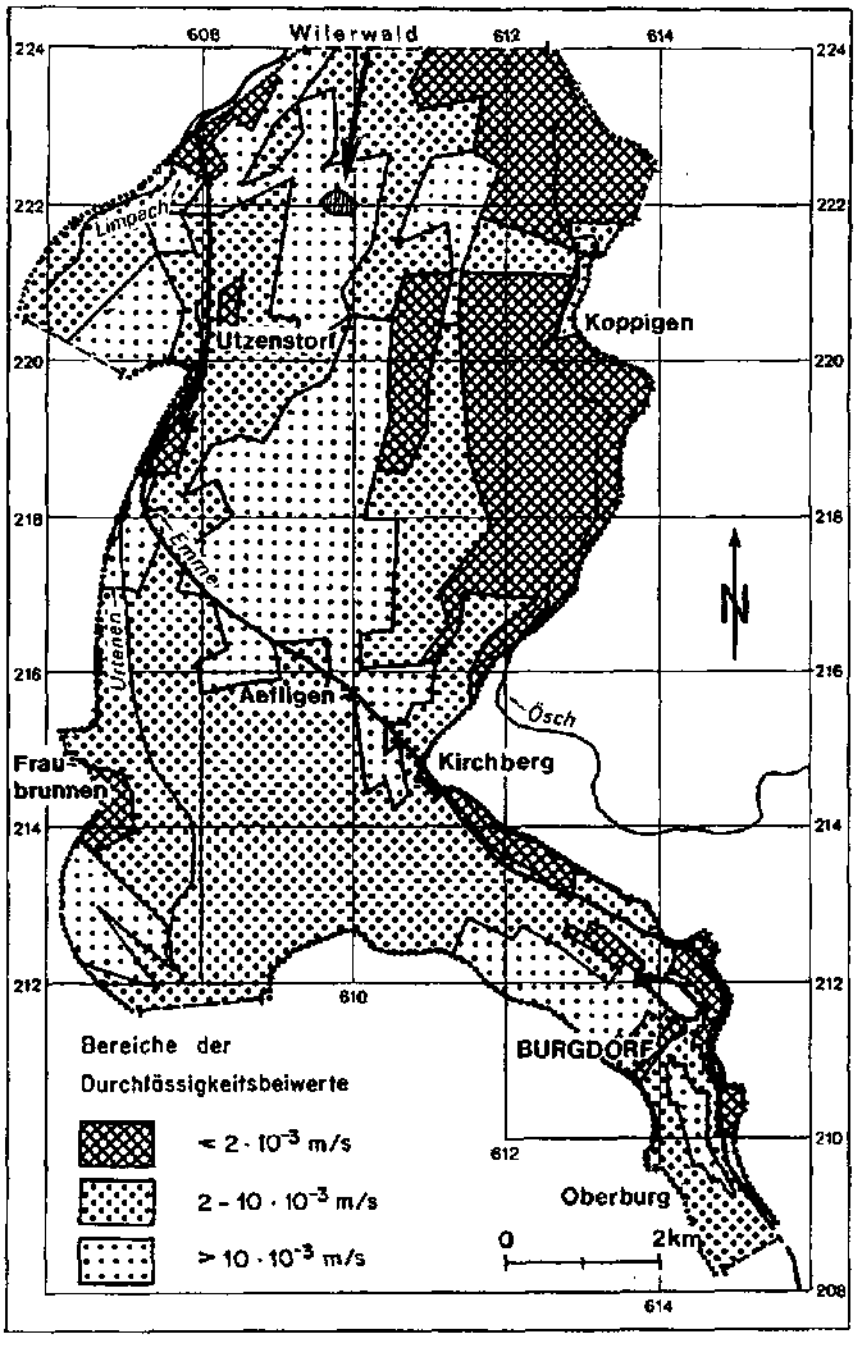

Fig. 2B-1 Map of the distribution of permeabilities,after **WEA,1981.** = Wilerwald

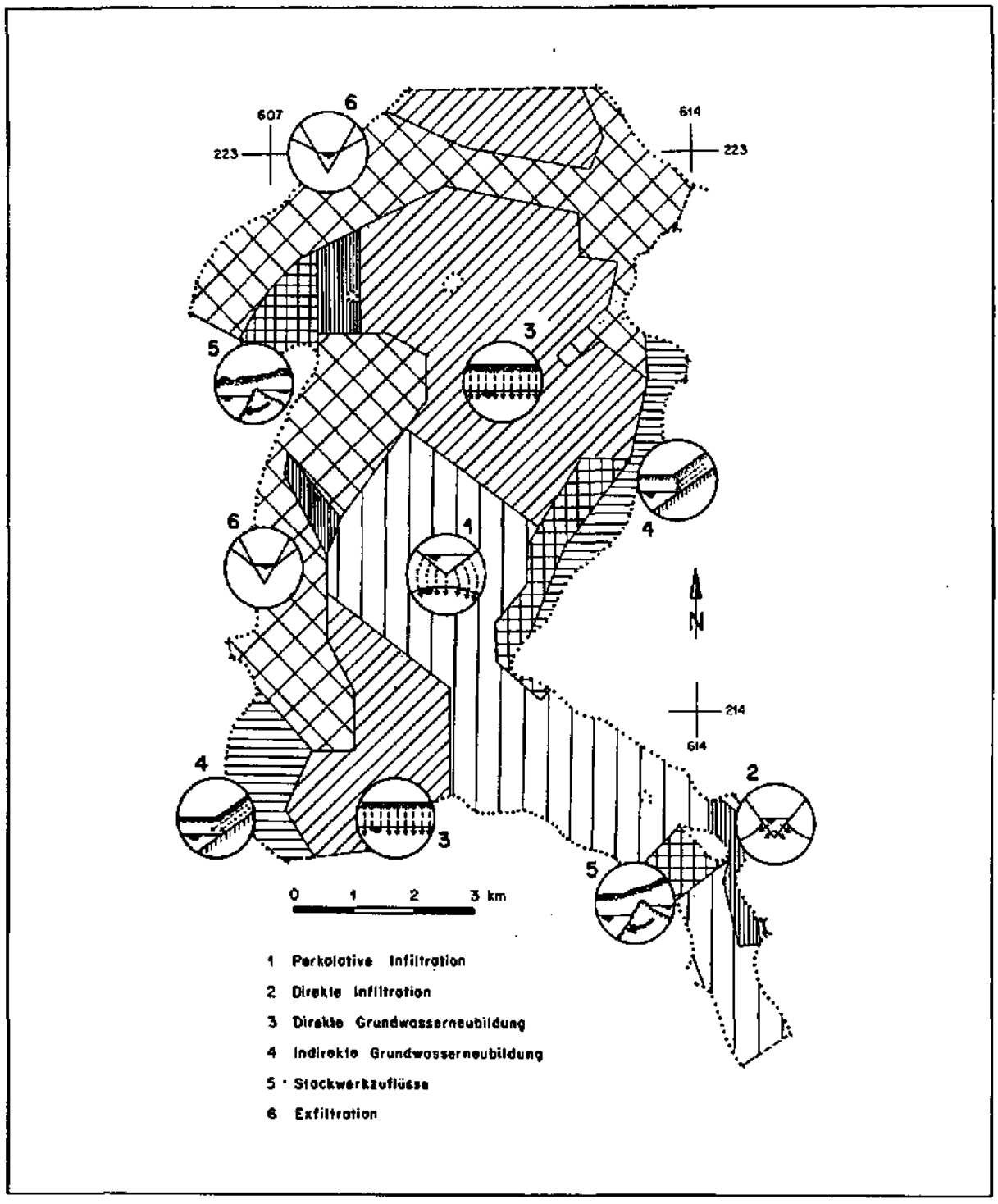

Fig. 2B-2 Map of discharging and recharging areas (WEA,1981).

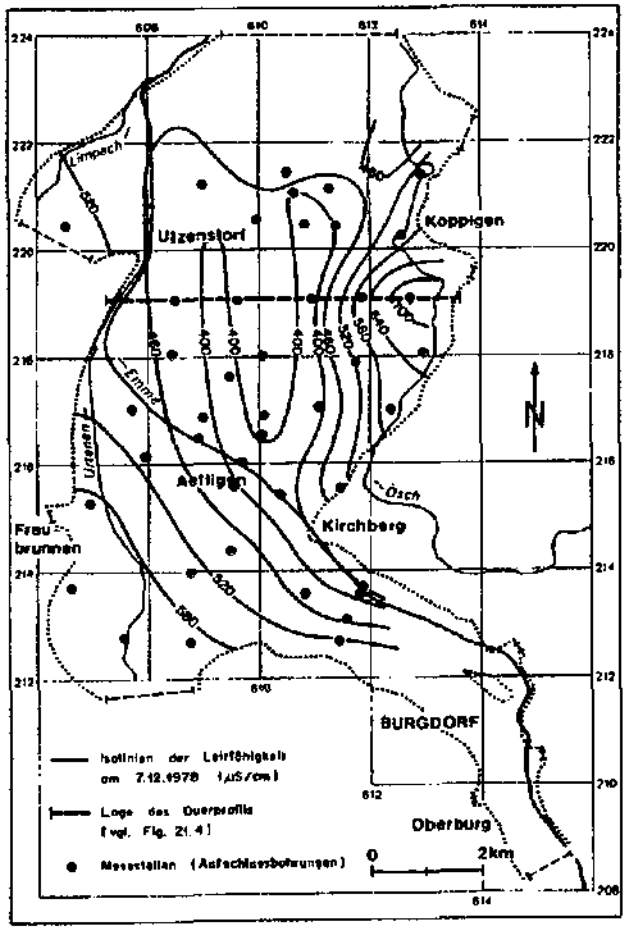

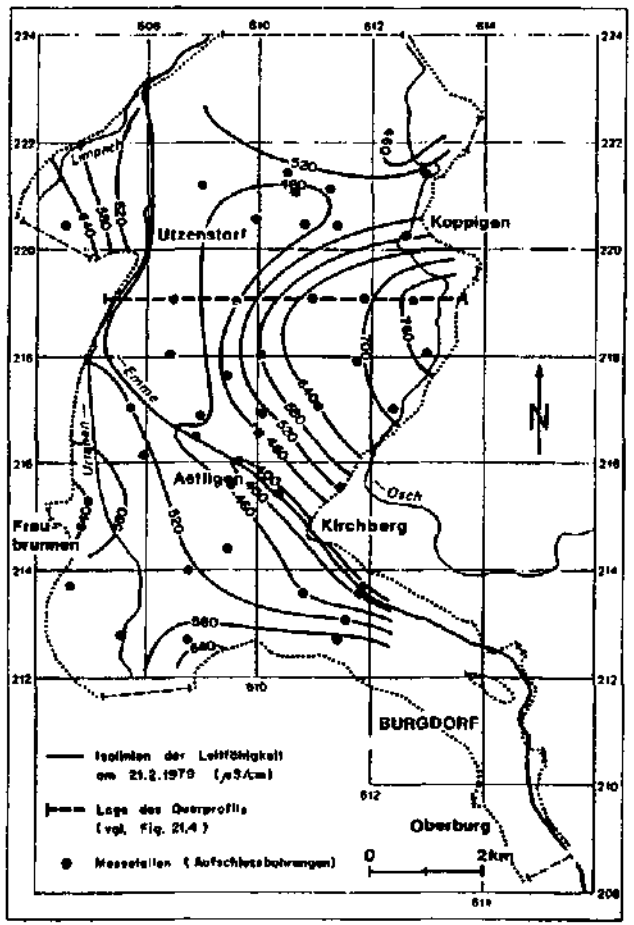

Fig. 2C-1. Map with distribution of conductivity adapted from **WEA (1981)** for the dry period (7.12.1978) and after rain fall event (21.2.1979). It is visible the importance of the Emme water infiltration lowering the conductivity values mainly in the region where the main infiltration takes place.

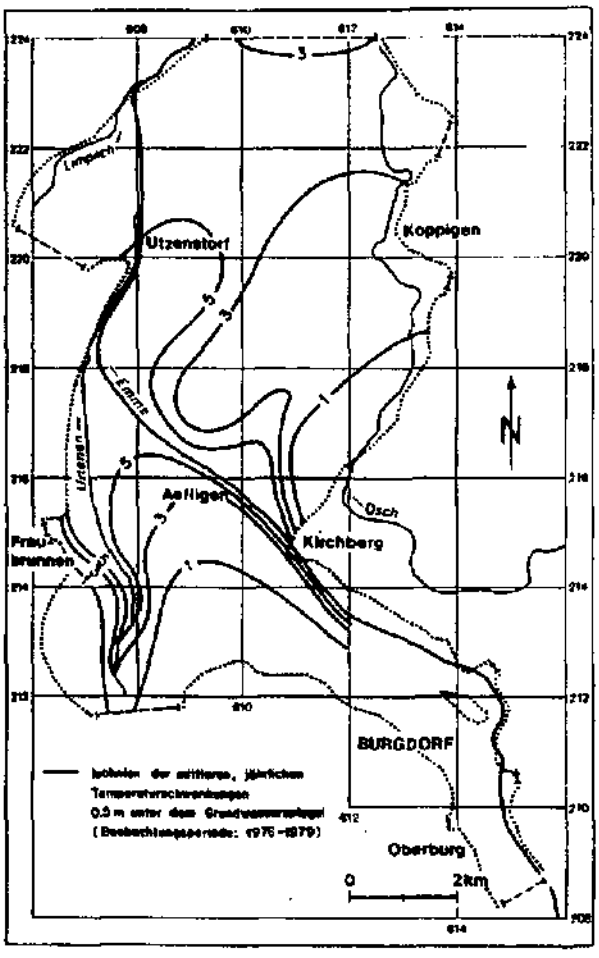

Fig. 2C-2 Map of distribution of the middle annual temperature oscilation isolines, taken 0,5 m under the groundwater level, for the period 1976-1979, adapted from WEA (1981).

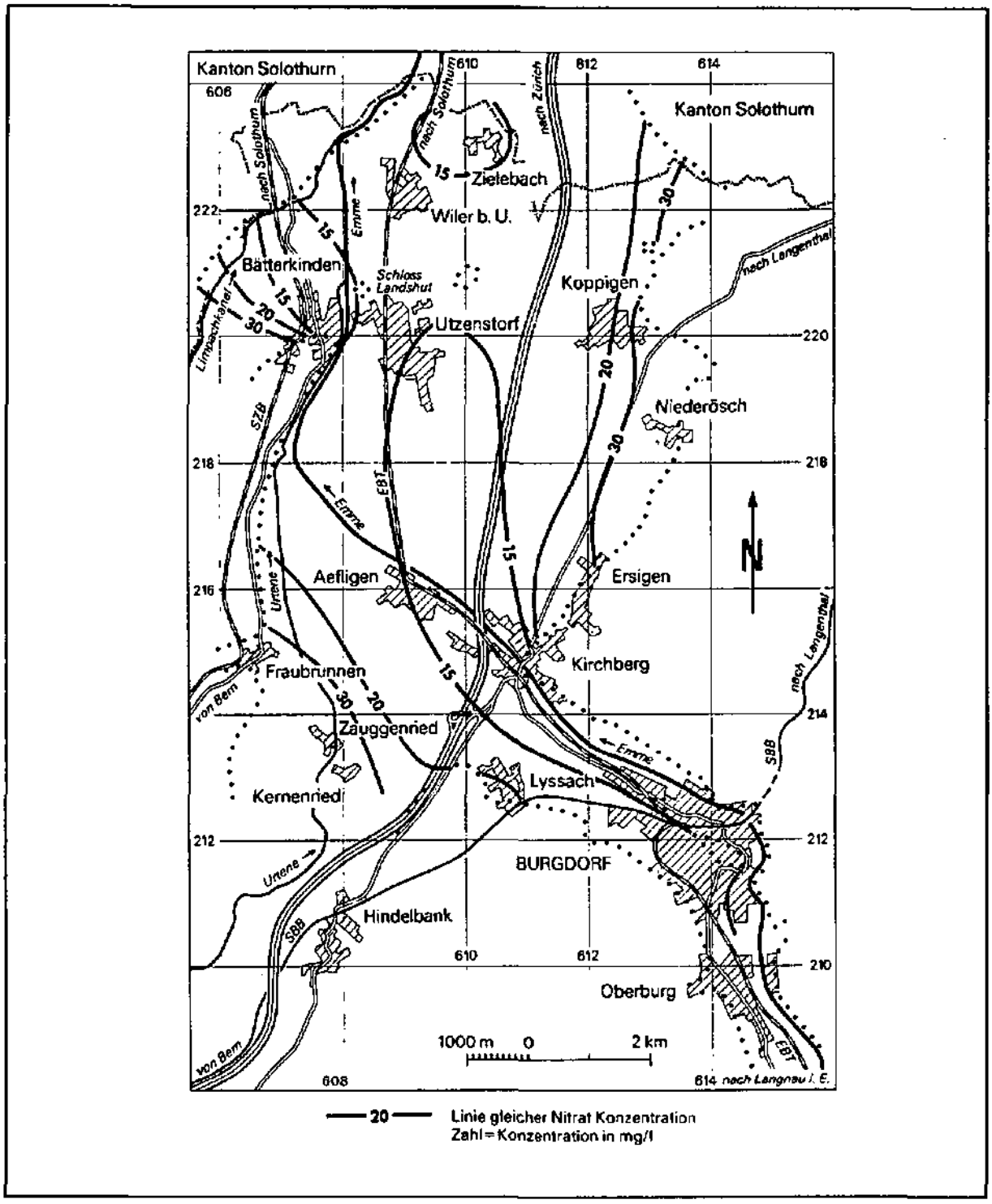

Fig. 2C-3 Nitrate distribution map (1971/1972) retired from **WEA (1981).**

Table 2B-1 Groundwater level evolution for the period Nov. 9th till Dec. 16th.

Obs. well	09-Nov	10-Nov	11-Nov	12-Nov	13-Nov	14-Nov	15-Nov	16-Nov	17-Nov	18-Nov	19-Nov
[AEH03]	482.4	482.43	482.48	482.46	482.46	482.44	482.7	482.64	482.58	482.55	482.67
[BAH14]	468.25	468.25	468.28	468.32	468.33	468.32	468.41	468.64	468.66	468.6	468.67
[WAB25]	483.97	485.94	483.96	485.99	484.01	484.02	484.05	484.17	484.27	484.33	484.39
[WAB13]	477.36	477.37	477.98	477.38	477.4	477.4	477.53	477.46	477.45	477.49	477.41
[UTB31]	465.33	465.22	465.33	465.34	465.36	465.39	465.46	465.53	465.68	465.69	465.72
[WIB01]	460.48	460.5	460.51	460.52	460.34	460.54	460.74	460.76	460.74	460.74	460.83
[WAB06]	477.48	477.5	477.52	477.35	477.38	477.6	477.7	477.84	477.88	477.9	477.84
[ZIB01]	455.18	455.22	455.28	455.34	455.38	455.38	455.6	455.82	455.74	455.66	455.82
[WAB21]	464.	464.01	464.02	464.03	464.04	464.05	464.08	464.18	464.28	464.36	464.44
[WAB23]	476.68	476.1	476.12	476.14	476.17	476.19	476.22	476.34	476.43	476.5	476.57
[WAB06]	493.26	493.27	493.28	493.3	493.31	493.33	495.34	493.37	495.41	493.44	493.48
[WAB67]	483.89	482.94	483.95	483.96	483.01	483.07	485.22	485.61	485.66	465.72	483.84
[WAB26]	475.88	479.9	475.92	475.95	479.97	476	476.12	476.28	476.34	476.4	476.5
[WAB29]	465.64	465.65	465.66	465.67	465.69	465.68	465.95	465.8	465.75	465.72	465.78

Obs. well	20-Nov	21-Nov	22-Nov	23-Nov	24-Nov	25-Nov	26-Nov	27-Nov	28-Nov	29-Nov	30-Nov
[AEH03]	482.62	482.69	482.69	482.62	482.57	482.56	483.78	482.67	482.64	482.63	482.62
[BAH14]	468.67	468.69	468.73	468.76	468.68	468.61	468.48	468.73	468.68	468.48	468.56
[WAB25]	464.65	484.5	484.57	484.61	484.64	484.64	484.65	484.73	484.75	484.77	484.78
[WAB13]	477.47	477.48	477.49	477.48	477.47	477.47	477.32	477.5	477.49	477.47	477.49
[UTB31]	465.75	465.78	465.8	465.84	465.84	465.81	465.82	465.86	465.86	465.84	465.82
[WIB01]	460.81	460.83	460.9	460.82	460.86	460.84	460.94	460.93	460.9	460.89	460.87
[WAB06]	477.98	478	478.05	478.09	476.1	476.12	478.18	478.2	476.32	478.22	478.22
[ZIB01]	455.77	455.77	455.91	455.88	455.78	455.72	455.87	455.85	455.79	455.73	455.67
[WAB21]	464.51	464.58	464.64	464.71	464.78	464.82	464.84	464.88	464.92	464.95	464.97
[WAB23]	476.62	476.66	476.71	476.77	476.81	476.83	476.87	476.91	476.95	476.97	476.98
[WAB06]	493.52	493.56	493.6	493.64	495.67	493.7	493.72	493.77	493.79	495.83	493.87
[WAB67]	465.95	484.02	484.12	484.23	484.3	484.34	484.42	484.56	484.64	484.65	484.66
[WAB26]	476.57	476.61	476.69	476.74	476.78	476.79	476.88	476.93	476.97	476.99	476.98
[WAB29]	465.73	465.73	465.79	465.76	465.74	465.73	465.83	465.78	465.76	465.74	465.74

Obs. well	01-Déc	02-Déc	03-Déc	04-Déc	05-Déc	06-Déc	07-Déc	08-Déc	09-Déc	10-Déc	11-Déc
[AEH03]	482.6	482.6	482.65	482.67	482.71	482.66	482.7	482.72	482.7	482.68	482.66
[BAH14]	468.49	468.43	468.43	468.45	468.55	468.58	468.59	468.64	468.68	468.65	468.58
[WAB25]	484.78	484.79	484.79	484.8	484.83	484.89	484.93	484.97	485.04	485.99	485.12
[WAB13]	477.49	477.48	477.51	477.56	477.53	477.52	477.56	477.36	477.54	477.54	477.53
[UTB31]	465.78	465.76	465.74	465.74	465.82	465.88	465.9	465.94	465.89	465.89	465.87
[WIB01]	460.86	460.84	460.86	460.91	461	460.98	461.02	461.1	461.07	461.84	461.02
[WAB06]	476.3	478.2	478.22	478.24	478.34	478.35	478.36	478.46	478.46	478.46	478.46
[ZIB01]	455.62	455.38	455.62	455.7	455.89	455.84	455.85	455.96	455.93	455.83	455.77
[WAB21]	464.98	464.99	464.98	464.97	465	465.07	465.13	465.17	465.25	465.32	465.35
[WAB23]	476.99	477	477	477.02	477.08	477.15	477.2	477.27	477.33	477.39	477.42
[WAB06]	493.89	493.92	493.93	493.95	493.98	494.01	494.05	494.11	494.16	494.22	494.28
[WAB67]	484.68	484.71	484.73	484.8	485.02	485.14	485.22	485.34	485.52	485.59	485.63
[WAB26]	476.99	477	477.02	477.08	477.19	477.25	477.33	477.41	477.47	477.47	477.48
[WAB29]	465.73	465.73	465.76	465.84	465.85	465.8	465.83	465.91	465.85	465.82	465.8

Obs. well	12-Déc	13-Déc	14-Déc	15-Déc	16-Déc	Max	# Max	Min	Delta
[AEH03]	482.72	482.69	482.66	482.64	482.64	482.78	26. Nov	482.4	0.38
[BAH14]	468.56	468.58	468.54	468.5	468.45	468.77	22. Nov	468.25	0.52
[WAB25]	485.13	485.15	485.16	485.13	485.12	485.16	14. Dec	483.92	1.24
[WAB13]	477.55	477.53	477.52	477.52	477.52	477.56	4. Dec	477.36	0.2
[UTB31]	465.83	465.8	465.78	465.76	465.73	465.94	8.Dec	465.33	0.61
[WIB01]	461.03	461.02	460.99	460.97	460.96	461.1	8. Dec	460.48	0.62
[WAB06]	478.47	478.48	478.48	478.45	478.44	478.48	13. Dec	477.48	1
[ZIB01]	455.76	455.72	455.68	455.84	455.6	455.96	8. Dec	455.18	0.78
[WAB21]	465.37	465.36	465.36	465.35	465.34	465.37	12. Dec	464.00	1.37
[WAB23]	477.43	477.43	477.43	477.42	477.4	477.43	13. Dec	476.08	1.35
[WAB06]	494.33	494.37	494.4	494.41	494.42	494.42	16. Dec	493.26	1.16
[WAB67]	485.63	485.65	485.67	485.66	485.61	485.67	14. Dec	483.89	2.78
[WAB26]	477.49	477.49	477.48	477.46	477.44	477.49	12. Dec	475.88	1.61
[WAB29]	465.82	465.8	465.79	465.78	465.77	465.95	15. Nov	465.64	0.31

Appendix 3A : local studies (Wilerwald and Merdingen)

Fig. 3A-1 Results of the AMT survey (true resistivities)at Wilerwald testsite (NNE region) determined by MT inversion

Fig. 3A-2 Longitudinal profiles showing the change in geometry and the true resistivity values variability.

Fig. 3A-3 Block diagram pointing out the geometry of the aquifer between the injection point and the C & D galleries.

Fig. 3A-4 Map with the aquitard's isolines.

Fig. 3A-5 True resistivity contour map, calculated with the MT. inversion **(Fischer et al, 1981)**.

Fig. 3A-6 VLF-EM profiles inside the Merdingen testsite, illustrating the greater degree in homogeneity (compared with Wilerwald).

Fig. 3A-7 Block diagram from Merdingen (based on MT inversion) showing the geometry of the aquifer in relation to the two subsites galleries.

Table 3A-1 RMT-R measurements

Table 3A-2 Wilerwald's equations of the spherical functions (variogram).

Table 3A-3 Merdingen's equations of the spherical functions (variogram).

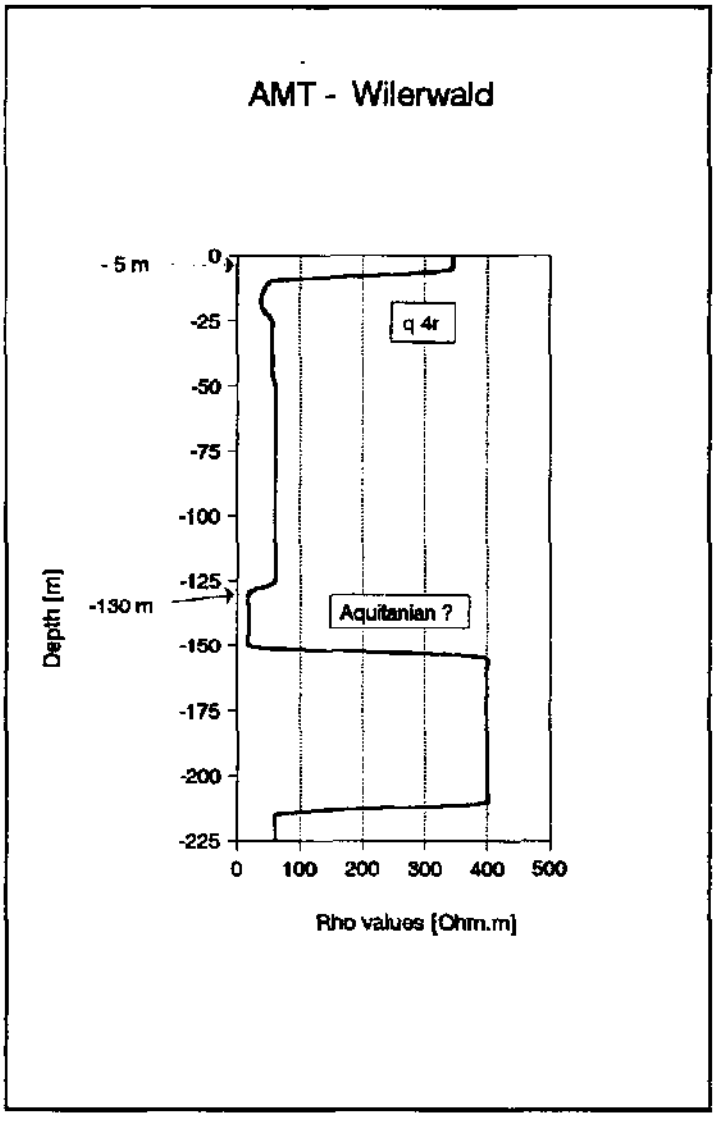

Fig. 3A-1 Results of the AMT survey at Wilerwald test site (NNE region): a resistant layer (aquifer) of about 5 meters, followed by the lacustrine unity (?) q4r. The passage to the aquitanian is probably localised at -130 m depth. These results have to be taken with prudence because of the extreme sensibility of this method towards electromagnetic interferences occurring in high industrialised countries.

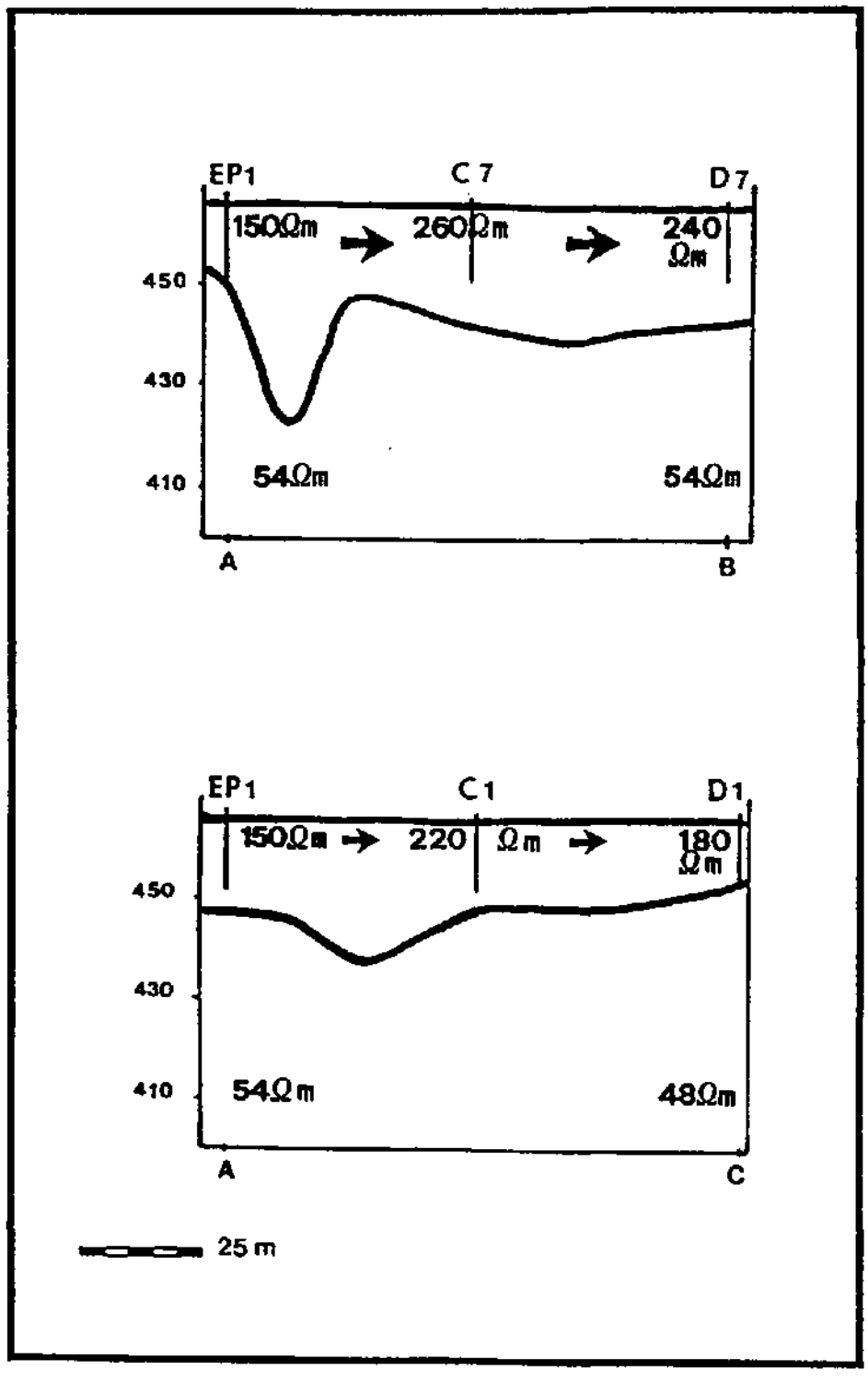

Fig. 3A-2 Longitudinal profiles showing the change in geometry and the true resistivity values variability. EP1 (injection borehole), C7 and D7 = observation wells more affected by the channel, D1 lying on the more conductive part of the site (for the location of the wells, please see **Fig. 3**.

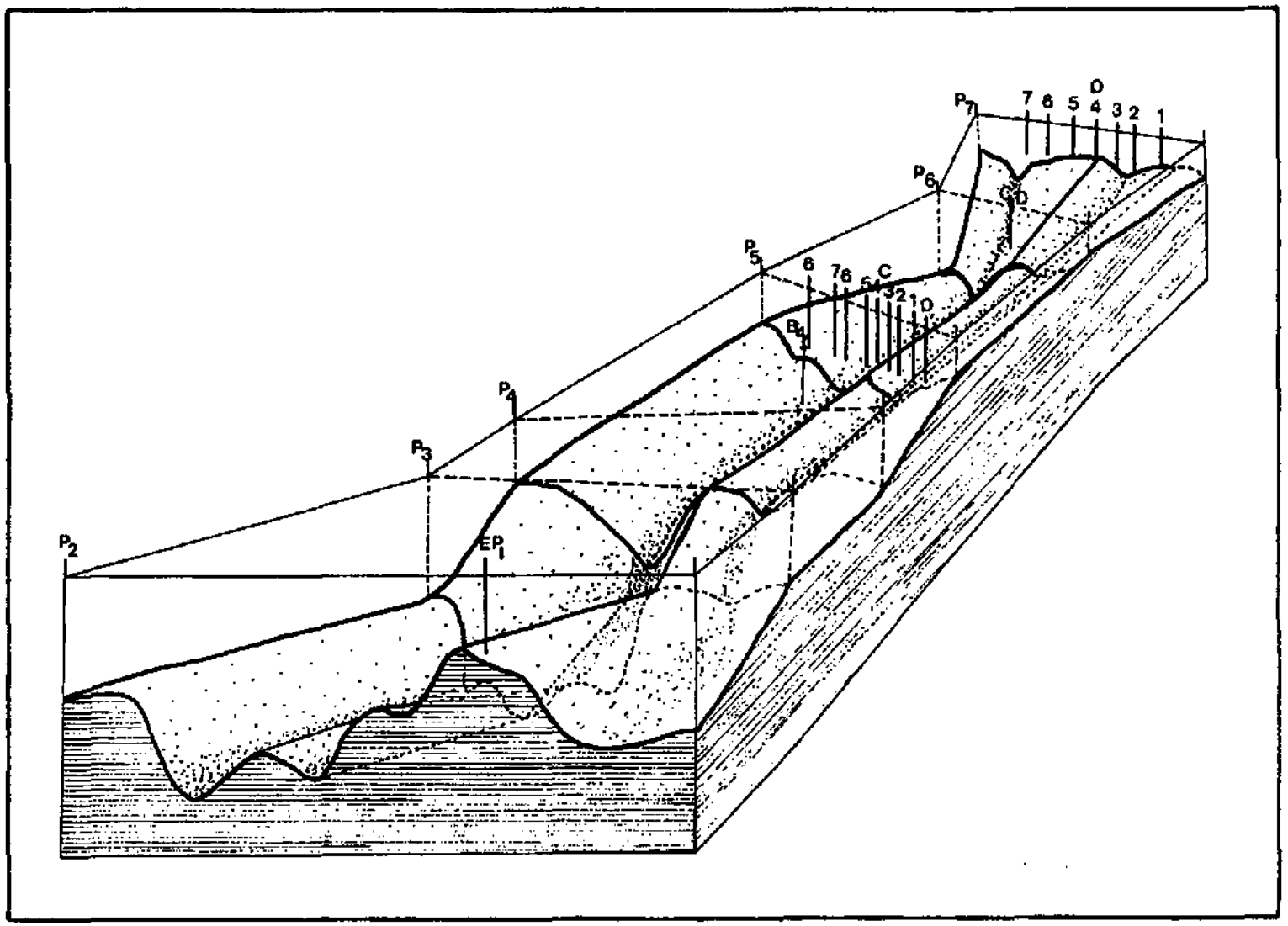

Fig. 3A-3 Block diagram pointing out the geometry of the aquifer between the injection well EP1 and the C & D galleries.

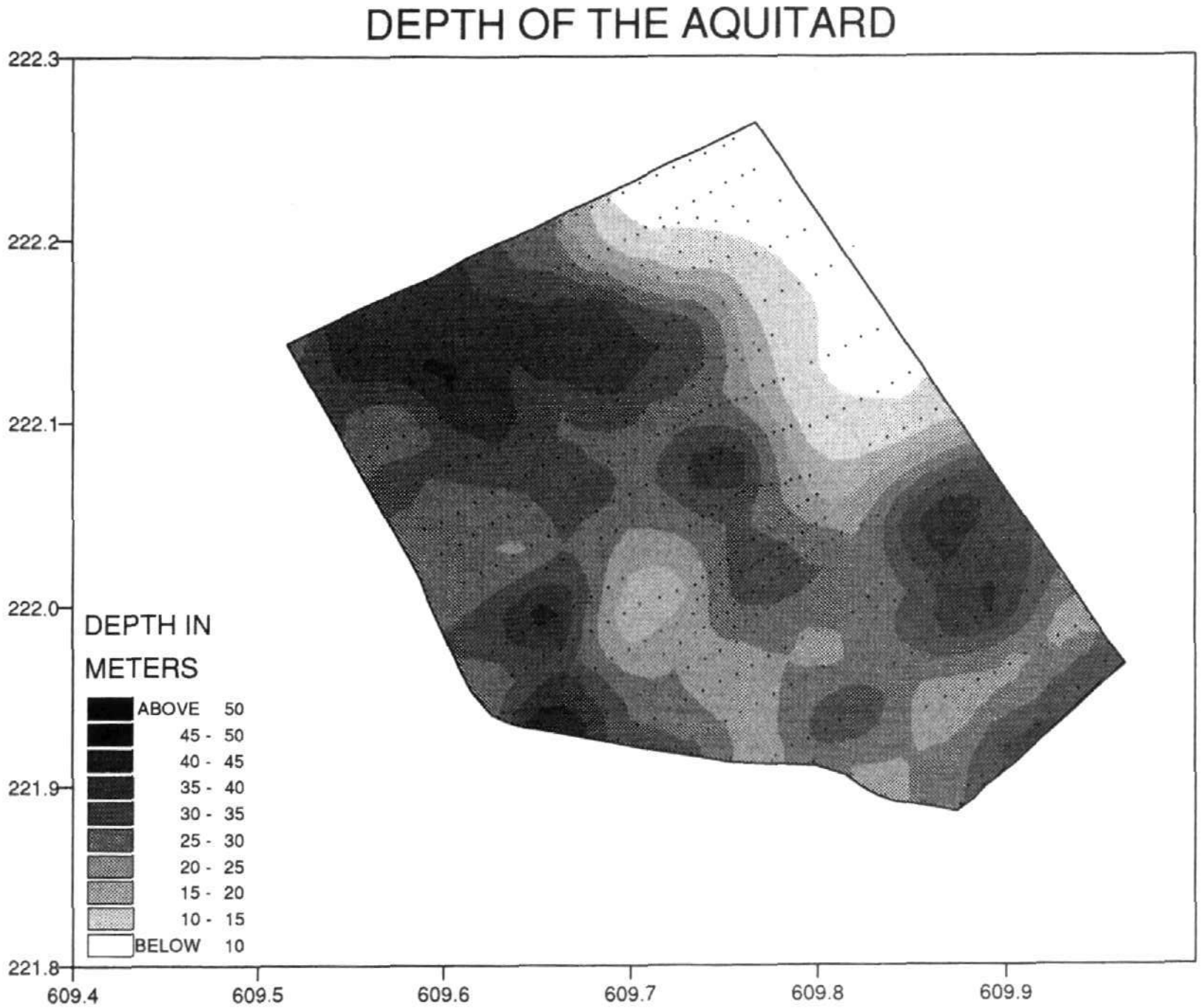

Fig. 3A-4 Map with the representation of the aquitard's isolines

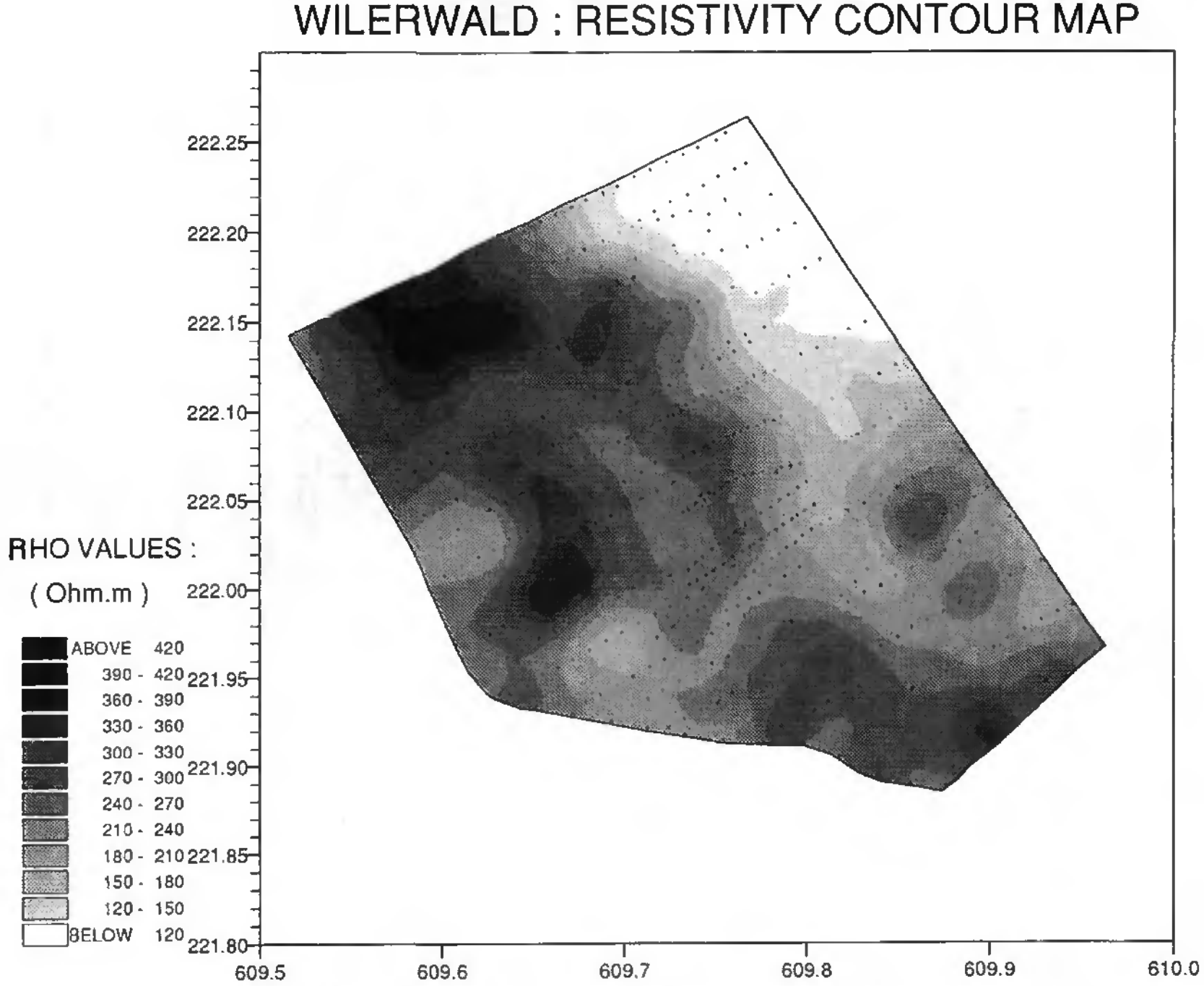

Fig. 3A-5 True resistivity contour map, calculated with the MT. inversion (**Fischer et al, 1981**).

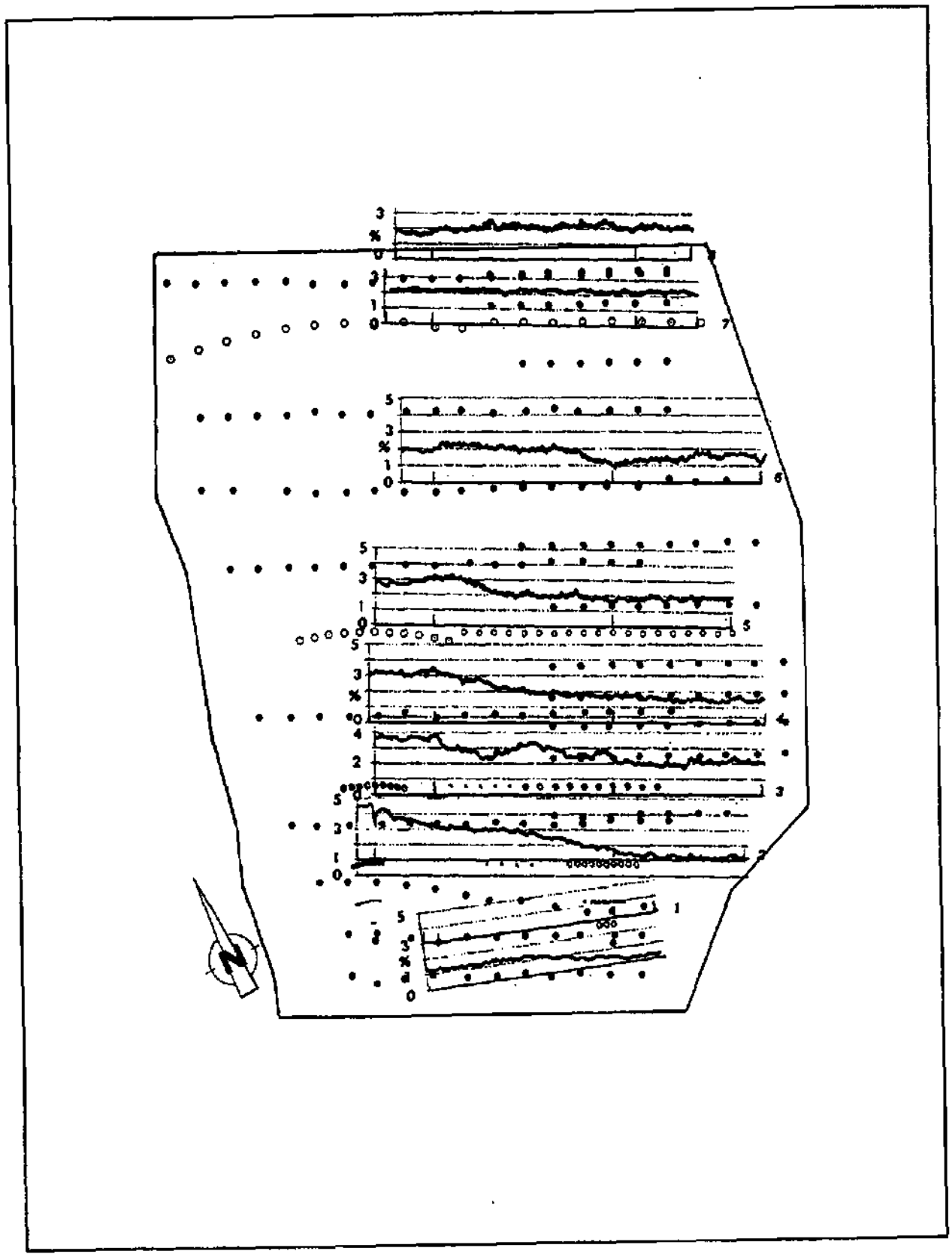

Fig . 3A-6 VLF-EM profiles inside the Merdingen test site , illustrating the greater degree in homogeneity (when compared with Wilerwald - Fig.33)

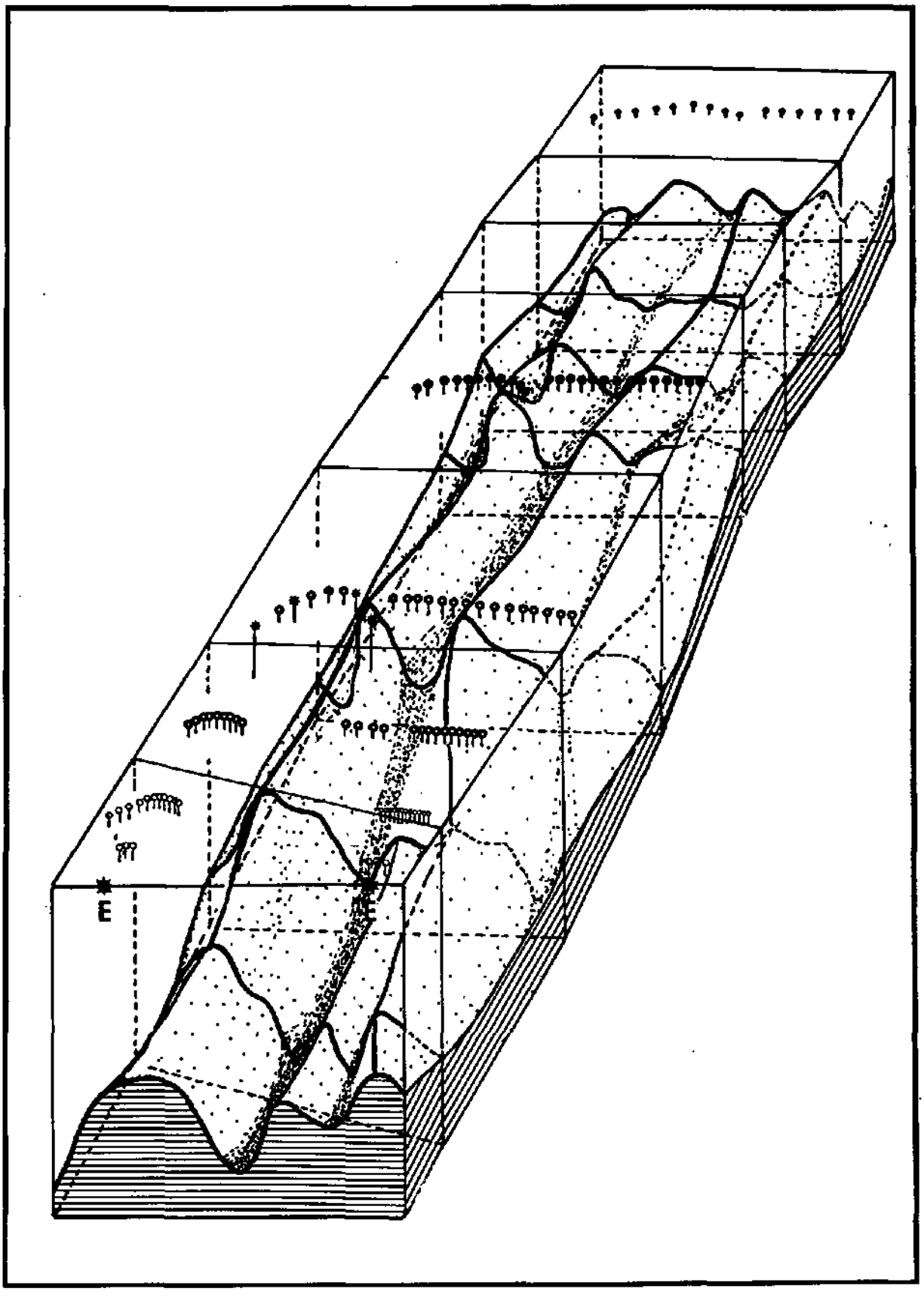

Fig. 3A-7 Block diagram from Merdingen (based on MT inversion) showing the geometry of the aquifer in relation to the two subsites galleries.

Table 3A-1 RMT-R measurements

RMT-R measurements

	Coordinates [Km]		ρα 183	Φ 183	ρα 70	Φ 70	ρα 19	Φ 19
	x	y	[Ohm.m]	[°]	[Ohm.m]	[°]	[Ohm.m]	[°]
1	609.632	221.941	128	24	190	40	153	49
2	609.652	221.934	273	31	80	42	36	49
3	609.672	221.930	225	39	292	47	140	54
4	609.693	221.926	172	32	211	40	153	49
5	609.713	221.922	136	38	146	45	104	51
6	609.733	221.918	92	37	77	43	89	50
7	609.754	221.915	160	36	154	43	136	51
8	609.776	221.914	92	30	113	40	90	51
9	609.798	221.913	97	31	102	37	132	30
10	609.818	221.906	150	28	197	38	177	50
11	609.836	221.894	134	33	152	41	147	52
12	609.257	221.890	172	32	170	37	212	51
13	609.876	221.889	218	34	249	46	190	55
14	609.880	221.899	181	35	200	50	155	55
15	609.887	221.905	70	44	74	48	58	55
16	609.895	221.912	290	33	316	46	257	53
17	609.902	221.920	383	31	453	43	375	52
18	609.909	221.927	319	32	383	44	326	51
19	609.917	221.933	208	37	352	44	202	52
20	609.923	221.939	198	37	234	46	176	53
21	609.931	221.947	260	30	300	44	228	53
22	609.938	221.953	244	28	345	39	303	30
23	609.953	221.968	220	32	266	44	268	50
24	609.945	221.991	134	23	159	44	125	52
25	609.937	221.987	119	41	110	51	87	54
26	609.928	221.982	140	41	132	49	190	55
27	609.919	221.977	112	44	99	53	74	56
28	609.910	221.972	167	41	140	51	117	54
29	609.902	221.967	90	39	92	47	80	53
30	609.894	221.962	110	37	124	47	102	53
31	609.885	221.958	156	34	190	45	158	52
32	609.877	221.953	190	32	338	43	195	52
33	609.868	221.949	109	35	130	45	111	54
34	609.258	221.943	140	33	188	44	151	53

	Coordinates [Km]		ρα 183	Φ 183	ρα 70	Φ 70	ρα 19	Φ 19
	x	y	[Ohm.m]	[°]	[Ohm.m]	[°]	[Ohm.m]	[°]
35	609.829	221.945	268	33	324	42	260	54
36	609.821	221.941	226	37	260	44	201	53
37	609.812	221.936	275	35	369	43	246	53
38	609.804	221.931	282	31	410	42	250	55
39	609.795	221.926	257	28	403	46	260	49
40	609.786	221.922	298	26	380	38	335	53
41	609.778	221.917	203	28	228	43	235	52
42	609.724	221.922	240	33	295	43	221	50
43	609.733	221.927	250	31	363	42	213	53
44	609.742	221.932	253	33	399	43	208	54
45	609.751	221.936	149	37	217	43	192	54
46	609.759	221.941	151	32	122	39	166	53
47	609.768	221.946	153	27	231	37	192	52
48	609.777	221.951	163	30	220	31	169	52
49	609.786	221.956	190	30	152	39	160	53
50	609.794	221.961	180	31	245	39	190	53
51	609.803	221.966	127	28	175	38	147	52
52	609.841	221.968	137	29	183	41	162	51
53	609.850	221.973	180	30	191	43	169	30
54	609.858	221.978	212	34	247	43	210	51
55	609.866	221.982	197	40	200	48	163	52
56	609.875	221.987	230	37	234	45	185	53
57	609.884	221.992	250	36	265	46	216	51
58	609.892	221.997	278	42	254	51	196	54
59	609.902	222.001	280	43	258	50	192	54
60	609.911	222.007	234	41	209	30	162	54
61	609.919	222.011	141	41	132	49	190	54
62	609.928	222.016	141	37	149	47	121	52
63	609.911	222.040	165	42	175	47	140	52
64	609.902	222.035	241	41	217	50	167	53
65	609.892	222.031	162	40	140	50	113	53
96	609.884	222.026	210	42	205	49	164	52
67	609.876	222.021	211	41	198	49	100	52
68	609.867	332.016	155	42	140	49	115	53

RMT-R measurements

	Coordinates	[Km]	ρα 183	Φ 183	ρα 70	Φ 70	ρα 19	Φ 19
	x	y	[Ohm.m]	[°]	[Ohm.m]	[°]	[Ohm.m]	[°]
69	609.858	222.012	192	37	190	47	136	52
70	609.849	222.007	166	36	178	46	152	51
71	609.841	222.002	146	36	162	43	144	50
72	609.832	221.998	184	32	220	42	298	49
73	609.823	221.992	206	29	276	42	244	50
74	609.609	221.986	127	30	204	39	143	51
75	609.792	221.982	151	27	222	37	198	51
76	609.783	221.976	180	29	367	38	211	52
77	609.774	221.972	176	30	233	38	210	51
78	609.765	221.967	146	31	224	39	168	51
79	609.757	221.962	122	22	162	34	180	50
80	609.748	221.958	98	32	164	40	111	51
81	609.739	221.953	136	33	183	41	126	51
82	609.730	221.948	160	36	172	44	146	53
83	609.721	221.963	151	38	170	44	138	53
84	609,713	221.938	203	35	253	43	170	53
85	609.704	221.934	210	33	291	42	176	52
86	609,679	221.937	270	39	337	45	211	51
87	609,687	221.941	218	36	314	43	183	50
88	609,696	221.966	130	42	168	48	103	56
89	609.705	221.951	133	42	118	52	93	57
90	609,714	221.956	121	35	142	45	123	51
91	609.722	221.961	182	36	192	47	165	53
92	609.731	221.966	241	32	280	46	229	55
93	609.740	221.970	137	31	180	41	161	51
94	609.746	221.975	119	31	178	41	153	51
95	609.757	221.980	121	33	135	44	137	52
96	609.766	221.985	166	29	247	38	213	51
97	609,819	221.996	148	28	198	38	137	49
98	609,827	222.004	111	29	157	39	123	48
99	609,834	222.011	128	36	137	43	122	51
100	609.842	222.018	140	32	185	42	121	50
101	609.851	222.023	199	38	186	46	156	52
102	609.859	222.029	609	32	453	43	330	51

	Coordinates	[Km]	ρα 183	Φ 183	ρα 70	Φ 70	ρα 19	Φ 19
	x	y	[Ohm.m]	[°]	[Ohm.m]	[°]	[Ohm.m]	[°]
103	609.867	222.035	288	34	326	45	218	52
104	609.875	222.041	262	33	250	46	212	52
105	609.883	222.046	303	38	272	47	242	51
106	609.892	222.051	230	38	186	46	181	52
107	609.899	222.056	193	38	177	47	158	51
108	609.796	222.012	198	22	188	40	182	47
109	609.788	222.007	174	27	242	36	205	47
110	609.780	222.002	219	24	265	38	244	47
111	609.774	221.998	143	31	140	40	143	49
112	609.768	221.995	232	28	250	40	213	48
113	609.762	221.991	244	28	274	40	246	49
114	609.756	221.988	136	24	147	37	139	46
115	609.718	221.973	163	30	188	42	165	30
116	609.727	221.979	126	33	202	38	152	49
117	609.735	221.985	253	24	340	37	297	47
118	609.740	221.988	205	22	270	36	254	47
119	609.744	221.990	155	24	218	36	211	47
120	609.747	221.994	181	23	238	37	220	48
121	609.752	221.990	244	30	284	40	262	50
122	609.756	222.000	210	33	261	41	224	51
123	609.761	222.003	123	40	159	43	120	52
124	609.766	222.007	165	37	222	42	170	50
125	609.771	222.010	130	41	175	47	122	51
126	609.776	222.014	106	36	104	42	80	51
EP1	609.781	222.017	136	32	125	42	114	50
128	609.785	222.020	131	33	144	45	120	50
129	609.789	222.023	180	23	205	41	185	47
130	609.794	222.026	214	30	225	41	194	49
131	609.798	222.030	204	34	246	42	192	50
132	609.803	222.033	183	26	213	40	188	47
133	609.808	222.036	163	20	199	41	174	47
134	609.813	222.039	99	33	156	40	87	30
135	609.823	222.044	110	31	178	39	118	46
136	609.832	222.048	158	30	275	40	135	49

RMT-R measurements

	Coordinates	[Km]	ρα 183	Φ 183	ρα 70	Φ 70	ρα 19	Φ 19
	x	y	[Ohm.m]	[°]	[Ohm.m]	[°]	[Ohm.m]	[°]
137	609.841	222.052	202	35	226	44	182	52
138	609.850	222.057	212	32	232	42	203	50
139	609.858	222.062	226	33	219	43	220	50
140	609.868	222.067	220	37	218	40	183	52
141	609.877	222.072	233	37	253	47	206	51
142	609.885	222.077	171	36	178	44	147	50
143	609.804	222.047	115	35	122	44	92	48
144	609.799	222.044	107	35	115	43	97	48
145	609.795	222.061	125	30	143	40	110	47
146	609.792	222.039	165	30	177	44	140	50
147	609.787	222.036	150	32	152	44	125	30
148	609.783	222.033	178	35	178	44	134	50
149	609.779	222.031	167	35	140	44	123	50
150	609.775	222.028	231	27	347	40	280	48
151	609.771	222.025	402	32	436	44	337	52
152	609.769	222.024	311	30	356	42	296	49
153	609.765	222.021	250	31	257	41	231	48
154	609.759	222.018	273	29	330	40	282	49
155	609.734	222.014	365	20	498	36	427	48
156	609.749	222.011	177	30	263	38	226	48
157	609.745	222.008	235	22	417	38	350	47
158	609.740	222.905	133	25	170	38	152	49
159	609.736	222.003	140	30	174	39	155	48
160	609.743	222.000	117	27	193	37	142	51
161	609.734	221.995	131	20	168	36	139	49
162	609.725	221.990	120	33	158	42	123	52
163	609.717	221.986	80	35	83	50	77	52
164	609.708	221.981	148	35	178	44	149	52
165	609.699	221.976	142	37	135	47	106	53
166	609.690	221.971	118	41	117	48	84	56
167	609.681	221.966	187	42	152	49	136	54
168	609.672	221.961	206	44	133	51	125	55
169	609.664	221.956	186	39	212	49	119	55
170	609.656	221.952	220	40	275	47	149	45

	Coordinates	[Km]	ρα 183	Φ 183	ρα 70	Φ 70	ρα 19	Φ 19
	x	y	[Ohm.m]	[°]	[Ohm.m]	[°]	[Ohm.m]	[°]
171	609.647	221.946	288	37	298	45	213	56
172	609.637	221.941	240	33	350	45	182	53
173	609.636	221.962	167	36	230	49	110	55
174	609.684	221.966	140	41	151	51	78	56
175	609.653	221.972	213	39	277	50	124	50
176	609.662	221.926	256	40	248	50	157	56
177	609.670	221.981	166	41	155	51	97	56
178	609.670	221.986	148	38	150	49	96	55
179	609.688	221.991	85	43	70	49	61	56
180	609.697	221.996	102	33	110	45	85	50
181	609.705	222.001	129	29	148	41	133	53
182	609.716	222.004	135	24	190	38	146	50
183	609.725	222.008	115	32	151	41	130	52
184	609.725	222.011	131	30	161	43	126	51
185	609.739	222.015	121	28	127	42	107	49
186	609.743	222.018	163	32	152	44	122	51
187	609.748	222.022	180	33	217	42	168	51
188	609.752	222.025	237	31	225	44	183	51
189	609.757	222.029	335	30	332	44	270	51
190	609.761	222.032	177	35	172	45	135	53
191	609.766	222.036	121	41	122	49	86	54
192	609.770	222.039	149	35	137	45	112	50
193	609.775	222.042	230	26	258	42	204	49
194	609.780	222.046	185	25	190	44	166	48
195	609.785	222.050	128	50	155	42	122	50
196	609.790	222.053	117	30	130	42	105	49
197	609.795	222.057	135	28	143	41	127	49
198	609.800	222.060	172	28	170	42	155	48
199	609.863	222.100	77	35	122	39	88	51
200	609.855	222.101	66	32	101	36	89	50
201	609.846	222.096	68	30	116	34	90	49
202	609.837	222.091	58	29	118	35	76	49
203	609.828	222.087	46	30	88	33	67	46
204	609.796	222.070	98	32	110	44	85	50

RMT-R meesurements

	Coordinates	[Km]	ρα 183	Φ 183	ρα 70	Φ 70	ρα 19	Φ 19
	x	y	[Ohm.m]	[°]	[Ohm.m]	[°]	[Ohm.m]	[°]
205	609.701	222.069	110	33	114	46	92	50
206	609.786	222.068	140	28	145	46	116	50
C0	609.784	222.066	173	28	150	45	122	51
C1	609.777	222.066	186	50	173	45	150	50
C2	609.772	222.065	192	35	122	46	130	50
C3	609.767	222.064	207	35	192	47	125	51
C4	609.763	222.062	228	36	206	50	134	54
C5	609.758	222.060	166	38	148	50	103	55
C6	609.754	222.057	261	35	215	49	140	52
C7	609.751	222.055	313	30	212	49	106	51
215	609.746	222.054	270	31	192	49	140	52
216	609.742	222.053	140	37	116	50	77	56
C8	609.745	222.050	155	32	168	47	126	50
218	609.739	222.048	272	33	180	50	138	52
219	609.735	222.045	183	50	152	47	117	51
220	609.732	222.045	114	50	122	42	103	50
221	609.696	222.015	140	37	192	46	119	56
222	609.688	222.010	175	36	224	48	122	57
223	609.679	222.005	245	46	162	48	183	57
224	609.670	222.000	561	56	805	50	356	55
225	609.669	221.995	443	37	429	48	296	55
226	609.651	221.990	360	37	343	49	230	56
227	609.643	221.985	326	38	268	50	211	54
228	609.634	221.980	227	35	233	42	157	56
229	609.626	221.975	209	37	223	48	139	56
230	609.655	222.020	180	30	230	45	116	55
231	609.669	222.025	225	36	298	46	140	56
232	609.684	222.057	145	32	170	48	112	55
233	609.692	222.041	230	35	244	46	171	55
234	609.701	222.046	144	38	148	50	105	55
235	609.709	222.051	188	38	175	52	123	55
236	609.718	222.055	217	37	179	52	131	55
237	609.727	222.060	150	46	123	53	98	55
238	609.736	222.065	192	39	156	53	105	55

	Coordinates	[Km]	ρα 183	Φ 183	ρα 70	Φ 70	ρα 19	Φ 19
	x	y	[Ohm.m]	[°]	[Ohm.m]	[°]	[Ohm.m]	[°]
239	609.849	222.126	60	29	85	32	101	48
240	609.840	222.121	66	26	101	50	106	47
241	609.832	222.116	69	28	113	32	111	48
242	609.823	222.112	68	25	120	31	114	47
243	609.814	222.107	80	37	146	43	99	50
244	609.805	222.102	83	36	106	40	106	50
245	609.796	222.097	75	32	90	38	98	50
246	609.786	222.997	85	33	91	45	74	50
247	609.782	222.995	109	31	113	45	88	51
248	609.777	222.094	166	28	173	46	138	50
249	609.773	222.092	185	32	170	46	126	52
250	609.768	222.091	207	32	219	47	148	52
251	609.764	222.089	195	32	198	46	140	51
252	609.760	222.087	195	37	167	49	117	52
253	609.756	222.086	270	37	210	50	137	54
254	609.749	222.083	237	35	238	50	162	52
255	609.746	222.080	380	35	288	48	209	52
256	609.738	222.077	330	31	266	50	185	55
257	609.732	222.074	280	35	276	48	183	53
258	609.717	222.071	138	39	119	51	86	56
259	609.209	222.066	209	46	237	50	119	56
260	609.200	222.061	230	39	284	50	127	57
261	609.691	222.057	162	53	212	46	118	56
262	609.682	222.052	132	37	165	49	78	57
263	609.673	222.047	227	56	250	46	150	56
264	609.664	222.043	237	32	258	47	168	50
265	609.656	222.038	218	32	218	46	162	50
266	609.467	222.033	199	31	200	45	155	55
267	609.637	222.038	135	37	159	49	87	56
268	609.628	222.022	146	36	105	49	290	53
269	609.620	222.018	153	39	158	50	92	56
270	609.611	222.013	177	39	194	51	91	50
271	609.602	222.008	122	43	157	51	101	56
272	609.599	222.039	199	43	240	41	103	56

RMT-R meesurements

	Coordinates [Km]		ρα 183	Φ 183	ρα 70	Φ 70	ρα 19	Φ 19
	x	y	[Ohm.m]	[°]	[Ohm.m]	[°]	[Ohm.m]	[°]
273	609.609	222.034	190	43	212	51	104	56
274	609.616	222.039	183	41	197	52	99	50
275	609.626	222.045	131	43	197	51	92	56
276	609.635	222.049	136	41	159	51	80	57
277	609.644	222.054	122	31	210	45	129	55
276	609.653	222.059	247	33	264	46	182	55
279	609.662	222.064	294	36	284	49	188	56
280	609.670	222.069	225	43	210	53	116	58
281	609.679	222.074	260	39	307	50	140	56
282	609.888	222.078	156	41	150	52	88	51
283	609.697	222.083	194	41	241	53	96	57
284	609.702	222.085	174	28	193	45	129	52
285	609.710	222.089	226	30	194	46	135	50
286	609.715	222.093	270	35	245	49	162	52
D7	609.721	222.096	270	37	209	51	131	54
288	609.724	222.097	256	34	204	49	140	53
D6	609.729	222.099	213	35	188	49	124	54
290	609.731	222.101	196	35	167	47	118	53
D5	609.736	222.105	113	27	122	42	102	47
292	609.738	222.106	187	37	140	51	103	52
D4	609.744	222.109	184	39	135	51	02	53
294	609.748	222.109	165	37	140	40	99	54
D3	609.750	222.111	220	40	169	51	113	54
296	609.757	222.112	207	37	190	48	131	53
D2	609.763	222.113	180	35	161	50	117	52
298	609.767	222.116	127	35	130	46	94	52
D1	609.772	222.120	88	32	108	43	88	49
300	609.777	222.122	81	30	104	41	84	49
301	609.782	222.123	92	35	120	41	91	50
302	609.797	222.132	46	33	94	38	85	50
303	609.806	222.136	66	34	100	39	81	50
304	609.815	222.141	52	32	81	37	46	50
305	609.823	222.146	45	31	22	36	60	49
306	609.832	222.150	52	32	98	37	74	49

	Coordinates [Km]		ρα 183	Φ 183	ρα 70	Φ 70	ρα 19	Φ 19
	x	y	[Ohm.m]	[°]	[Ohm.m]	[°]	[Ohm.m]	[°]
307	609.749	222.139	73	36	97	45	75	52
308	609.740	222.134	132	39	140	49	98	55
309	609.752	222.130	188	41	165	53	110	56
310	609.743	222.124	155	39	142	52	97	50
311	609.734	222.120	160	42	147	53	99	56
312	609.725	222.115	216	41	197	53	124	57
313	609.716	222.110	228	37	190	53	126	57
314	609.707	222.105	171	39	160	53	103	57
315	609.698	222.100	152	39	133	54	88	57
316	609.689	222.095	122	42	97	55	68	58
317	609.680	222.090	165	40	146	53	97	56
318	609.671	222.085	266	42	218	55	135	58
319	609.661	222.081	173	43	233	53	70	59
320	609.653	222.076	220	37	217	48	139	50
321	609.644	222.071	192	36	203	49	119	57
322	609.635	222.067	230	39	235	50	136	57
323	609.626	222.062	270	37	324	50	140	56
324	609.617	222.057	171	41	152	52	100	57
325	609.608	222.051	165	41	160	51	94	57
326	609.599	222.046	161	39	115	51	111	55
327	609.590	222.042	156	40	180	49	84	50
328	609.576	222.061	204	33	261	50	121	54
329	609.585	222.067	280	38	298	50	170	57
330	609.594	222.072	207	40	184	50	128	50
331	609.603	222.077	161	41	110	51	102	57
332	609.612	222.081	150	45	140	50	80	59
333	609.619	222.082	428	37	300	51	197	53
334	609.629	222.086	170	37	155	50	106	54
335	609.638	222.089	257	36	222	49	140	53
336	609.647	222.093	280	35	224	47	158	57
337	609.656	222.097	137	41	91	57	60	56
338	609.666	222.101	146	40	114	53	73	55
339	609.675	222.105	196	35	122	46	120	53

	Coordinates [Km]		ρα 183	Φ 183	ρα 70	Φ 70	ρα 19	Φ 19
	x	y	[Ohm.m]	[°]	[Ohm.m]	[°]	[Ohm.m]	[°]
340	609.684	222.108	351	36	274	50	183	53
341	609.693	222.112	266	35	224	49	146	53
342	609.702	222.116	210	36	180	50	115	54
343	609.711	222.120	225	37	185	50	126	55
344	609.720	222.124	248	43	220	51	126	55
345	609.730	222.128	193	39	160	48	111	55
346	609.739	222.131	192	41	160	47	122	52
347	609.749	222.135	151	36	144	47	110	52
344	609.757	222.139	102	35	108	42	86	51
349	609.766	222.143	78	31	97	40	88	49
350	609.776	222.147	101	37	152	42	121	50
351	609.807	222.185	50	26	89	33	81	46
352	609.799	222.180	62	33	92	37	84	50
353	609.790	222.175	66	32	101	37	91	49
354	609.781	222.171	62	26	100	33	92	47
355	609.772	222.160	60	30	98	37	84	49
356	609.759	222.169	22	35	98	41	83	48
357	609.750	222.165	100	25	146	38	125	47
358	609.740	222.161	280	35	262	47	188	54
359	609.730	222.157	254	35	223	47	169	52
E4	609.726	222.156	270	33	241	48	156	52
561	609.719	222.153	234	35	206	47	144	52
362	609.711	222.150	182	35	164	47	113	56
363	609.702	222.148	240	38	191	51	132	55
364	609.692	222.144	284	36	250	51	152	56
365	609.683	222.142	222	31	270	46	180	56
366	609.673	222.139	241	38	190	51	130	56
367	609.684	222.136	303	35	255	50	170	54
368	609.654	222.133	224	40	214	50	130	55
360	609.644	222.130	257	35	252	48	173	54
370	609.635	222.128	274	32	306	47	200	55
371	609.624	222.124	127	39	93	51	65	55
372	609.614	222.122	370	37	335	50	211	55
373	609.605	222.119	316	37	236	52	154	54

	Coordinates [Km]		ρα 183	Φ 183	ρα 70	Φ 70	ρα 19	Φ 19
	x	y	[Ohm.m]	[°]	[Ohm.m]	[°]	[Ohm.m]	[°]
374	609.598	222.102	250	41	242	52	140	58
375	609.588	222.097	217	38	261	50	122	57
376	609.579	222.093	167	36	164	49	107	57
377	609.570	222.087	150	38	176	50	87	57
378	609.561	222.082	218	41	250	53	114	58
379	609.583	222.122	236	46	253	53	116	59
380	609.575	222.118	151	56	141	46	115	56
381	609.566	222.112	245	36	278	48	142	57
382	609.557	222.107	173	39	147	49	104	58
383	609.535	222.125	177	41	230	51	88	57
384	609.544	222.129	280	46	252	57	139	58
385	609.554	222.133	261	46	273	53	131	56
386	609.562	222.137	230	41	271	52	126	57
387	609.571	222.142	231	36	248	50	136	57
388	609.582	222.138	460	40	380	51	238	57
389	609.591	222.141	336	40	292	56	173	57
390	609.600	222.146	270	38	245	51	157	56
391	609.610	222.147	307	37	208	52	143	57
392	609.619	222.149	407	37	358	50	234	57
393	609.629	222.152	356	40	290	52	181	57
394	609.639	222.155	322	28	319	46	225	53
395	609.648	222.158	290	35	280	47	188	55
396	609.658	222.161	128	38	105	49	73	54
397	609.667	222.164	278	35	272	49	190	54
398	609.677	222.160	361	33	280	47	217	53
399	609.687	222.170	285	56	260	47	184	53
400	609.696	222.172	277	31	275	48	170	55
401	609.705	222.175	246	31	236	40	187	52
402	609.715	222.179	82	36	97	42	72	53
403	609.725	222.181	60	35	82	42	67	50
406	609.734	222.184	60	35	62	39	77	49
405	609.743	222.188	79	35	96	40	90	50
406	609.753	222.190	71	35	81	38	87	50
407	609.767	222.192	60	32	85	38	70	49

RMT-R measurements

	Coordinates	[Km]	ρα 183	Φ 183	ρα 70	Φ 70	ρα 19	Φ 19
	x	y	[Ohm.m]	[°]	[Ohm.m]	[°]	[Ohm.m]	[°]
408	609.775	222.196	60	31	87	37	88	49
409	609.784	222.201	53	29	25	56	86	47
410	609.793	222.205	51	56	77	38	75	48
411	609.780	222.221	41	36	63	41	58	48
412	609.763	222.210	41	54	62	38	58	47
413	609.746	222.201	45	28	76	54	74	47
414	609.727	222.193	61	30	77	36	82	49
415	609.706	222.186	70	29	97	38	87	50
416	609.687	222.181	102	32	115	41	107	52
417	609.668	222.174	129	32	127	42	126	52
418	609.649	222.169	190	32	223	46	160	56
419	609.630	222.163	206	35	203	48	146	50
420	609.610	222.157	194	36	223	48	153	50
421	609.591	222.151	144	39	119	50	97	39
422	609.570	222.145	148	38	130	49	95	57
423	609.550	222.159	258	35	257	48	177	56
424	609.532	222.133	122	39	143	47	90	53
425	609.569	222.100	244	37	188	54	116	57
426	609.579	222.143	317	35	250	56	162	55
427	609.590	222.165	334	42	260	53	170	57
428	609.599	222.167	303	40	215	50	153	53
429	609.609	222.170	282	37	251	50	170	57
430	609.618	222.173	210	32	213	48	140	55
431	609.628	222.175	186	35	170	48	120	55
432	609.643	222.179	196	36	176	49	119	56
433	609.652	222.181	240	34	210	47	144	53
434	609.661	222.184	224	54	175	50	123	55
F8	609.673	222.188	185	35	160	47	117	56
436	609.678	222.191	90	54	110	44	80	52
437	609.688	222.195	66	26	92	40	77	49
438	609.697	222.200	56	28	83	38	71	48
F4	609.708	222.206	60	27	91	37	83	47
440	609.718	222.207	42	22	82	33	80	45
441	609.726	222.209	59	28	86	35	87	46

	Coordinates	[Km]	ρα 183	Φ 183	ρα 70	Φ 70	ρα 19	Φ 19
	x	y	[Ohm.m]	[°]	[Ohm.m]	[°]	[Ohm.m]	[°]
442	609.736	222.212	20	31	89	40	87	47
F2	609.748	222.215	58	33	76	40	70	47
446	609.755	222.218	52	30	70	40	60	47
445	609.766	222.238	53	30	78	37	78	48
446	609.760	222.235	60	36	84	36	85	49
447	609.751	222.231	61	35	80	38	81	50
448	609.743	222.226	63	36	88	40	75	50
449	609.734	222.221	56	32	88	37	79	48
450	609.725	222.217	60	33	96	39	77	49
451	609.716	222.212	55	30	84	36	80	48
452	609.708	222.207	53	33	82	39	68	50
453	609.733	222.255	46	31	72	36	68	48
454	609.750	222.231	53	33	86	38	75	49
455	609.740	222.247	56	33	81	37	77	49
456	609.732	222.263	53	32	79	56	76	48
457	609.723	222.239	55	37	75	59	75	49
458	609.714	222.235	51	33	73	37	76	49
459	609.705	222.231	46	34	73	36	70	48
460	609.696	222.226	52	33	75	37	78	49
461	609.688	222.222	67	30	89	39	90	52
462	609.679	222.218	52	33	91	39	68	52
463	609.671	222.214	100	37	130	46	85	54
466	609.662	222.210	139	43	128	53	101	57
465	609.656	222.206	183	41	157	51	119	54
466	609.645	222.201	140	39	158	40	90	56
467	609.637	222.197	180	38	210	49	114	57
468	609.618	222.188	313	36	368	47	209	53
469	609.609	222.184	215	40	253	52	118	58
470	609.609	222.180	261	47	237	55	128	60
471	609.591	222.176	244	42	230	53	127	58
472	609.582	222.172	298	47	254	55	148	60
473	609.574	222.167	166	43	136	55	88	59
474	609.567	222.164	233	42	216	53	112	56
475	609.557	222.159	297	42	238	54	150	60

Table 3A-2

Wilerwald

1) Rho 183 kHz

$$\gamma(h) = 8000\left[\left[\frac{3}{2}\frac{|h|}{0.3} - \frac{1}{2}\left(\frac{|h|}{0.3}\right)^3\right]\right] + 3000 \quad h \le 0.3 \text{ Km}$$

$\gamma(h) = 11000$ $\quad$ $h > 0.3$ Km

2) Rho 70 kHz

$$\gamma(h) = 8100\left[\left[\frac{3}{2}\frac{|h|}{0.25} - \frac{1}{2}\left(\frac{|h|}{0.25}\right)^3\right]\right] + 400; \quad h \le 0.25 \text{ Km}$$

$\gamma(h) = 12100$ $\quad$ $h > 0.25$ Km

3) Rho 19 kHz

$$\gamma(h) = 4000\left[\frac{3}{2}\frac{|h|}{0.3} - \frac{1}{2}\left(\frac{|h|}{0.3}\right)^3\right] + 2000; \; h \le 0.3 \text{ Km}$$

$\gamma(h) = 6000$ $\quad$ $h > 0.3$ Km

4)Log Rho 183 kHz

$$\gamma(h) = 0.075\left[\left[\frac{3}{2}\frac{|h|}{0.26} - \frac{1}{2}\left(\frac{|h|}{0.26}\right)^3\right]\right] + 0.01; \; h \le 0.26 \text{ Km}$$

$\gamma(h) = 0.085$ $\quad$ $h > 0.26$ Km

5) Log Rho 70 kHz

$$\gamma(h) = 0.049\left[\left[\frac{3}{2}\frac{|h|}{0.33} - \frac{1}{2}\left(\frac{|h|}{0.33}\right)^3\right]\right] + 0.015; h \le 0.33 \text{ Km}$$

$\gamma(h) = 0.064$ $\quad$ $h > 0.33$ Km

6) Log Rho 19 kHz

$$\gamma(h) = 0.045\left[\left[\frac{3}{2}\frac{|h|}{0.45} - \frac{1}{2}\left(\frac{|h|}{0.45}\right)^3\right]\right] + 0.015; h \le 0.45 \text{ km}$$

$\gamma(h) = 0.06$ $\quad$ $h > 0.45$ Km

7) Phase 183 kHz

$$\gamma(h) = 26\left[\frac{3}{2}\frac{|h|}{0.15} - \frac{1}{2}\left(\frac{|h|}{0.15}\right)^3\right] + 11 \quad h \le 0.15 \text{ Km}$$

$\gamma(h) = 37$ $\quad$ $h > 0.15$ Km

8) Phase 70 kHz

$$\gamma(h) = 33\left[\frac{3}{2}\frac{|h|}{0.15} - \frac{1}{2}\left(\frac{|h|}{0.15}\right)^3\right] + 1 \quad h \le 0.15 \text{ Km}$$

$\gamma(h) = 34$ $\quad$ $h > 0.15$ Km

9) Phase 19 kHz

$$\gamma(h) = 12.2\left[\frac{3}{2}\frac{|h|}{0.22} - \frac{1}{2}\left(\frac{|h|}{0.22}\right)^3\right] + 2 \quad h \le 0.22 \text{ Km}$$

$\gamma(h) = 14.2$ $\quad$ $h > 0.22$ Km

Table 3A-3

Merdingen

1) Rho 183 kHz

$$\gamma(h) = 1900\left[\left[\frac{3}{2}\frac{|h|}{0.2} - \frac{1}{2}\left(\frac{|h|}{0.2}\right)^3\right]\right] + 900 \quad h \le 0.200 \text{ Km}$$

$\gamma(h) = 2800$ $\quad$ $h > 0.200$ Km

2) Rho 70 kHz

$$\gamma(h) = 1600\left[\left[\frac{3}{2}\frac{|h|}{a} - \frac{1}{2}\left(\frac{|h|}{a}\right)^3\right]\right] + 850 \quad h \le 0.300 \text{ Km}$$

$\gamma(h) = 2450$ $\quad$ $h > 0.300$ Km

3) Rho 19 kHz

$$\gamma(h) = 430\left[\left[\frac{3}{2}\frac{|h|}{0.2} - \frac{1}{2}\left(\frac{|h|}{0.2}\right)^3\right]\right] + 320 \quad h \le 0.200 \text{ Km}$$

$\gamma(h) = 750$ $\quad$ $h > 0.200$ Km

4) Log Rho 183 kHz

$$\gamma(h) = 0.008\left[\left[\frac{3}{2}\frac{|h|}{0.25} - \frac{1}{2}\left(\frac{|h|}{0.25}\right)^3\right]\right] + 0.0038 \quad h \le 0.25 \text{ Km}$$

$\gamma(h) = 0.0118$ $\quad$ $h > 0.25$ Km

5) Log Rho 70 kHz

$$\gamma(h) = 0.009\left[\left[\frac{3}{2}\frac{|h|}{0.3} - \frac{1}{2}\left(\frac{|h|}{0.3}\right)^3\right]\right] + 0.0055 \quad h \le 0.300 \text{ Km}$$

$\gamma(h) = 0.0145$ $\quad$ $h > 0.300$ Km

6) Log Rho 19 kHz

$$\gamma(h) = 0.0064\left[\left[\frac{3}{2}\frac{|h|}{0.21} - \frac{1}{2}\left(\frac{|h|}{0.21}\right)^3\right]\right] + 0.004 \; ; h \le 0.210 \text{ Km}$$

$\gamma(h) = 0.0104$ $\quad$ $h > 0.210$ Km

7) Phase 183 kHz

$$\gamma(h) = 5\left[\left[\frac{3}{2}\frac{|h|}{0.25} - \frac{1}{2}\left(\frac{|h|}{0.25}\right)^3\right]\right] + 1.1 \quad h \le 0.250 \text{ Km}$$

$\gamma(h) = 6.1$ $\quad$ $h > 0.250$ Km

8) Phase 70 kHz

$$\gamma(h) = 6.6\left[\left[\frac{3}{2}\frac{|h|}{0.19} - \frac{1}{2}\left(\frac{|h|}{0.19}\right)^3\right]\right] + 3.4 \quad h \le 0.190 \text{ Km}$$

$\gamma(h) = 10$ $\quad$ $h > 0.190$ Km

9) Phase 19 kHz

$$\gamma(h) = 2.45\left[\left[\frac{3}{2}\frac{|h|}{0.265} - \frac{1}{2}\left(\frac{|h|}{0.265}\right)^3\right]\right] + 0.5 \quad h \le 0.265 \text{ Km}$$

$\gamma(h) = 2.95$ $\quad$ $h > 0.265$ Km

Appendix 3B Local hydraulic aspects

Fig. 3B-1 Piezometric maps drawed by Sansoni et al, 1987.

Fig. 3B-2 Scattered groundwater level measurements at some chosen piezometers.

Table 3B-1 Goundwater level measurements at the Wilerwald testsite.

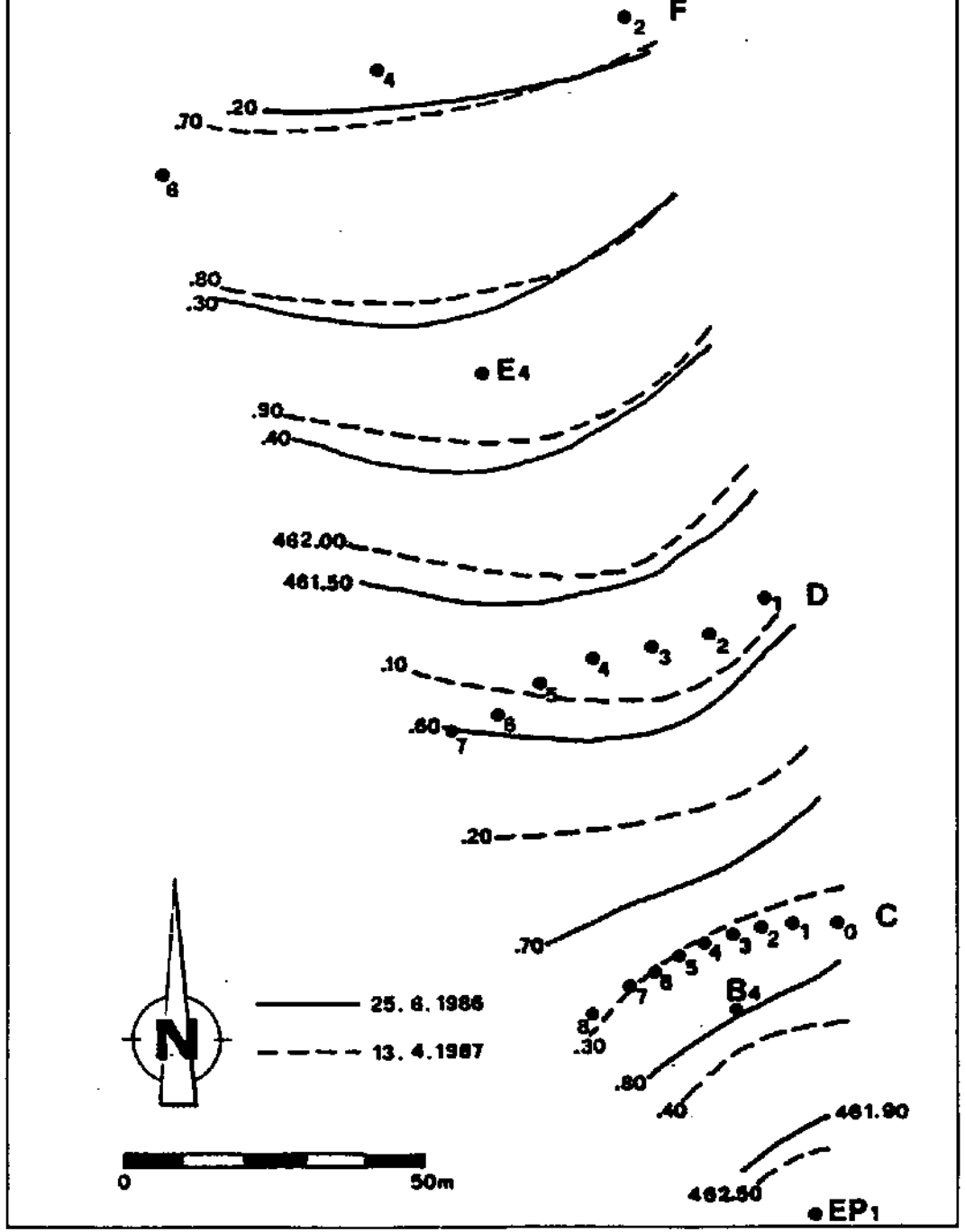

Fig. 3B-1 Piezometric map drawed by Sansoni et al, 1987.

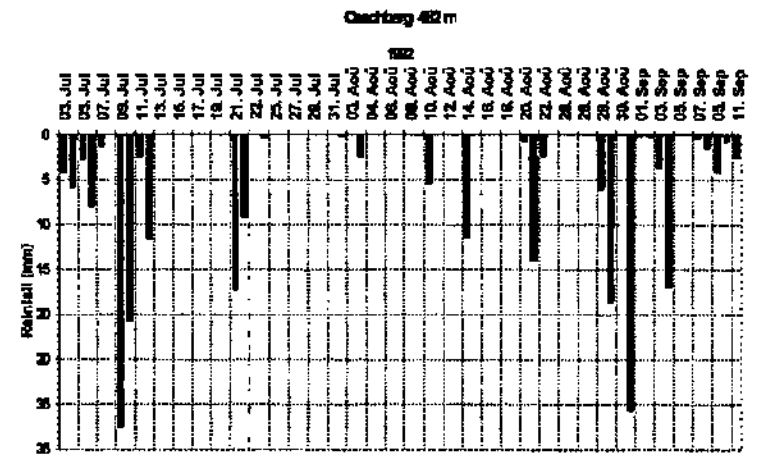

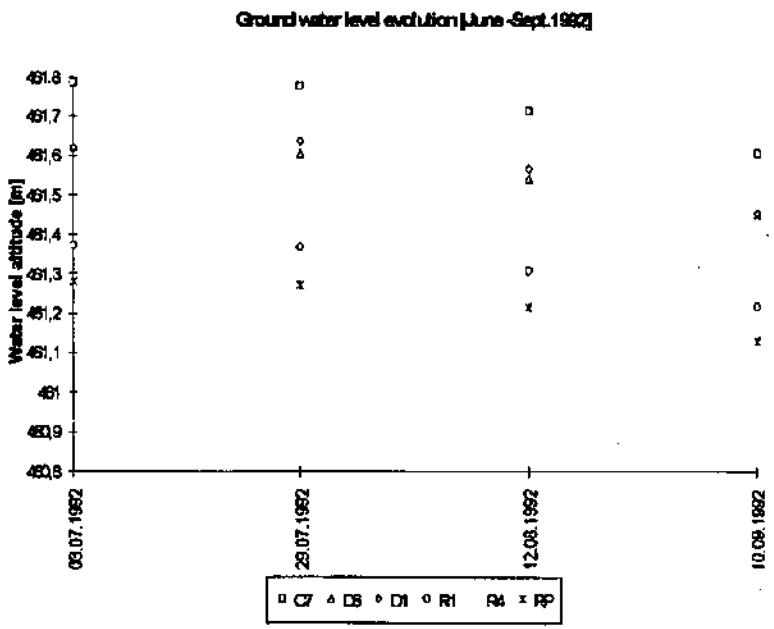

Fig 3B-2 Scattered groundwater level measurements at some chosen piezometers.

Table 3B-1 Goundwater level measurements at the Wilerwald testsite.

	03. Jul	29. Jul	12. Aug	10. Sep	10. Nov	17. Nov	18. Nov	19. Nov	20. Nov	23. Nov	24. Nov	25. Nov	26. Nov
BP1	462.029	462.009	461.899	461.829	461.949		462.309	462.369	462.419	462.529	462.549	462.549	462.549
B4	461.817	461.802	461.722	461.632	461.752		462.102	462.157	462.192	462.272	462.282	462.312	462.312
C8	461.784	461.774	461.714	461.604	461.754	462.049	462.074	462.124	462.174	462.294	462.294	462.294	462.284
C7	461.787	461.777	461.712	461.607	461.757	462.047	462.077	462.117	462.177	462.287	462.297	462.297	462.287
C6	461.793	461.768	461.708	461.603	461.733	462.043	462.073	462.123	462.173	462.293	462.303	462.293	462.283
C5	461.79	461.77	461.71	461.61	461.750	462.05	462.07	462.13	462.17	462.29	462.3	462.29	462.28
C4	461.798	461.778	461.718	461.613	461.733	462.063	462.083	462.133	462.193	462.293	462.303	462.303	462.293
C3	461.806	461.781	461.716	461.611	461.761	462.051	462.091	462.131	462.181	462.291	462.311	462.311	462.301
C2	461.801	461.786	461.721	461.616	461.756	462.066	462.096	462.136	462.186	462.206	462.306	462.306	462.306
C1	461.806	461.791	461.716	461.626	461.756			462.146	462.196	462.286	462.306	462.306	462.306
C0	461.881	461.871	461.781	461.676	461.806			462.196	462.246	462.316	462.386	462.396	462.386
R6	461.682	461.682	461.622	461.532	461.662	461.947	461.992	462.042	462.092	462.202	462.212	462.202	462.202
R5	461.695	461.625	461.615	461.532	461.655	461.955	461.985	462.045	462.085	462.195	462.205	462.205	462.195
C0	461.704	461.694	461.624	461.529	461.659	461.959	461.989	462.039	462.069	462.169	462.199	462.189	462.189
D7	461.642	461.632	461.567	461.472	461.552	461.912	461.942	461.992	462.032	462.142	462.152	462.142	462.132
D6	461.621	461.606	461.541	461.451	461.591	461.881	461.901	461.951	462.001	462.121	462.111	462.111	462.101
D5	461.623	461.613	461.553	461.463	461.603	461.863	461.913	461.973	462.003	462.113	462.113	462.113	462.103
D4	461.599	461.609	461.549	461.459	461.589	461.879	461.899	461.969	461.909	462.109	462.119	462.109	462.099
D3	461.599	461.599	461.544	461.454	461.584	461.854	461.894	461.954	461.984	462.084	462.094	462.084	462.084
D2	461.604	461.614	461.544	461.45	461.570	461.87	461.904	461.974	461.994	462.104	462.114	462.104	462.104
D1	461.621	461.636	461.566	461.455	461.655	461.896	461.926	461.996	462.116	462.126	462.136	462.126	462.126
R4	461.399	461.409	461.359	461.279	461.409	461.659	461.719	461.779	461.819	461.919	461.939	461.929	461.919
E4	461.404	461.399	461.334	461.254	461.364	461.674	461.694	461.754	461.784	461.894	461.894	461.884	461.874
R1	461.373	461.368	461.308	461.218	461.338	461.638	461.658	461.748	461.738	461.858	461.848	461.838	461.848
R3	461.275	461.27	461.215	461.125	461.235	461.57	461.585	461.635	461.665	461.775	461.775	461.765	461.755
R2	461.264	461.254	461.199	461.119	461.249	461.559	461.569	461.629	461.659	461.759	461.759	461.749	461.739
F6	461.262	461.257	461.197	461.117	461.217	461.557	461.557	461.627	461.647	461.747	461.747	461.727	461.727
F4	461.234	461.229	461.169	461.089	461.239	461.539	461.499	461.599	461.619	461.719	461.709	461.699	461.699
F2													
RP	461.281	461.271	461.216	461.131		461.696	461.611	461.661	461.771	461.891	461.881	461.821	461.781

Groundwater level variations at the testsite Wilerwald

Table 3B-1 Goundwater level measurements at the Wilerwald testsite.

	27. Nov	28 Nov.	30. Nov	01. Déc	02. Déc	03. Déc	04. Déc	06. Déc	07. Déc	08. Déc	10. Déc	11. Déc	14. Déc	16. Déc
EP1	462.619	462.629	462.619	462.599	462.589	462.579	462.589	462.739	462.759	462.839	462.889	462.879	462.849	462.809
B4	462.392	462.392	462.382	462.362	462.352	462.342	462.352	462.492	462.502	462.592	462.632	462.612	462.582	462.542
C8	462.354	462.374	462.354	462.334	462.324	462.314	462.324	462.464	462.474	462.574	462.594	462.584	462.564	462.514
C7	462.357	462.367	462.357	462.337	462.327	462.317	462.327	462.467	462.477	462.567	462.597	462.582	462.557	462.517
C6	462.363	462.373	462.353	462.333	462.323	462.313	462.323	462.468	462.473	462.563	462.603	462.583	462.563	462.513
C5	462.36	462.37	462.35	462.34	462.33	462.32	462.33	462.465	462.48	462.56	462.6	462.58	462.56	462.51
C4	462.383	462.383	462.353	462.353	462.333	462.323	462.333	462.473	462.483	462.573	462.613	462.593	462.573	462.533
C3	462.381	462.391	462.371	462.351	462.341	462.331	462.341	462.481	462.491	462.571	462.611	462.601	462.571	462.531
C2	462.376	462.386	462.366	462.346	462.336	462.336	462.346	462.476	462.496	462.576	462.616	462.596	462.576	462.536
C1	462.386	462.386	462.376	462.356	462.346	462.336	462.346	462.486	462.496	462.586	462.616	462.606	462.576	462.536
C0	462.466	462.476	462.456	462.436	462.426	462.426	462.426	462.566	462.586	462.686	462.716	462.696	462.676	462.626
R6	462.272	462.282	462.262	462.252	462.232	462.222	462.232	462.372	462.382	462.472	462.502	462.482	462.462	462.412
R5	462.275	462.285	462.255	462.245	462.225	462.215	462.235	462.365	462.375	462.465	462.505	462.485	462.455	462.415
CD	462.269	462.269	462.249	462.229	462.219	462.209	462.219	462.359	462.369	462.459	462.499	462.469	462.439	462.409
D7	462.212	462.222	462.202	462.182	462.172	462.162	462.172	462.312	462.322	462.412	462.442	462.422	462.392	462.352
D6	462.181	462.181	462.161	462.151	462.141	462.131	462.141	462.271	462.281	462.381	462.401	462.381	462.361	462.321
D5	462.183	462.183	462.163	462.143	462.133	462.123	462.143	462.273	462.283	462.373	462.403	462.383	462.353	462.313
D4	462.179	462.189	462.159	462.149	462.129	462.129	462.139	462.269	462.279	462.379	462.399	462.379	462.359	462.309
D3	462.164	462.174	462.144	462.134	462.124	462.114	462.124	462.254	462.264	462.364	462.384	462.364	462.344	462.294
D2	462.174	462.184	462.164	462.144	462.134	462.134	462.144	462.284	462.284	462.334	462.394	462.384	462.364	462.31
D1	462.206	462.196	462.176	462.166	462.156	462.146	462.146	462.286	462.286	462.386	462.426	462.386	462.366	462.295
R4	462.009	462.009	461.979	461.959	461.949	461.939	461.939	462.069	462.079	462.179	462.199	462.179	462.149	462.099
E4	461.964	461.954	461.934	461.914	461.904	461.894	461.914	462.044	462.044	462.144	462.154	462.134	462.104	462.064
R1	461.938	461.918	461.898	461.878	461.868	461.858	461.878	462.008	462.008	462.128	462.118	462.098	462.068	462.028
R3	461.835	461.845	461.815	461.805	461.785	461.765	461.795	461.935	461.925	462.025	462.045	462.015	461.985	461.945
R2	461.819	461.819	461.789	461.769	461.759	461.749	461.769	461.899	461.899	461.999	462.009	461.989	461.959	461.919
F6	461.817	461.807	461.787	461.757	461.747	461.737	461.757	461.887	461.887	461.987	461.997	461.977	461.947	461.902
F4	461.779	461.769	461.749	461.729	461.719	461.709	461.729	461.839	461.869	461.959	461.949	461.919	461.899	461.849
F2	461.793	461.753	461.733	461.713	461.713	461.703	461.713	461.863	461.843	461.953	461.953	461.933	461.913	461.863
RP	461.991	461.951	461.921	461.861	461.831	461.801	461.811	462.151	462.101	462.221	462.251	462.141	462.021	461.956

Table 3C Chemical, Isotopes and Tracer Results

Table 3C2-1 Conductivity measurements at the test site Wilerwald.

Table 3C2-2 Groundwater temperature measurements at the test site Wilerwald.

Table 3C2-3 Total hardness **(a)** Carbonate hardness **(b)** Calcium hardness **(c)** and Magnesium hardness values **(d)** (test site Wilerwald).

Table 3C2-4 Conductivity and temperature profiles measured in the observation wells: C2, C3, C4, C5.

Table 3C2-5 Conductivity and temperature profiles measured in the observation well : C6.

Table 3C2-6 Conductivity and temperature profiles measured in the observation wells: C7.

Table 3C2-7 Conductivity and temperature profiles measured in the observation wells: C8.

Table 3C2-8 Conductivity and temperature profiles measured in the observatioo wells: D1, D2, D3, D4.

Table 3C2-9 Conductivity and temperature profiles measured in the observatioo wells: D5, E4, F4, F6.

Table 3C2-10 Conductivity and temperature profiles measured io the observation wells: D6.

Table 3C2-11 Conductivity and temperature profiles measured in the observation wells: D7.

Table 3C3 Isotopes analyses (O-18 and tritium) performed at the site, Emme and Burgdorf's precipitation.

Table 3C4-1 Na-Naphtionate results - 1992 tracer experiment.

Table 3C4-2 Amidorhodamine G results - 1992 tracer experiment.

Table 3C4-3 Uranine results - 1992 tracer experiment.

Table 3C4-4 Na-Naphtionate breakthrough curves at the observation wells C8, C7, C6 & C5.

Table 3C4-5 Na-Naphtionate breakthrough curves at the observation wells C4, C3, C3 & CD.

Table 3C4-6 Na-Naphtionate breakthrough curves at the observation wells D7, D6, D5 & D4.

Table 3C4-8 Na-Naphtionate breakthrough curves at the observatioo wells D3, D2, & D1.

Table 3C4-9 Amidorhodamine G breakthrough curves at the observation wells C8, C7, C6 & C5.

Table 3C4-10 Amidorhodamine G breakthrough curves at the observation wells C4, C3, C3 & CD.

Table 3C4-11 Amidorhodamine G breakthrough curves at the observation wells D7, D6, D5 & D4.

Table 3C4-12 Amidorhodamine G breakthrough curves at the observation wells D3, D2, & D1.

Table 3C4-13 Uranine breakthrough curves at the observatioo wells C8, C7, C6 & C5.

Table 3C4-14 Uranine breakthrough curves at the observatioo wells C4, C3, C3 & CD.

Table 3C4-15 Uranine breakthrough curves at the observation wells D7, D6, D5 & D4.

Table 3C4-16 Uranine breakthrough curves at the observation wells D3, D2, & D1.

CHEMICAL TABLES

Table 3C2-1 Conductivity Results

μScm^{-1}	20.07.92	06.08.92	19.08.92	17.09.92	26.09.92	09.11.92	12.11.92	13.11.92	14.11.92
F6	503	563	596	-	-	588	-	-	-
F4	472	567	591	-	-	545	-	-	-
E4	481	525	548	-	-	531	-	-	-
D7	498	552	582	-	537	581	579	579	580
D6	488	553	580	-	538	582	579	579	579
D5	495	563	593	-	550	596	577	577	576
D4	491	555	583	-	539	579	570	574	572
D3	496	535	558	-	514	547	539	543	544
D2	484	536	559	-	513	549	548	548	548
D1	488	547	573	-	526	559	561	577	561
CD	-	-	585	-	543	-	589	588	589
C8	496	553	583	584	535	584	574	574	574
C7	493	551	581	584	534	577	577	578	578
C6	489	550	580	577	529	580	575	576	577
C5	489	548	585	573	525	569	567	566	568
C4	493	555	585	588	536	587	581	581	580
C3	503	556	588	589	542	591	589	590	592
C2	489	569	581	563	517	578	579	580	583
EP1	-	-	-	562	521	-	-	-	-
Emma	-	363	306	-	-	-	-	-	-
Zielebach	-	534	560	-	-	-	-	-	-

μScm^{-1}	16.11.92	17.11.92	18.11.92	19.11.92	20.11.92	23.11.92	25.11.92
D7	579	581	583	581	584	584	-
D6	581	583	583	583	583	586	-
D5	555	574	584	579	582	587	-
D4	569	570	573	574	575	577	-
D3	550	544	547	549	551	551	-
D2	545	548	548	546	549	547	-
D1	579	565	556	575	565	562	-
CD	590	596	598	598	599	600	-
C8	576	582	583	577	583	584	587
C7	576	579	579	581	582	585	587
C6	573	579	580	579	582	584	586
C5	562	567	570	565	572	570	573
C4	579	587	589	588	590	590	589
C3	594	595	595	595	596	599	599
C2	578	594	600	601	604	605	-

Table 3C2-2 Temperature measurements

[°C]	20.07.92	06.08.92	19.08.92	17.09.92	26.09.92	09.11.92	12.11.92	13.11.92	14.11.92
F6	10	10.7	10.3	-	-	-	-	-	-
F4	9.6	9.8	11.1	-	-	9.7	-	-	-
E4	11.3	10	10.3	-	-	-	-	-	-
D7	11	10.3	10.8	-	10.3	10.1	9	9	8.8
D6	10.2	10.4	10.9	-	10.5	9.9	8.9	9	8.7
D5	10.9	10.5	11.1	-	10.9	10.3	9	9	8.5
D4	10.9	10.2	10.6	-	10.6	10.2	8.7	9.1	8.5
D3	11.2	10	10.4	-	10	9.6	8.5	8.7	8
D2	10.5	10.2	10.2	-	10.2	9.5	8.3	8.4	7.8
D1	10.3	9.7	9.9	-	9.7	9.7	8.9	8.7	7.9
CD	-	-	11.2	-	10.6	10.3	9.1	9.2	8.5
C8	11	10.4	10.7	10.9	10.7	10.5	8.5	9.3	8.5
C7	10.8	10.1	10.7	10.7	10.5	9.9	9.1	9.1	8.6
C6	10.6	10.1	10.8	10.6	10	10.1	9	9.3	8.8
C5	10.6	10.1	10.8	10.7	9.9	10	8.5	8.8	8.4
C4	10.5	10.2	10.8	10.9	10.2	10.1	9	9.1	8
C3	10.6	10.2	10.8	11	10.4	10.3	9	9	7.8
C2	10.3	10.4	11	10.7	10.3	10	8.9	9	8.8
EP1	-	-	-	10.9	10	-	-	-	-
Emme	-	21.2	24.2	-	-	-	-	-	
Zielebach	-	9.7	13.3	-	-	-	-	-	-

[°C]	16.11.92	17.11.92	18.11.92	19.11.92	20.11.92	23.11.92	25.11.92
F6	-	-	-	-	-	-	-
F4	-	-	-	-	-	-	-
E4	-	-	-	-	-	-	-
D7	9.5	8.5	8.9	9.6	9.1	9.8	-
D6	9.5	8.6	8.7	9.4	9.4	9.8	-
D5	9.2	8.9	8.6	9.4	9.2	9.6	-
D4	9.2	9	8.8	9.6	9.1	9.7	-
D3	9.2	8.6	8.4	9.3	8.8	9.5	-
D2	8.9	8.5	8.2	9.1	8.8	9.3	-
D1	9.2	8.7	8.4	9.2	8.9	9.6	-
CD	9.3	8.9	8.7	9.5	9	9.9	-
C8	9.5	8.7	8.8	9.2	9.4	9.9	9.3
C7	9.3	9	9	9.3	9.3	9.9	9.4
C6	9.6	8.8	9	9.6	9.3	10.1	9.6
C5	9.1	8.5	8.5	9.2	8.9	9.7	9
C4	9.3	8.5	9	9.3	9.3	9.8	9.3
C3	9.7	8.8	9.2	9.5	9.1	9.9	9.4
C2	9.4	9	9.2	9.4	9.1	9.7	-

Table 3C2-3a Total hardness

Total hardness	11.6.1992 [mg $CaCO_3$/l]	20.07.1992 [mg $CaCO_3$/l]	06.08.1992 [mg $CaCO_3$/l]	19.08.1992 [mg $CaCO_3$/l]	17.09.1992 [mg $CaCO_3$/l]	26.09.1992 [mg $CaCO_3$/l]
Emme	98,49	206,8	181,14	132,29	-	190,95
Zielebach	115,62	283,5	290,9	284,66	-	281,67
F4	113,79	-	-	305,77	-	-
F6	107,1	270,4	-	307,86	-	-
E4	153,31	237,4	-	276,36	-	273,22
D7	144,23	280,2	294,72	297,1	-	294,8
D6	290,9	282,2	-	294,22	-	295,6
D5	135,16	288	299,03	304,45	-	300
D4	255,3	283,9	-	294,23	-	294,6
D3	139,11	260,2	-	283,87	-	279,6
D2	105,8	282,4	-	282,75	-	279,5
D1	135,32	285,3	303,05	289,67	-	285,6
C8	248,32	265,1	293,68	298,61	354,39	295,86
C7	132,01	287,5	295,45	295,03	297,15	293,25
C6	193,68	225,1	294,18	294,41	293,08	291,06
C5	211,13	229,6	-	296,47	290,63	288,4
C4	269,1	282,5	-	304,28	300,51	294,1
C3	103,18	243,6	297,15	299,69	299,7	289,1
C2	119,4	249,4	-	297,03	285,46	280,44
CD	-	-	-	297,06	-	298,4
EP1	-	-	-	-	301,42	283,21

Table 3C2-3b Carbonate hardness

Carbonate Hardness	11.6.1992 [mg $CaCO_3$/l]	20.07.1992 [mg $CaCO_3$/l]	06.08.1992 [mg $CaCO_3$/l]	19.08.1992 [mg $CaCO_3$/l]	17.09.1992 [mg $CaCO_3$/l]	26.09.1992 [mg $CaCO_3$/l]
Emme	124,3	239,5	211,6	160,8	-	187,8
Zielebach	130,1	292,6	301,4	295	-	258,9
F4	136,5	-	-	312,9	-	-
F6	128,7	278,6	-	315,4	-	-
E4	174,2	243,1	-	287,3	-	253,5
D7	164,4	286,6	298,4	304,1	-	272,2
D6	305,8	288,3	-	301,7	-	272,4
D5	147,9	292,8	312,9	315,9	-	278,2
D4	265,9	289,2	-	303,8	-	268,6
D3	154,9	265	-	293,7	-	261,9
D2	123,9	288,4	-	292,7	-	259,6
D1	158	290,9	313,5	299	-	261,7
C8	230,5	269	305,6	303,2	287,4	276,7
C7	143,4	295,9	297,3	304	278,3	272,8
C6	205	233,3	304,6	303,7	273,4	268,7
C5	136	237,3	-	308,7	273	267,6
C4	278,5	289,5	-	311,7	282,6	272,6
C3	108,8	250,7	309,1	309,6	280,8	265,4
C2	138,6	255,2		306,7	266,3	259,8
CD	-	-	-	309,4		275,3
EP1	-	-	-	-	276,6	262,7

Table 3C2-3c Calcium hardness

Calcium hardness	11.6.1992 Ca^{++} [mg/l]	20.07.1992 Ca^{++} [mg/l]	06.08.1992 Ca^{++} [mg/l]	19.08.1992 Ca^{++} [mg/l]	17.09.1992 Ca^{++} [mg/l]	26.09.1992 Ca^{++} [mg/l]
Emme	30,1	-	60,83	40,09	-	63,92
Zielebach	32,06	-	103,06	99,19	-	99,27
F4	31,45	-	-	109,98	-	-
F6	30,59	-	-	110,16	-	-
E4	49,67	-	-	96,64	-	95,77
D7	45,64	-	109,99	105,26	-	-
D6	-	-		104,2	-	-
D5	40,13	-	105,98	107,96	-	-
D4	-	-	-	104,37	-	-
D3	44,58	-	-	99,09	-	-
D2	29,67	-	-	99,45	-	-
D1	43,38	-	108,5	102,65	-	-
C8	74,53	-	104,14	106,09	128,33	105,18
C7	39,65	-	103,65	104,39	105,4	104,14
C6	61,94	-	104,66	104,28	103,83	103,15
C5	32,79	-	-	105,17	102,93	-
C4	-	-	-	108,03	106,26	-
C3	27,13	-	105,32	106,37	-	-
C2	37,35	-	-	104,9	100,7	98,44
CD	-	-	-	105,33	-	-
EP1	-	-	-	-	106,32	99,89

Table 3C2-3d Magnesium hardness

Magnesium hardness	11.6.1992 Mg^{++} [mg/l]	20.07.1992 Mg^{++} [mg/l]	06.08.1992 Mg^{++} [mg/l]	19.08.1992 Mg^{++} [mg/l]	17.09.1992 Mg^{++} [mg/l]	26.09.1992 Mg^{++} [mg/l]
Emme	5,65	-	7,07	7,79	-	7,57
Zielebach	8,62	-	7,94	8,92	-	8,14
F4	8,55	-	-	7,49	-	-
F6	7,44	-	-	7,89	-	-
E4	7,08	-	-	8,45	-	8,22
D7	7,33	-	4,8	8,25	-	-
D6	-	-	-	8,2	-	-
D5	8,47	-	8,28	8,4	-	-
D4	-	-	-	8,1	-	-
D3	6,72	-	-	8,79	-	-
D2	7,69	-	-	8,3	-	-
D1	6,53	-	7,73	8,04	-	-
C8	15,07	-	8,1	8,12	8,16	8
C7	7,99	-	8,83	8,28	8,18	8
C6	9,44	-	7,91	8,19	8,15	8,07
C5	31,4	-	-	8,16	8,1	-
C4	-	-	-	8,32	8,47	-
C3	8,6	-	8,23	8,21	-	-
C2	6,32	-	-	8,46	8,19	8,35
CD	-	-	-	8,2	-	-
EP1	-	-	-	-	8,66	8,14

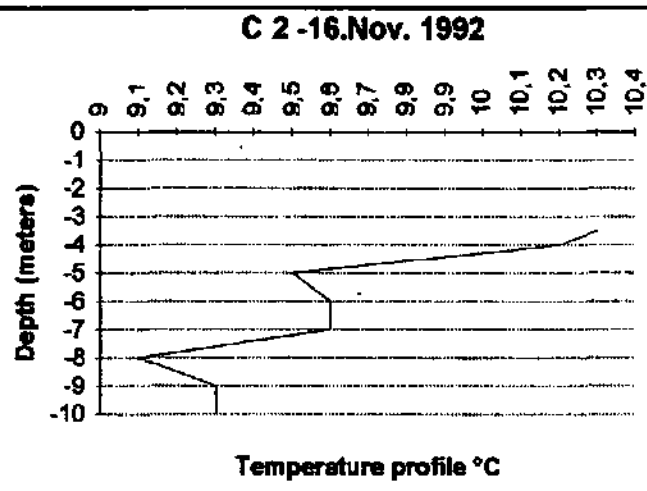

a.1

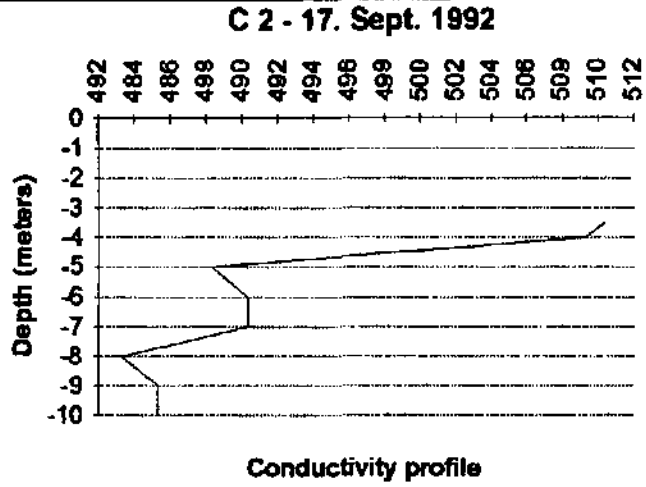

a.2

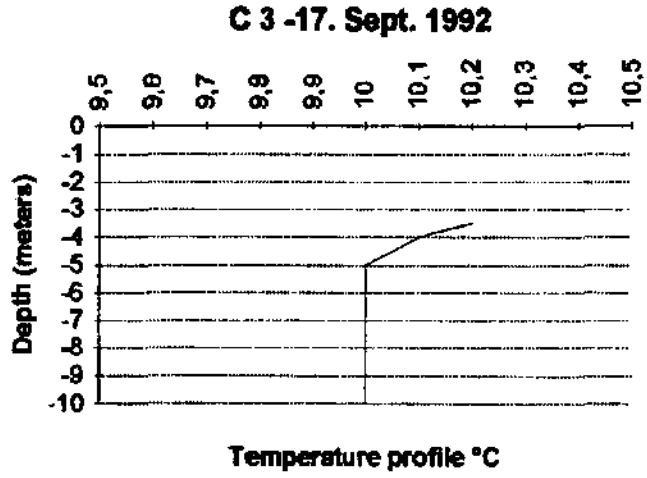

b.1

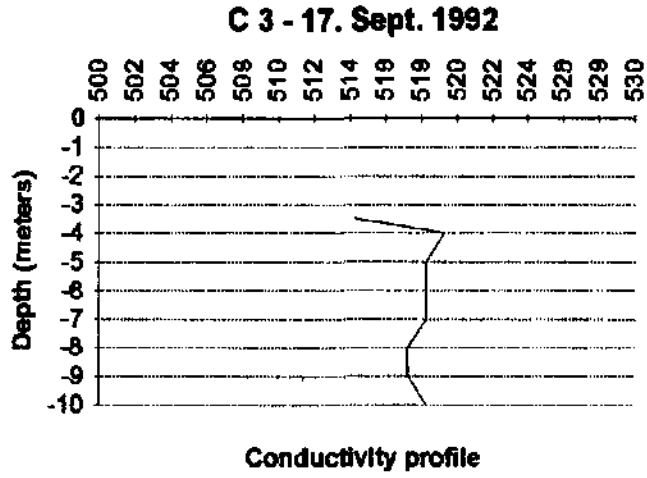

b.2

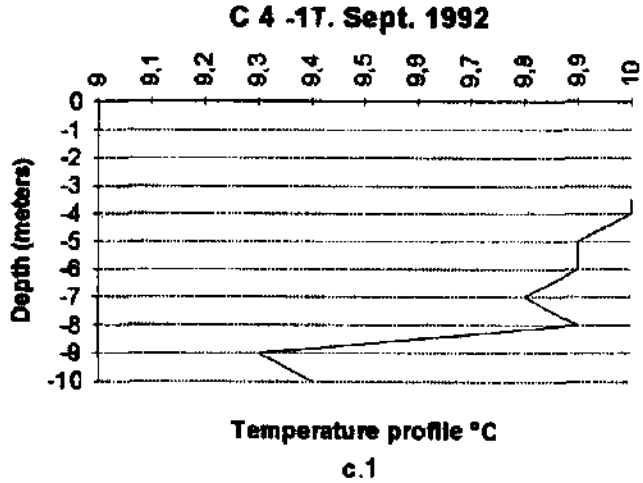

c.1

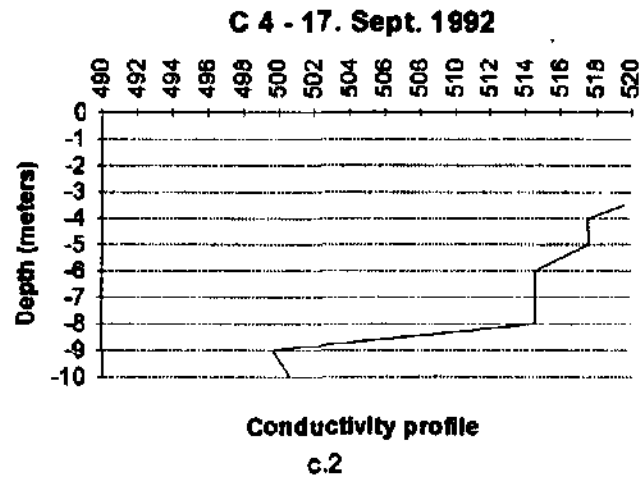

c.2

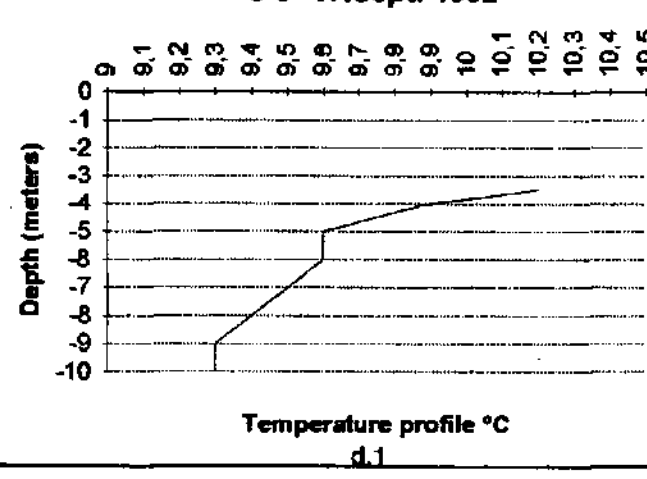

d.1

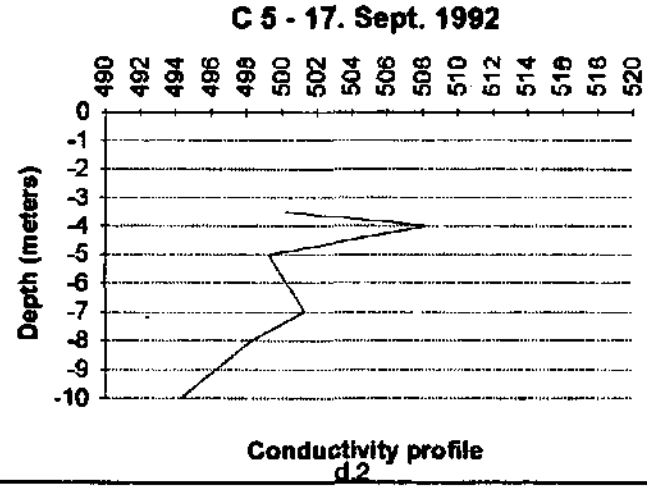

d.2

Table 3C2-4 Conductivity and temperature profiles measured in the observation wells: C2, C3, C4, C5.

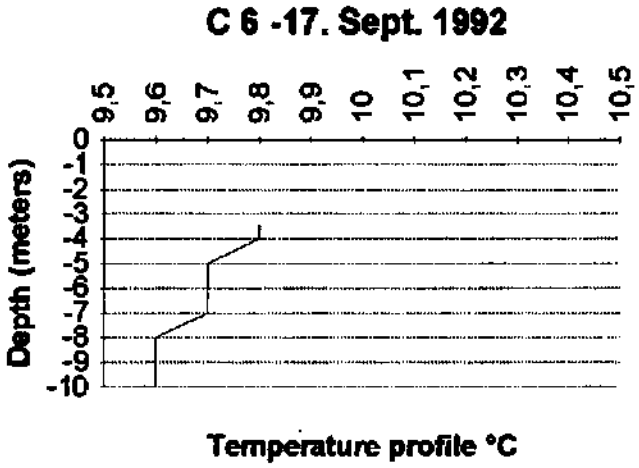

a.1

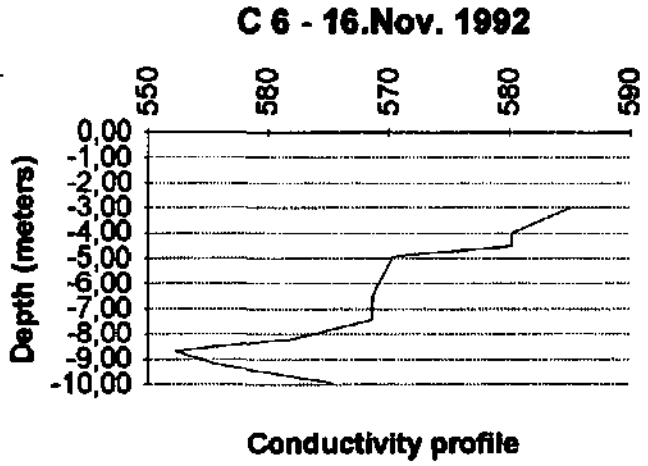

a.2

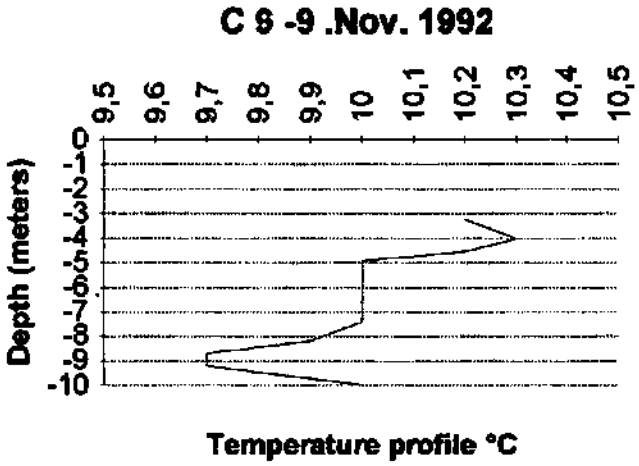

b.1

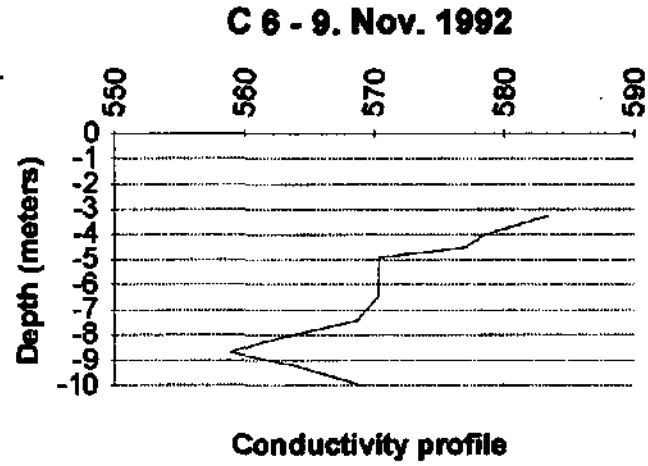

b.2

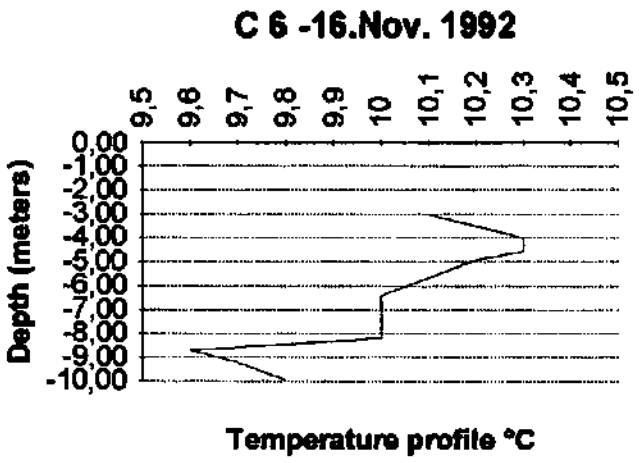

c.1

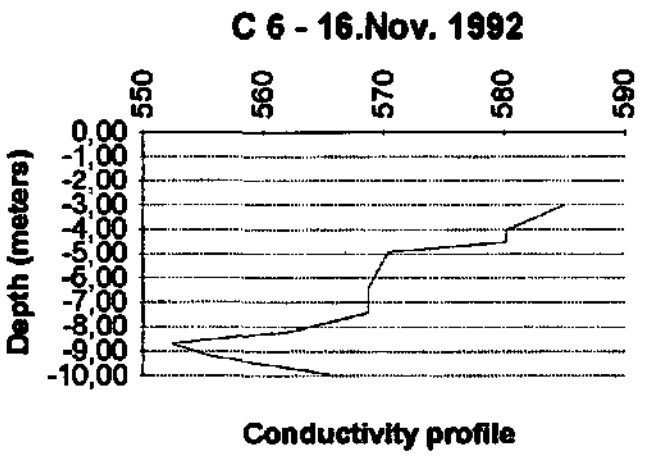

c.2

Table 3C2-5 Conductivity and temperature profiles measured in the observation well : C6.

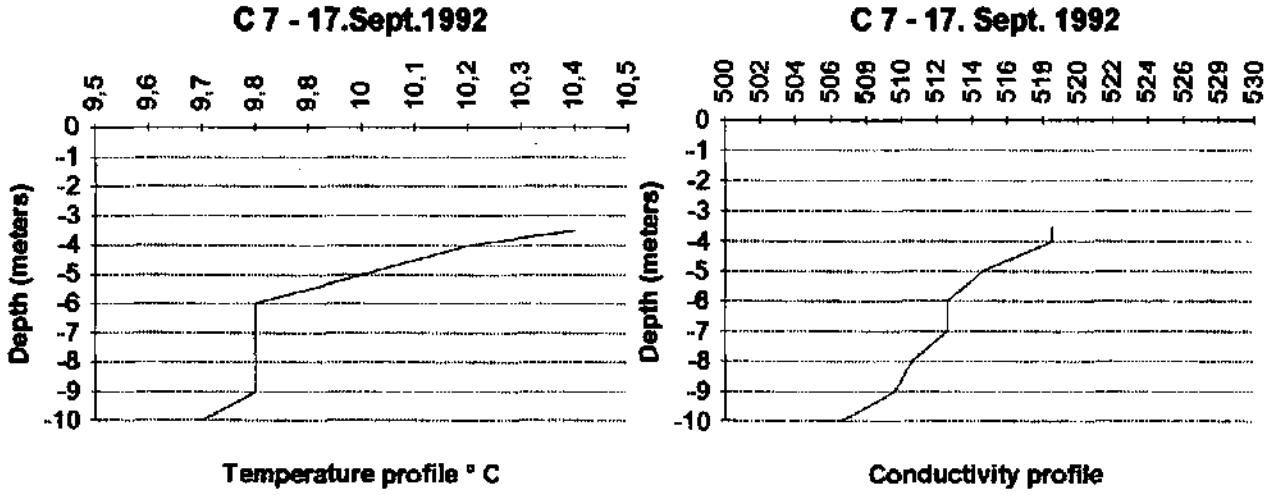

a.1

a.2

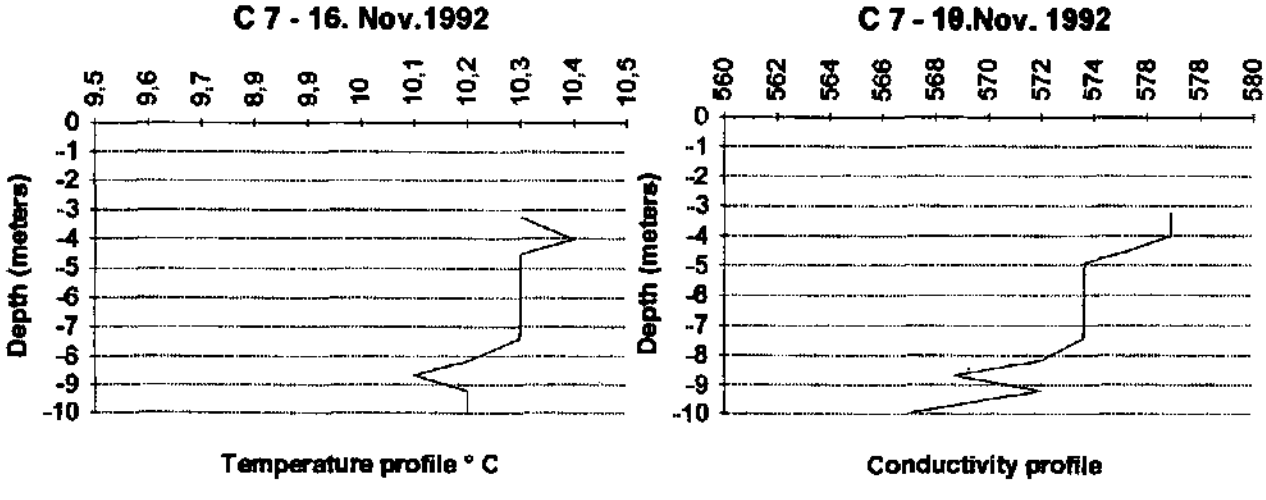

b.1

b.2

Table 3C2-6 Conductivity and temperature profiles measured in the observation wells: C7.

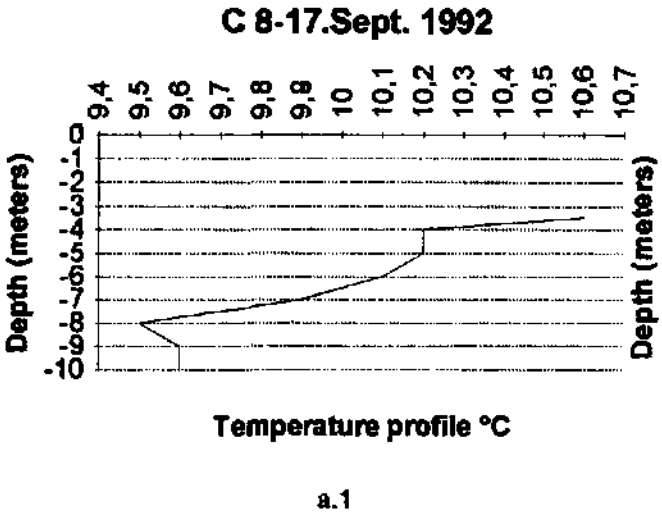

a.1

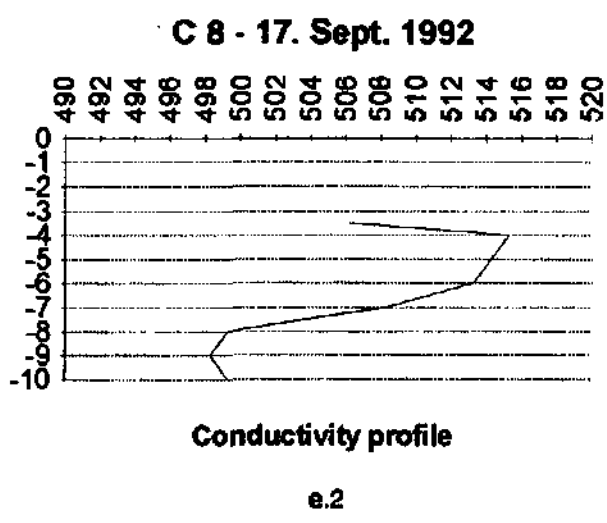

e.2

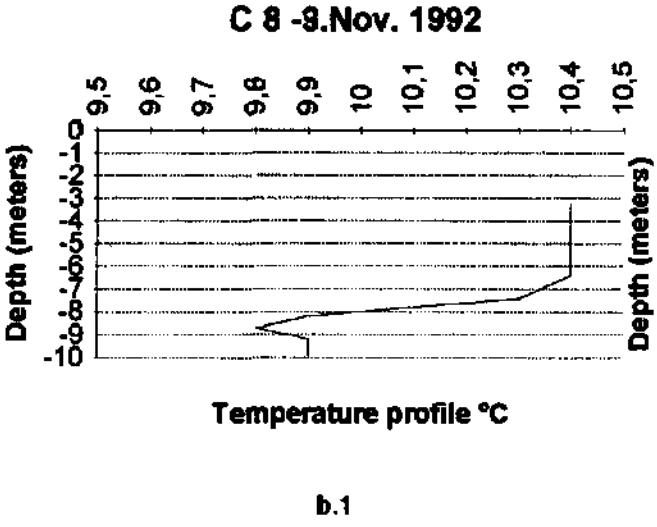

b.1

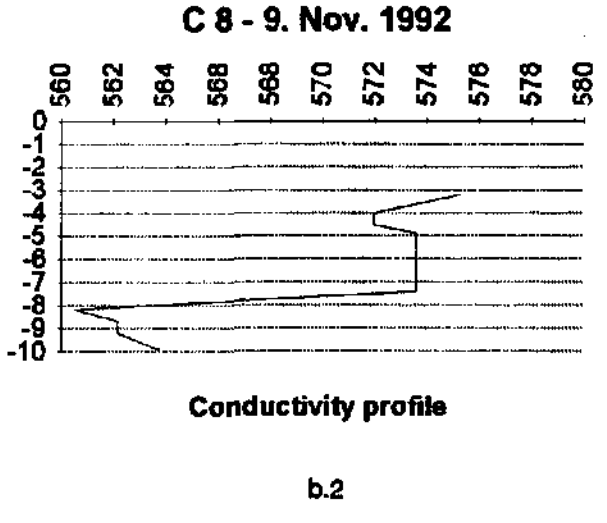

b.2

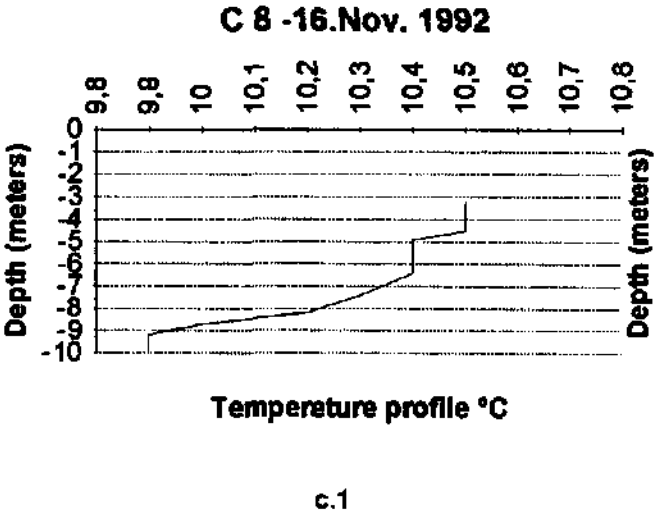

c.1

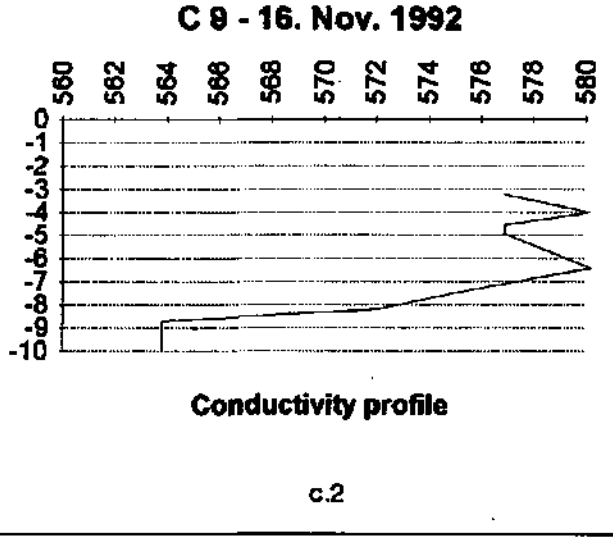

c.2

Table 3C2-7 Conductivity and temperature profiles measured in the observation wells: C8.

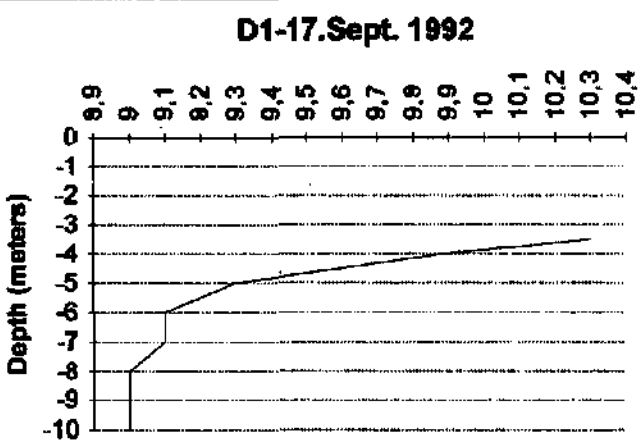

a.1

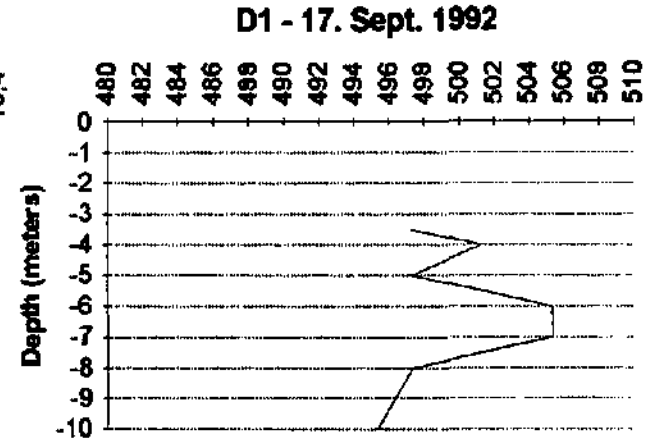

a.2

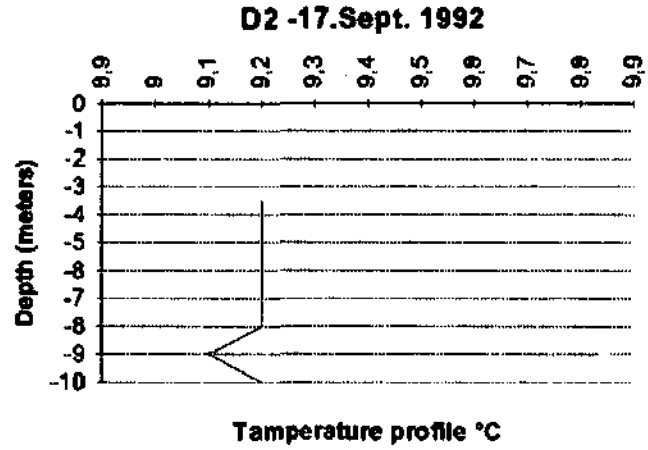

b.1

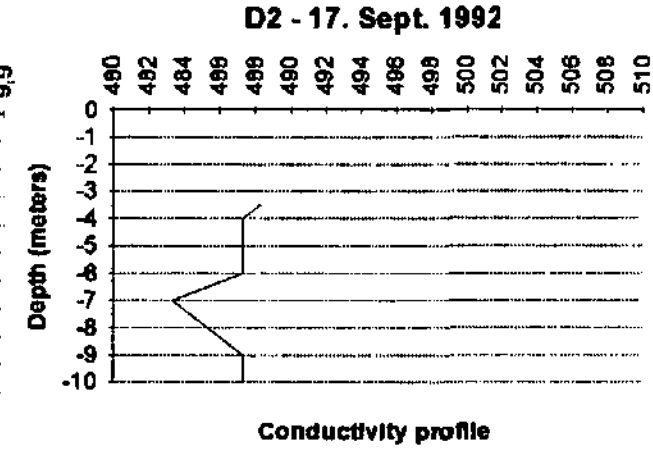

b.2

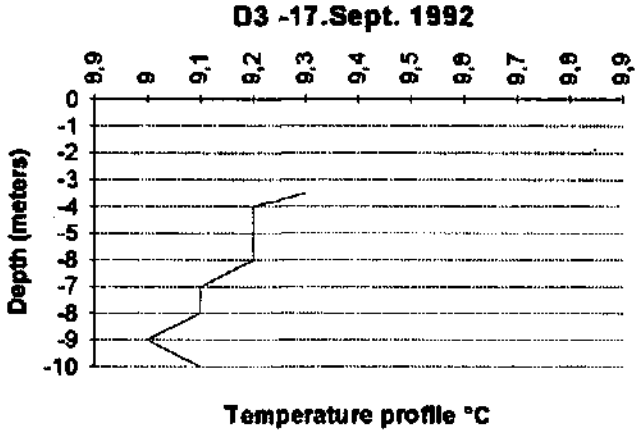

c.1

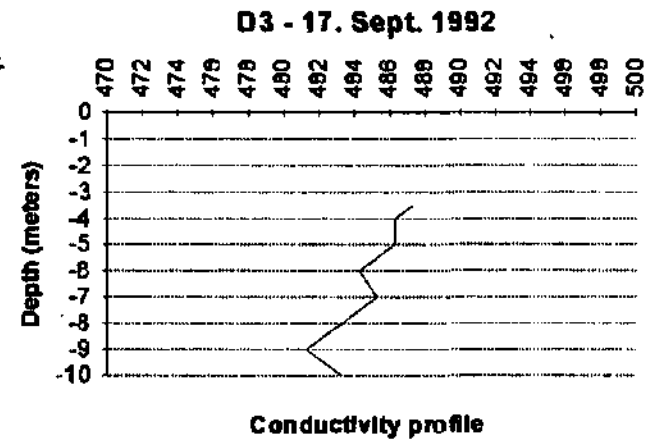

c.2

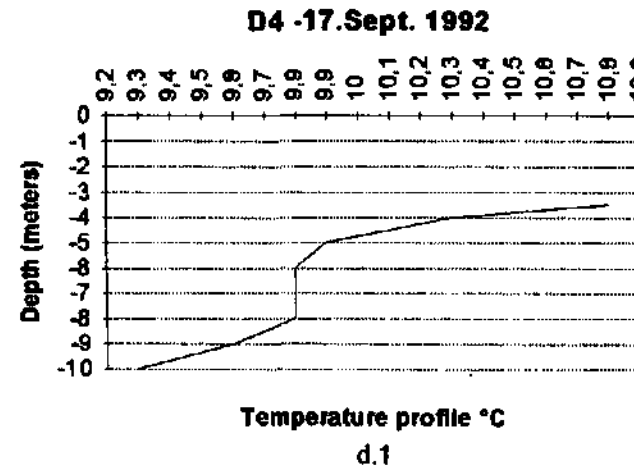

d.1

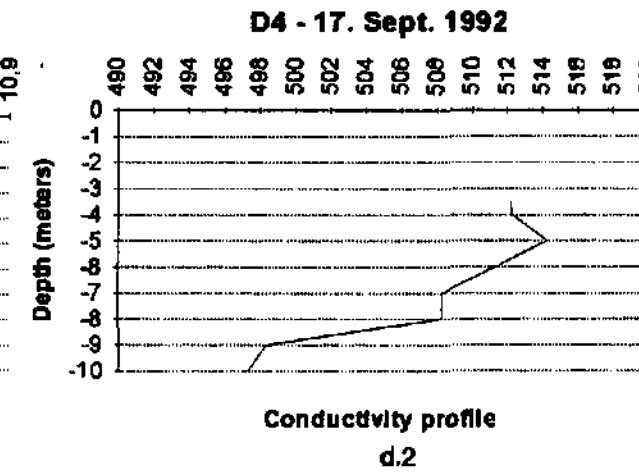

d.2

Table 3C2-8 Conductivity and temperature profiles measured in the observation wells: D1, D2, D3, D4.

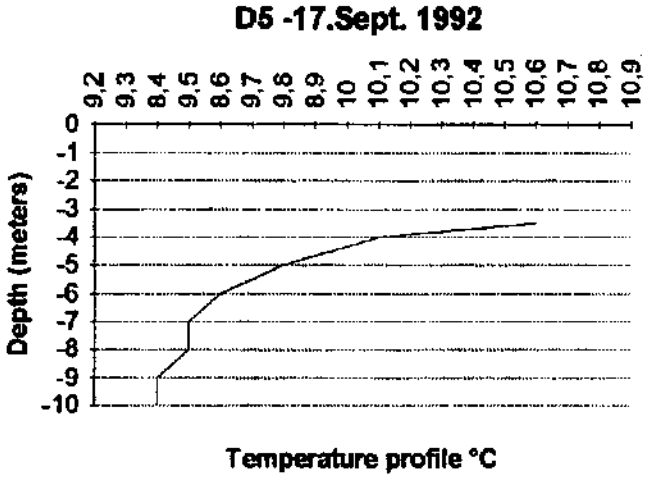

a.1

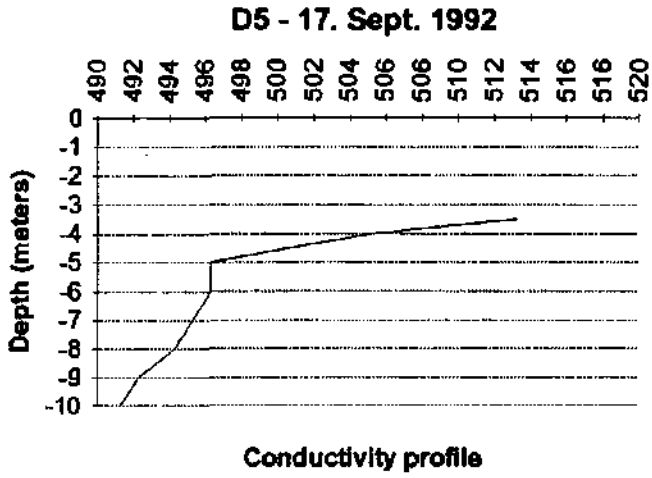

e.2

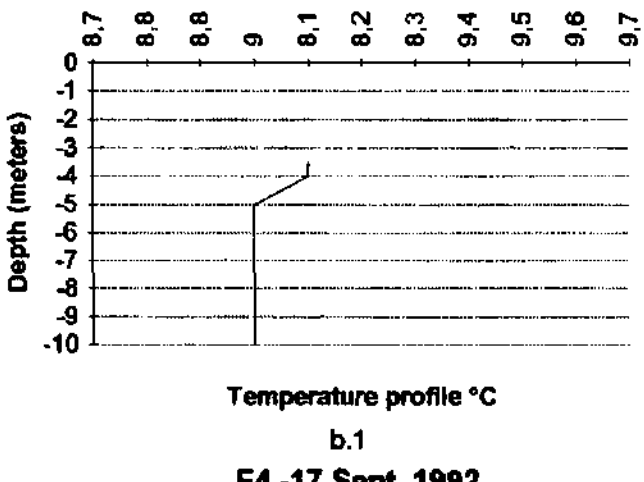

b.1

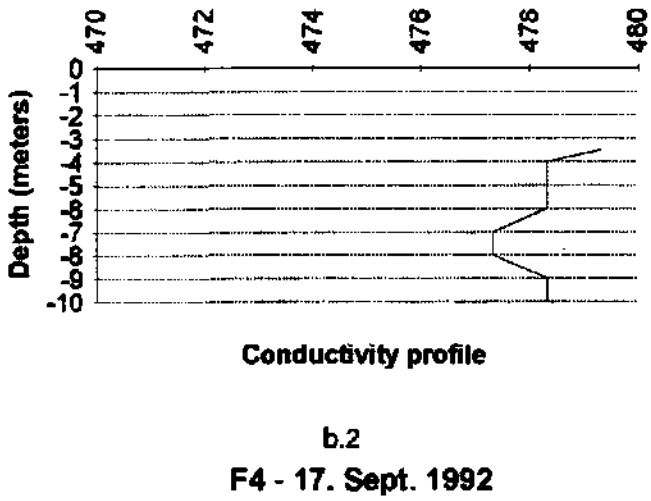

b.2

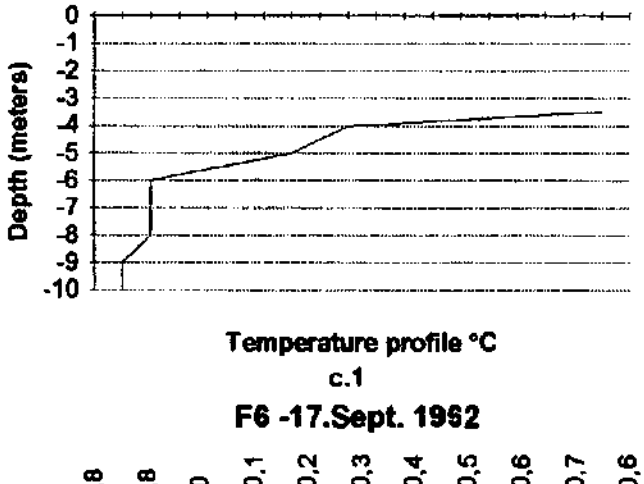

c.1

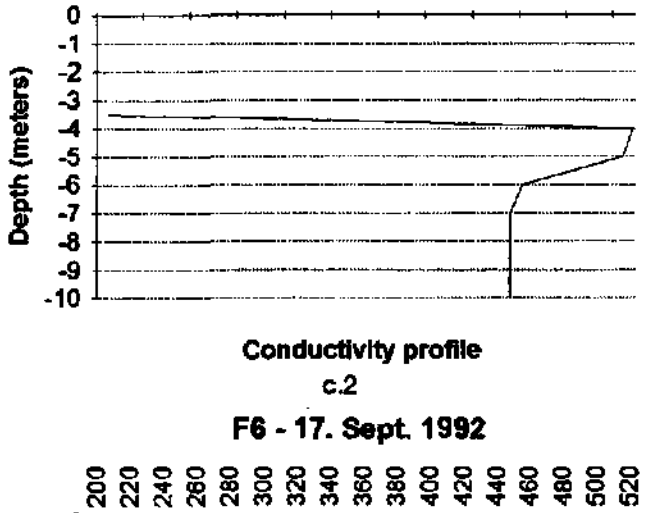

c.2

d.1

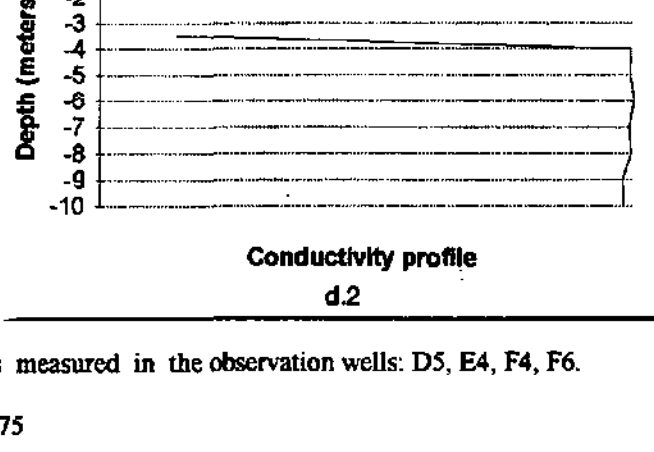

d.2

Table 3C2-9 Conductivity and temperature profiles measured in the observation wells: D5, E4, F4, F6.

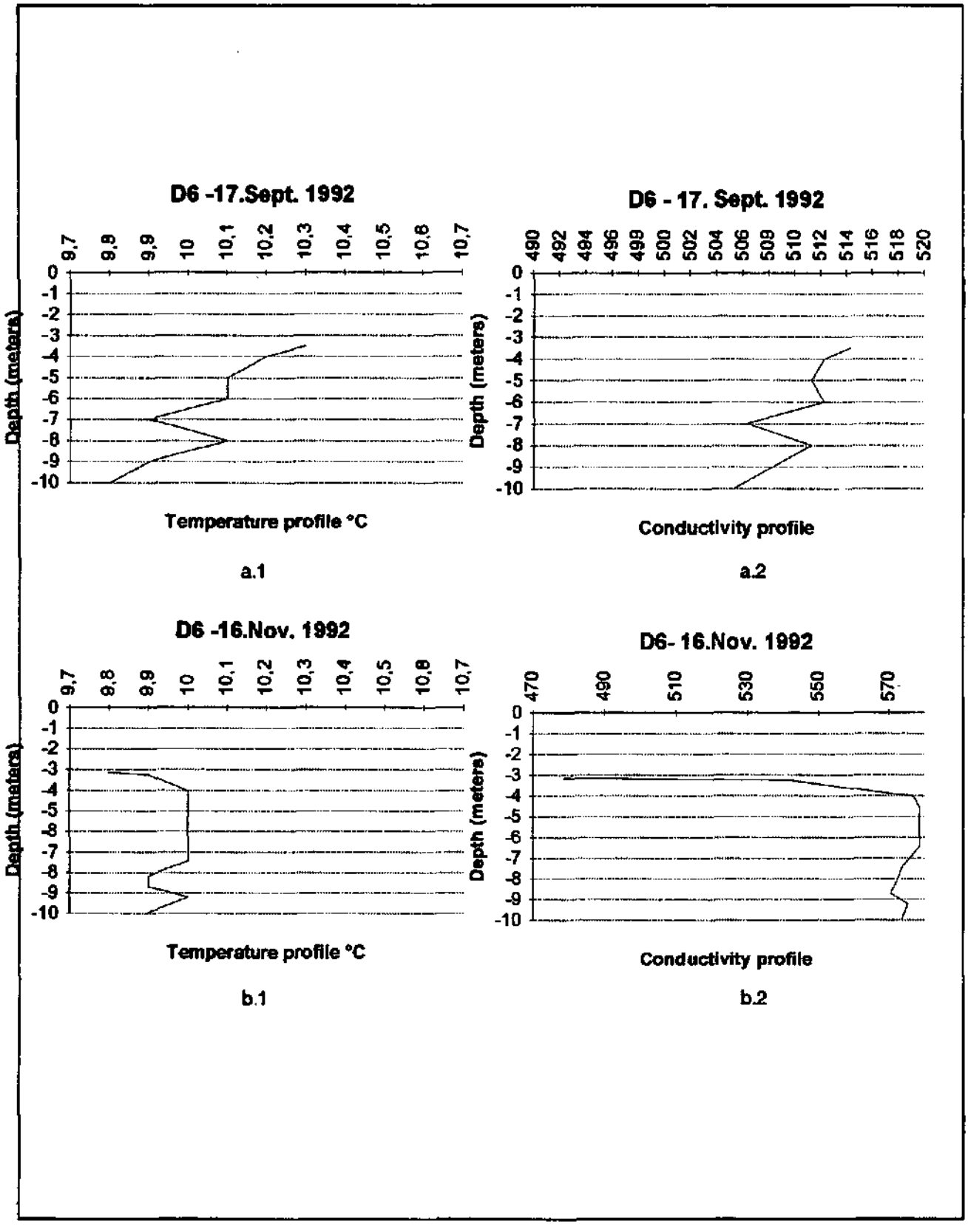

Table 3C2-10 Conductivity and temperature profiles measured in the observation wells: D6.

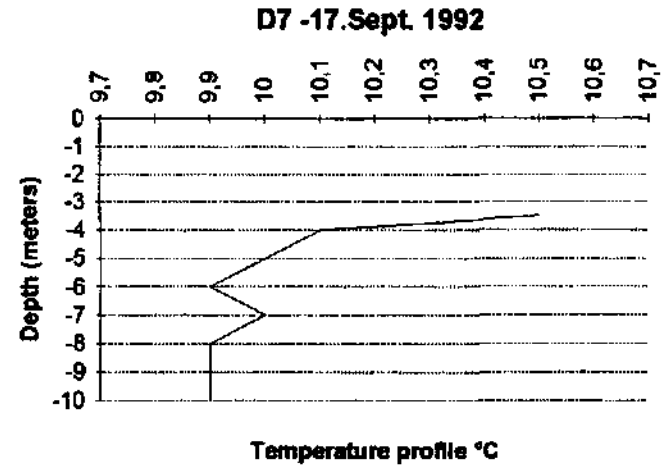

a.1

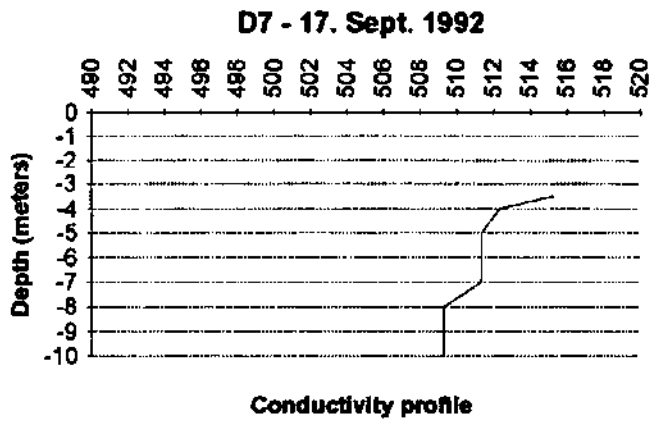

a.2

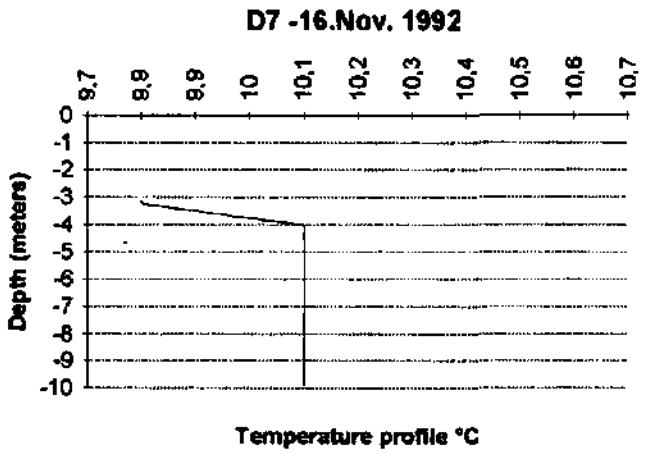

b.1

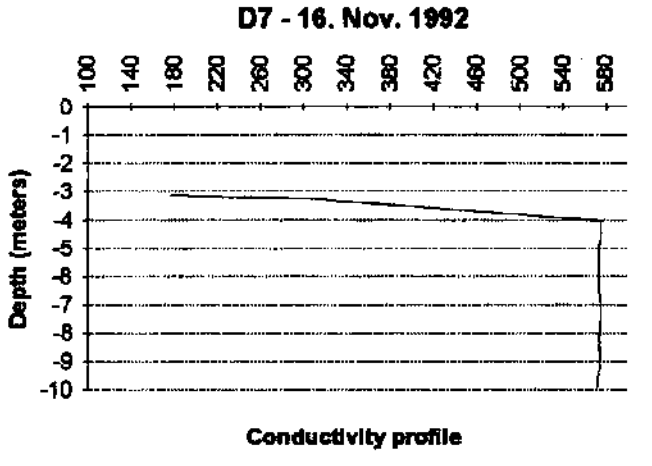

b.2

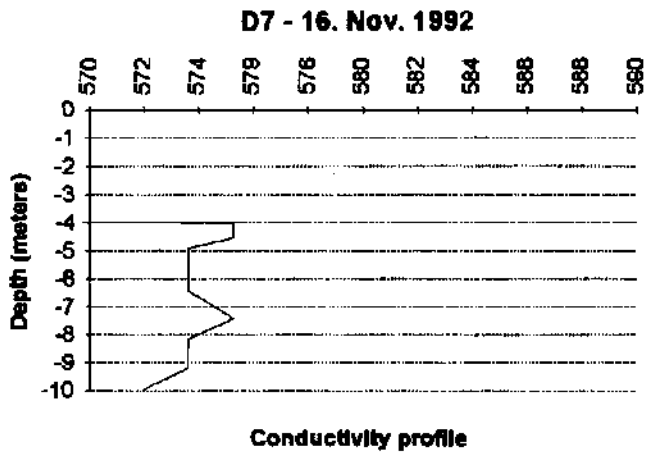

b.3

Table 3C2-11 Conductivity and temperature profiles measured in the observation wells: D7.

ISOTOPES

		EntnDat	TU ±Err	18O BE	18 O (SMOW)
Emme		11.03.91	26.7 ±3.1	-11.43	-11.27
Zielebach		11.03.91	27.3 ±3.1	-10.01	-9.85
Wilerwald C2 4m		11.03.91		-9.79	-9.63
Wilerwald C2 8m		11.03.91		-9.92	-9.76
Wilerwald C5 8m		11.03.91		-9.94	-9.78
Wilerwald C7 4m		11.03.91	32.5 ±3.2	-9.75	-9.59
Wilerwald C7 8m		11.03.91	26.0 ±2.7	-9.81	-9.65
Wilerwald D1 4m		11.03.91		-9.85	-9.69
Wilerwald D1 8m		11.03.91	28.0 ±2.7	-10.00	-9.84
Wilerwald D4 8m		11.03.91		-9.91	-9.75
Wilerwald D7 8m		11.03.91		-9.79	-9.63
Wilerwald D7 4m		11.03.91		-9.78	-9.62
Wilerwald E4 8m		11.03.91		-9.84	-9.68
Wilerwald F4 8m		11.03.91		-10.01	-9.85
Wilerwald F8 8m		11.03.91	29.9 ±2.7	-9.83	-9.67
Emme		09.05.91	17.4 ±2.8	-11.27	-11.11
Zielebach		09.05.91	21.9 ±2.8	-10.07	-9.91
Emme		14.09.91	24.9 ±2.8	-10.26	-10.10
Zielebach		14.09.91		-10.17	-10.01
Zielebach	Pumpwerk	14.09.91		-10.19	-10.03
Zielebach		14.09.91	28.2 ±3.1	-10.18	-10.02
Wilerwald D1 4m		14.09.91		-9.80	-9.64
Wilerwald D1 4m nach 10Min pumpen		14.09.91		-9.92	-9.76
Wilerwald D1 11m		14.09.91		-10.30	-10.14
Wilerwald D7 11m		14.09.91		-10.08	-9.90
Wilerwald D7 11m nach 10Min pumpen		14.09.91	35.3 ±3.0	-10.15	-9.99
Wilerwald D7 4m		14.09.91		-10.07	-9.91
Wilerwald D7 4m nach 10Min pumpen		14.09.91		-10.15	-9.99
Emme	Aefligen	05.12.91	28.2 ±3.4	-10.59	-10.43
Zielebach		05.12.91	23.0 ±3.2	-10.38	-10.22
Wilerwald C4 4m		05.12.91		-10.20	-10.04
Wilerwald C4 8m		05.12.91		-10.38	-10.22
Wilerwald D1 4m		05.12.91		-9.78	-9.62
Wilerwald D1 8m		05.12.91		-10.29	-10.13
Wilerwald D7 4m		05.12.91		-10.18	-10.02
Wilerwald D7 8m		05.12.91		-10.21	-10.05
Emme		20.03.92	17.3 ±3.0	-11.07	-10.91
Zielebach		20.03.92	25.8 ±3.4	-10.50	-10.34
Wilerwald C 4 4m		20.03.92		-10.31	-10.15
Wilerwald C 4 11m		20.03.92		-10.43	-10.27
Wilerwald C 7 11m		20.03.92		-10.25	-10.09
Wilerwald D 1 4m		20.03.92		-10.14	-9.98
Wilerwald D 1 8m		20.03.92		-10.39	-10.23
Wilerwald D 7 8m		20.03.92		-10.29	-10.13
Emme		11.04.92	25.7 ±3.3	-11.21	-11.05
Zielebach		11.04.92	21.9 ±3.1	-10.52	-10.36
Wilerwald C 4 4m		11.04.92		-10.25	-10.09
Wilerwald C 4 11m		11.04.92		-10.42	-10.26
Wilerwald C 7 8m		11.04.92		-10.37	-10.21
Wilerwald D 1 4m		11.04.92		-10.25	-10.09
Wilerwald D 1 8m		11.04.92		-10.42	-10.26
Wilerwald D 7 8m		11.04.92		-10.28	-10.12
Emme		14.05.92	18.6 ±3.2	-11.26	-11.10
Zielebach		14.05.92	23.5 ±3.3	-10.51	-10.35

Table 3C3 Isotopes analyses (O-18 and tritium) performed at the site, Emme and Burgdorf's precipitation.

	EntnDat	TU ±Err	18O ΘE	1a O (SMOW)
Wilerwald C 4 11m	14.05.92		-10.41	-10.25
Wilerwald C 4 4m	14.05.92		-10.32	-10.16
Wilerwald C 7 6m	14.05.92		-10.36	-10.20
Wilerwald D 1 4m	14.05.92		-10.23	-10.07
Wilerwald D 1 6m	14.05.92		-10.39	-10.23
Wilerwald D 7 8m	14.05.92		-10.35	-10.19
Emme	11.06.92	26.5 ±3.2	-11.09	-10.93
Zielebach	11.06.92	26.0 ±3.2	-10.47	-10.31
Wilerwald C 2 6m	11.06.92		-10.38	-10.22
Wilerwald C 3 6m	11.06.92		-10.40	-10.24
Wilerwald C 4 8m	11.06.92		-10.39	-10.23
Wilerwald C 5 8m	11.06.92		-10.45	-10.29
Wilerwald C 6 6m	11.06.92		-10.39	-10.23
Wilerwald C 7 8m	11.06.92		-10.39	-10.23
Wilerwald C 6 8m	11.06.92		-10.39	-10.23
Wilerwald D 1 8m	11.06.92		-10.31	-10.15
Wilerwald D 2 8m	11.06.92		-10.39	-10.23
Wilerwald D 3 6m	11.06.92		-10.34	-10.18
Wilerwald D 4 8m	11.06.92		-10.38	-10.22
Wilerwald D 5 8m	11.06.92		-10.39	-10.23
Wilerwald D 6 8m	11.06.92		-10.33	-10.17
Wilerwald D 7 6m	11.06.92		-10.34	-10.18
Wilerwald E 4 6m	11.06.92		-10.19	-10.03
Wilerwald F 4 6m	11.06.92		-10.46	-10.30
Wilerwald F 6 8m	11.06.92		-10.38	-10.22
Wilerwald C 2	12.06.92		-10.28	-10.12
Wilerwald C 3	12.06.92		-10.38	-10.22
Wilerwald C 4	12.06.92		-10.35	-10.19
Wilerwald C 5	12.06.92		-10.36	-10.20
Wilerwald C 6	12.06.92		-10.45	-10.29
Wilerwald C 7	12.06.92		-10.43	-10.27
Wilerwald C 6	12.06.92		-10.39	-10.23
Wilerwald D 1	12.06.92		-10.32	-10.16
Wilerwald D 2	12.06.92		-10.36	-10.22
Wilerwald D 3	12.06.92		-10.38	-10.22
Wilerwald D 4	12.06.92		-10.29	-10.13
Wilerwald D 5	12.06.92		-10.36	-10.20
Wilerwald D 6	12.06.92		-10.37	-10.21
Wilerwald D 7	12.06.92		-10.36	-10.22
Wilerwald E 4	12.06.92		-10.50	-10.34
Wilerwald F 4	12.06.92		-10.32	-10.16
Wilerwald F 6	12.06.92		-10.61	-10.45
Emme	24.06.92	24.0 ±3.3	-10.73	-10.57
Zielebach	24.06.92	29.8 ±3.4	-10.47	-10.31
Emme	26.06.92	20.1 ±3.3	-10.83	-10.67
Zielebach	26.06.92	16.7 ±3.1	-10.46	-10.30
Wilerwald C 4	26.06.92		-10.35	-10.19
Wilerwald C 7	26.06.92		-10.35	-10.19
Wilerwald C 6	26.06.92		-10.38	-10.22
Wilerwald D 1	26.06.92		-10.29	-10.13
Wilerwald D 7	26.06.92		-10.44	-10.28
Emme	20.07.92	25.2 ±3.2	-10.81	-10.65
Zielebach	20.07.92	21.0 ±3.0	-10.51	-10.35
Wilerwald C 2	20.07.92		-10.46	-10.30

Table 3C3 Isotopes analyses (O-18 and tritium) performed at the site, Emme and Burgdorf's precipitation.

	EmtnDat	TU ±Err	18O BE	18 O (SMOW)
Wilerwald C 3	20.07.92		-10.41	-10.25
Wilerwald C 4	20.07.92		-10.50	-10.34
Wilerwald C 5	20.07.92		-10.47	-10.31
Wilerwald C 6	20.07.92		-10.50	-10.34
Wilerwald C 7	20.07.92		-10.48	-10.32
Wilerwald C 8	20.07.92		-10.47	-10.31
Wilerwald D 1	20.07.92		-10.43	-10.27
Wilerwald D 2	20.07.92		-10.42	-10.26
Wilerwald D 3	20.07.92		-10.44	-10.28
Wilerwald D 4	20.07.92		-10.44	-10.28
Wilerwald D 5	20.07.92		-10.40	-10.24
Wilerwald D 6	20.07.92		-10.42	-10.26
Wilerwald D 7	20.07.92		-10.39	-10.23
Wilerwald E 4	20.07.92		-10.45	-10.29
Wilerwald F 4	20.07.92		-10.45	-10.29
Wilerwald F 6	20.07.92		-10.41	-10.25
Emme	06.08.92	25.2 ±3.4	-10.55	-10.39
Zielebach	08.08.92	27.8 ±3.2	-10.44	-10.28
Wilerwald C 2	06.08.92		-10.42	-10.26
Wilerwald C 3	06.08.92		-10.43	-10.27
Wilerwald C 4	06.08.92		-10.53	-10.37
Wilerwald C 5	08.08.92		-10.52	-10.36
Wilerwald C 6	06.08.92		-10.46	-10.30
Wilerwald C 7	06.08.92		-10.47	-10.31
Wilerwald C 8	06.08.92		-10.55	-10.39
Wilerwald D 1	06.08.92		-10.32	-10.16
Wilerwald D 2	06.08.92		-10.46	-10.30
Wilerwald D 3	06.08.92		-10.48	-10.32
Wilerwald D 4	06.08.92		-10.40	-10.24
Wilerwald D 5	06.08.92		-10.41	-10.25
Wilerwald D 6	06.08.92		-10.48	-10.32
Wilerwald D 7	06.08.92		-10.54	-10.38
Wilerwald E 4	06.08.92		-10.53	-10.37
Wilerwald F 4	06.08.92		-10.36	-10.20
Wilerwald F 6	06.08.92		-10.37	-10.21
Emme	19.08.92	22.9 ±3.3	-10.51	-10.35
Zielebach	19.08.92	23.4 ±3.1	-10.51	-10.35
Wilerwald C 2	19.08.92		-10.48	-10.30
Wilerwald C 3	19.08.92		-10.47	-10.31
Wilerwald C 4	19.08.92		-10.47	-10.31
Wilerwald C 5	19.08.92		-10.48	-10.30
Wilerwald C 6	19.08.92		-10.44	-10.28
Wilerwald C 7	19.08.92		-10.45	-10.29
Wilerwald C 8	19.08.92		-10.50	-10.34
Wilerwald C/d	19.08.92		-10.52	-10.36
Wilerwald D 1	19.08.92		-10.39	-10.23
Wilerwald D 2	19.08.92		-10.51	-10.35
Wilerwald D 3	19.08.92		-10.55	-10.39
Wilerwald D 4	19.08.92		-10.43	-10.27
Wilerwald D 5	19.08.92		-10.41	-10.25
Wilerwald D 6	19.08.92		-10.46	-10.30
Wilerwald D 7	19.08.92		-10.47	-10.31
Wilerwald E 4	19.08.92		-10.56	-10.40
Wilerwald F 4	19.08.92		-10.37	-10.21

Table 3C3 Isotopes analyses (O-18 and tritium) performed at the site, Emme and Burgdorf's precipitation.

	EntnDat	TU ±Err	18O BE	18 O (SMOW)
Wilerwald F 6	19.08.92		-10.46	-10.30
Emme	26.09.92	25.8 ±3.1	-10.46	-10.30
Zielebach	26.08.92	21.8 ±3.0	-10.55	-10.39
Wilerwald C 2	26.09.92		-10.49	-10.33
Wilerwald C 3	26.09.92		-10.45	-10.29
Wilerwald C 4	26.09.92		-10.50	-10.34
Wilerwald C 5	26.09.92		-10.47	-10.31
Wilerwald C 6	26.09.92		-10.45	-10.29
Wilerwald C 7	26.09.92		-10.44	-10.28
Wilerwald C 8	26.09.92		-10.47	-10.31
Wilerwald C/d	26.09.92		-10.47	-10.31
Wilerwald D 1	26.09.92		-10.43	-10.27
Wilerwald D 2	26.09.92		-10.54	-10.38
Wilerwald D 3	26.09.92		-10.59	-10.43
Wilerwald D 4	26.09.92		-10.43	-10.27
Wilerweld D 5	26.09.92		-10.36	-10.20
Wilerwald D 7	26.09.92		-10.48	-10.32
Wilerwald D6	26.09.92		-10.48	-10.32
Wilerweld E4	26.09.92		-10.59	-10.43
Wilerwald EP1	26.09.92		-10.40	-10.24
Wilerwald F4	26.09.92		-10.61	-10.45
Emme	09.11.92	20.2 ±3.1	-10.65	-10.69
Zielebach	09.11.92	16.5 ±2.9	-10.61	-10.45
Wilerweld C 2	09.11.92		-10.54	-10.38
Wilerweld C 3	09.11.92		-10.50	-10.34
Wilerweld C 4	09.11.92		-10.51	-10.35
Wilerwald C 5	09.11.92		-10.57	-10.41
Wilerwald C 6	09.11.92		-10.54	-10.38
Wilerwald C 7	09.11.92		-10.54	-10.38
Wilerwald C 8	09.11.92		-10.54	-10.38
Wilerwald C/d	09.11.92		-10.51	-10.35
Wilerwald D 1	09.11.92		-10.53	-10.37
Wilerwald D 2	09.11.92		-10.62	-10.46
Wilerwald D 3	09.11.92		-10.64	-10.48
Wilerwald D 4	09.11.92		-10.51	-10.35
Wilerwald D 5	09.11.92		-10.54	-10.38
Wilerwald D 7	09.11.92		-10.55	-10.39
Wilerwald D6	09.11.92		-10.56	-10.40
Wilerwald E4	09.11.92		-10.73	-10.57
Wilerwald EP1	09.11.92		-10.54	-10.38
Wilerweld F4	09.11.92		-10.71	-10.55
Wilerwald F6	09.11.92		-10.53	-10.37
Emme	25.11.92	17.4 ±3.0	-10.92	-10.76
Zielebach	25.11.92	19.1 ±3.0	-10.66	-10.50
Wilerwald C 2	25.11.92		-10.44	-10.28
Wilerwald C 3	25.11.92		-10.50	-10.34
Wilerwald C 4	25.11.92		-10.48	-10.32
Wilerwald C 5	25.11.92		-10.50	-10.34
Wilerwald C 6	25.11.92		-10.53	-10.37
Wilerwald C 7	25.11.92		-10.45	-10.29
Wilerwald C 8	25.11.92		-10.43	-10.27
Wilerwald C/d	25.11.92		-10.43	-10.27
Wilerwald D 1	25.11.92		-10.47	-10.31
Wilerwald D 2	25.11.92		-10.57	-10.41

Table 3C3 Isotopes analyses (O-18 and tritium) performed at the site, Emme and Burgdorf's precipitation.

	EntnDat	TU ±Err	18O BE	18 O (SMOW)
Wilerwald D 3	25.11.92		-10.59	-10.43
Wilerwald D 4	25.11.92		-10.49	-10.33
Wilerwald D 5	25.11.92		-10.43	-10.27
Wilerwald D 7	25.11.92		-10.45	-10.29
Wilerwald D6	25.11.92		-10.46	-10.30
Wilerweld E4	25.11.92		-10.57	-10.41
Wilerwald EP1	25.11.92		-10.49	-10.33
Wilerwald F4	25.11.92		-10.65	-10.49
Wilerwald F6	25.11.92		-10.46	-10.30
Emme	10.12.92	18.6 ±2.8	-10.90	-10.74
Zielebach	10.12.92	21.2 ±3.0	-10.68	-10.52
Wilerwald C 2	10.12.92		-10.43	-10.27
Wilerwald C 3	10.12.92		-10.40	-10.24
Wilerwald C 4	10.12.92		-10.45	-10.29
Wilerwald C 5	10.12.92		-10.50	-10.34
Wilerwald C 6	10.12.92		-10.44	-10.28
Wilerwald C 7	10.12.92		-10.47	-10.31
Wilerwald C 8	10.12.92		-10.58	-10.42
Wilerwald C/d	10.12.92		-10.42	-10.26
Wilerweld D 1	10.12.92		-10.63	-10.47
Wilerwald D 2	10.12.92		-10.69	-10.53
Wilerwald D 3	10.12.92		-10.60	-10.44
Wilerwald D 4	10.12.92		-10.52	-10.36
Wilerwald D 5	10.12.92		-10.43	-10.27
Wilerwald D 7	10.12.92		-10.40	-10.24
Wilerwald D8	10.12.92		-10.41	-10.25
Wilerwald E4	10.12.92		-10.51	-10.35
Wilerwald EP1	10.12.92		-10.42	-10.26
Wilerwald F4	10.12.92		-10.66	-10.50
Wilerwald F8	10.12.92		-10.41	-10.25

Table 3C3 Isotopes analyses (O-18 and tritium) performed at the site, Emme and Burgdorf's precipitation.

1992 TRACER EXPERIMENT RESULTS

Time	[ ]	Time	[ ]	Time	[ ]	Time	[ ]	Time	[ ]	Time	[ ]
C2	C2	C3	C3	C4	C4	C5	C5	C6	C6	C7	C7
10.11.1992 10:00	0	10.11.1992 10:00	0	10.11.1992 10:00	0	10.11.1992 10:00	0	10.11.1992 10:00	0	10.11.1992 10:00	0
				10.11.1992 11:11	0,5	10.11.1992 11:15	0,63	10.11.1992 11:05	0,5	10.11.1992 11:00	10,5
10.11.1992 16:50	0,75	10.11.1992 16:00	0,75	10.11.1992 16:25	10,5	10.11.1992 16:30	2605	10.11.1992 16:30	5220	10.11.1992 15:42	0,3
10.11.1992 19:45	9,1	10.11.1992 21:10	0,22	10.11.1992 19:15	16,3	10.11.1992 19:06	2790	10.11.1992 19:34	2100	10.11.1992 18:42	0,57
10.11.1992 21:20	0,67			10.11.1992 21:01	20,4	10.11.1992 20:52	1965	10.11.1992 20:44	1467	10.11.1992 19:58	0,21
11.11.1992 10:12	0,16	11.11.1992 10:05	0,38	11.11.1992 09:38	3,2	11.11.1992 09:51	457	11.11.1992 09:44	336	11.11.1992 09:57	0
				10.11.1992 12:10	4,2	10.11.1992 11:59	577	10.11.1992 11:51	397	10.11.1992 11:41	0
12.11.1992 17:50	0			12.11.1992 17:20	8,8	12.11.1992 17:20	274	12.11.1992 17:10	184	12.11.1992 17:00	0
12.11.1992 10:00	0	12.11.1992 08:50	0,05	12.11.1992 09:40	0,52	12.11.1992 09:30	136	12.11.1992 09:20	83	12.11.1992 09:10	0
12.11.1992 13:00	0	12.11.1992 17:50	0,07	12.11.1992 17:40	0,82	12.11.1992 17:30	111	12.11.1992 17:20	65	12.11.1992 17:10	0
13.11.1992 10:50	0	13.11.1992 10:50	0,04	13.11.1992 10:10	0	13.11.1992 10:00	52	13.11.1992 09:50	34,7	13.11.1992 09:40	0
13.11.1992 17:00	0	13.11.1992 16:50	0	13.11.1992 16:40	0	13.11.1992 16:30	43	13.11.1992 16:20	28,8	13.11.1992 16:10	0
14.11.1992 11:00	0	14.11.1992 10:50	0	14.11.1992 10:40	0	14.11.1992 10:30	24	14.11.1992 10:20	8,6	14.11.1992 10:10	0
16.11.1992 11:00	0	16.11.1992 10:50	0	16.11.1992 10:40	0	16.11.1992 10:30	7,3	16.11.1992 10:20	2,8	16.11.1992 10:10	0
17.11.1992 11:00	0	17.11.1992 10:50	0	17.11.1992 10:40	0	17.11.1992 10:30	5,6	17.11.1992 10:20	1,19	17.11.1992 10:10	0
18.11.1992 11:00	0	18.11.1992 10:50	0	18.11.1992 10:40	0	18.11.1992 10:30	4,7	18.11.1992 10:20	0,65	18.11.1992 10:10	0
19.11.1992 11:00	0	19.11.1992 10:50	0	19.11.1992 10:40	0	19.11.1992 10:30	3,2	19.11.1992 10:20	0,7	19.11.1992 10:10	0
20.11.1992 11:00	0	20.11.1992 10:50	0	20.11.1992 10:40	0	20.11.1992 10:30	2,8	20.11.1992 10:20	0,61	20.11.1992 10:10	0
23.11.1992 11:00	0	23.11.1992 10:50	0	23.11.1992 10:40	0	23.11.1992 10:30	1,57	23.11.1992 10:20	0,17	23.11.1992 10:10	0
25.11.1992 11:00	0	25.11.1992 10:50	0	25.11.1992 10:40	0	25.11.1992 10:30	1,27	25.11.1992 10:20	0,16	25.11.1992 10:10	0
27.11.1992 11:00	0	27.11.1992 10:50	0	27.11.1992 10:40	0	27.11.1992 10:30	0,98	27.11.1992 10:20	0,01	27.11.1992 10:10	0
30.11.1992 11:00	0	30.11.1992 10:50	0	30.11.1992 10:40	0	30.11.1992 10:30	0,95	30.11.1992 10:20	0	30.11.1992 10:10	0
04.12.1992 11:00	0	04.12.1992 10:50	0	04.12.1992 10:40	0	04.12.1992 10:30	0,7	04.12.1992 10:20	0	04.12.1992 10:10	0
10.12.1992 11:00	0	10.12.1992 10:50	0	10.12.1992 10:40	0	10.12.1992 10:30	0,46	10.12.1992 10:20	0,12	10.12.1992 10:10	0,36
14.12.1992 11:00	0	14.12.1992 10:50	0	14.12.1992 10:40	0	14.12.1992 10:30	0,36	14.12.1992 10:20	0,12	14.12.1992 10:10	0,45
25.01.1993 11:00	0	25.01.1993 10:50	0	25.01.1993 10:40	0	25.01.1993 10:30	0,3	25.01.1993 10:20	0,15	25.01.1993 10:10	0,23

Time	[ ]	Time	[ ]	Time	[ ]	Time	[ ]	Time	[ ]	Time	[ ]
C8	C8	C9	C9	D0	D1	D2	D2	D3	D3	D4	D4
10.11.1992 10:00	0	10.11.1992 10:00	0	10.11.1992 10:00	0	10.11.1992 10:00	0	10.11.1992 10:00	0	10.11.1992 10:00	0
10.11.1992 12:00	0	10.11.1992 17:00	0,1	10.11.1992 18:01	0,2	10.11.1992 17:55	0,63	10.11.1992 17:45	0,2	10.11.1992 17:31	0,22
10.11.1992 18:30	0,07	10.11.1992 19:00	8,7								
10.11.1992 10:30	0,05	10.11.1992 21:30	53	10.11.1992 22:00	169	10.11.1992 22:00	0,6	10.11.1992 21:33	9,9	10.11.1992 23:00	4,1
11.11.1992 09:30	0	11.11.1992 10:20	187	10.11.1992 11:00	278	11.11.1992 11:25	2,01	11.11.1992 11:13	125	11.11.1992 11:00	26
11.11.1992 16:50	0	11.11.1992 16:40	147	11.11.1992 16:55	117	11.11.1992 16:00	6,9	11.11.1992 16:24	169	11.11.1992 16:12	34
12.11.1992 09:00	0	12.11.1992 10:10	79	12.11.1992 11:00	27	12.11.1992 10:50	35	12.11.1992 10:45	224	12.11.1992 10:30	16,2
12.11.1992 17:00	0	12.11.1992 18:30	58	12.11.1992 19:00	19	12.11.1992 18:51	46	12.11.1992 18:46	213	12.11.1992 18:40	13,8
13.11.1992 09:30	0	13.11.1992 10:40	35	13.11.1992 11:50	8,9	13.11.1992 11:40	68	13.11.1992 11:20	169	13.11.1992 11:00	9,6
13.11.1992 16:00	0	13.11.1992 17:10	27	13.11.1992 17:20	9,1	13.11.1992 17:20	61	13.11.1992 18:00	148	13.11.1992 17:50	9,5
14.11.1992 10:00	0	14.11.1992 11:10	17,9	14.11.1992 11:50	3,9	14.11.1992 11:10	70	14.11.1992 12:00	83	14.11.1992 11:50	7
16.11.1992 10:00	0	16.11.1992 11:10	4,9	16.11.1992 11:50	1,08	16.11.1992 12:10	45	16.11.1992 12:00	24	16.11.1992 11:50	4,8
17.11.1992 10:00	0	17.11.1992 11:10	3,2	17.11.1992 12:20	1,43	17.11.1992 12:10	48	17.11.1992 13:00	13,8	17.11.1992 11:50	3,2
18.11.1992 10:00	0	18.11.1992 11:10	2,2	18.11.1992 12:20	1,29	18.11.1992 12:10	41	18.11.1992 13:00	9,3	18.11.1992 11:50	2,7
19.11.1992 10:00	0	19.11.1992 11:10	1,51	19.11.1992 11:50	0,81	19.11.1992 12:10	28	19.11.1992 12:00	7	19.11.1992 11:50	2,6
20.11.1992 10:00	0	20.11.1992 11:10	1,01	20.11.1992 11:50	0,52	20.11.1992 12:10	23	20.11.1992 12:00	4,9	20.11.1992 11:50	2,24
23.11.1992 10:00	0	23.11.1992 11:10	0,63	23.11.1992 10:50	0,3	23.11.1992 12:10	10,5	23.11.1992 13:00	2,7	23.11.1992 11:50	1,9
25.11.1992 10:00	0	25.11.1992 11:10	0,83	25.11.1992 11:20	0,07	25.11.1992 12:10	5,8	25.11.1992 12:00	1,6	25.11.1992 11:50	1,5
27.11.1992 10:00	0	27.11.1992 11:10	0,31	27.11.1992 11:20	0,25	27.11.1992 12:10	3,2	27.11.1992 12:00	1,1	27.11.1992 11:50	1,4
30.11.1992 10:00	0	30.11.1992 11:10	0,02	30.11.1992 12:20	0	30.11.1992 12:10	1,59	30.11.1992 12:00	0,64	30.11.1992 11:50	0,74
04.12.1992 10:00	0	04.12.1992 11:10	0,1	04.12.1992 11:50	0	04.12.1992 12:10	1,31	04.12.1992 12:00	0,42	04.12.1992 11:50	0,46
10.12.1992 10:00	1,9	10.12.1992 11:10	0,36	10.12.1992 11:50	0,38	10.12.1992 12:10	0,93	10.12.1992 12:00	0,28	10.12.1992 11:50	0,44
14.12.1992 10:00	0,77	14.12.1992 11:10	0,30	14.12.1992 12:20	0,29	14.12.1992 12:10	0,16	14.12.1992 12:00	0,26	14.12.1992 11:50	3,8
25.01.1993 10:00	0,33	25.01.1993 11:10	0,35	25.01.1993 11:20	0,07	25.01.1993 12:10	0,33	25.01.1993 12:00	0	25.01.1993 11:50	0,31

Time	[ ]	Time	[ ]	Time	[ ]
D5	D5	D6	D6	D7	D7
10.11.1992 10:00	0	10.11.1992 10:00	0	10.11.1992 10:00	0
10.11.1992 17:34	0,6	10.11.1992 17:37	0,3	10.11.1992 17:10	0,19
10.11.1992 21:35	0,1	10.11.1992 21:47	18,6	10.11.1992 21:40	47
11.11.1992 10:39	2,65	11.11.1992 10:57	544	11.11.1992 10:50	480
11.11.1992 16:12	10,5	11.11.1992 16:06	454	11.11.1992 16:00	366
12.11.1992 10:57	21	12.11.1992 12:08	159	12.11.1992 10:50	136
12.11.1992 10:51	22	12.11.1992 10:27	137	12.11.1992 10:20	92
13.11.1992 11:10	18,6	13.11.1992 11:00	86	13.11.1992 10:50	53
13.11.1992 17:50	16,5	13.11.1992 17:39	69	13.11.1992 17:30	41
14.11.1992 11:40	13,8	14.11.1992 11:30	44	14.11.1992 11:20	25
16.11.1992 11:40	3,5	16.11.1992 11:30	15,3	16.11.1992 11:20	7,3
17.11.1992 11:40	4	17.11.1992 11:30	9,5	17.11.1992 11:20	3,97
18.11.1992 11:40	3,8	18.11.1992 11:30	6,16	18.11.1992 11:20	2,4
19.11.1992 11:40	2,8	19.11.1992 11:30	4,3	19.11.1992 11:20	2
20.11.1992 11:40	1,64	20.11.1992 11:30	2,76	20.11.1992 11:20	1,3
23.11.1992 11:40	0,96	23.11.1992 11:30	1,26	23.11.1992 11:20	0,44
25.11.1992 11:40	0,82	25.11.1992 11:30	0,99	25.11.1992 11:20	0,29
27.11.1992 11:40	0,36	27.11.1992 11:30	0,44	27.11.1992 11:20	0,17
30.11.1992 11:40	0,01	30.11.1992 11:30	0,41	30.11.1992 11:20	0,14
04.12.1992 11:40	0,01	04.12.1992 11:30	0,4	04.12.1992 11:20	0,15
10.12.1992 11:40	0,29	10.12.1992 11:30	0,33	10.12.1992 11:20	0,7
14.12.1992 11:40	0,3	14.12.1992 11:30	0,31	14.12.1992 11:20	0,22
25.01.1993 11:40	0,1	25.01.1993 11:30	0,19	25.01.1993 11:20	0,24

[ ] Concentration in microgramm/ liter

Table 3C4-1 Na-Naphtionate results - 1992 tracer experiment.

Time	[ ]	Time	[ ]	Time	[ ]	Time	[ ]	Time	[ ]	Time	[ ]
C1	C2	C3	C3	C4	C4	C5	C5	C6	C6	C7	C7
10.11.1992 10:00	0	10.11.1992 10:00	0	10.11.1992 10:00	0	10.11.1992 10:00	0	10.11.1992 10:00	0	10.11.1992 10:00	0
				10.11.1992 17:13	0,16	10.11.1992 13:10	0,17	10.11.1992 13:05	0,15	10.11.1992 11:00	0,3
10.11.1992 19:30	0,12	10.11.1992 19:30	0,47	10.11.1992 16:25	0,9	10.11.1992 16:10	1645	10.11.1992 15:53	1803	10.11.1992 15:42	0,06
10.11.1992 19:45	0,29	10.11.1992 21:10	0,26	10.11.1992 19:10	3,1	10.11.1992 19:05	1170	10.11.1992 18:54	1183	10.11.1992 18:42	0,04
10.11.1992 21:20	0,15			10.11.1992 21:01	0,06	10.11.1992 20:05	854	10.11.1992 20:44	1116	10.11.1992 10:00	0,09
11.11.1992 09:13	0,06	11.11.1992 10:05	0,078	11.11.1992 09:58	0,0	11.11.1992 09:53	309	11.11.1992 09:44	336	11.11.1992 09:37	0,02
				10.11.1992 11:20	0,29	10.11.1992 11:59	235	10.11.1992 11:51	266	10.11.1992 11:43	0,02
11.11.1992 17:30	0,06			10.11.1992 17:20	1,43	13.11.1992 17:20	226	11.11.1992 17:06	104	11.11.1992 17:00	0,02
12.11.1992 10:00	0,03	12.11.1992 09:20	0,055	12.11.1992 09:40	0,16	12.11.1992 09:30	360	12.11.1992 09:20	114	12.11.1992 09:20	0,02
12.11.1992 10:40	0,07	12.11.1992 17:20	0,037	12.11.1992 17:40	0,58	12.11.1992 17:30	166	12.11.1992 17:20	68	12.11.1992 17:10	0,01
13.11.1992 10:20	0,04	13.11.1992 10:20	0,025	13.11.1992 10:45	0,11	13.11.1992 10:05	70	13.11.1992 09:55	49	13.11.1992 09:40	0,02
13.11.1992 17:00	0,07	13.11.1992 10:50	0,02	13.11.1992 10:50	0,16	13.11.1992 10:30	70	13.11.1992 10:20	50	13.11.1992 10:10	0,03
14.11.1992 11:00	0,01	14.11.1992 10:30	0,018	14.11.1992 10:40	0,14	14.11.1992 10:20	67	14.11.1992 10:00	28	14.11.1992 10:10	0,02
16.11.1992 11:00	0,01	16.11.1992 10:50	0,01	16.11.1992 10:40	0,1	16.11.1992 10:20	30	16.11.1992 10:00	16,0	16.11.1992 10:20	0,02
17.11.1992 11:00	0,01	17.11.1992 10:50	0,01	17.11.1992 10:40	0,1	17.11.1992 10:20	27	17.11.1992 10:00	9,6	17.11.1992 10:10	0,02
18.11.1992 11:00	0,01	18.11.1992 10:50	0,01	18.11.1992 10:40	0,1	18.11.1992 10:20	32	18.11.1992 10:00	7,4	18.11.1992 10:10	0,01
19.11.1992 11:00	0,01	19.11.1992 10:50	0,01	19.11.1992 10:40	0,1	19.11.1992 10:20	37,9	19.11.1992 10:00	6,4	19.11.1992 10:10	0,01
20.11.1992 11:00	0,01	20.11.1992 10:50	0,02	20.11.1992 10:40	0,1	20.11.1992 10:20	15,4	20.11.1992 10:00	5,5	20.11.1992 10:10	0,01
23.11.1992 11:00	0,01	23.11.1992 10:50	0,03	23.11.1992 10:40	0,1	23.11.1992 10:20	10,4	23.11.1992 10:00	3,7	23.11.1992 10:10	0,02
25.11.1992 11:00	0,01	25.11.1992 10:50	0,05	25.11.1992 10:40	0,1	25.11.1992 10:20	8,5	25.11.1992 10:00	2,6	25.11.1992 10:10	0,06
27.11.1992 11:00	0,01	27.11.1992 10:50	0,04	27.11.1992 10:40	0,1	27.11.1992 10:20	6,6	27.11.1992 10:00	2,2	27.11.1992 10:10	0,07
30.11.1992 11:00	0	30.11.1992 10:50	0,03	30.11.1992 10:40	0,1	30.11.1992 10:20	8,9	30.11.1992 10:00	2	30.11.1992 10:10	0,05
04.12.1992 11:00	0	04.12.1992 10:50	0,02	04.12.1992 10:40	0,05	04.12.1992 10:20	4,3	04.12.1992 10:00	1,5	04.12.1992 10:10	0,01
08.12.1992 11:00	0	10.12.1992 10:50	0,05	08.12.1992 10:40	0,12	10.12.1992 10:20	3	10.12.1992 10:00	1,12	10.12.1992 10:10	0,04
16.12.1992 11:00	0	16.12.1992 10:50	0,04	16.12.1992 10:40	0,1	16.12.1992 10:20	1,5	16.12.1992 10:00	0,62	16.12.1992 10:10	0,05
25.01.1993 11:00	0	25.01.1993 10:50	0,02	25.01.1993 10:40	0,04	25.01.1993 10:20	1,33	25.01.1993 10:05	0,9	25.01.1993 10:10	0

Time	[ ]	Time	[ ]	Time	[ ]	Time	[ ]	Time	[ ]	Time	[ ]
C8	C8	C9	C9	D1	D1	D2	D2	D3	D3	D4	D4
10.11.1992 10:30	0	10.11.1992 10:00	0	10.11.1992 10:00	0	10.11.1992 10:00	0	10.11.1992 10:00	0	10.11.1992 10:10	0
26.11.1992 17:40	0	10.11.1992 17:00	0,06	10.11.1992 16:05	0	10.11.1992 17:20	0	10.11.1992 17:00	0	10.11.1992 17:05	0
09.11.1992 10:20	0,045	10.11.1992 06:00	0,66								
10.11.1992 10:30	0,066	10.11.1992 21:00	3,5	10.11.1992 12:20	0,01	10.11.1992 22:20	0	10.11.1992 22:10	0,03	10.11.1992 10:00	0,09
11.11.1992 09:30	0,04	11.11.1992 10:30	16,5	11.11.1992 10:00	0,06	11.11.1992 11:20	0	11.11.1992 11:10	0,97	11.11.1992 11:05	1,27
11.11.1992 10:20	0,03	11.11.1992 16:40	17,5	11.11.1992 16:55	0,06	11.11.1992 10:30	0	11.11.1992 16:54	1	11.11.1992 16:18	2,3
12.11.1992 09:30	0,03	12.11.1992 09:20	16,6	12.11.1992 11:00	0,07	12.11.1992 10:50	0	12.11.1992 10:45	1,34	12.11.1992 10:35	1,88
12.11.1992 17:00	0,03	12.11.1992 18:30	18	12.11.1992 19:00	0,08	25.11.1992 20:50	0	12.11.1992 19:00	1,3	12.11.1992 18:40	1,43
13.11.1992 10:30	0,03	13.11.1992 10:40	14,3	13.11.1992 11:00	0,07	13.11.1992 11:40	0	13.11.1992 11:30	1,42	13.11.1992 11:20	1,39
13.11.1992 16:00	0,02	13.11.1992 17:10	19,5	11.11.1992 18:20	0,08	13.11.1992 19:10	0	13.11.1992 16:00	1,3	13.11.1992 17:50	1,51
14.11.1992 09:00	0,02	14.11.1992 11:10	12	14.11.1992 12:20	0,07	14.11.1992 12:10	0,01	14.11.1992 12:00	1,28	14.11.1992 11:50	1,83
15.11.1992 10:00	0,02	14.11.1992 11:10	7,4	14.11.1992 12:20	0,06	14.11.1992 12:10	0,07	13.11.1992 12:00	1,57	14.11.1992 11:50	1,71
17.11.1992 10:00	0,02	17.11.1992 11:10	6,9	17.11.1992 12:20	0,08	17.11.1992 12:10	0,01	17.11.1992 12:00	0,93	17.11.1992 11:50	1,23
18.11.1992 10:00	0,02	18.11.1992 11:10	6,4	18.11.1992 12:20	0,16	18.11.1992 12:10	0,02	18.11.1992 12:00	1	18.11.1992 11:50	0,93
19.11.1992 10:10	0,02	19.11.1992 11:10	5,6	19.11.1992 12:20	0,13	19.11.1992 12:10	0,02	19.11.1992 12:00	1,1	19.11.1992 11:50	0,93
20.11.1992 10:00	0,02	20.11.1992 11:30	5	20.11.1992 12:20	0,17	20.11.1992 12:10	0,03	20.11.1992 12:00	1	20.11.1992 11:50	0,77
23.11.1992 10:00	0,03	23.11.1992 11:10	3,9	23.11.1992 12:20	0,17	23.11.1992 12:10	0,06	23.11.1992 12:00	0,8	23.11.1992 11:50	0,66
25.11.1992 10:00	0,03	25.11.1992 11:30	3,3	25.11.1992 12:20	0,06	25.11.1992 12:30	0,05	25.11.1992 12:20	0,84	25.11.1992 11:50	0,57
27.11.1992 10:20	0,04	27.11.1992 11:10	2,7	27.11.1992 12:20	0,18	27.11.1992 12:10	0,09	27.11.1992 11:50	0,78	27.11.1992 11:50	0,51
30.11.1992 10:00	0,03	30.11.1992 11:10	2,5	30.11.1992 12:20	0,06	30.11.1992 12:30	0,07	30.11.1992 12:20	0,77	30.11.1992 11:20	0,46
04.12.1992 10:00	0,03	04.12.1992 11:10	1,93	04.12.1992 12:20	0,16	04.12.1992 12:10	0,02	04.12.1992 12:00	0,62	04.12.1992 11:20	0,48
08.12.1992 10:00	0,02	10.12.1992 11:10	1,39	08.12.1992 12:20	0,16	10.12.1992 12:30	0,26	10.12.1992 12:20	0,27	10.12.1992 11:50	0,41
16.12.1992 10:20	0,05	16.12.1992 11:10	1,29	16.12.1992 12:20	0,37	16.12.1992 12:10	0,11	16.12.1992 12:00	0,54	16.12.1992 11:50	0,37
25.01.1993 10:00	0	25.01.1993 11:10	0,45	25.01.1993 12:20	0,49	25.01.1993 12:10	0,05	25.01.1993 12:00	0,36	25.01.1993 11:50	0,3

Time	[ ]	Time	[ ]	Time	[ ]
D5	D5	D6	D6	D7	D7
10.11.1992 10:00	0	10.11.1992 10:00	0	10.11.1992 10:00	0
10.11.1992 17:24	0	10.11.1992 17:17	0	10.11.1992 17:10	0,03
10.11.1992 23:55	0,03	10.11.1992 21:47	0,5	10.11.1992 22:40	3
11.11.1992 10:13	0,05	11.11.1992 09:27	33	11.11.1992 10:35	70
11.11.1992 16:32	0,05	11.11.1992 16:08	66	11.11.1992 10:00	77
12.11.1992 10:31	0,15	12.11.1992 09:58	50	12.11.1992 10:10	61
12.11.1992 18:01	0,43	12.11.1992 18:27	47	12.11.1992 18:10	53
13.11.1992 11:10	0,44	13.11.1992 11:00	43	13.11.1992 10:30	43
13.11.1992 17:40	0,46	13.11.1992 17:30	40	13.11.1992 17:05	39
14.11.1992 10:40	0,59	14.11.1992 11:30	34	14.11.1992 11:15	35
16.11.1992 11:40	0,72	16.11.1992 11:30	22	16.11.1992 11:10	19,9
17.11.1992 11:40	0,65	17.11.1992 11:30	19,3	17.11.1992 11:20	16
18.11.1992 11:40	0,67	18.11.1992 11:30	16	18.11.1992 11:20	13,3
19.11.1992 11:40	0,68	19.11.1992 11:30	13,6	19.11.1992 11:20	11,3
20.11.1992 11:40	0,81	20.11.1992 11:30	11,9	20.11.1992 11:20	10
23.11.1992 11:40	0,84	23.11.1992 11:30	8,5	23.11.1992 11:20	7,4
23.11.1992 11:40	0,78	25.11.1992 11:30	6,9	25.11.1992 11:20	6,2
27.11.1992 11:40	0,75	27.11.1992 11:30	5,9	27.11.1992 11:20	5,3
30.11.1992 11:40	0,79	30.11.1992 11:30	5,3	30.11.1992 11:20	4,7
04.12.1992 11:40	0,68	04.12.1992 11:30	4,4	04.12.1992 11:20	3,7
08.12.1992 11:40	0,66	08.12.1992 11:30	3,7	10.12.1992 11:20	3,1
16.12.1992 11:40	0,67	16.12.1992 11:30	3	16.12.1992 11:20	2,6
25.01.1993 11:40	0,26	25.01.1993 11:30	0,145	25.01.1993 11:20	1

[ ] Concentration in microgramm/ liter

Table 3C4-2 Amidorhodamine G results - 1992 tracer experiment.

Time	[ ]	Time	[ ]	Time	[ ]	Time	[ ]	Time	[ ]	Time	[ ]	Time	[ ]
C1	C1	C3	C3	C4	C4	C5	C5	C6	C6	C7	C7		
10.11.1992 09:50	0	10.11.1992 10:00	0	10.11.1992 10:00	0	10.11.1992 10:00	0	10.11.1992 10:00	0	10.11.1992 10:00	0		
				10.11.1992 19:15	0	10.11.1992 19:10	0	10.11.1992 19:05	0	10.11.1992 19:03	0,3		
10.11.1992 16:50	0	10.11.1992 19:30	0	10.11.1992 16:25	0,004	10.11.1992 16:10	0,99	10.11.1992 16:55	0,63	10.11.1992 15:42	0,02		
10.11.1992 19:45	0	10.11.1992 23:10	0	10.11.1992 19:18	0,017	10.11.1992 19:00	2,82	10.11.1992 18:54	0,33	10.11.1992 19:40	0,04		
10.11.1992 21:20	0			10.11.1992 21:01	0,44	10.11.1992 20:52	0,43	10.11.1992 20:46	0,07	10.11.1992 20:26	0,03		
11.11.1992 10:12	0,118	11.11.1992 10:05	0,06	11.11.1992 09:58	13,7	11.11.1992 09:51	11,9	11.11.1992 09:44	2,53	11.11.1992 09:37	0,23		
				10.11.1992 12:40	21	10.11.1992 11:59	20,3	10.11.1992 11:51	5,56	10.11.1992 11:45	0,26		
11.11.1992 17:30	0,72			11.11.1992 17:20	20	11.11.1992 17:10	28	11.11.1992 17:10	9,33	11.11.1992 17:00	0,62		
12.11.1992 10:00	2,17	12.11.1992 09:50	0,91	12.11.1992 09:40	27,3	12.11.1992 09:30	28	12.11.1992 09:20	9,67	12.11.1992 09:10	0,01		
12.11.1992 16:00	2,42	12.11.1992 17:50	0,28	12.11.1992 17:45	27,3	12.11.1992 17:30	32	12.11.1992 17:20	7,24	13.11.1992 17:10	0,02		
13.11.1992 10:30	1,38	13.11.1992 10:20	0,105	13.11.1992 09:40	19,7	13.11.1992 09:30	27	13.11.1992 09:20	7,01	13.11.1992 09:40	0,02		
13.11.1992 17:00	3,54	13.11.1992 10:20	0,3	13.11.1992 10:40	11,8	13.11.1992 10:30	25	13.11.1992 16:20	7,51	13.11.1992 16:10	0,03		
14.11.1992 11:50	3,12	14.11.1992 10:51	0,093	14.11.1992 10:40	8,9	14.11.1992 10:30	20,3	14.11.1992 10:20	5,44	14.11.1992 10:10	0,02		
28.11.1992 11:00	2,6	16.11.1992 10:20	0,07	16.11.1992 10:40	8,66	16.11.1992 10:20	11,58	16.11.1992 10:20	0,96	16.11.1992 10:10	0,02		
17.11.1992 11:00	1,07	17.11.1992 10:51	0,153	17.11.1992 10:40	8,66	17.11.1992 10:30	8,66	17.11.1992 10:20	0,36	17.11.1992 10:10	0,01		
18.11.1992 10:03	0,62	18.11.1992 10:50	0,11	18.11.1992 10:40	3,23	18.11.1992 10:30	6,66	18.11.1992 10:50	1,66	28.11.1992 10:10	0,01		
19.11.1992 11:00	0,71	19.11.1992 10:50	0,085	19.11.1992 10:40	2,9	19.11.1992 10:20	4,39	19.11.1992 10:00	3,93	19.11.1992 10:10	0,01		
20.11.1992 11:00	0,62	20.11.1992 10:50	0,092	20.11.1992 10:40	2,1	20.11.1992 10:01	3,71	20.11.1992 10:20	2,3	20.11.1992 10:10	0,28		
23.11.1992 11:00	0,25	23.11.1992 10:01	0,07	23.11.1992 10:40	1,23	23.11.1992 10:30	6,66	23.11.1992 10:20	1,49	23.11.1992 10:10	0,37		
25.11.1992 11:00	0,91	25.11.1992 10:50	0,088	25.11.1992 10:40	1,01	25.11.1992 10:20	1,54	25.11.1992 10:50	1,05	25.11.1992 10:10	0,47		
27.11.1992 11:00	0,19	27.11.1992 10:01	0,06	27.11.1992 10:40	0,85	27.11.1992 10:30	1,13	27.11.1992 10:20	0,78	27.11.1992 10:10	0,16		
28.11.1992 11:00	0,1	30.11.1992 10:01	0,085	30.11.1992 10:40	0,56	30.11.1992 10:01	0,9	30.11.1992 10:20	2,44	30.11.1993 10:20	0,08		
04.12.1992 11:00	0,08	04.12.1992 10:50	0,019	04.12.1992 10:01	0,35	04.12.1992 10:20	0,57	04.12.1992 10:20	0,42	04.12.1992 10:10	0,2		
08.12.1992 11:00	0,44	08.12.1992 10:51	0,026	10.12.1992 10:40	0,31	10.12.1992 10:00	0,33	10.12.1992 10:20	0,35	10.12.1992 10:20	0,16		
14.12.1992 11:00	0,3	08.12.1992 10:01	0,01	10.12.1992 10:40	0,21	10.12.1992 10:00	0,31	16.12.1992 10:20	0,14	16.12.1992 10:15	0,17		
25.01.1993 11:00	0,16	25.01.1993 10:51	0,009	25.01.1993 10:01	0,05	25.01.1993 10:00	0,075	25.01.1993 10:20	0,04	25.01.1993 10:10	0,009		

Time	[ ]	Time	[ ]	Time	[ ]	Time	[ ]	Time	[ ]	Time	[ ]	Time	[ ]
C8	C8	C9	C9	D1	D1	D2	D2	D3	D3	D4	D4		
10.11.1992 10:00	0	10.11.1992 10:00	0	10.11.1992 09:00	0	10.11.1992 10:00	0	10.11.1992 10:00	0	10.11.1992 10:00	0		
10.11.1992 15:30	0	10.11.1992 17:00	0	10.11.1992 09:51	0	10.11.1992 17:55	0	10.11.1992 17:45	0	10.11.1992 17:33	0		
10.11.1992 19:40	0	10.11.1992 20:40	0										
10.11.1992 20:26	0	10.11.1992 21:50	0,11	10.11.1992 12:20	0	10.11.1992 22:01	0	10.11.1992 22:11	0,05	10.11.1992 22:09	0		
11.11.1992 09:30	0,03	11.11.1992 10:20	0,01	11.11.1992 11:30	0,045	11.11.1992 11:21	0	11.11.1992 11:13	0,08	11.11.1992 11:50	0		
11.11.1992 09:20	0,28	11.11.1992 10:00	0,21	11.11.1992 10:25	0,08	11.11.1992 14:20	0	11.11.1992 10:21	2,44	11.11.1992 16:18	0		
12.11.1992 09:00	1,19	12.11.1992 10:20	1,13	12.11.1992 11:20	0,295	12.11.1992 10:13	0,09	12.11.1992 10:45	6,57	12.11.1992 10:39	1,04		
13.11.1992 17:00	1,32	12.11.1992 18:10	1,49	12.11.1992 14:58	0,36	12.11.1992 18:53	0,23	13.11.1992 10:09	7,46	12.11.1992 19:00	1,3		
13.11.1992 09:30	1,98	13.11.1992 10:03	1,62	13.11.1992 11:30	0,28	13.11.1992 11:00	0,78	13.11.1992 11:50	9,08	13.11.1992 13:20	2,49		
13.11.1992 16:00	2,01	13.11.1992 19:30	1,68	13.11.1992 16:20	0,38	13.11.1992 18:50	1,01	13.11.1992 10:02	9,2	13.11.1992 17:50	3,18		
14.11.1992 09:50	2,16	14.11.1992 11:50	1,64	14.11.1992 11:20	0,245	14.11.1992 12:20	0,66	14.11.1992 12:00	9,19	14.11.1992 11:50	4,91		
16.11.1992 09:00	2,62	16.11.1992 11:30	0,98	10.11.1992 12:50	0,11	16.11.1992 11:20	2,21	16.11.1992 11:00	8,68	16.11.1992 11:50	3,76		
17.11.1992 09:50	2,62	17.11.1992 11:30	0,95	17.11.1992 12:20	0,36	17.11.1992 12:00	4,3	17.11.1992 12:00	8,98	17.11.1992 11:50	3,96		
18.11.1992 09:00	1,85	18.11.1992 11:30	0,31	18.11.1992 12:50	0,31	18.11.1992 14:20	5,26	18.11.1992 12:00	6,54	28.11.1992 11:50	3,21		
19.11.1992 09:00	1,75	19.11.1992 11:50	0,60	19.11.1992 12:50	0,24	19.11.1992 12:20	4,82	19.11.1992 11:00	5,71	19.11.1992 11:50	2,78		
20.11.1992 09:00	1,52	20.11.1992 11:30	0,58	20.11.1992 12:20	0,34	20.11.1992 12:20	3,47	20.11.1992 12:50	5,47	20.11.1992 11:50	3,86		
21.11.1992 09:00	1,02	21.11.1992 11:10	0,39	21.11.1992 12:20	0,37	21.11.1992 14:01	0,6	23.11.1992 12:50	3,53	21.11.1992 11:50	1,53		
23.11.1992 09:00	0,65	23.11.1992 11:10	0,29	23.11.1992 12:50	0,22	23.11.1992 12:50	4,3	23.11.1992 11:00	3,45	23.11.1992 11:50	1,27		
27.11.1992 10:00	0,98	27.11.1992 11:10	0,25	27.11.1992 12:20	0,22	27.11.1992 11:20	1	27.11.1992 11:00	3,14	27.11.1992 11:50	0,91		
30.11.1992 09:50	0,91	30.11.1992 11:30	0,195	30.11.1992 12:20	0,22	30.11.1992 12:20	2,73	30.11.1992 12:00	1,72	30.11.1992 11:50	0,91		
04.12.1992 09:00	0,38	04.12.1992 14:58	0,165	04.12.1992 12:20	0,08	04.12.1992 12:20	1,58	04.12.1992 12:00	1,16	04.12.1992 11:50	0,6		
10.12.1992 09:00	0,91	08.12.1992 11:50	0,1	10.12.1992 08:20	0,07	10.12.1992 12:10	1,14	10.12.1992 12:00	0,72	10.12.1992 11:50	0,78		
16.12.1992 10:00	0,11	16.12.1992 11:50	0,07	16.12.1992 12:20	0,17	16.12.1992 12:10	0,54	16.12.1992 12:00	0,3	16.12.1992 16:53	0,005		
25.01.1993 10:00	0,03	25.01.1993 11:50	0,03	25.01.1993 12:20	0,01	25.01.1992 12:10	0,78	25.01.1992 11:00	0,085	25.01.1993 11:50	0,1		

Time	[ ]	Time	[ ]	Time	[ ]
D5	D5	D6	D6	D7	D7
10.11.1992 10:00	0	10.11.1992 10:00	0	10.11.1992 10:00	0
10.11.1992 17:26	0	10.11.1992 17:17	0	10.11.1992 17:10	0
10.11.1992 22:53	0	10.11.1992 21:47	0	10.11.1992 21:40	0,01
11.11.1992 10:55	0	11.11.1992 10:47	0,015	11.11.1992 10:30	0,11
11.11.1992 10:41	0	11.11.1992 10:00	0,17	11.11.1992 10:00	0,16
12.11.1992 10:53	0,01	12.11.1992 10:26	1,1	12.11.1992 09:50	0,91
12.11.1992 10:53	0,00	12.11.1992 10:43	1,85	12.11.1992 10:20	1,07
13.11.1992 11:10	0,11	13.11.1992 11:00	2,74	13.11.1992 09:50	1,41
13.11.1992 17:40	0,24	13.11.1992 17:30	0,47	13.11.1992 17:20	1,07
14.11.1992 11:40	0,91	14.11.1992 11:30	3,44	14.11.1992 11:20	1,61
16.11.1992 11:40	0,01	16.11.1992 11:03	1,9	16.11.1992 11:20	1,38
17.11.1992 12:40	0,7	17.11.1992 11:50	1,65	17.11.1992 11:20	1,34
18.11.1992 11:40	0,64	18.11.1992 11:30	1,45	18.11.1992 11:20	1,05
19.11.1992 11:40	0,39	19.11.1992 11:30	1,13	19.11.1992 11:20	0,31
20.11.1992 11:40	0,91	20.11.1992 11:30	0,16	20.11.1992 11:00	0,79
23.11.1992 11:40	0,46	23.11.1992 11:30	0,74	23.11.1992 11:20	0,01
23.11.1992 11:40	0,35	23.11.1992 11:30	0,47	23.11.1992 11:20	0,11
27.11.1992 11:40	0,31	27.11.1992 11:30	0,01	27.11.1992 11:20	0,31
30.11.1992 11:40	0,29	30.11.1992 11:30	0,31	30.11.1992 11:20	0,11
04.12.1992 11:40	0,11	04.12.1992 11:30	0,31	04.12.1992 11:00	0,31
10.12.1992 11:40	0,16	10.12.1992 11:30	0,11	10.12.1992 11:50	0,01
16.12.1992 11:40	0,11	16.12.1992 11:30	0,085	16.12.1992 11:20	0,05
25.01.1993 11:40	0,013	25.01.1993 11:30	0,045	25.01.1992 11:20	0,022

[ ] Concentration in microgramm/ liter

Table 3C4-3 Uranine results - 1992 tracer experiment .

Table 3C4-4 Na-Naphtionate breakthrough curves at the observation wells C8, C7, C6 & C5.

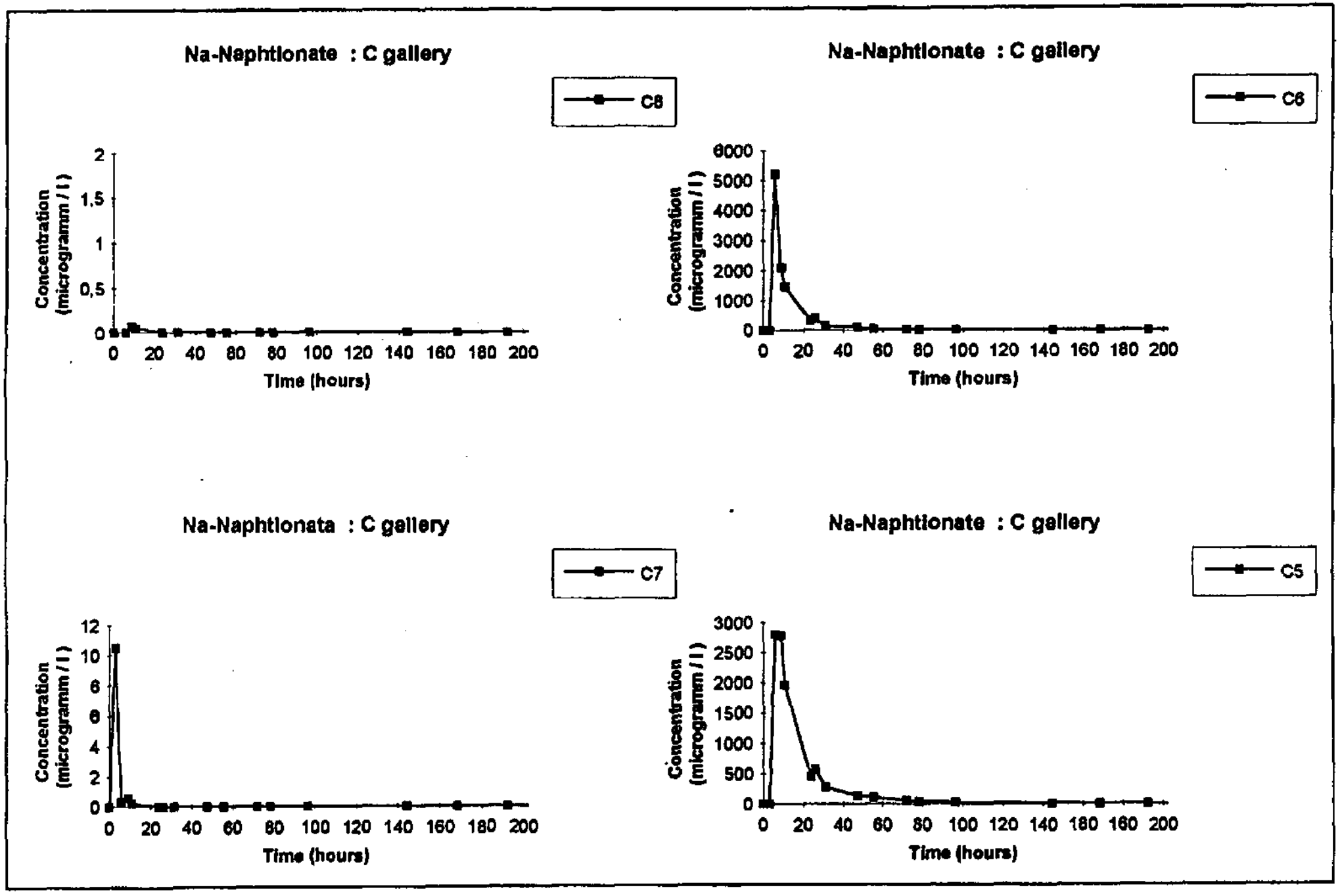

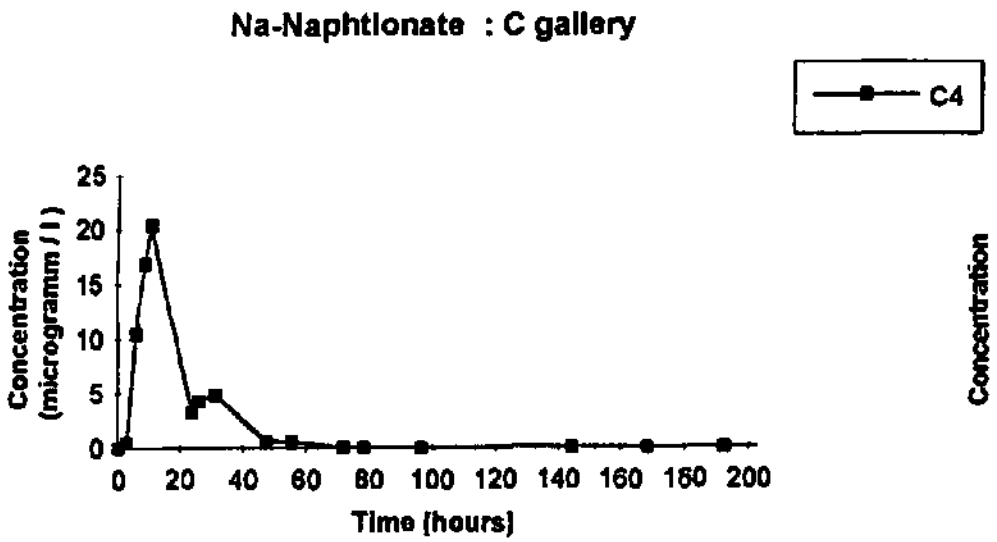
Na-Naphtionate : C gallery
C4
Concentration (microgramm / l)
25
20
15
10
5
0
0 20 40 60 80 100 120 140 160 180 200
Time (hours)

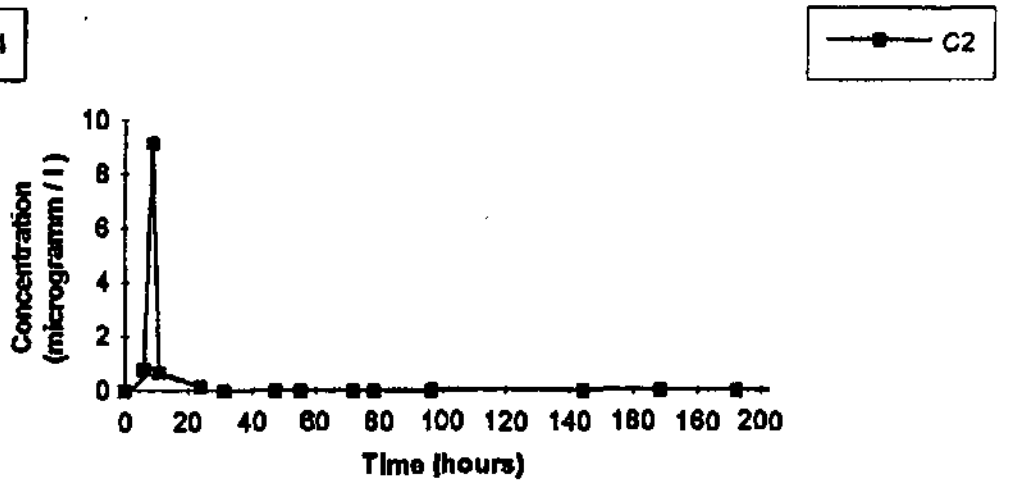
Na-Naphtionate : C gallery
C2
Concentration (microgramm / l)
10
8
6
4
2
0
0 20 40 60 80 100 120 140 160 180 200
Time (hours)

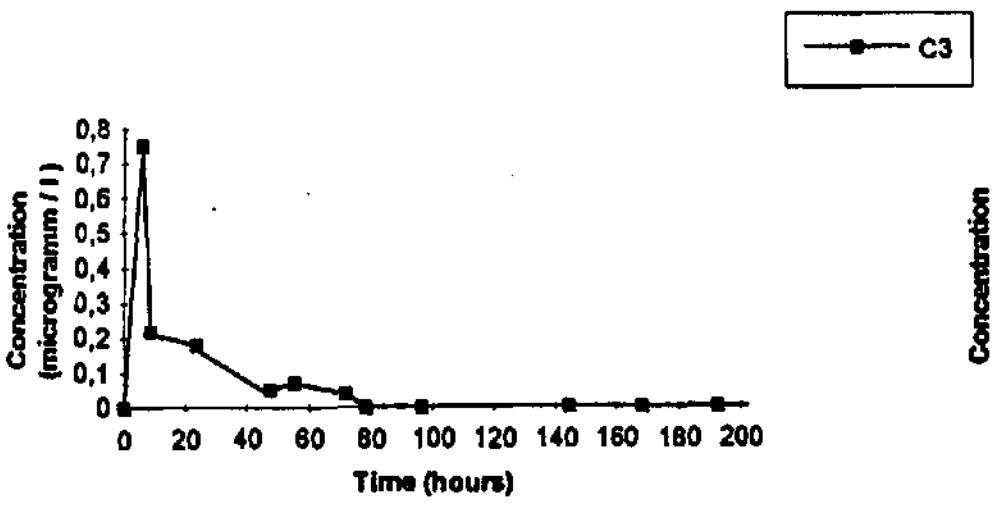
Na-Naphtionate : C gallery
C3
Concentration (microgramm / l)
0,8
0,7
0,6
0,5
0,4
0,3
0,2
0,1
0
0 20 40 60 80 100 120 140 160 180 200
Time (hours)

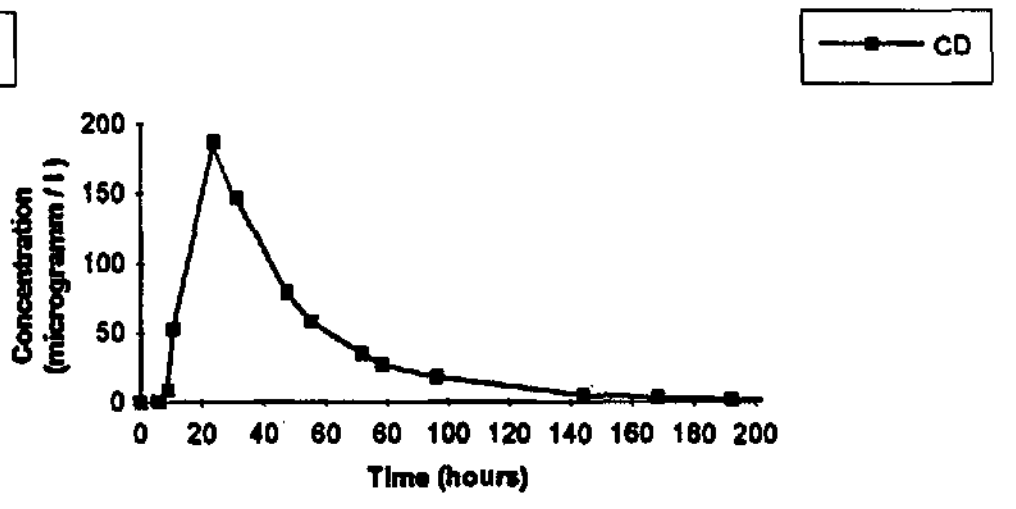
Na-Naphtionate : C gallery
CD
Concentration (microgramm / l)
200
150
100
50
0
0 20 40 60 80 100 120 140 160 180 200
Time (hours)

Table 3C4-6 Na-Naphtionate breakthrough curves at the observation wells D7, D6, D5 & D4.

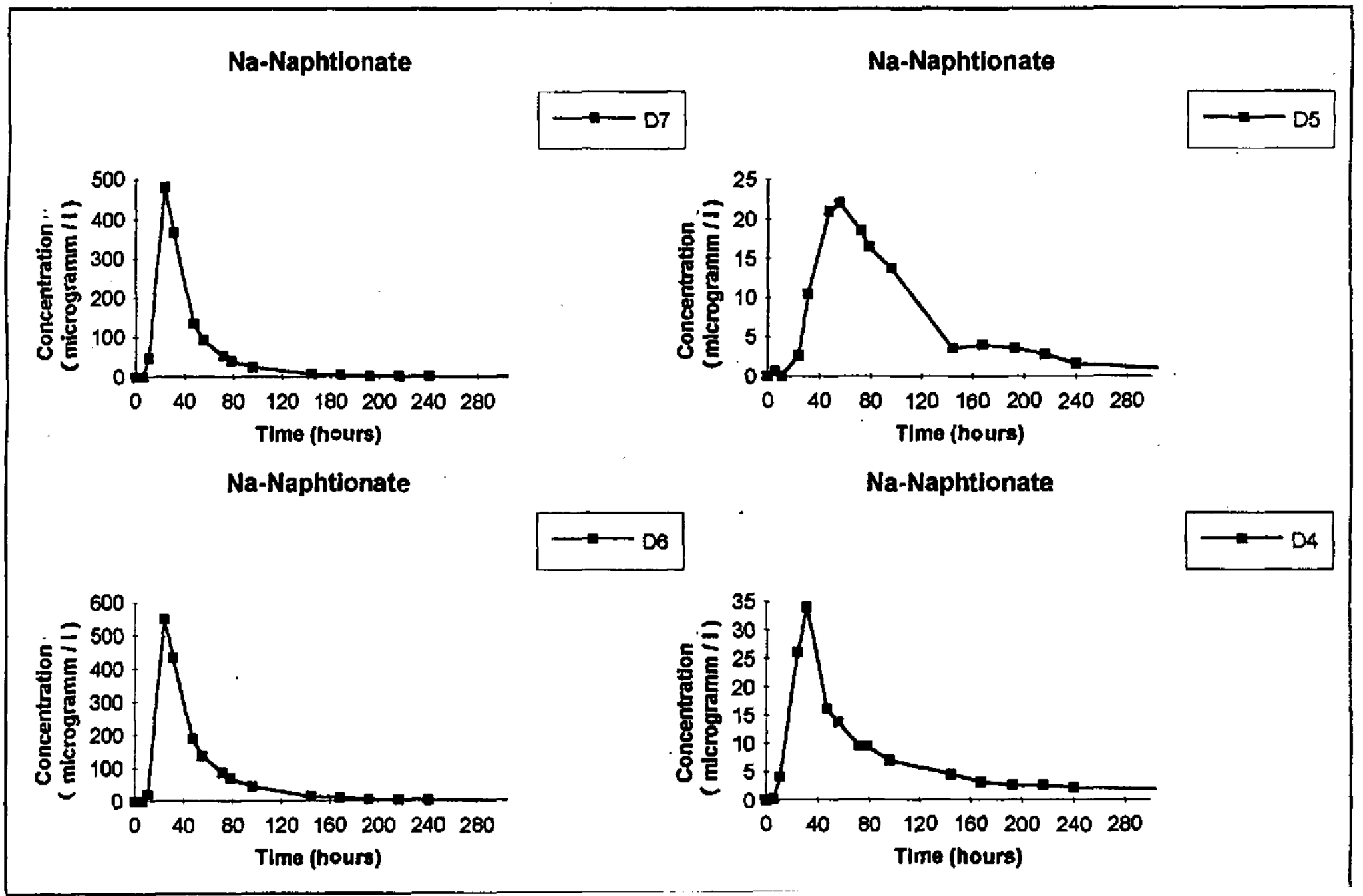

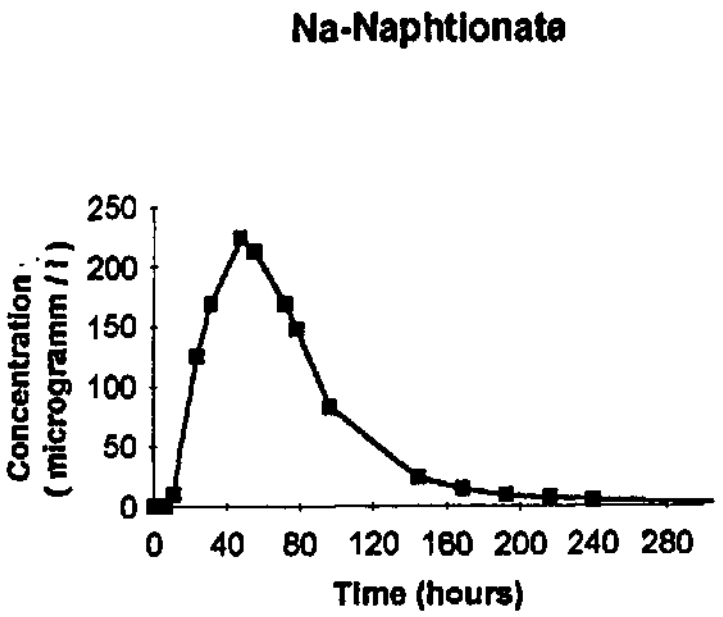
Na-Naphtionate
D3
Concentration (microgramm / l)
250
200
150
100
50
0
0 40 80 120 160 200 240 280
Time (hours)

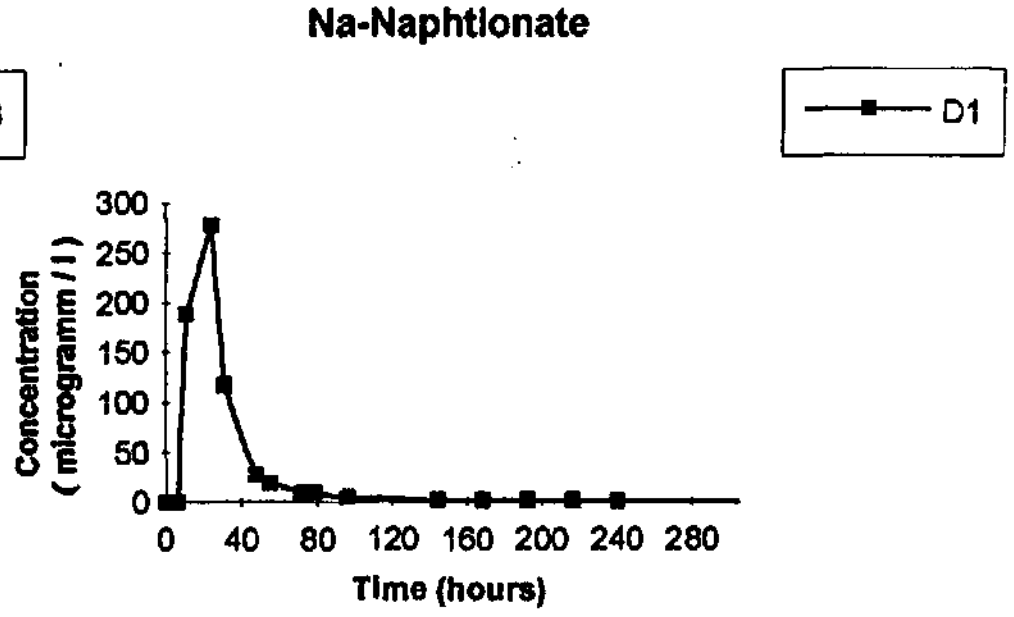
Na-Naphtionate
D1
Concentration (microgramm / l)
300
250
200
150
100
50
0
0 40 80 120 160 200 240 280
Time (hours)

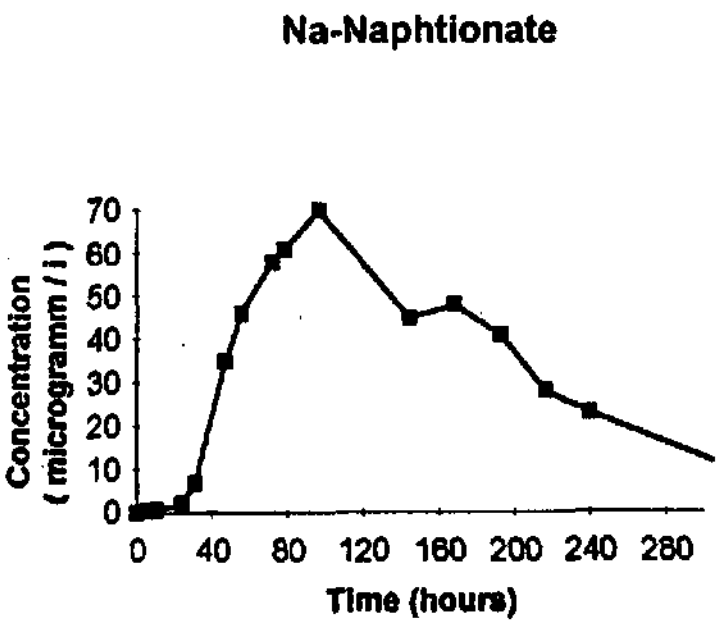
Na-Naphtionate
D2
Concentration (microgramm / l)
70
60
50
40
30
20
10
0
0 40 80 120 160 200 240 280
Time (hours)

Table 3C4-9 Amidorhodamine G breakthrough curves at the observation wells C8, C7, C6 & C5.

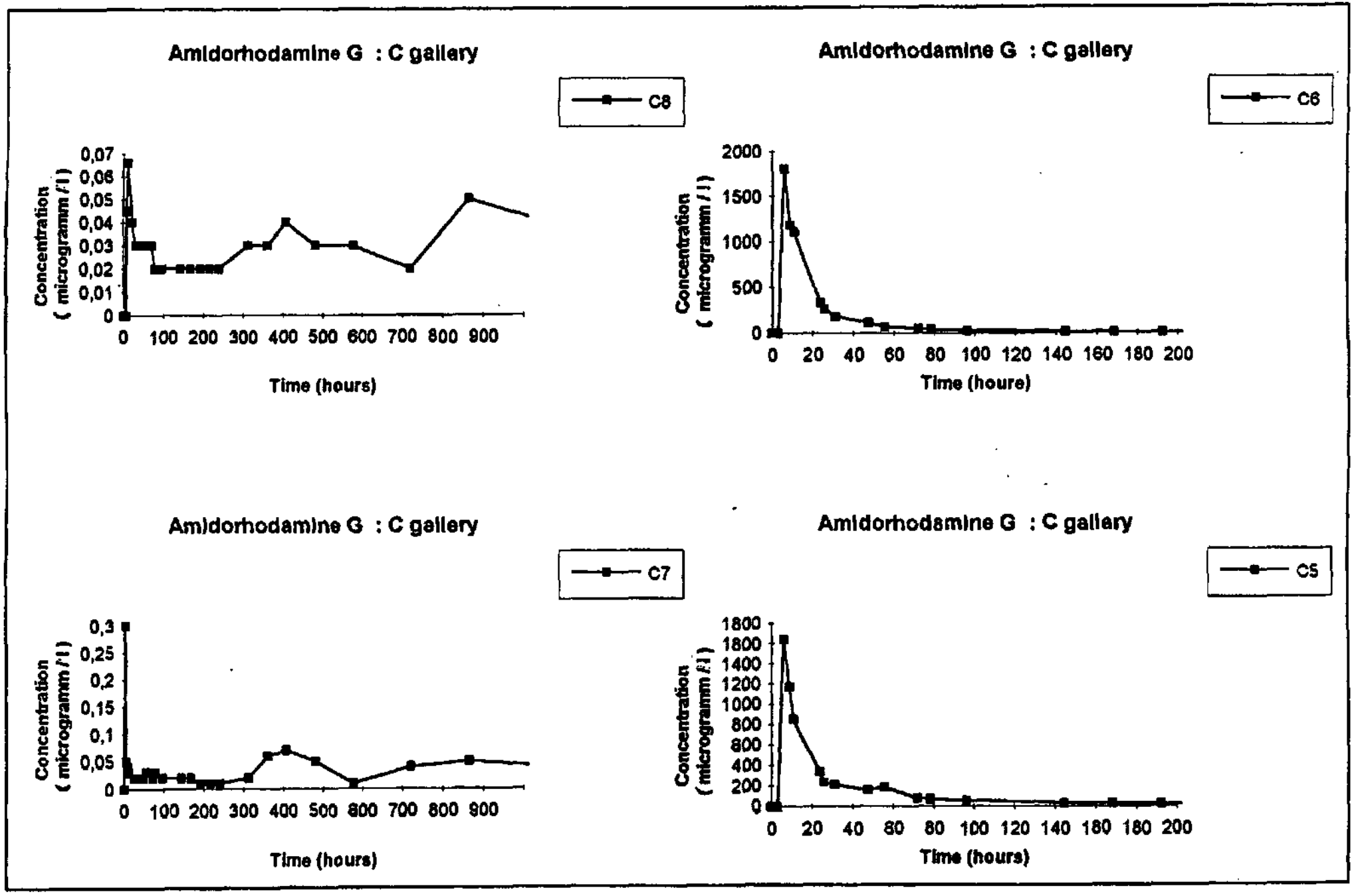

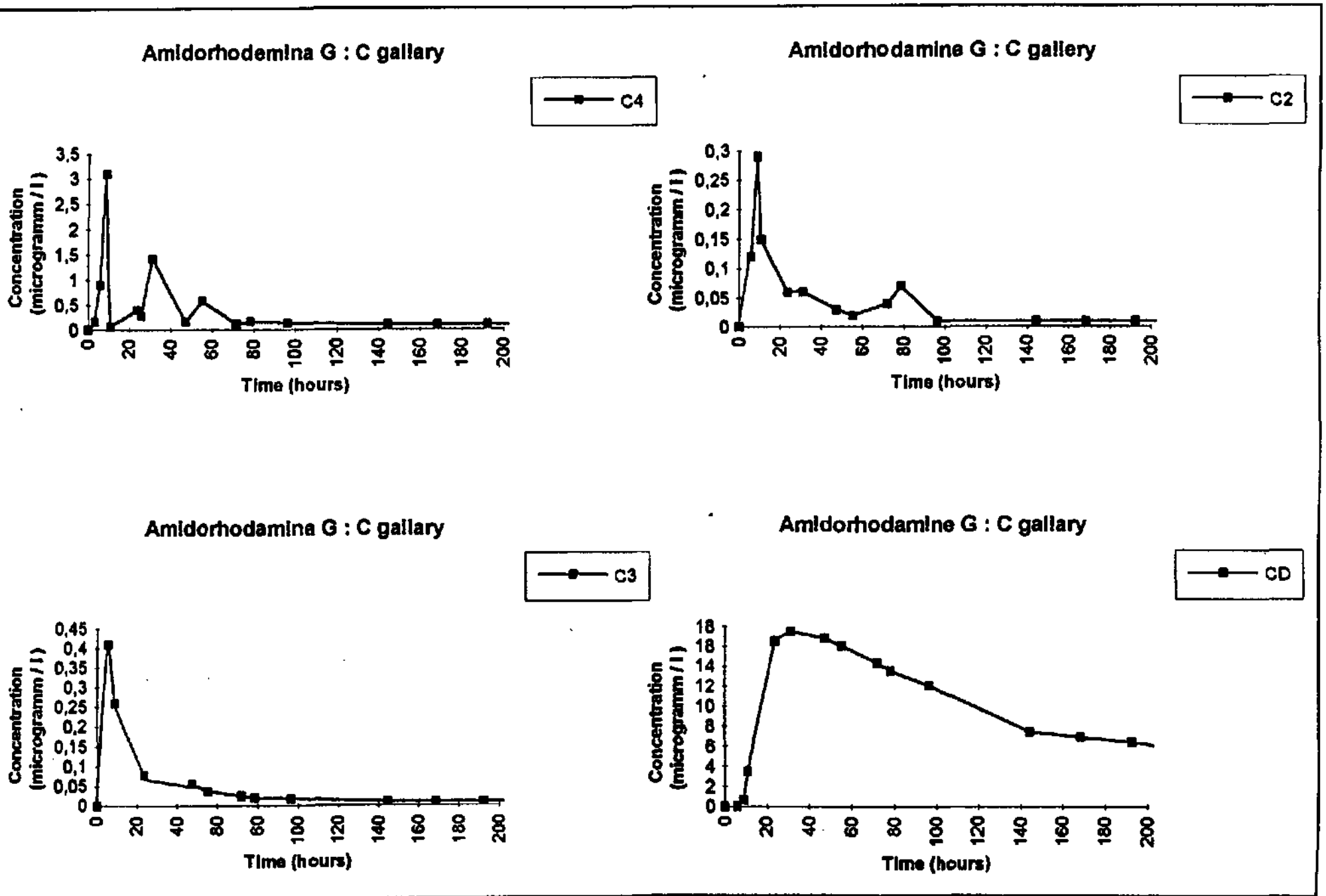
Amidorhodemina G : C gallary
C4
Concentration (microgramm / l)
Time (hours)
Amidorhodamine G : C gallery
C2
Concentration (microgramm / l)
Time (hours)
Amidorhodamina G : C gallary
C3
Concentration (microgramm / l)
Time (hours)
Amidorhodamine G : C gallary
CD
Concentration (microgramm / l)
Time (hours)

Table 3C4-11 Amidorhodamine G breakthrough curves at the observation wells D7, D6, D5 & D4.

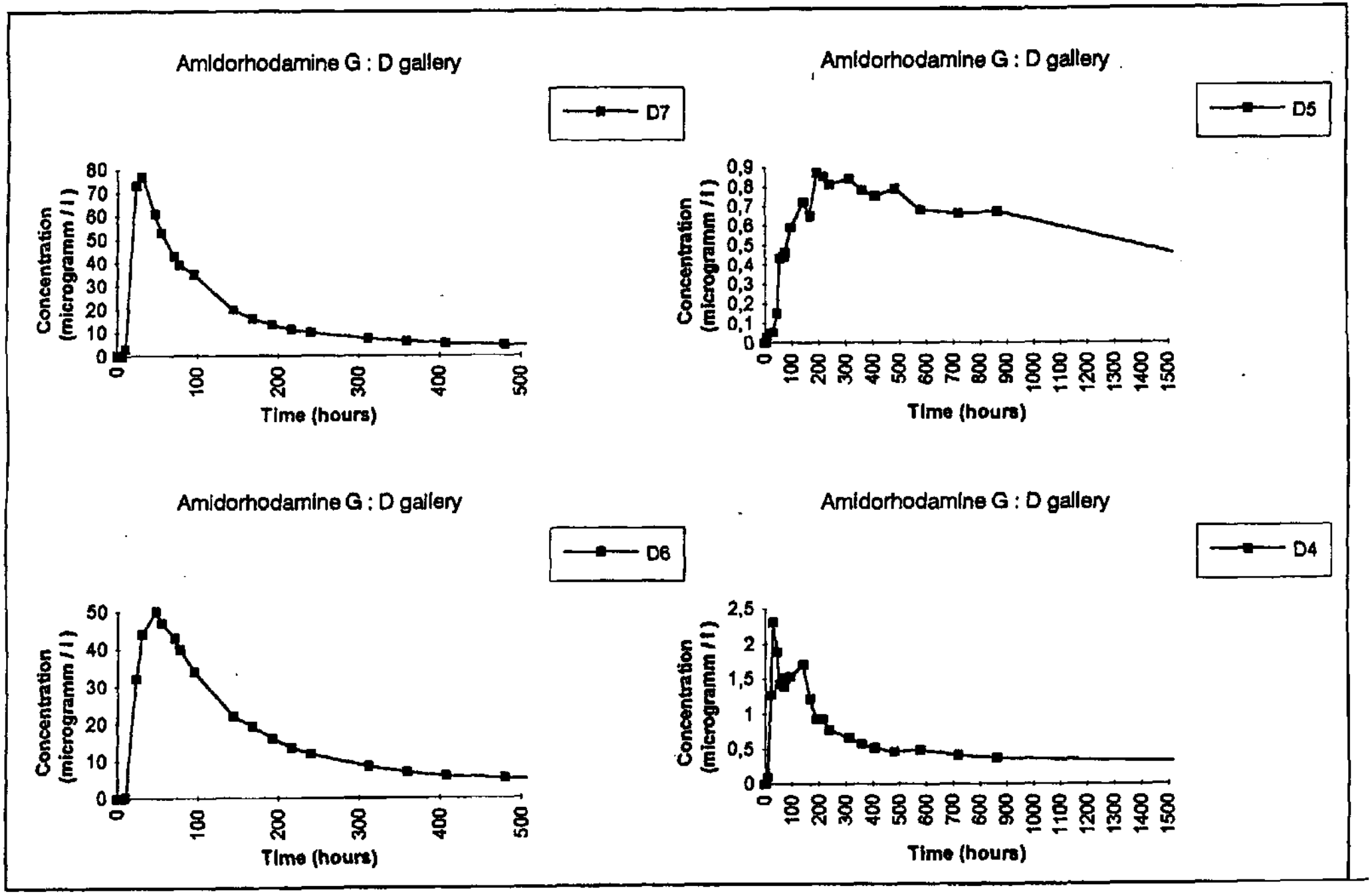

Table 3C4-12 Amidorhodamine G breakthrough curves at the observation wells D3, D2, & D1.

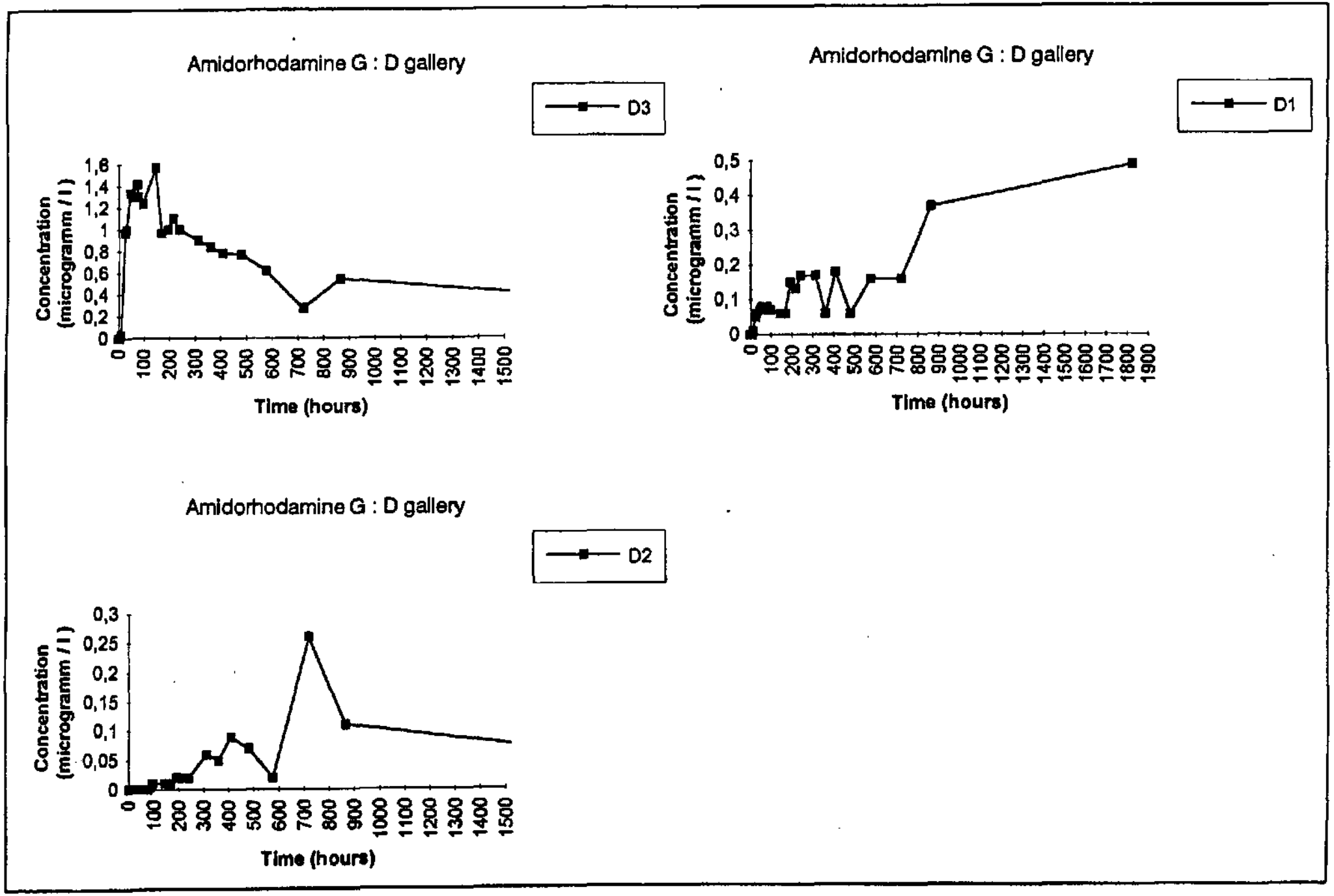

Table 3C4-13 Uranine breakthrough curves at the observation wells C8, C7, C6 & C5.

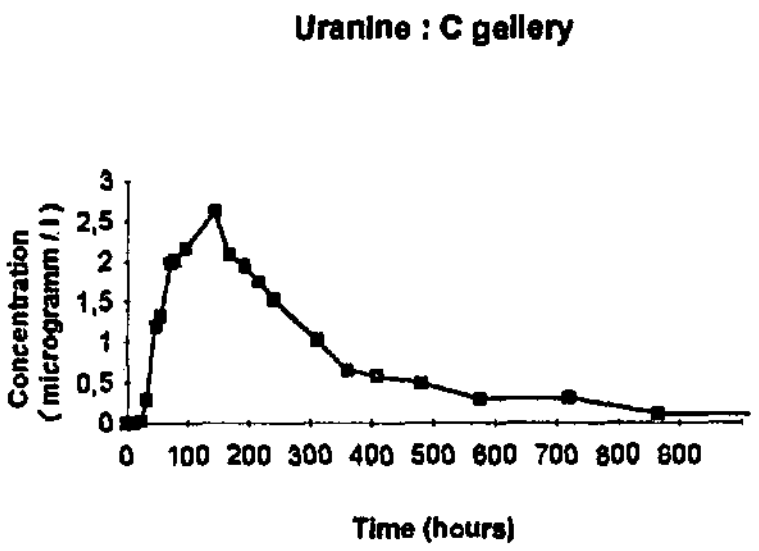

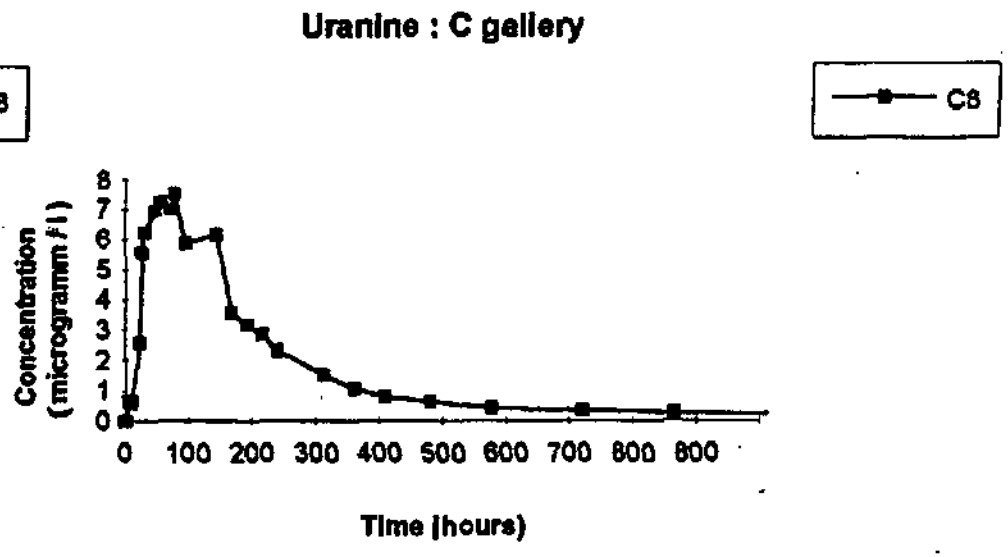

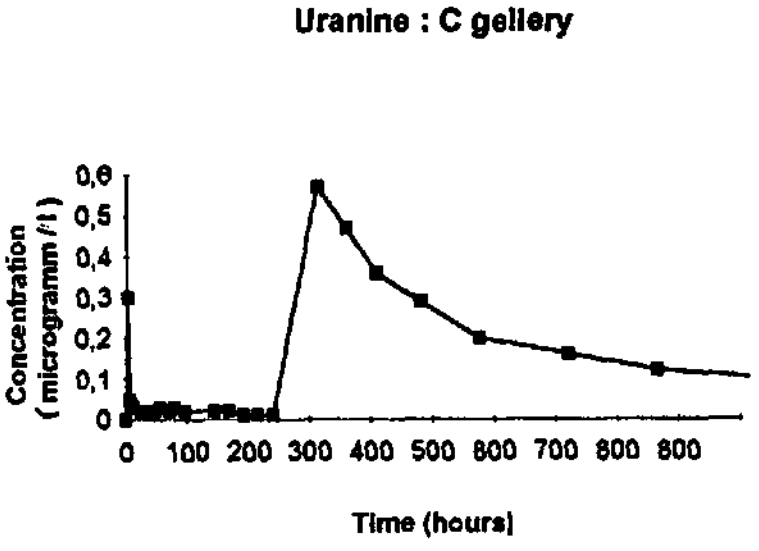

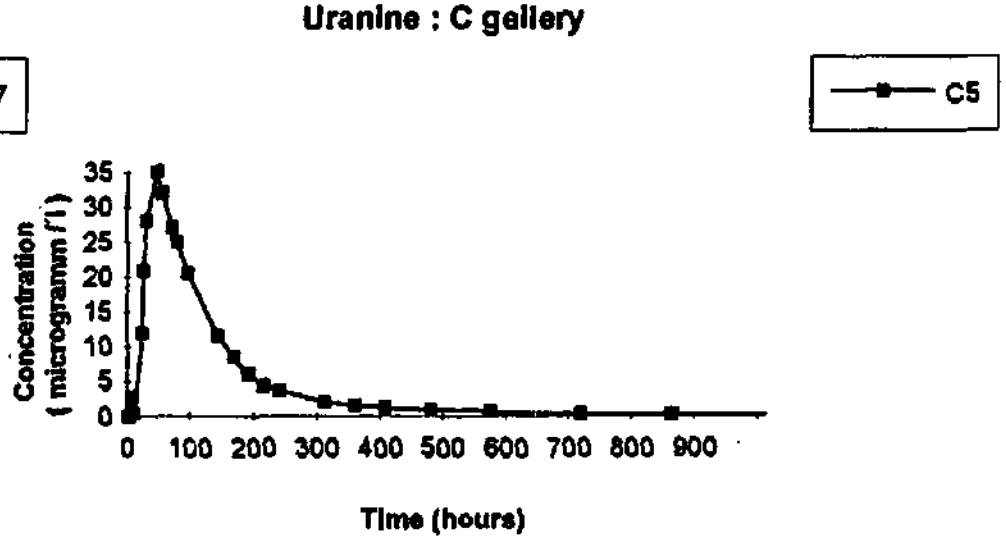

Table 3C4-14 Uranine breakthrough curves at the observation wells C4, C3, C3 & CD.

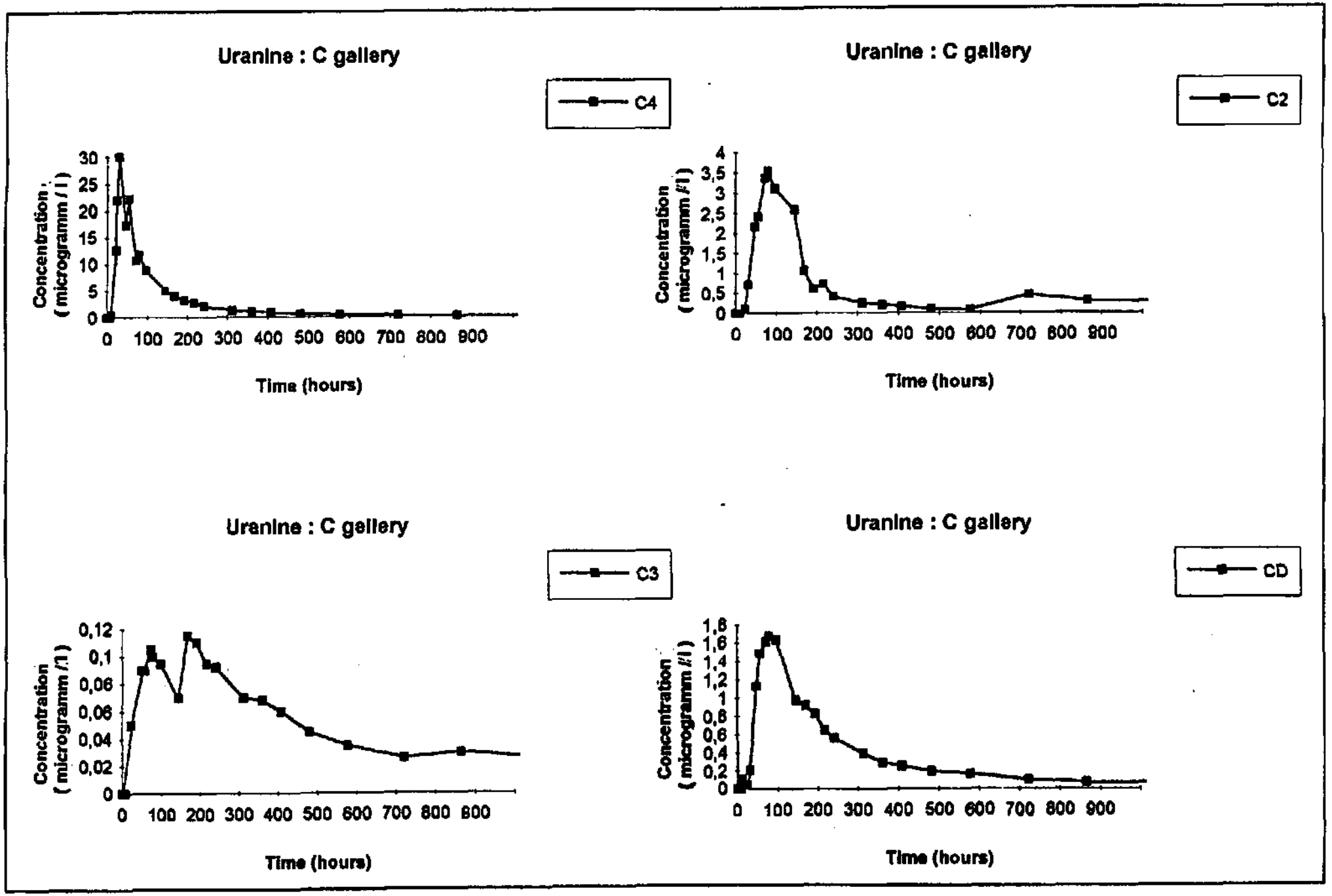

Table 3C4-15 Uranine breakthrough curves at the observation wells D7, D6, D5 & D4.

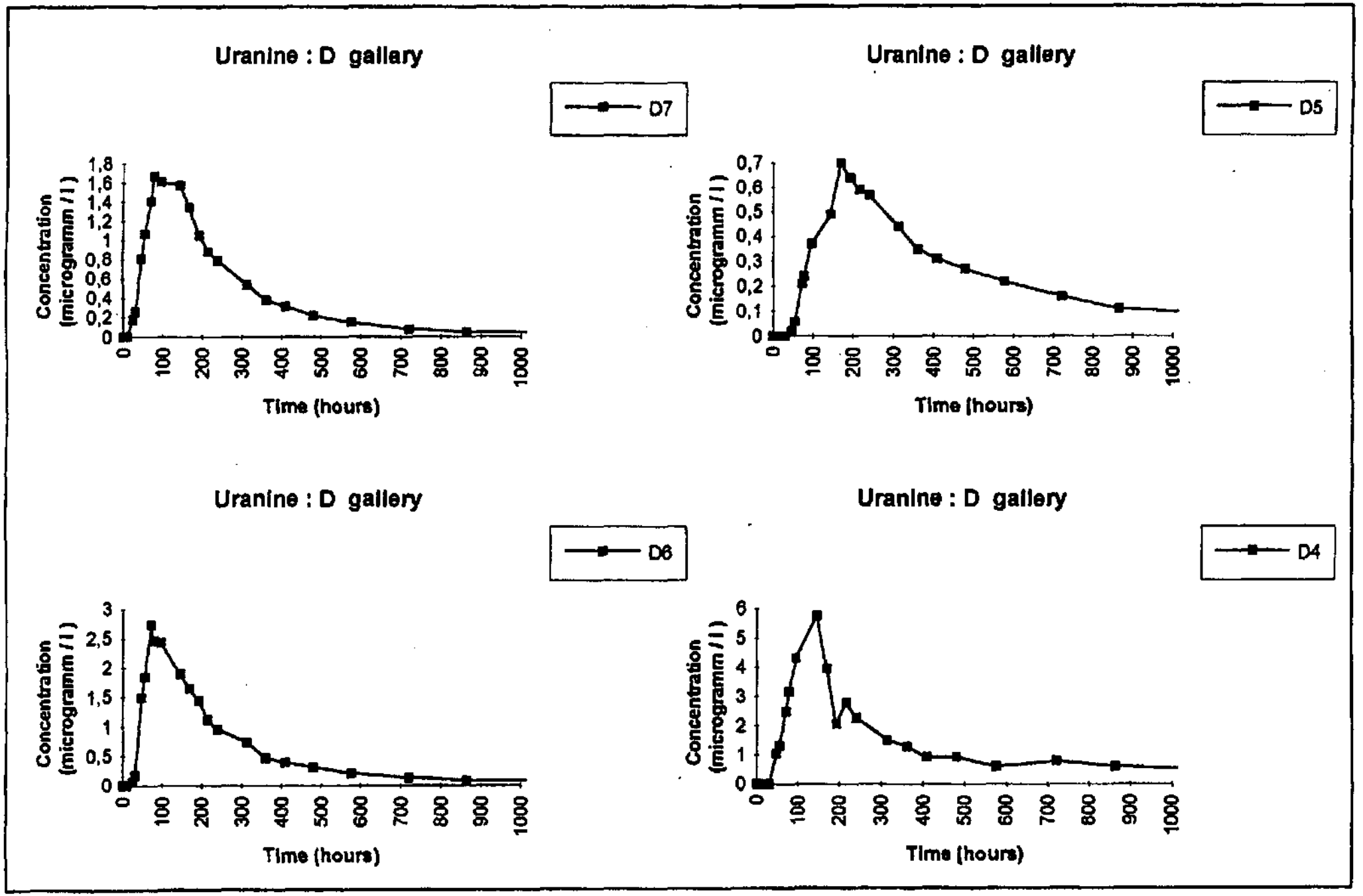

Table 3C.4-16 Uranine breakthrough curves at the observation wells D3, D2, & D1.

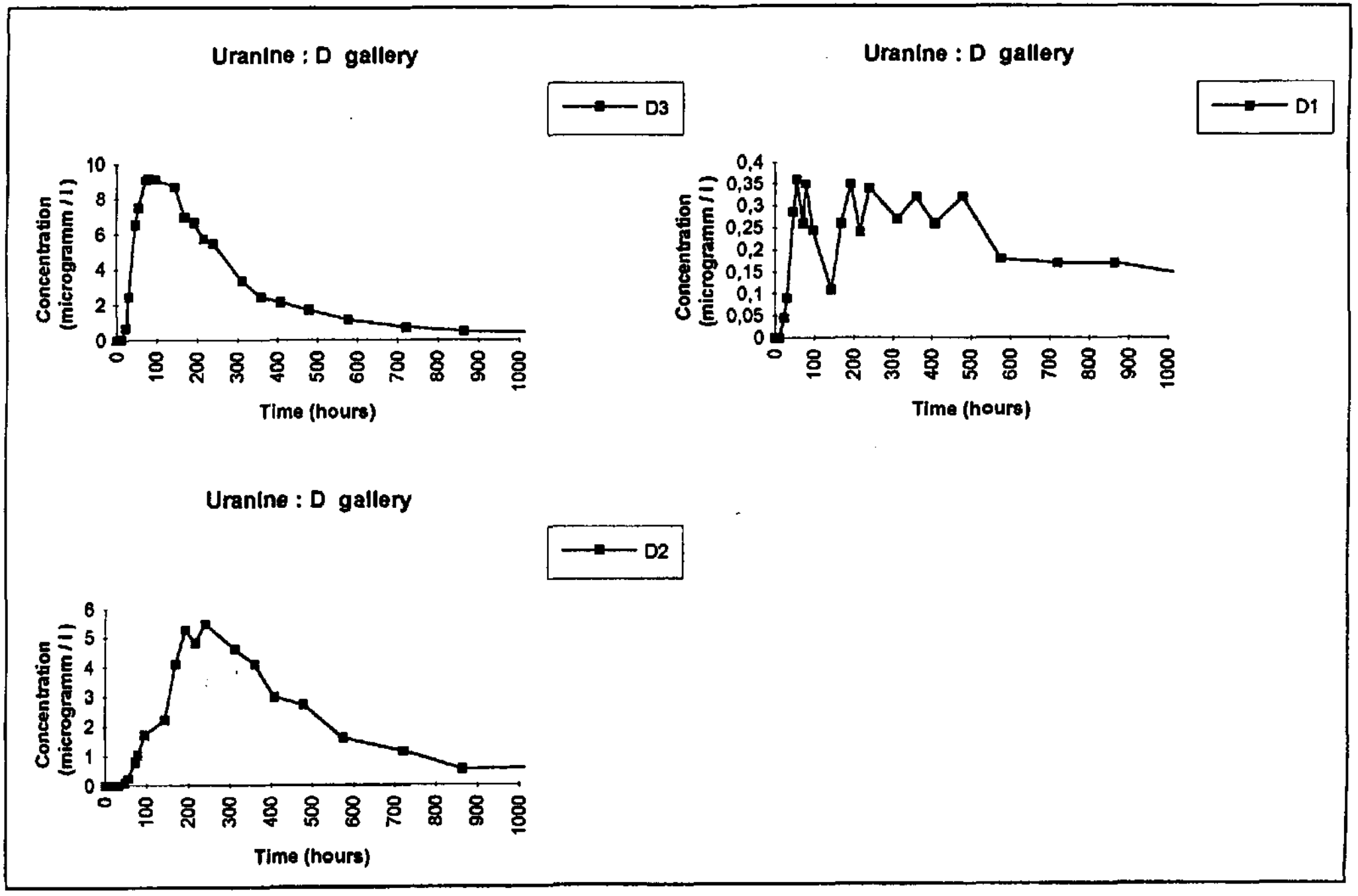

Curriculum vitae

Amélia de Carvalho Dill
Unidade de Ciências e Tecnologias dos Recursos Aquáticos
(UCTRA)
Universidade do Algarve
Campus de Gambelas
8000 Faro (Portugal)
Phone: 89 - 817166 ; Fax: 89 - 818353

Amélia de Carvalho Dill was born in Lisbon in 1955. She lived for 12 years in Mozambique, where she went to High School in Maputo. In 1974 she started her studies in Geology at the Universidade de Lourenço Marques (today Maputo). After the independence was proclaimed (1975), the University closed and she was forced to move to Lisboa. She obtained her degree (Licenciatura) in Geology at the Universidade Clássica de Lisboa in 1981. In 1982 she completed a post-graduate degree in Geology for Civil Engineering (Geotecnic) at the Universidade Nova de Lisboa.

She then worked as an assistant at the Universidade de Trás-os-Montes e Alto Douro, in 1983. Since 1985 she is linked to the University of the Algarve. In 1987 she received a portuguese scholarship to contioue her studies in Switzerland . She succesfully presented her doctorate dissertation (Ph.D) in 1993.

She is a member of the I' International Association of Tracer Hydrologists and is co-author of the folllowing papers:

Carvalho Dill, A.; Gerlinger, K., Hahn, T., Hötzl, H., Käss, W., Leibundgut, Ch., Maloszewski, P., Müller, I., Oetzel S., Rank, D., Teutsch, G., Werner, A. (1992).- Porous aquifer- testsite Merdingen (Germany). Steir. Beitr. z. Hydrogeologie, 43, 251-280, Graz.

Carvalho Dill, A., Müller, I.(1992). Comparative results to structure analyses in the porous aquifer testsite Wilerwald (BE, Switzerland) with very low frequency geophysics : VLF-R, VLF-EM. in Tracer Hydrology, Hötzl&Werner (eds), 139-142.Balkema, Rotterdam.

Leibundgut,CH., Carvalho Dill,A., Maloszewski,P.,Müller,I. and Schneider, J. (1992).- Investigation of solute transport in the porous aquifer of the test site Wilerwald (Switzerland). Steir. Beitr. z. Hydrogeologie, 43, 229-250, Graz.

Rossi, P., Carvalho Dill, A., Müller, I. & Aragno, M. (1993)- Comparative tracing experiments in a porous aquifer using bacteriophages and fluorescent dye on a test field located at Wilerwald (Switzerland) and simultaneously surveyed in detail on local scale by Radio-Magneto-Tellury (12-240 kHz). J. Environmental Geology, in Press.

Steiner,T., de Carvalho Dill, A., Szarka, L. & Müller, I.(1992).- Comparative studies of VLF-R and VLF-EM geophysical methods; 1-D and 2-D numerical modelling at the tracer test-field Wilerwald (BE, Switzerland) - Bull. du Centre d'hydrogeologie de l'Université de Neuchâtel, 11 ,97-112.

Amélia de Carvalho Dill est née à 1955 à Lisbonne. Elle a vecu 12 ans au Mozambique, où en 1974 elle a commencé ses études universitaires en géologie à l'Université de Maputo.

En 1976 la fermeture de l'université pendant l'indépendance la contraint de se déplacer à Lisbonne. Elle y obtient son diplôme (Licenciatura) de géologue en 1981 à l'Universidade Classique de Lisbonne.

En 1982 elle a complété sa formation post-grade en géologie l'ingénieur à l'Universidade Nova de Lisboa.

De 1983-85 elle a travaillé comme assistante à l'Universidade de Trás-os-Montes e Alto Douro, puis, dès 1985 à l'Universidade do Algarve. Depuis Nov. 1987 elle étudie à Berne grâce à une bourse portugaise . En 1993 elle obtient soo doctorat ès Sciences en hydrogéolngie au Centre d'Hydrogéologie de l'Université de Neuchâtel, Suisse.

Elle est membre de l'International Association of Tracer Hydrologists et a publié conjointement les articles suivants:

Carvalho Dill, A.; Gerlinger, K., Hahn, T., Hötzl, H., Käss, W., Leibundgut, Ch., Maloszewski, P., Müller, I., Oetzel S., Rank, D., Teutsch, G., Werner, A. (1992).- Porous aquifer- testsite Merdingen (Germany). Steir. Beitr. z. Hydrogeologie, 43, 251-280, Graz.

Carvalho Dill, A., Müller, I.(1992). Comparative results to structure analyses in the porous aquifer testsite Wilerwald (BE, Switzerland) with very low frequency geophysics : VLF-R, VLF-EM. in Tracer Hydrology, Hötzl&Werner (eds), 139-142.Balkema, Rotterdam.

Leibundgut,CH., Carvalho Dill,A., Maloszewski,P.,Müller,I. and Schneider, J. (1992).- Investigation of solute transport in the porous aquifer of the test site Wilerwald (Switzerland). Steir. Beitr. z. Hydrogeologie, 43, 229-250, Graz.

Rossi, P., Carvalho Dill, A., Müller, I. & Aragno, M. (1993)- Comparative tracing experiments in a porous aquifer using bacteriophages and fluorescent dye on a test field located at Wilerwald (Switzerland) and simultaneously surveyed in detail on local scale by Radio-Magneto-Tellury (12-240 kHz). J. Environmental Geology, in Press.

Steiner,T., de Carvalho Dill, A., Szarka, L. & Müller, I.(1992).- Comparative studies of VLF-R and VLF-EM geophysical methods; 1-D and 2-D numerical modelling at the tracer test-field Wilerwald (BE, Switzerland) - Bull. du Centre d'hydrogeologie de l'Université de Neuchâtel, 11 *(in Press)*.

Spatial variability in porous aquifer properties.

Synthetical approach by geophysics, tracer techniques and groundwater flow parameters.*

by

Amélia Carvalho Dill

Universidade do Algarve
Unidade de Ciências e Tecnologias dos Recursos Aquáticos (UCTRA)
Campus de Gambelas, 8000 Faro, PORTUGAL
Phone: 89 - 817166 Fax: 89 - 818353

133p., 74 fig., 18 tabl., 3 append.

Abstract

Natural porous formations are quite heterogeneous and of a complex nature, with highly variable geometrical and hydraulic properties. They are often important water reservoirs, very vulnerable to contamination by agriculture or other pollution sources. Therefore, tracer tests under field conditions, simulating contamination problems, have become of increasing importance.

This work was developed on a test site - Wilerwald [canton Bern, Swiss Plateau] - equipped to perform tracer experiments on post glacial Holocene sandy gravels. Artificial tracer tests had already been made, but gave results very inconsistent with what had been expected :

- In wells lying just 7 meters apart, differences of several orders of magnitudes in arrival times as well as in concentrations were observed!
- Simultaneously, we repeatedly observed a deflection of the tracer, diverging from what was considered the main direction of water flow.

In order to interpret solute transport in such formations, it is necessary to have sufficient information about the aquifer, that is, about the mechanisms of flow and about its structure and permeability distribution. Electromagnetical surveys* - Radio Magnetotelluric - Resistivity (RMT-R 12-240 kHz) and Very Low Frequency - Electromagnetic (VLF-EM) were fundamental for collecting such detailed data, otherwise impossible to obtain, by classical geoelectrics or drilling.

We discovered a paleochannel, responsible for the above-mentioned deflection, as well as significant differences in resistivities (and consequently in permeabilities) around each piezometer, thus plausibly explaining the erratic behaviour of the tracers.

In November 1992, the last tracer campaign using classical dyes (Naphtionate, Uranin and Amidorhodamine) and bacteriophages, once again confirmed the electromagnetic conclusions. Almost daily observations of the piezometric level, performed simultaneously, exposed the spatial and temporal variations of the groundwater level, inducing each time new directions and velocities of flow.

To interpret RMT-R raw data a new approach was used, based on the indirect relationship between resistivities and grain size distribution. This is a rapid method for determining both the horizontal and vertical distribution of heterogeneities. It differentiates the vertical distribution of layers and resistivities, and also defines the influence of the upper conductive layer on the resistivity data.

According to the prevailing heterogeneities a regional flow system can thus be differentiated into local systems, each with a different flow-line pattern, a different residence time of the water, and consequently different chemical properties. The same applies to the test-site scale. Some chemical analyses (conductivity , nitrate, sulphate, chloride determinations and hardness) were carried out : they showed only small differences but quite significant ones.

The concentration of two water isotopes was measured

- oxygen 18, to evaluate the respective contributions of rain water and the river Emme to the renewal of the water reserves.
- Tritium, to determine the residence-time of the water in the aquifer.

This work points out:

1) the real degree of heterogeneity of Wilerwald's quaternary formation,
2) the importance of this factor in the evaluation of hydraulic parameters,
3) its implications for transport processes,
4) and the importance of electromagnetical methods for hydrogeological studies.

Keywords:
Porous aquifers, electromagnetics, heterogeneities, piezometry, dyes, isotopes, water chemistry, Swiss Plateau (Wilerwald), Upper Rhine Valley (Merdingen,Germany).

*Thesis presented to the Science Faculty of the University of Neuchâtel, for the grade ofDocteur ès Sciences, at November the 5 th, 1993.